Seafloor Atlas

of the Northern Norwegian-Greenland Sea

EDITED BY KATHLEEN CRANE AND ANDERS SOLHEIM

NORSK POLARINSTITUTT

REGIONES
SVB POLO ARCTICO.
Auctore Guilielmo Blaeu
FRIGVS iners illic habitant, Pallorque, Tremorque,
Et jejuna FAMES.
New South Wales.
Buttons Bay
New North Wales
Iames his Bay.
NOVA BRITANNIA.
Fretum Hudson
Baffins Bay.
FRETUM DAVIS.
GROENLANDIA.
YSLANDIA.
Terra de Corterealis.
TERRA NOVA
Amplissimo Spectatissimo Prudentiss.o Viro
GVILIELMO BACKER DE CORNELIIS,
Reip. Amstelodamensis Consuli et Senatori, nec non in Consessu Societatis Indicæ Orientalis Assessori Tabulam hance D.D.
Joh: Blaeu.

Circulus sub Circulo Arctico.
Tenduc
Cambalu
CATHAIA.
ASIÆ
TARTARIÆ
PARS.
C. Tabin
MARE
TARTARICUM.
Taxata Insula
Eylanden van Orangie
NOVA ZEMLA
C. de Troost
C. Nassau
NIAREN
MORE.
Lomsbay
Molgomzaia.
Obi reca
Obdora.
Staten eyland
Nova Hollandia
SAMOIEDA.
RUSSIÆ PARS.
Petzora
MOURMANSKOY
MORÆ.
Fretum Nassovicum
I. Colgoyen
C. Candenos
Spitsberge
Vogelhoeck
Suydhoeck
t'Beren Eyland
Willoughbys Landt
Noordkaep
Noordkyn
Wardhuys
Kola
Jockenga
LAPPONIA.
Finmarchia
EVROPÆ
Mare Album
S. Michael Archangel
Europæ terminus
SVECIÆ PARS.
NORVEGIÆ PARS
Dronthem
Sinus Bothnicus
culo Arctico.
Milliaria Germanica communia pro 60. latit. gradu
pro 70 latit. gradu
pro 80 lat. gradu

SEAFLOOR ATLAS OF THE NORTHERN NORWEGIAN-GREENLAND SEA

Edited by:
KATHLEEN CRANE
AND ANDERS SOLHEIM

NORSK POLARINSTITUTT

MEDDELELSER NR. 137
OSLO 1995

Technical editor of text and illustrations: Annemor Brekke
Graphic design and production: Grimshei Grafiske, Lørenskog, Norway
Front cover: Low-angle oblique view of the Molloy Ridge and Deep, constructed from merged SeaMARC II side-looking sonar and bathymetric data.
Production: Milanostampa S.p.A, Italy/Knut Hässlers Bokbinderi, Sweden
Printed 1995

ISBN 82-7666-089-4

CONTENTS

The reproductions of old maps as well as the historical photographs from the Nansen Fram-expedition to the North Pole in 1893-96, are from the archives of Norsk Polarinstitutt.

PREFACE

Of all the regions on planet Earth that have yet to be explored and mapped, the Arctic Ocean and its neighboring seas remain the most obscure, difficult to penetrate, and for decades, seemingly unchartable. Where swath mapping systems may routinely be used in temperate and tropical seas, towed or attached acoustic arrays can be shredded rapidly by even a random encounter with ice. Only penetrated by nuclear submarines, (until recently off limits to the research oceanographer), and the costly and small oceanographic icebreaker fleet, whose progress is limited to only a few knots through sea ice, the vast majority of the Arctic Seas remain poorly mapped.

As a result, charts of the world's oceans are often truncated north of 72°N. Because of the difficulties of actually getting to these regions with ships and then penetrating the ice cover, large scale geophysical mapping techniques (primarily from aircraft) have been the most common means of determining the location of plate boundaries and the shape of neighboring seafloor.

Efforts by Norwegians, Swedes and Danes in the last and early part of this century, capped by the epic voyages of Fridtjof Nansen, strove to document the vagaries of the Nordic Sea's physical, chemical and biological oceanography. While the eminent Norwegian oceanographer Håkon Mosby declared that since 1909, more observations about the world's oceans have been collected in the Nordic Seas than in any other, sadly the same could not be said about observations of the seafloor beneath these Arctic waters.

With the advent of single and multichannel seismic systems, the construction of several oceanographic ice-strengthened vessels and the growing international interest in the resources of the Arctic marginal seas, investigation of the Norwegian-Greenland Sea and the neighboring Barents Sea expanded rapidly during the 1980s. Even with the growing interest, most expeditions are still limited to the narrow August-September weather window for exploration east and north of Svalbard. However, in spite of these limitations, voyages from France, Germany, the USA, the USSR (Russia), Norway, Denmark, Sweden, Great Britain and Canada have been successful in mapping restricted regions in great detail.

The most recent compilations of Arctic seafloor data were published in two large books called *The Nordic Seas* (Hurdle 1986), and Volume L of the Decade of North American Geology Series, *The Arctic Ocean Region,* (Grantz et al. 1990). A third compilation of seismic data collected over the Svalbard margin was published by Eiken (1994). The need for a seafloor atlas of the Norwegian-Greenland Sea arose from discussion about how one could present the large format, high resolution multibeam and side-looking sonar information recently collected on numerous expeditions. Because of the long standing interest of the Norwegian Polar Institute in the geographical region, it seemed fitting that the compilation be published in one of the institute's research series.

The information that we present is an international effort to publish several detailed high-resolution maps representing data collected primarily within the last fifteen years. French multibeam data from the Mohns Ridge, German multibeam data from the Fram Strait and the western Norwegian-Greenland Sea, Norwegian-American Sea-MARC II side-looking sonar and bathymetric data from the eastern and central Norwegian-Greenland Sea, to the Arctic Ocean north of Svalbard, British and German GLORIA coverage of the Greenland margin, Canadian compilations of multinational magnetic data (including recently released Russian data near Svalbard), Norwegian compilations of gravity data and Norwegian, American and German compilations of sediment and seismic data extracted from multinational expeditions, are presented in this atlas.

Funding for the publication of the *Seafloor Atlas of the Norwegian-Greenland Sea* comes from the Norwegian Polar Institute and from the Joint Oceanographic Institutions, in Washington DC, whose recent interest in the Arctic stems from the efforts of the Ocean Drilling Program to investigate the role of the Fram Strait tectonic gateway on the changing climate of the world.

It is our hope that these newly compiled maps of the Norwegian-Greenland Seafloor reach a wide audience whose interest lies in fields as diverse as paleo-oceanography, climate change and the evolution of a very young ocean basin. They are organized from regional to small-scale, with the majority of the images representing high resolution multibeam and swath mapping surveys. All citations and references are collated at the end of the atlas to allow the interested individual to search out sources for more detailed information about the respective subject.

We gratefully acknowledge the Norwegian Polar Institute, Oslo, Norway, and the Joint Oceanographic Institutions of Washington DC, USA, for their financial support, as well as the numerous multinational funding agencies that sponsored the expeditions represented in this atlas and the individuals who spent countless hours in the production of their compilations and maps. We also thank Terje Sundberg, Einar Heltne, Espen Kopperud, and Anne Kari Bjørge for refining and massaging the numerous forms of imagery. Annemor Brekke played a major role in designing the lay-out of the atlas. To all these assistants, authors and funders we are grateful.

KATHLEEN CRANE,
Washington DC, USA

ANDERS SOLHEIM,
Oslo, Norway

TABLE OF PLATES

LIST OF CONTRIBUTORS

Kathleen Crane, Editor,
Marine Physics, Code 7420, Naval Research Laboratory, Washington DC, 20375, USA
Department of Geology and Geography, Hunter College, 695 Park Avenue, NY, NY 10021, USA and Lamont-Doherty Earth Observatory, Palisades, NY 10964, USA

Anders Solheim, Editor,
Norsk Polarinstitutt, Middelthuns gate 29, P.O. Box 5072, Majorstua, N-0301 Oslo, Norway

Espen S. Andersen
Institutt for geologi, Universitetet i Oslo, P.O. Box 1047, Blindern, N-0316 Oslo, Norway

Susan Barr
Norsk Polarinstitutt, Middelthuns gate 29, P.O. Box 5072, Majorstua, N-0301 Oslo, Norway

Norman Z. Cherkis
Marine Physics, Code 7420, Naval Research Laboratory, Washington DC, 20375, USA

Conoco Norway, Inc.
P.O. Box 488, N-4001 Stavanger, Norway

Ola Eiken
STATOIL, P. O. Box 2123, N-6501, Kristiansund, Norway

Jan Inge Faleide
Institutt for geologi, Universitetet i Oslo, P.O. Box 1047, Blindern, N-0316 Oslo, Norway

Louis Geli
IFREMER, Centre de Brest, BP 337, 29273, Brest, France

Hannes Grobe,
Alfred Wegener Institut für Polar und Meeresforschung, Columbusstrasse, Postfach D-27515, Bremerhaven, Germany

Klemens Heidland
Alfred Wegener Institut für Polar und Meeresforschung, Columbusstrasse, Postfach D-27515, Bremerhaven, Germany

Karl Hinz
Bundesanstalt fur Geowissenschaften und Rohstoffe, Alfred-Bentz-Haus, Stillweg 2, Postfach 510153, Hannover 51, Germany

Heinrich Hinze
Alfred Wegener Institut für Polar und Meeresforschung, Columbusstrasse, Postfach D-27515, Bremerhaven, Germany

Franz Josef Hollender
SFB 313 der Christian-Albrechts Universität zu Kiel, Olshausen-strasse 40-60, D-24118 Kiel, Germany

Heidemarie Kassens
GEOMAR, Forschungszentrum für Marine Geowissenschaften der Christian-Albrechts-Universität zu Kiel, Wischhofstrasse 1-3, D-24148 Kiel , Germany

Neil H. Kenyon
Institute of Ocean Sciences, Deacon Laboratory, Brook Road, Wormley, Godallming, Surrey, GU 5 UB, UK

Jan Sverre Laberg
Institutt for Biologi og Geologi, Universitetet i Tromsø, N-9037 Tromsø, Norway

Ron Macnab
Atlantic Geoscience Centre, Geological Survey of Canada, PO Box 1006, Dartmuth, Nova Scotia, Canada, B2Y 4A2

Jürgen Mienert
GEOMAR, Forshungszentrum für Marine Geowissenschaften der Christian-Albrechts-Universität zu Kiel, Wischhofstrasse 1-3, D-24148 Kiel , Germany

Jürgen Monk
Alfred Wegener Institut für Polar und Meeresforschung, Columbusstrasse, Postfach D-27515, Bremerhaven, Germany

Fred Niederjasper
Alfred Wegener Institut für Polar- und Meeresforschung, Columbusstrasse, Postfach D-27515, Bremerhaven, Germany

Oljedirektoratet (Norwegian Petroleum Directorate)
P.O. Box 600, N-4001 Stavanger, Norway

Stephanie L. Pfirman
Barnard College/Columbia University, 3009 Broadway, New York, NY 10027, U.S.A.

Thomas Reed IV
Hawaii Institute of Geophysics, 2525 Correa Road, Honolulu, Hawaii, 96822 USA

Vincent Renard
IFREMER, Centre de Brest, BP 337, 29273, Brest, France

Hans-Werner Schenke
Alfred Wegener Institut für Polar und Meeresforschung, Columbusstrasse, Postfach D-27515, Bremerhaven, Germany

Telo Schöne
Alfred Wegener Institut für Polar und Meeresforschung, Columbusstrasse, Postfach D-27515, Bremerhaven, Germany

Alexander Shor
Hawaii Institute of Geophysics, 2525 Correa Road, Honolulu, Hawaii, 96822 USA

Reidar Skilbrei
Norges Geologiske Undersøkelse, PO Box 3006, Lade, N-7002, Trondheim, Norway

Robert Spielhagen
GEOMAR, Forschungszentrum für Marine Geowissenschaften der Christian-Albrechts-Universität zu Kiel, Wischhofstrasse 1-3, D-24148 Kiel, Germany

Eirik Sundvor
Institutt for den faste jords fysikk, Universitetet i Bergen, Allegaten 41, 5000, Bergen, Norway

Jörn Thiede
GEOMAR, Forschungszentrum für Marine Geowissenschaften der Christian-Albrechts-Universität zu Kiel, Wischhofstrasse 1-3, D-24148 Kiel, Germany

Jacob Verhoef
Atlantic Geoscience Centre, Geological Survey of Canada, PO Box 1006, Dartmouth, Nova-Scotia, Canada B2Y 4A2

Peter R. Vogt
Marine Physics, Code 7420, Naval Research Laboratory, Washington DC, 20375, USA

Tore O. Vorren
Institutt for Biologi og Geologi, Universitetet i Tromsø, N-9037 Tromsø, Norway

I. REGIONAL MAPS

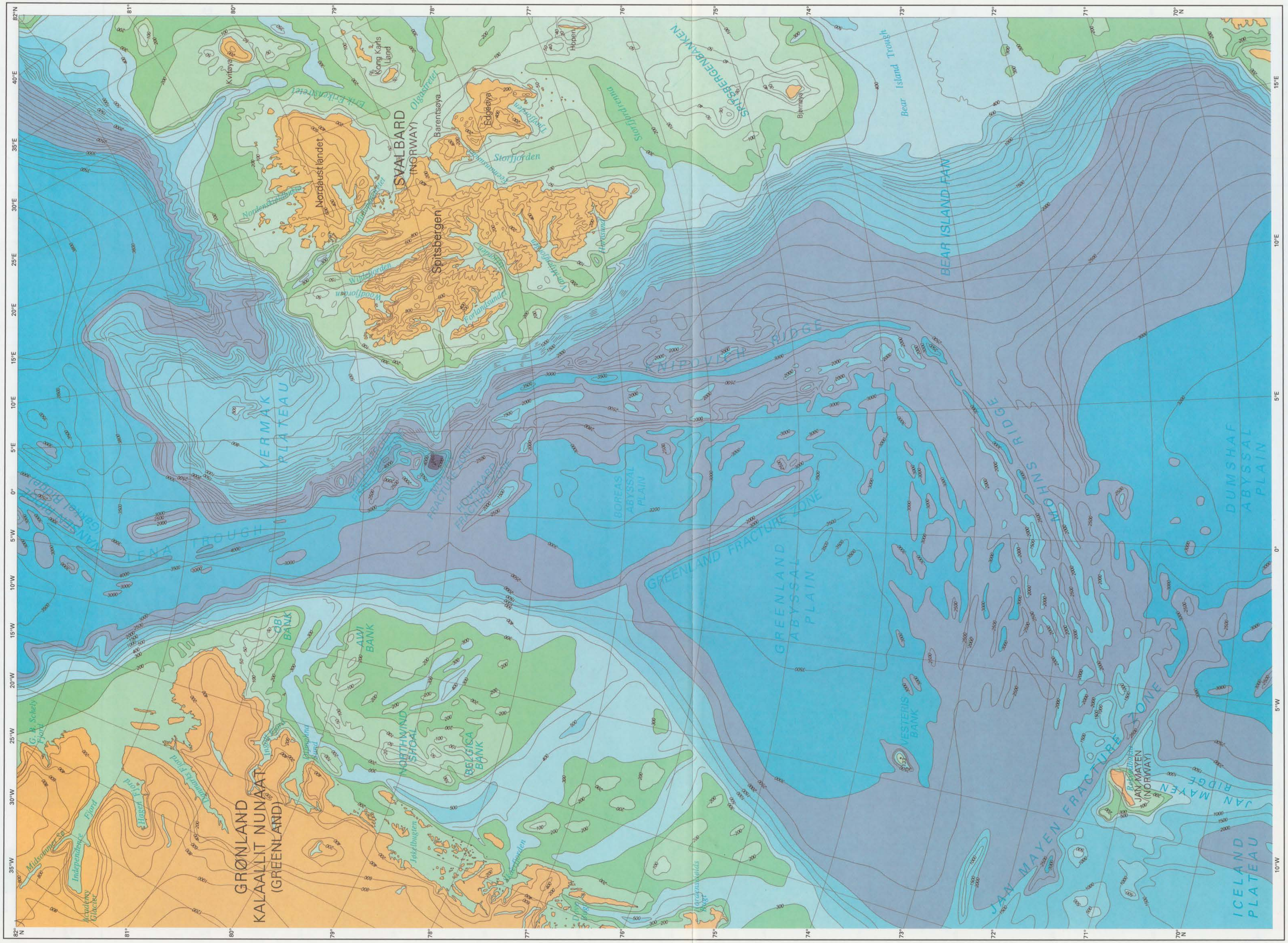

BATHYMETRY OF THE NORTHERN NORWEGIAN - GREENLAND SEA

Compiled by N. Z. Cherkis and P. R. Vogt

1994

Polar Stereographic Projection

Scale 1:3,000,000 at Latitude 71°N

HYPSOMETRIC TINTS

Meters: Land Mass, Sea Level 0, 100, 200, 300, 500, 1000, 1000, 2000, 3000, 4000, 5000

PLATE 2

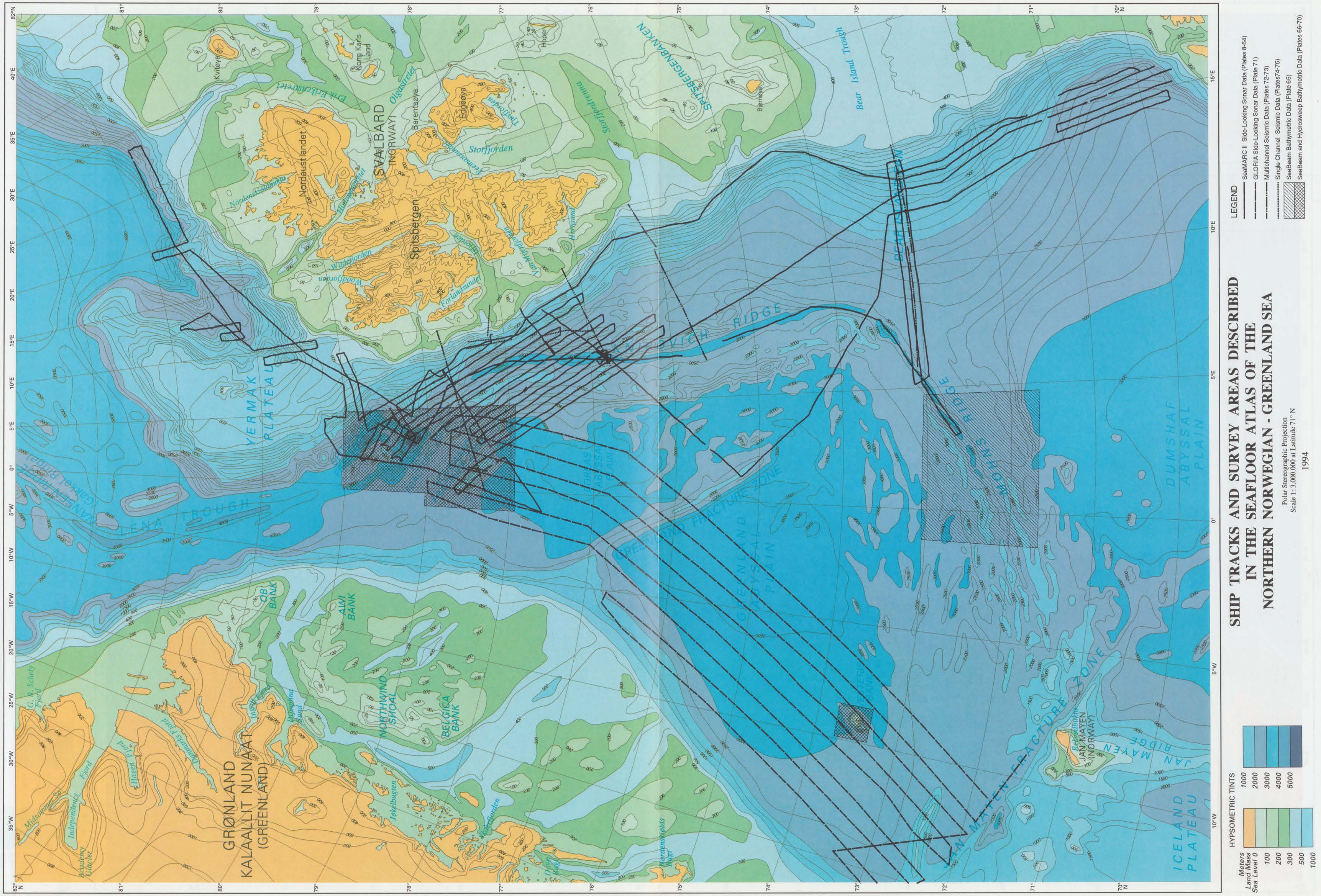

SHIP TRACKS AND SURVEY AREAS DESCRIBED
IN THE SEAFLOOR ATLAS OF THE
NORTHERN NORWEGIAN - GREENLAND SEA
Polar Stereographic Projection
Scale 1: 3,000,000 at Latitude 71° N
1994
LEGEND
SeaMARC II Side-Looking Sonar Data (Plates 8-64)
GLORIA Side-Looking Sonar Data (Plate 71)
Multichannel Seismic Data (Plates 72-73)
Single Channel Seismic Data (Plates74-75)
SeaBeam Bathymetric Data (Plate 65)
SeaBeam and Hydrosweep Bathymetric Data (Plates 66-70)
HYPSOMETRIC TINTS
Meters
Land Mass
Sea Level 0
100
200
300
500
1000
1000
2000
3000
4000
5000
SVALBARD
(NORWAY)
Spitsbergen
Nordaustlandet
Kong Karls Land
Barentsøya
Edgeøya
Kvitøya
Hopen
Bjørnøya
Storfjorden
SPITSBERGENBANKEN
Bear Island Trough
YERMAK PLATEAU
LENA TROUGH
GRØNLAND
KALAALLIT NUNAAT
(GREENLAND)
OB BANK
AWI BANK
NORTHWIND SHOAL
BELGICA BANK
GREENLAND FRACTURE ZONE
GREENLAND ABYSSAL PLAIN
MOHNS RIDGE
DUMSHAF ABYSSAL PLAIN
JAN MAYEN
(NORWAY)
JAN MAYEN FRACTURE ZONE
JAN MAYEN RIDGE
ICELAND PLATEAU

PLATES 1 & 2

BATHYMETRY OF THE NORTHERN NORWEGIAN-GREENLAND SEA

NORMAN Z. CHERKIS AND PETER R. VOGT

The bathymetric map of the Norwegian-Greenland Sea produced by Perry et al. (1980), contained a compilation of single-beam bathymetric data collected through 1978 and was published at a scale of ~1:2.3 million. Further refinements were made to this map and published as part of a subsequent Naval Research Laboratory (NRL)-produced chart: *Bathymetry of the Arctic Ocean* (Perry et al. 1986), at a scale of ~1:4.7 million. The 1986 version contained German multibeam bathymetry collected in 1984 and 1985 in the Fram Strait and over Vesteris Seamount (Alfred Wegener Institute (AWI); GEOMAR), as well as data from several early 1980s at-sea geophysical programs conducted by NRL. A 1991 compilation (Cherkis et al. 1991a): *The Bathymetry of the Barents and Kara Seas*, portrayed the shelf break area between the Barents and Norwegian-Greenland Seas, and included refinements of the Fram Strait, Yermak Plateau and Nordaustlandet areas obtained from new data collected by AWI, GEOMAR, NRL, the University of Bergen and Lamont-Doherty Earth Observatory.

The present compilation contains major revisions to the 1980 and 1986 works, including new multibeam bathymetry from the Fram Strait, Vesteris Seamount and the Knipovich Ridge (AWI; GEOMAR; NRL), Mohns Ridge (IFREMER; AWI; GEOMAR; NRL), Bear Island Fan (GEOMAR; NRL) and the Svalbard archipelago (Norsk Polarinstitutt and Norges Sjøkartverk). Enhanced single-beam bathymetry and sidescan sonar imagery data were collected over Jan Mayen Fracture Zone, Knipovich Ridge, Bear Island Fan and Yermak Plateau by the *R/V Kane* and *R/V Håkon Mosby*, during NRL and University of Bergen; NRL, Lamont-Doherty Earth Observatory, Scripps Institution of Oceanography and Hunter College field programs. The east Greenland shelf data were enhanced by single-beam bathymetry collected by researchers from the US Naval Post Graduate School. In areas where no new data had been collected (or were unknown to the compilers), contours are based on the maps of Perry et al. (1980; 1986) and Cherkis et al. (1991a).

Ship tracks and survey regions which contributed to this new bathymetry compilation are presented in detail in this atlas and are illustrated on Plate 2. Sources of data are taken from the following references: Alekshin & Verba (1979), AWI & GIK (1989), Baturin (1987; 1988), Baturin & Yunov (1987), Baturin & Nechkhaev (1989), Baturin & Yunov (1989), Beal (1969), Birkenmajer (1981), Boyd (1935; 1948), Briseid & Mascle (1975), Buchardt (1981), Bugge et al. (1987), Charov & Krasil'shchikov (1981), Cherkis et al. (1989; 1991a, b; 1992; 1994), Cherkis & Max (1991; 1992), Dekko & Rokoengen (1980), Dibner et al. (1970), Eggvin (1963), Eldholm & Ewing (1971), Gramberg (1988), Grønlie & Talwani (1979), Gudlaugsson et al. (1987), Guterch et al. (1978), Hagevang (1978), Heezen & Ewing (1961), Heezen & Tharp (1975), Helland-Hansen & Nansen (1909), Hempel et al. (1991), Herman (1974), Hjelle & Lauritzen (1982), Holtedahl (1940), Holtedahl & Holtedahl (1961) Houtz & Windisch (1977), Hurdle (1986), Johnson & Eckhoff (1966), Johnson & Heezen (1967), Johnson et al. (1979), Klenova (1960), Kovacs & Vogt (1982), Kristoffersen et al. (1989), Laktionov (1959), Lauritzen & Ohta (1984), Litvin (1965), Lowell (1972), Løvø et al. (1990), Malod & Mascle (1975), Matishov (1975; 1979; 1986a; 1986b; 1987), Matishov et al. (1984), Medvedev & Pavlidis (1984), Meyer et al. (1972), Nansen (1904), Neprochnov et al. (1984), Norges Sjøkartverk (1988), Nunns (1980; 1982), Ohta (1982), Perry et al. (1980; 1986), Perry (1986), Renard & Malod (1974), Rice et al. (1989), Riis et al. (1986), Rønnevik (1981), Rønnevik & Motland (1979), Rønnevik et al. (1982a, b; 1984), Rønnevik & Jacobsen (1984), Savostin & Karasik (1981), Sorokin (1987), Sverdrup (1933), Thiede et al. (1990), Volkov (1961), Winsnes & Worsley (1981), and Åm (1975).

Acknowledgements:

The following institutions contributed data used in the construction of this map:

Alfred Wegener Institut für Polar und Meeresforschung, Bremerhaven, Germany
British Hydrographic Office, Taunton, Great Britain
Bundesamt für Seeschiffahrt und Hydrographie, Hamburg, Germany
Bundesanstalt für Geowissenschaften und Rohstoffe, Hannover, Germany
Defense Mapping Agency Hydrographic-Topographic Center, Bethesda, MD, USA
Farvandsvæsenet, Copenhagen, Denmark
Fiskeridirektoratets Havforskningsinstitutt, Bergen, Norway
Forsvarets Forskningsinstitutt, Horten, Norway
Geologisch-Paläontologisches Institut, Kiel, Germany
GEOMAR/Forschungszentrum für Marine Geowissenschaften, Kiel, Germany
Grønlands Geologiske Undersøgelse, Copenhagen, Denmark
Glavnoe Upravleniye Navigatsii i Okeanograpfii, MO, St. Petersburg, Russia
Hydrographic Service of the Netherlands, LS's Gravenhague, The Netherlands
IFREMER, Brest, France
Institute of Oceanographic Sciences, Wormley, Great Britain
Institutt for Kontinentalsokkelundersøkelser og Petroleumsteknologi A/S, IKU, Trondheim, Norway
International Council for the Exploration of the Seas, Copenhagen, Denmark
Lamont-Doherty Earth Observatory, Palisades, NY, USA
National Geophysical Data Center, Boulder, CO, USA
Naval Oceanographic Office, Stennis Space Center, MS, USA
Naval Postgraduate School, Monterey, CA, USA
Naval Research Laboratory, Washington, DC, USA
Norsk Oseanografisk Datasenter, Bergen, Norway
Norsk Polarinstitutt, Oslo, Norway
Oljedirektoratet, Stavanger, Norway
Service Hydrographique et Oceanographique de la Marine, Brest, France
Statens Kartwerk, Norges Sjøkartverk, Stavanger, Norway
Universität Bremen, Bremen, Germany
Universität Hamburg, Hamburg, Germany
Universitetet i Bergen, Bergen, Norway
Universitetet i Oslo, Oslo, Norway
Universitetet i Tromsø, Tromsø, Norway
US Coast Guard, Washington, DC, USA

PLATE 3

SEAFLOOR ECHO CHARACTER OF THE NORTHERN NORWEGIAN-GREENLAND SEA

Stephanie L. Pfirman and Heidemarie Kassens

Acoustic echo character of the seafloor in the Norwegian-Greenland Sea was originally investigated by Damuth (1978). Our echo character compilation extends his analysis using a similar echo classification scheme with 3.5 kHz profiles courtesy of the Alfred Wegener Institute for Polar and Marine Research, the US Naval Research Laboratory, as well as Lamont-Doherty Earth Observatory.

Echo Classifications

Echo classifications reflect those defined by Damuth (1978), with modifications as noted (see types IB*, IIIA*, IIID, IV):

Type IA-2: distinct bottom echoes with intense, closely spaced hummocks.

Type IB: continuous sharp bottom echoes with several continuous, sharp, parallel subbottom reflectors which persist for tens to hundreds of kilometers. Within the Boreas Basin, a region where type IB reflectors are underlain by one or more acoustically transparent deposits (type IB*) was mapped.

Type IC: continuous, sharp bottom echoes with one or more sharp, wedging or lens-shaped subbottom reflectors.

Type IIA: semiprolonged bottom echoes with intermittent zones of discontinuous, subbottom reflectors.

Type IIB: prolonged bottom echoes with few or no subbottom reflectors.

Type IIIA: large, irregular, overlapping hyperbolae with widely varying vertex elevations above the sea floor. This echo type was separated into two categories: one with common intervening sediment pockets (type IIIA*) and one without (type IIIA).

Type IIIC: regular overlapping hyperbolae with varying vertex elevations above the sea floor.

Type IIID: regular, semi-periodic features with subbottom reflectors. This echo type is modified from that used by Damuth (1978). Here it encompasses migrating and non-migrating sediment waves, and may also include some channel levee deposits, slumps and periodic faulting.

Type IV: periodic focusing of the acoustic return. This type was not identified by Damuth (1978).

Regional Characteristics

Sediments on the continental shelves in this region are often disturbed by iceberg gouging, resulting in a hummocky surface return (type IA-2). Iceberg gouging is apparent down to more than 400 m water depth. Here the surface becomes smooth and returns a prolonged signal (types IIA and IIB). The prolonged return probably represents an increase in the amount of bedded silt/sand (Damuth 1978) perhaps due to mass wasting and winnowing of seafloor sediments by currents flowing along the continental margins. A region heavily influenced by mass wasting exists just to the west of the Bear Island Trough. The unusual wedging reflectors (type IC) observed by Damuth (1978) are due to mud flows that form elongated tongues on the continental slope and rise (Sundvor et al. 1991; Vogt et al. 1991a, b; Vogt et al. 1993; Laberg & Vorren 1995).

The Mohns and Knipovich Ridges extend through the center of the study area. These active plate margins are represented by hyperbolic returns from basement highs, either with (type IIIA*) or without (type IIIA) pockets of sediment.

The sedimentary section in the Boreas Basin (Boreas Abyssal Plain) and much of the deeper portions of Fram Strait consist of conformable reflectors, most likely representing bedded sediment with little silt or sand (type IB: Damuth 1978). Generally, evidence for sediment disturbances is confined to the vicinity of basement highs along the basin margins. In water depths exceeding 3,200 m, two deep transparent layers (type IB*) are observed at approximately 20 msec subbottom depth (Pfirman 1987). Because they are confined to the deepest part of the basin, these layers appear to represent large-scale gravity-influenced sediment flows.

Sediment characteristics of the Greenland Basin (Greenland Abyssal Plain) are quite different. Damuth (1978) and Pfirman (1987) noted that large regions of the western basin have hyperbolic returns (IIIC), and prolonged reflectors (IIA and IIB), with numerous erosional channels and patches of migrating sediment waves (IIID). These echo characteristics indicate sediment redeposition including mass wasting. A large sediment drift (1 sec thick) with a pronounced moat, observed on seismic profiles run parallel to the 3.5 kHz profiles, indicates long-term contour current activity in this region.

To the northeast of Vesterisbanken is a region with an unusual sediment characteristic: the acoustic return is periodically focused and defocused in patches slightly raised above the adjacent sea floor (called here type IV). These features resemble so-called “pagoda” structures (Emery 1974) and may represent current-influenced sedimentation.

The sediment disturbances observed in the Greenland Basin are in marked contrast to the comparatively quiescent accumulation of the Boreas Basin. One reason for the difference could be the fact that numerous cross-shelf troughs extend across the Greenland shelf just west of the Greenland Basin, while there is a large bank, (Belgica Bank), on the shelf to the west of the Boreas Basin (Pfirman 1987). Transverse shelf troughs are thought to have formed by glacial erosion and can act as conduits for water and sediment under certain conditions. Supply of sediment and cascading dense water from the shelf and slope into the Greenland Basin may have contributed to the sediment disturbances observed there. Additional evidence for downslope transport can be seen in the GLORIA image presented by Mienert et al. (1995).

PLATE 3

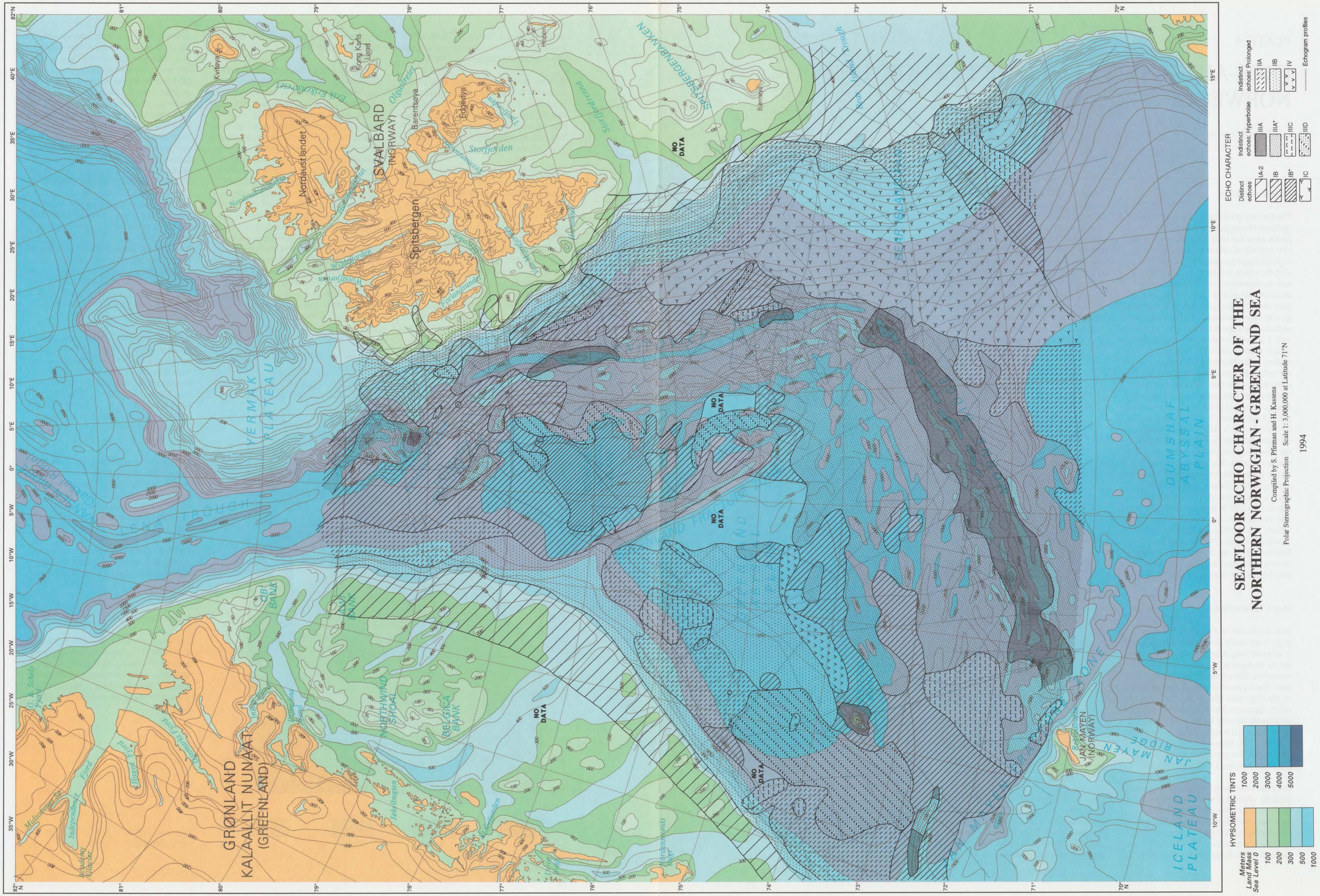
SEAFLOOR ECHO CHARACTER OF THE
NORTHERN NORWEGIAN - GREENLAND SEA
Compiled by S. Pfirman and H. Kassens
Polar Stereographic Projection Scale 1:3,000,000 at Latitude 71°N
1994
ECHO CHARACTER
HYPSOMETRIC TINTS
SVALBARD (NORWAY)
Spitsbergen
Nordaustlandet
Barentsøya
Edgeøya
Storfjorden
Bjørnøya
Kong Karls Land
Kvitøya
Hopen
GRØNLAND
KALAALLIT NUNAAT
(GREENLAND)
JAN MAYEN (NORWAY)
YERMAK PLATEAU
NORTHWIND SHOAL
BELGICA BANK
DUMSHAF ABYSSAL PLAIN
ICELAND PLATEAU
JAN MAYEN RIDGE
NO DATA

PLATE 4

FREE-AIR GRAVITY FIELD OF THE NORTHERN NORWEGIAN-GREENLAND SEA

JAN INGE FALEIDE

Map construction

The free-air gravity anomaly map of the northern Norwegian-Greenland Sea and adjacent areas has been compiled from several new sources of data incorporating two regional maps presented by Faleide et al. (1984b) which included a large number of new measurements carefully evaluated in terms of data quality. After corrections had been made for the systematic differences of gravity values measured at ship track intersections, the maps were manually contoured with a 10 mGal contour interval, with less weight given to the data considered of low quality. In the Norwegian-Greenland Sea, the bathymetry was used as a guideline for contouring when there were limited data. Structural information from multichannel seismic data guided the contouring in some parts of the Barents Sea. The data coverage for Faleide et al.'s (1984b) map was in general quite satisfactory, with the exception of the western Norwegian-Greenland Sea and northern Barents Sea which were poorly mapped due to the ice conditions. Using the same approach, Faleide (in Breivik 1991) made a similar gravity map covering the area south of 73°N and east of 0°. The present map is based on maps and data from Faleide et al. (1984a, b), Breivik (1991), Talwani & Grønlie (1976), Austegard & Sundvor (1991), the Norwegian Geological Survey, NGU (unpublished), and the Norwegian Mapping Authority (unpublished).

Map Characteristics

Both the Mohns and Knipovich Ridges (Fig. 1) are easily distinguished in the gravity anomaly map where they are characterized by elongate negative or small positive anomalies. The continuity of this belt indicates that no transform faults presently offset the ridge axis. The Knipovich Ridge rift valley appears to be continuous, striking north-northwesterly between 74°N and 76°N. The axial trend changes to due north at about 77°N. Between 76°N and 77°N several positive gravity anomalies form a northwest-southeast lineament (Fig. 2).

The most prominent anomaly to the west of the ridge is associated with the Greenland Fracture Zone. West of 2°E the fracture zone has a well defined linear northwest-southeast trend. This positive gravity anomaly (with a maximum of 117 mGal) is associated with a basement ridge (Eldholm & Windisch 1974). Close to the mid-ocean ridge, no obvious lineaments in the gravity field outline the fracture zone. However, several positive gravity anomalies in this area indicate a more easterly azimuth for this part of the fracture zone. This change is probably related to the reorganization of relative plate motion at about 36 Ma (Talwani & Eldholm 1977). The different levels of the gravity field on either side of the Greenland Fracture Zone reflect the different crustal ages and basement elevations across the fracture zone. The bathymetry also shows a regional difference of approximately 500-700 m.

The decrease of the free-air anomalies towards the Hovgård Fracture Zone appears to be partly associated with an increasing depth to oceanic basement. Two pronounced gravity maxima coincide with the Hovgård Fracture Zone and in general reflect the bathymetry of the segmented submarine ridge. However, the (42 mGal) difference in maximum values between the two ridge segments does not appear to be any simple topographic effect because the eastern segment is even deeper than the western segment. It may be attributed to an important difference in the densities of the underlying

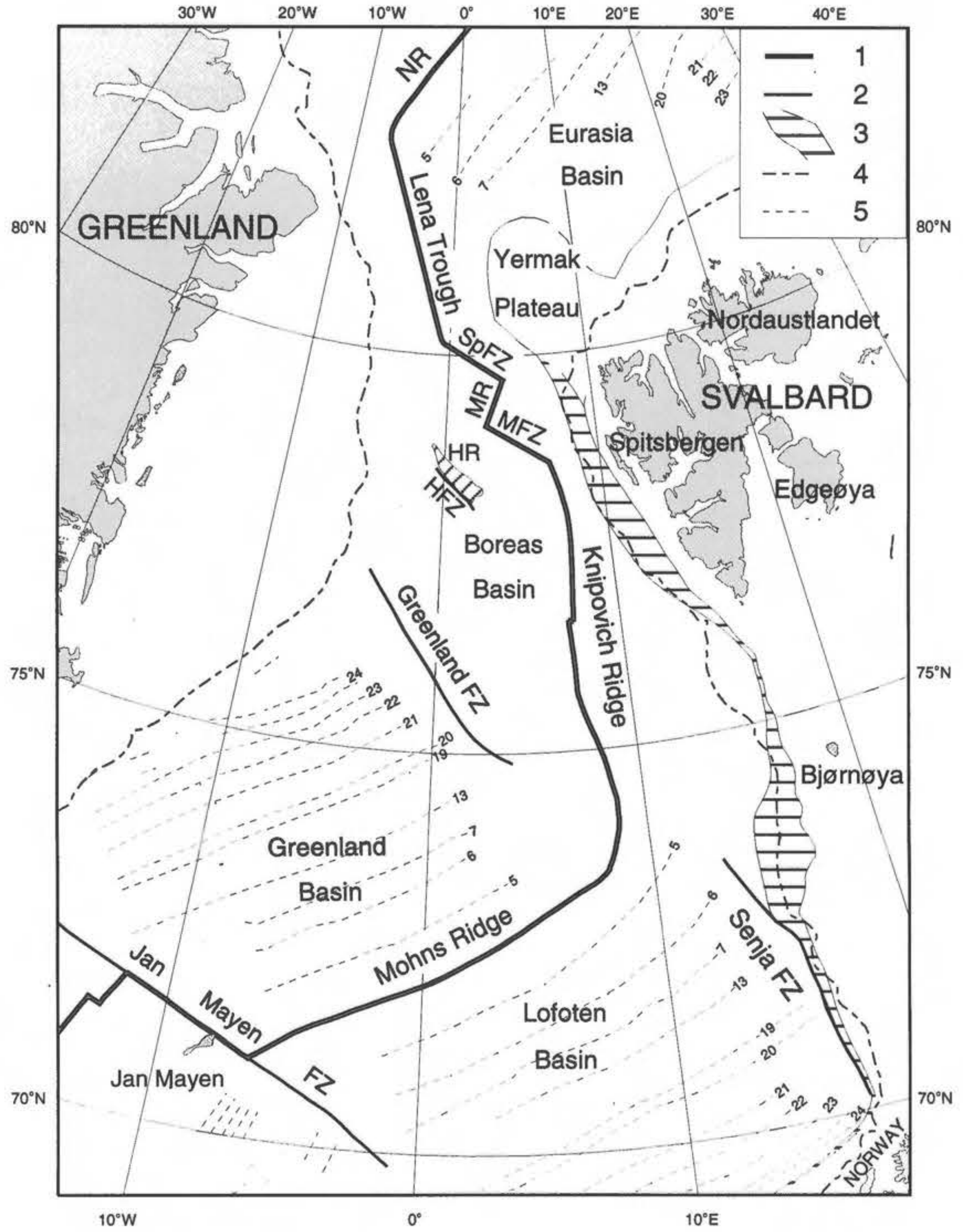

Figure 1. Major Tectonic Features in the Norwegian-Greenland Sea. Main structural features: MFZ = Molloy Fracture Zone; HFZ = Hovgård Fracture Zone; HR = Hovgård Ridge; MR = Molloy Ridge; NR = Nansen Ridge; SpFZ = Spitsbergen Fracture Zone; 1 = present plate boundary; 2 = fracture zones; 3 = continent-ocean transition along the western Barents Sea-Svalbard margin; 4 = shelf edge (500 m water depth); 5 = magnetic lineations.

rocks (Eldholm & Myhre 1977). Possibly, it reflects the different crustal nature of the two ridge blocks (Myhre et al. 1982).

Between the Knipovich Ridge axial province and the Svalbard margin the gravity field is subdued. Seismic reflection and refraction data indicate a thick sediment cover extending from the continental shelf to the eastern axial mountains (Eiken & Austegard 1987; Myhre & Eldholm 1988).

Large elongate positive free-air gravity anomalies are present seaward of the continent-ocean transition along the western Barents Sea continental margin. The anomalies are most pronounced at the sheared margin segments along the Senja Fracture Zone (SFZ) (70°-73°N and 11.5°-15.5°E) and the southern Hornsund Fault Zone (HFZ) (74.5°-76.5°N and 13°-16°E) (Fig. 1). Here, the crustal transition coincides with the gravity gradient on the eastern flank of the positive anomaly belts (Faleide et al. 1991). Between these belts, along the central rifted margin segment southwest of Bjørnøya, there is another well-defined but less prominent anomaly belt associated with the Vestbakken Volcanic Province.

The location of all three gravity anomaly belts strongly implies a relation between fundamental properties of the oldest oceanic crust and with structures formed during the initial phase of opening (Eldholm et al. 1987). Results from a transect of expanding spread profiles (ESP) across the Hornsund Margin (Kitterød 1986) reveal normal oceanic crust west of the gravity anomaly. Beneath the anomaly the crust maintains a normal oceanic thickness, but a 7.1 km/s velocity is measured just below the basement surface. In order to satisfy the observed gravity data along the transect, Myhre & Eldholm (1988) had to introduce a high-density crust, 3.0-3.1 g/cm^3, beneath the main anomaly seaward of the Hornsund Fault Zone. Similar results are obtained along a transect of Expanding Spread Profiles (ESP) across the Senja Fracture Zone where Jackson et al. (1990) reported higher velocities than normal for oceanic layer 2 and a slightly thinner crust.

Abnormally high seismic velocities near the top of the basement suggest that isolated high-density bodies produce the large gravity anomalies west of the Senja and Hovgård Fracture Zones. Eldholm et al. (1987) suggested that the anomalies are caused by intrusions of asthenospheric material from levels deeper than at a spreading ridge, within a leaky transform fault zone surrounded by relatively thick continental crust. The maximum positive gravity anomalies along the margin coincide with the maximum thickness of Cenozoic sediments associated with the Bjørnøya and Storfjorden Fans (Breivik 1991). The deep burial and loading by a thick (up to 4-6 km) wedge of sediments probably also contribute to the calculated high velocities of the oceanic crust.

Breivik (1991) modelled a series of crustal transects across the western Barents Sea-Svalbard margin. In order to obtain a match with the observed gravity field, he had to introduce lateral density contrasts in the mantle probably related to a thermal anomaly/gradient.

Along the western Svalbard margin the relationship between the gravity field and the continent-ocean boundary (Fig. 1) is much less clear, although the north-northwest structural trend is reflected by the anomalies. The narrow (132 mGal) local high at 77°N is believed to be caused by a local intrusive body surrounded by less dense continental crust along the Hornsund Fault Zone (Myhre & Eldholm 1988).

In the southwestern Barents Sea, the free-air gravity field reveals a first-order correlation with the subsurface structures of deep basins and intrabasinal highs/ridges. North of 74°N, a system of generally positive anomalies is associated with the Svalbard Platform.

Figure 2 illustrates the true gravity color scheme as a reference for Plate 4 which depicts free air gravity superimposed over bathymetry.

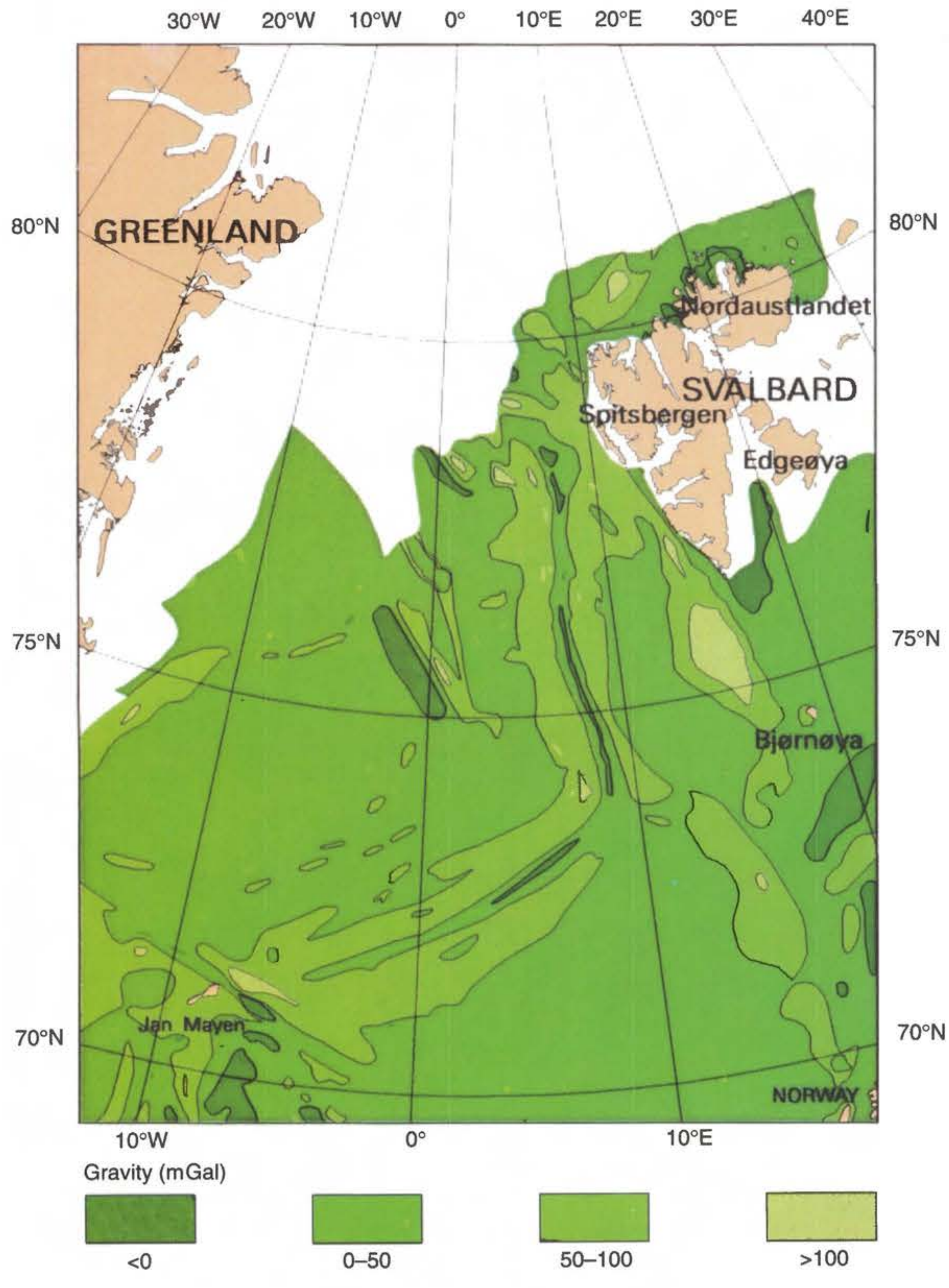

Figure 2. True color Free-Air Gravity Map of the Norwegian- Greenland Sea.

Acknowledgements

The author would like to thank Reidar Skilbrei at NGU who provided data from northern Svalbard, Asbjørn Breivik for assistance in the compilation of the gravity data, and Terje Sundberg of Norsk Polarinstitutt for digitizing and producing the final map.

PLATE 4

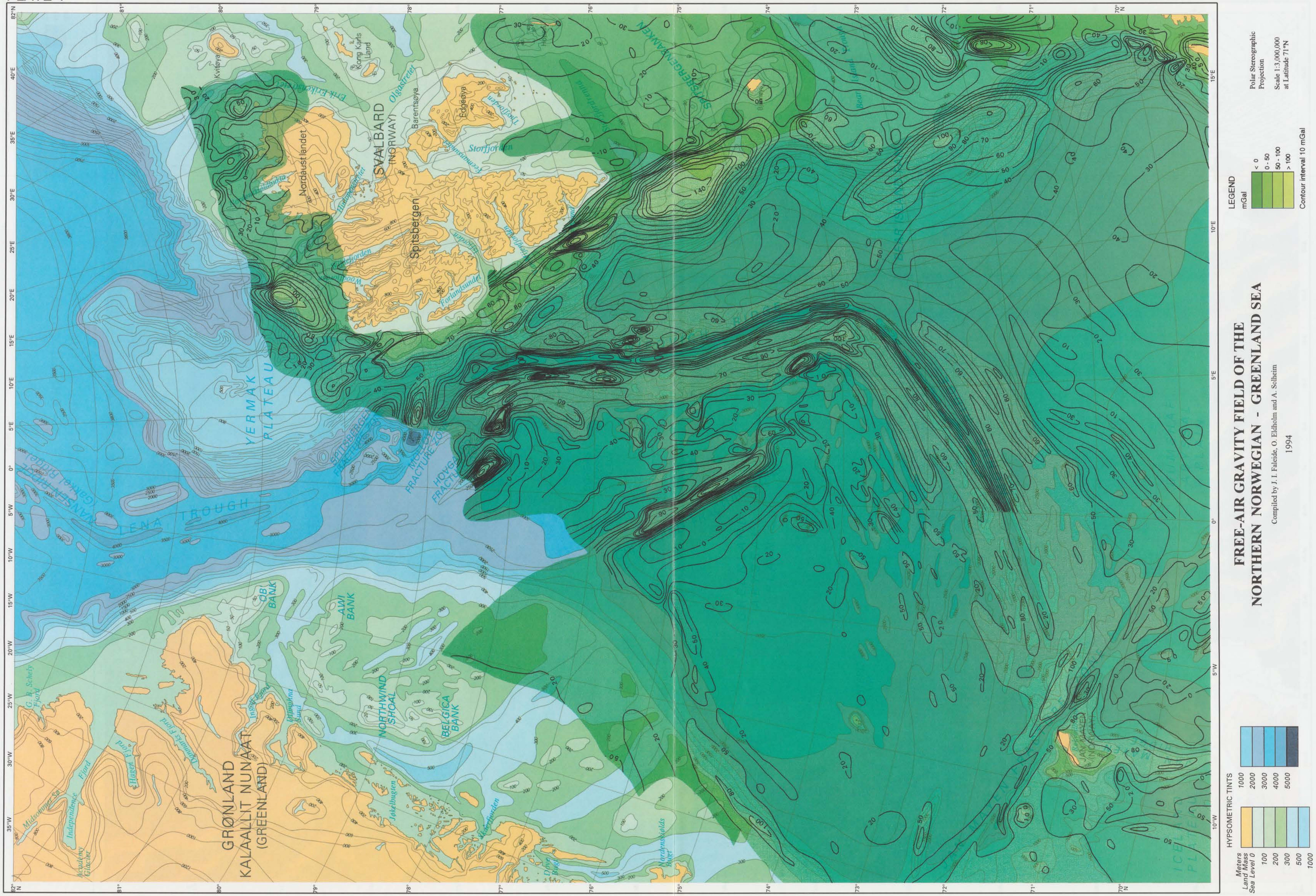
FREE-AIR GRAVITY FIELD OF THE
NORTHERN NORWEGIAN - GREENLAND SEA
Compiled by J. I. Faleide, O. Eldholm and A. Solheim
1994
Polar Stereographic Projection
Scale 1:3,000,000 at Latitude 71°N
LEGEND
mGal
< 0
0 - 50
50 - 100
> 100
Contour interval 10 mGal
HYPSOMETRIC TINTS
Meters
Land Mass
Sea Level 0
100
200
300
500
1000
1000
2000
3000
4000
5000
SVALBARD
(NORWAY)
Spitsbergen
Nordaustlandet
Barentsøya
Edgeøya
Storfjorden
YERMAK
PLATEAU
LENA TROUGH
GRØNLAND
KALAALLIT NUNAAT
(GREENLAND)
OB
BANK
AWI
BANK
NORTHWIND
SHOAL
BELGICA
BANK

PLATE 5

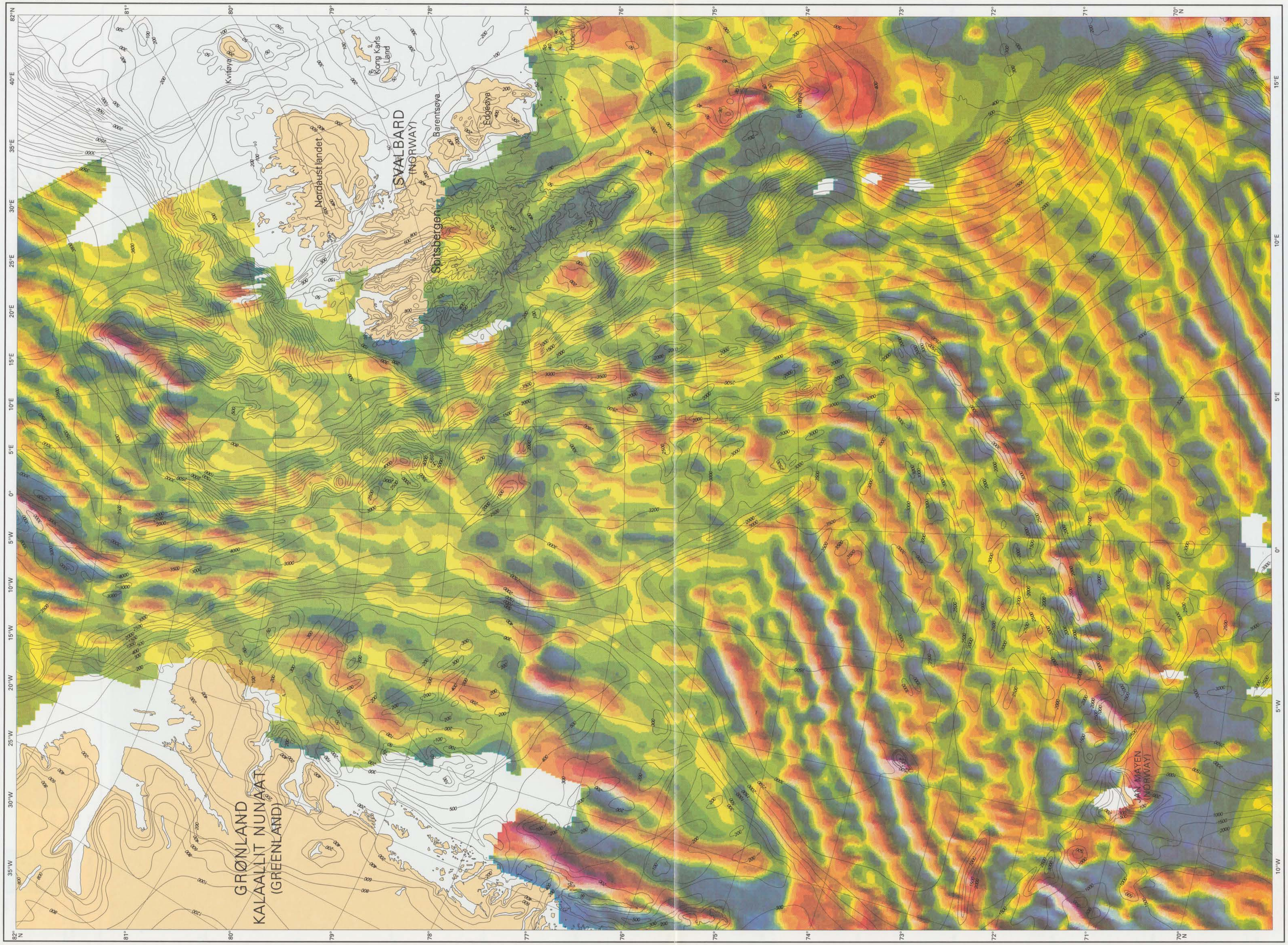
MAGNETIC ANOMALIES OF THE
NORTHERN NORWEGIAN - GREENLAND SEA
Compiled by R. Macnab and J. Verhoef
Polar Stereographic Projection Scale 1: 3,000,000 at Latitude 71°N
1994
LEGEND
Magnetic Anomaly Values (Nanotesla)
Bathymetry (Meters)
SVALBARD
(NORWAY)
Nordaustlandet
Spitsbergen
Barentsøya
Edgeøya
Kong Karls Land
Kvitøya
Hopen
GRØNLAND
KALAALLIT NUNAAT
(GREENLAND)
JAN MAYEN
(NORWAY)

PLATE 5

MAGNETIC ANOMALIES OF THE NORTHERN NORWEGIAN-GREENLAND SEA

RON MACNAB AND JACOB VERHOEF

Map Construction

This map was produced from a compilation of marine and airborne magnetic observations that were collected by or on behalf of the following organizations: the Lamont-Doherty Earth Observatory, Palisades NY, USA; the US Naval Research Laboratory, Washington DC, USA; the US Naval Oceanographic Office, Stennis Space Center MS, USA; the Marine Geology Institute, Murmansk, Russia; the Geological Survey of Norway, Trondheim, Norway; and the Geological Survey of Greenland, Copenhagen, Denmark.

The original data sets consisted of total magnetic field observations along ship and aircraft tracks, the latter flown at an average altitude of 300 metres above sea level. After initial editing to remove spikes and other obvious errors, the observations were reduced to anomaly values through application of the International Geomagnetic Reference Field (IGRF), and then merged. A technique of minimum curvature was used to grid the combined anomaly values over a grid spacing of 20 points per degree of latitude and longitude, yielding a grid density of 400 points per degree square. This grid was used to produce a color shaded relief map, with artificial illumination from the northwest to emphasize the anomaly field's fine structure.

The data sets used in the production of this map were assembled and merged at the Atlantic Geoscience Centre of the Geological Survey of Canada, within the framework of a larger project to compile magnetic observations from the Arctic and North Atlantic Oceans and adjacent land areas. The grid portrayed here is a preliminary product of that compilation effort. Users may place confidence in the major features that are shown, but some of the map's detailed aspects remain questionable pending more definitive adjustments that must still be applied to the final compilation grid.

Map Characteristics

The geomagnetic field patterns shown on this map are indicative of the general nature and distribution of material in the earth's crust beneath the seafloor. They also provide a record of tectonic plate movements over geological time. For example, the stripes in the northern and southern parts of the map reflect the formation of alternating bands of normally and reversely magnetized rock at mid-ocean spreading centers over the past 56 million years, while the polarity of the earth's magnetic field switched successively between positive and negative directions.

Both sets of magnetic stripes are truncated by prominent bathymetric features: the Jan Mayen, the Greenland, and the Spitsbergen Fracture Zones. Between the Greenland and Spitsbergen Fracture Zones, the magnetic field has a less well-defined pattern, suggesting a regional process of crustal fracturing and dislocation created while the Eurasian and Greenland plates changed the direction of their relative motion.

PLATE 6

CRUSTAL HEAT FLOW IN THE NORTHERN NORWEGIAN-GREENLAND SEA

EIRIK SUNDVOR AND KATHLEEN CRANE

Heat flow data were first collected on the Svalbard margin in the area south of the Hovgård Fracture Zone and reported by Lachenbruch & Marshall (1968), Lubimova et al. (1973), and Langseth & Zielinski (1974). Additional data along and north of the Molloy and Spitsbergen Transform Faults were reported by Crane et al. (1982) and Jackson et al. (1984). To study the basin evolution of the Norwegian continental margin, Elf Aquitaine, Norge, the Department of Geology, University of Oslo, the Seismological Observatory (now the Institute of Solid Earth Physics) of the University of Bergen and Lamont-Doherty Geological Observatory (now Lamont-Doherty Earth Observatory) of Columbia University, carried out a cooperative research project during the period of 1983-1986. It included a series of margin transects where heat flow measurements, cores and high resolution seismic data were collected. Two of the transects were undertaken on the Svalbard margin (Crane et al. 1988; Crane et al. 1991). Because of the poorly resolvable magnetic anomalies in the region, they used the data to model both the spreading rate of the Knipovich Ridge and the age of the adjacent oceanic crust. The Seismological Observatory of the University of Bergen undertook an additional heat flow expedition in 1984 (Sundvor 1986). A total of 96 measurements were taken in the area north of 78°N. In addition, measurements were made at 19 stations on the Barents Sea margin between 70°N and 73°N.

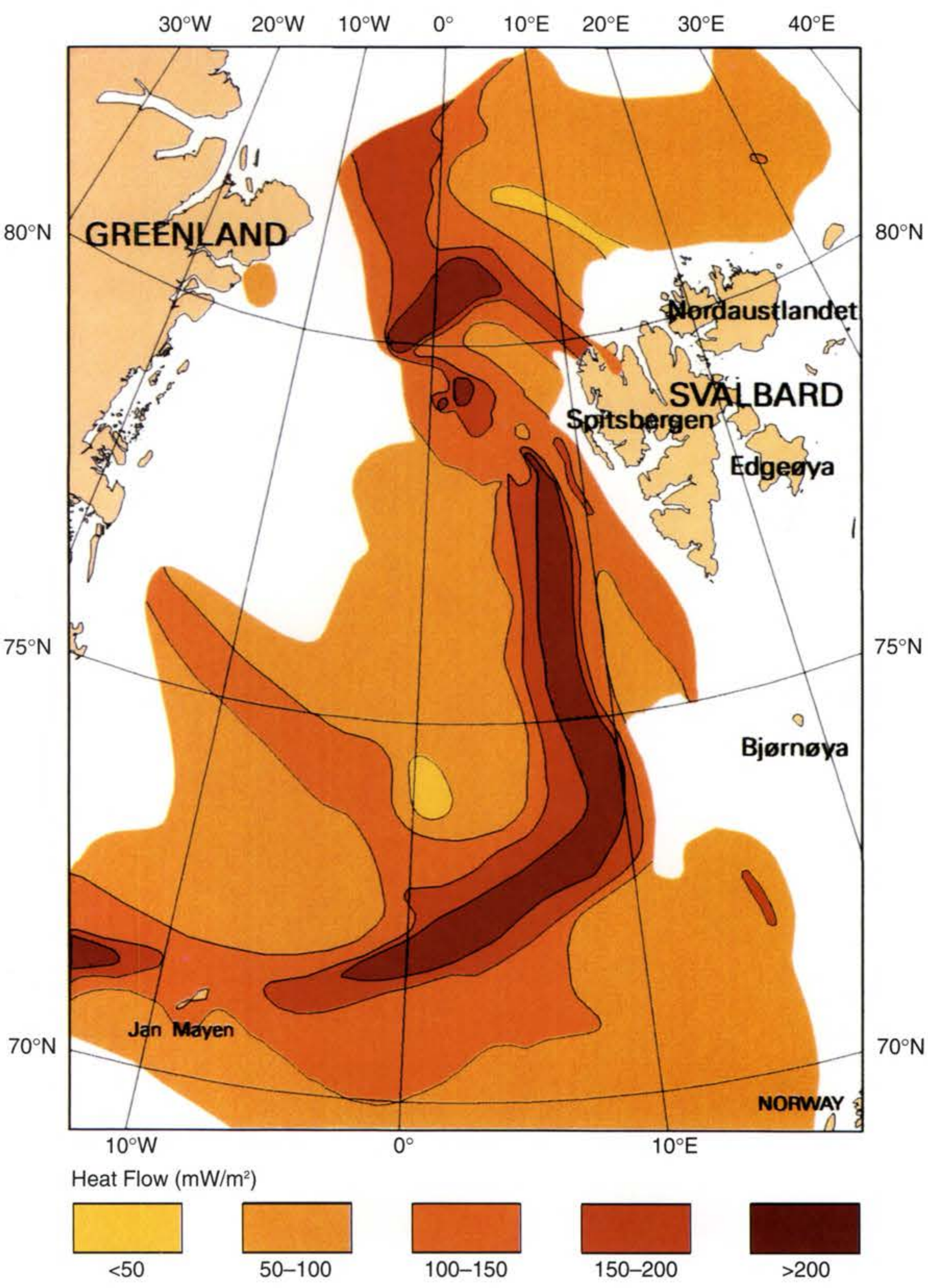

Methodology

The 1968 measurements were collected from an ice island that flowed into the Den-mark Straits (Lachenbruch & Marshall 1968). Measurements made by Lubimova et al. (1973), Langseth & Zielinski (1974), and Crane et al. (1982) were carried out using outrigger probes on a piston core achieving 3.5-5 m penetrations into the sediment. The 1984 and 1986 temperature gradient measurements were recorded using a Norwegian instrument built at the Lamont-Doherty Geological Observatory. The thermistor probes were mounted on outriggers several centimeters away from a solid lance that was attached to a corehead weight. The instrument was dropped into the sea bottom and left for several minutes, permitting a correction for the effect of transient frictional heating which occurs when the lance penetrates the sediments. The instrument also monitored the bottom water temperature and the tilt of the instrument package. The same instrument was used on the German Arctic Expedition ARK IV/3 (Sundvor & Torp 1987) where 21 measurements were made. The rest of the measurements included in the contoured map were recorded using the IFREMER heat flow instrument which is based on a modified Anderaa thermistor string refurbished for enhanced resolution and attached onto the outer part of the piston core barrel.

During the 1984 and 1986 surveys, thermal conductivities were measured on sediment samples retrieved from piston and gravity cores using the needle-probe method (von Herzen & Maxwell 1959). A Fenwal probe consisting of thermistor and heating wire was used. The thermal conductivities were measured at 10 cm intervals along the cores and the values corrected to 'in situ' conditions (Ratcliffe 1960). At temperature gradient stations where no cores were taken, conductivity measurements from neighboring stations were used to calculate heat flow. ▶

(continued page 29)

Figure 3. True Color Crustal Heat Flow Map of the northern Norwegian-Greenland Sea.

PLATE 6

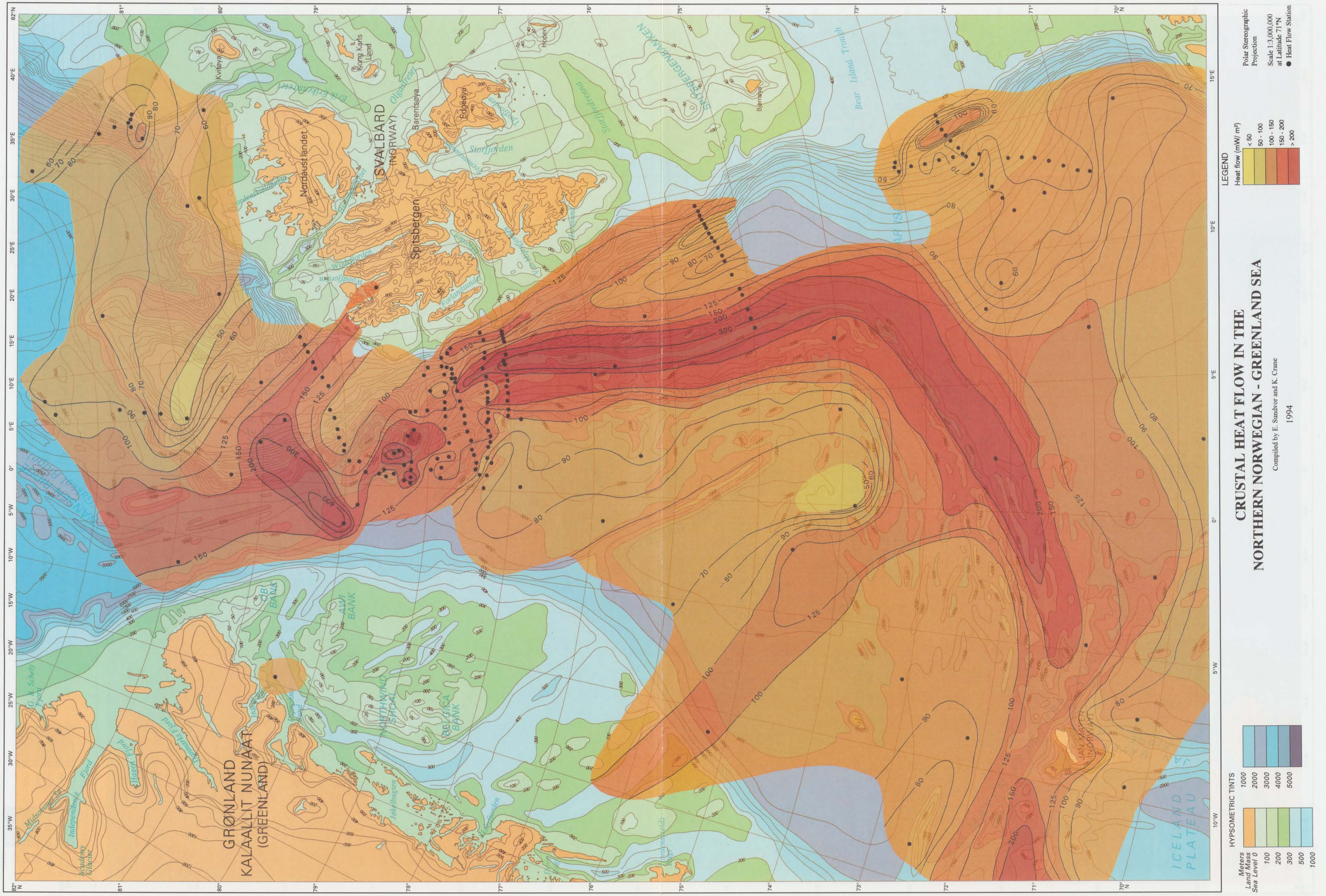

CRUSTAL HEAT FLOW IN THE
NORTHERN NORWEGIAN - GREENLAND SEA
Compiled by E. Sundvor and K. Crane
1994
LEGEND
Heat flow (mW/ m²)
< 50
50 - 100
100 - 150
150 - 200
> 200
Polar Stereographic Projection
Scale 1:3,000,000 at Latitude 71°N
● Heat Flow Station
HYPSOMETRIC TINTS
Meters
Land Mass
Sea Level 0
100
200
300
500
1000
1000
2000
3000
4000
5000
SVALBARD
(NORWAY)
Nordaustlandet
Spitsbergen
Barentsøya
Edgeøya
Kvitøya
Kong Karls Land
Hopen
Bjørnøya
Storfjorden
Bear Island Trough
GRØNLAND
KALAALLIT NUNAAT
(GREENLAND)
OB BANK
AWI BANK
NORTHWIND SHOAL
BELGICA BANK
JAN MAYEN
(NORWAY)
ICELAND PLATEAU

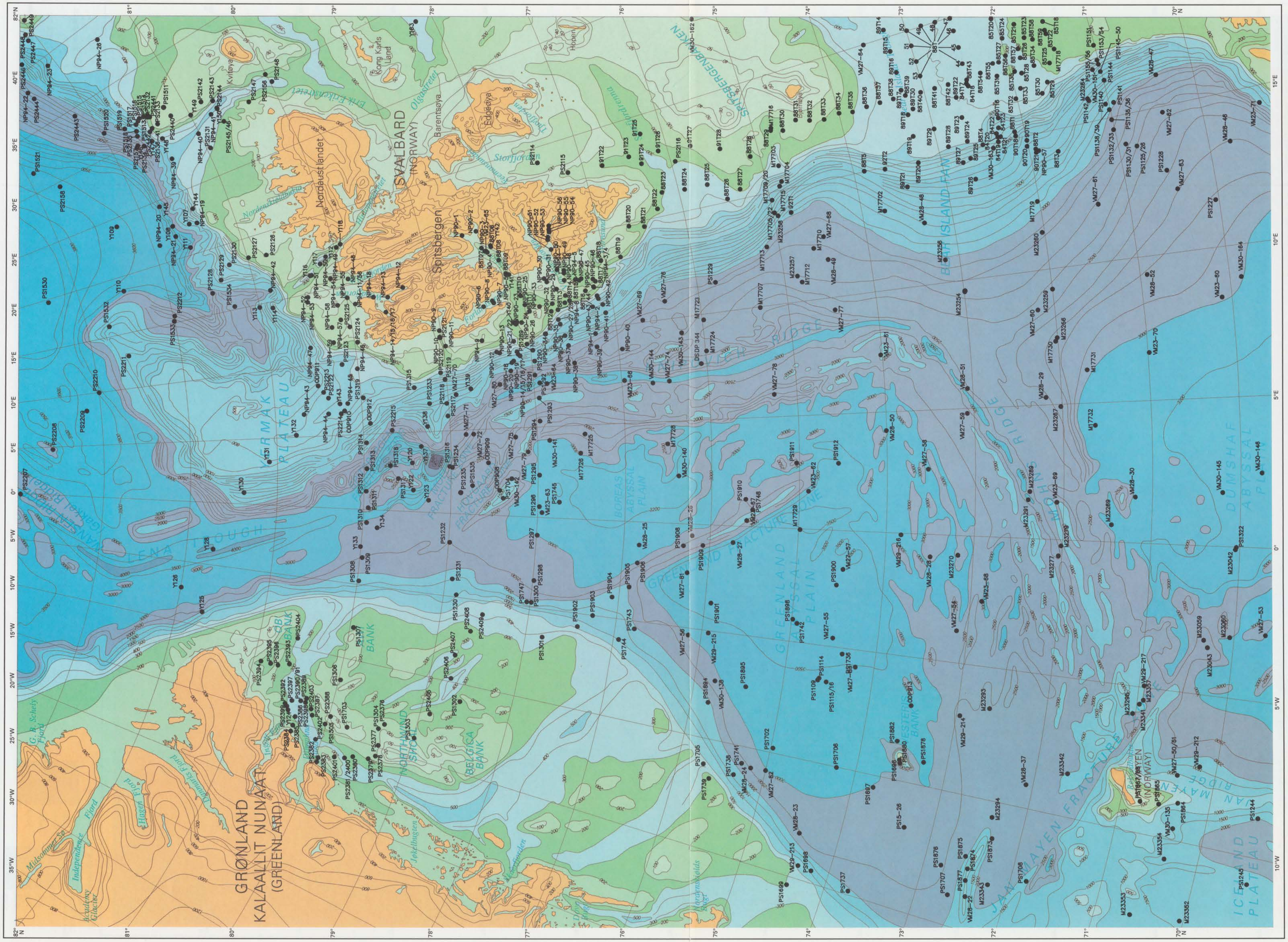

SEDIMENT CORE LOCATIONS IN THE NORTHERN NORWEGIAN - GREENLAND SEA

Compiled by H. Kassens, H. Grobe, S. L. Pfirman, R. Spielhagen and J. Thiede

Polar Stereographic Projection Scale 1: 3,000,000 at Latitude 71°N

1995

PS	Alfred-Wegener-Institute for Polar and Marine Research, Bremerhaven, Germany
M	Special Collaborative Program 313, University of Kiel, Germany
NP	Norwegian Polar Institute, Oslo, Norway
T	Institute for Biology and Geology, University of Tromsø, Norway
VM	Lamont Doherty Earth Observatory, U.S.A.
Y	Department of Geology, University of Stockholm, Sweden
DSDP	Deep Sea Drilling Project
ODP	Ocean Drilling Program

HYPSOMETRIC TINTS

Meters
Land Mass
Sea Level 0
100
200
300
500
1000
1000
2000
3000
4000
5000

PLATE 7

SEDIMENT CORE LOCATIONS IN THE NORTHERN NORWEGIAN-GREENLAND SEA

HEIDEMARIE KASSENS, HANNES GROBE, STEPHANIE PFIRMAN, ROBERT SPIELHAGEN AND JÖRN THIEDE

Core locations are compiled from data supplied by the Alfred Wegener Institut für Polar und Meeresforschung (AWI) in Bremerhaven, (Special Research Program 313), from GEOMAR, Forschungszentrum für Marine Geowissenschaften der Christian-Albrechts-Universität zu Kiel, from Christian-Albrects-Universität zu Kiel, from Norsk Polarinstitutt, from Institutt for biologi og geologi, Universitetet i Tromsø, and from Lamont-Doherty Earth Observatory of Columbia University in New York.

In addition, drill sites from the Deep Sea Drilling Project, Leg 38 (Talwani, Udintsev et al. 1976) and the Ocean Drilling Program, Leg 151 (ODP Leg 151 Shipboard Scientific Party 1994) are included.

A wide range of devices (such as box, gravity and piston cores) were used during these expeditions. The source institutions should be contacted about the cores and their contents.

(continued from page 24)

Map Characteristics

A glance at Plate 6 reveals the distribution of the stations of observed heat flow from which the contours are drawn. It is readily apparent that there is a paucity of data along the rise axis (which is expected due to the lack of sediment in the rift valley of the spreading center). The greatest density of data, adjacent to Svalbard, reveal three regions of elevated heat flow > 150 mW/m^2: the Knipovich Ridge, the entire Molloy and Spitsbergen Transform Region, and a parallel band of high heat flow atop the Yermak Plateau connecting with the Woodfjord volcanics on Svalbard.

Even though there is a paucity of bathymetric data along the northernmost Spitsbergen Transform, heat flow collected from the YMER icebreaker (Crane et al. 1982), reveal that there are most likely two pull-apart, short-segment spreading centers within the Spitsbergen Transform: the Molloy Ridge (already described in the above mentioned articles), and one trending NE reaching from the Spitsbergen Transform up to the Yermak Plateau. The thermal boundaries of the latter mid-transform "pull-apart basin" are poorly defined by only three heat flow values ranging from 212-442 mW/m^2.

Further south, high heat flow can be found along the Mohns Ridge in a linear shaped region trending perpendicular to the Mohns Ridge, NW towards Greenland and SE towards northern Norway. In addition, the Jan Mayen Transform Fault appears to be associated with high heat flow. The fact that transform faults in the northern Norwegian-Greenland Sea are "hot" rather than "cold" is in marked contrast to the theory that fracture zones are "heat sinks" that cut across oceanic crust. Certainly, tectonic evidence suggests that the evolution of the Norwegian-Greenland Sea is characterized by propagating ridges jumping or moving into preexisting fracture zones. The most recent example of this is the propagation of the Mohns Ridge into the ancient Spitsbergen Shear Zone forming the Knipovich Ridge in the process (Crane et al. 1991).

Figure 3 illustrates the true heat flow color scheme as a reference for Plate 6 which depicts crustal heat flow superimposed over bathymetry.

Acknowledgements

The authors would like to thank Terje Sundberg of Norsk Polarinstitutt for his assistance in digitizing and producing the final heat flow map.

II. SEAMARC II SURVEYS

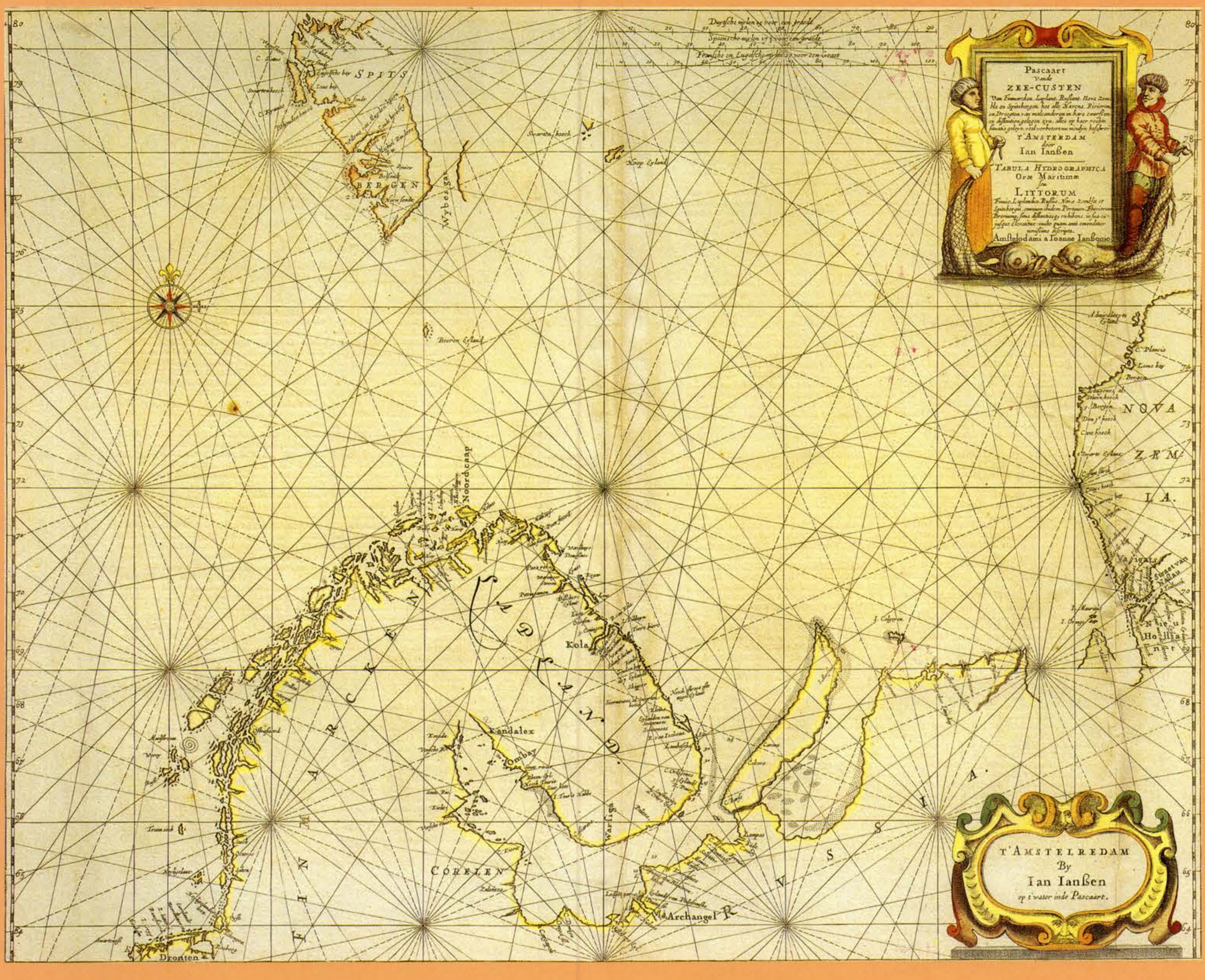

PLATES 8-64

SEAMARC II INVESTIGATIONS OF THE NORTHERN NORWEGIAN-GREENLAND SEA

KATHLEEN CRANE, PETER R.VOGT, EIRIK SUNDVOR, ALEXANDER SHOR AND THOMAS REED IV

The high latitude Norwegian-Greenland Sea is a natural laboratory to study the growth of a narrow, young ocean basin dominated by very slow opening across one of the world's longest fracture zones. Because of its proximity to the Arctic ice pack, this sea has remained relatively unexplored. It is a remote region that has been of great interest to the international scientific community because within it lies the only deep-water entrance into the Arctic Ocean (known as the Fram Strait). The strait was created by seafloor transtension across the lengthy Paleo-Spitsbergen Fracture Zone, which once was one of the longest shear zones on the surface of the Earth.

Fault-controlled passages between ocean basins influence the hydrography of the world ocean because their morphology and bathymetry control the exchange of water masses. The Fram Strait is one of the most important of these deep passages, because it plays a pivotal role in the Earth's recent ocean hydrography and paleo-environmental evolution (Gammelsrød & Rudels 1983). Heat exchange via transport of water and sea ice through this passage influences global climate and oceanography. However, this region is very complex, and nearly all geophysical parameters used to reconstruct seafloor geological history, are abnormal relative to the rest of the world ocean basins Chan & Mitchell (1985), Crane et al. (1982; 1988; 1991; 1992), Doss et al. (1991), Eldholm et al. (1984; 1990), Faleide & Gudlaugsson (1981), Feden et al. (1979), Gayer et al. (1966), Kellogg (1975), Myhre & Eldholm (1981; 1988), Myhre et al. (1982), Okay et al. (1991), Okay & Crane (1993), Okay (1994), Ostenso (1968), Phillips et al. (1982), Sundvor et al. (1975; 1977; 1978; 1979; 1982a,b; 1991), Sundvor & Eldholm (1976; 1979), Sundvor & Torp (1987), Vogt (1968; 1986), Vogt & Avery (1974), and Vogt et al. (1978; 1979; 1981; 1982; 1991a,b).

Therefore, deciphering when and at what ratė the Norwegian-Greenland Sea and the Fram Strait formed is a formidable task, but nonetheless it is a necessary goal if the paleoclimatic history is to be unraveled.

The complexity of the plate boundary in the Norwegian-Greenland Sea reflects the complex opening history in this area. Seafloor spreading in the Norwegian-Greenland Sea and the Arctic Ocean started at approximately 66-57 million years (Ma) before the present. The relative motion between Svalbard (Spitsbergen) and Greenland was approximately northeast-southwest from the Mohns Ridge, with no crustal extension in the northern Norwegian-Greenland Sea. The paleo-Spitsbergen Fracture Zone acted as the plate boundary between the incipient southern Norwegian-Greenland Sea and the Arctic Ocean linking the Mohns Ridge to the Nansen Ridge.

About 36 Ma the east-west component of opening increased allowing the mid-oceanic ridge to move northward into the Spitsbergen Fracture Zone. This started transtensional seafloor spreading in the northern Norwegian-Greenland Sea along the Knipovich Ridge. Heat flow data also confirm that spreading began earlier in the South than in the North. The rate of opening along the more northerly Knipovich Ridge is even slower. By using heat flow data, it has been estimated that the North American Plate in this region is growing 1.5 times faster than the Eurasian Plate

Analysis of heat flow data suggests that the Knipovich Ridge propagated northward at a rate of 1 degree per 10 Ma commencing at 60 Ma at a latitude of 75°N. Evidence for further northward rift propagation exists on the northerly Yermak Plateau adjacent to Svalbard. Additional heat flow data suggest that faults along the plateau (which were a part of the more extensive and ancient Spitsbergen Fracture Zone system) are serving as present-day channels through which heat from a subjacent body of magma escapes to the seafloor.

SeaMARC II Survey

To resolve the evolution of the northern Norwegian-Greenland Sea, two SeaMARC II side-looking sonar and bathymetric swath-mapping expeditions aboard the Norwegian ship *Håkon Mosby* took place in the fall of 1989 and 1990. The SeaMARC II system (operated out of the Hawaii Institute of Geophysics) is a shallow-tow vehicle (50-100 m) with port-starboard coverage and a tow-speed capability of up to 10 knots. It operates at frequencies of 11 and 12 kHz with short transmission pulses. The qualitative backscattering measurements from the imagery are useful for determination of bottom slope and texture and large-scale regional trends.

The program, a cooperative effort involving the University of Bergen, Norway, the US Naval Research Laboratory, the Lamont-Doherty Earth Observatory, Hunter College of CUNY, Scripps Institution of Oceanography, and the Hawaii Institute of Geophysics investigated the Knipovich Ridge, Molloy Ridge, Molloy Transform Fault, southwestern Yermak Plateau, the northern Svalbard margin, and the Svalbard-Barents Sea continental margin.

Navigation was by transit, Global Positioning System satellites and range-range mode Loran C. Sea ice placed a northern limit of 80°05'N on the first expedition and 82°N on the second expedition. Nevertheless, the shipboard teams collected 11,000 line-kilometers of geophysical data, including SeaMARC II sidescan and bathymetry, 3.5 kHz bathymetry, gravity and magnetics. In addition, high-resolution 38 kHz single-beam bathymetry was obtained at water depths less than 2,500 m. About 80,000 km^2 of the seafloor was mapped by side-looking sonar and roughly half that area was bathymetrically swath-mapped.

Processing the SeaMARC II Data

The usefulness of synoptic seafloor surveys has been limited in the past by the minimal extent to which the user can interact with the resulting survey data. Paper collage mosaics, while qualitatively spectacular at times, require significant manual effort, are fragile, limited in navigational accuracy and data dynamic range, and provide little in the way of quantitative information. Of late, significant efforts have been made to quantify both the physical products and the interpretations derived from these surveys.

In order to improve the noisy SeaMARC II bathymetric data and to geometrically correct the degraded images by warping them to the smoothed SeaMARC II bathymetric surface, the following processing scheme was recently adopted by K. Crane and T. Reed (Reed et al. 1992):

1. The bathymetric data were edited, filtered to produce a smooth bathymetric surface, and corrected within the bounds of previous contour data.

2. The sidescan image pixels were co-registered with the bathymetry on the basis of known pixel slant range. This procedure

removes both the distortion caused by bottom tracking errors and the layover distortion resulting from violation of the flat-bottom assumption. Like most sidescan sonar systems, SeaMARC II applies a slant range correction based upon the assumption that the depth across track is constant and equal to that detected at nadir for each ping. This 'flat-bottom' assumption will create a geometrically correct image provided that the bottom is flat athwartships, and the nadir depth detection is correct. In the Norwegian-Greenland Sea survey, the cross-track depth variations, often in excess of 2-3 km, severely violate the flat-bottom assumption. This is most noticeable in the Molloy Ridge rift valley.

The completed mosaics, corrected for depth variations, are presented in the atlas as regional maps representing merged bathymetry and side-looking sonar imagery (Plates 8-11), as 3-D low angle oblique views of the seafloor (Plates 12-13), and as 49 tiles (Plates 15-63). Each tile is comprised of two parts: a) the side-looking sonar backscatter information and b) the merged bathymetry and side-looking sonar data. These tiles are the basis for the following interpretation of geological features on the seafloor.

Sedimentary Processes

Volcanic/tectonic features and their modification by mass wasting dominate the active plate boundary (Plate 64). However, much of the seafloor adjacent to and at times including the northernmost tip of the Knipovich Ridge, is covered by thick layers of continentally derived sediment. Notable sedimentary fea-tures include pockmarks, iceberg plow marks, channels, gullies, slumps and bottom current effects (Vogt et al. 1991a, b, 1993, 1994a, b, c; Cherkis et al. 1992; Okay 1994).

Roughly 100 pockmarks were imaged, scattered across thickly sedimented parts of the area (Tile 16, Plate 30). The pockmarks appear as small dark speckles, barely resolvable in the side-looking sonar images and unresolvable in the swath bathymetry. At least half of the pockmarks occur in a narrow crestal belt along Vestnesa Ridge, a 1,300 - 1,500 m deep spur extending from the west Svalbard margin almost to the Molloy Ridge. Where crossed by single-channel echosounders, the pockmarks are bathymetric dimples around 100-200 m across and 10 m deep. The features are thought to have been derived by methane venting from a shallow clathrate (solid, ice-like gas hydrates) layer as also described by Solheim & Elverhøi (1993) from the Barents Sea. High heat flow from the nearby volcanically active spreading center could cause the transformation from the frozen to the gaseous phase. Gas trapped below the clathrate would migrate up and collect under the Vestnesa "anticline" escaping through available cracks and faults.

A reconnaissance made across the southwest Yermak Plateau revealed unambiguous iceberg plow marks to depths of 600 m (Vogt et al. 1994a) (Tiles 7, 15; Plates 21,29). Broader, more subtle lineations extend to 900 m; deep even for large Pleistocene icebergs. The depression between the Yermak Plateau and the Vestnesa Ridge is occupied by a narrow, isolated channel extending from the Kongsfjord continental margin to the Molloy Ridge axial valley (Tile 16; Plate 30).

One track from Svalbard along the 1,000 m contour south to the Bear Island Fan reveals the absence of large canyons along the western Svalbard margin (79°N - 75°N) (Tiles 29, 30, 31; Plates 43, 44, 45), but canyons are prominent on the steep margin between 74°15'N and 74°30'N (west of Bear Island) (Tile 33; Plate 47), with channels of lesser relief occurring intermittently from there southward. Three east-west transects down the Bear Island Fan suggest that the fan comprises long (more than one hundred kilometers), complex fingers 5-10 km wide and incised by channels (Tiles 36-39; Plates 50-53). See also Laberg & Vorren (1995, Plate 76) for a description of the Bear Island Fan.

Adjacent to the Norwegian margin, the seafloor is subjected to constant mass wasting. Large erosion channels and debris fields mark the imagery. Only a few slump scars were imaged, one at 74°55'N, 15°E and several on steep, thickly sedimented slopes in the Molloy Ridge/Transform area. Features that have possibly been generated by bottom currents appear in the side-looking sonar near the Molloy Transform. However, their proximity to this active fault means that a tectonic origin cannot be ruled out.

Volcanic/Tectonic Features

The SeaMARC II imaged the accreting Mohns and Knipovich Ridges, the Molloy Transform Fault, and the Molloy Ridge. Diagonal contiguous sidescan swaths mapped the outcropping rift mountain and ridge flank basement topography along the northern Knipovich Ridge. The rift valleys are characterized by scallop-shaped faults, which mark their boundaries, which from north to south are tiles 17, 18, 19, 20, 12, 13, 14, 37, 38, 40 (Plates 31, 32, 33, 26, 27, 28, 51, 52, 54). Within the rift valley, faults and fissures trend obliquely to the more regional rift valley trend. Young lava flows occur at 74°35'N 75°30'N 76°05'N and 76°50'N (approximately 65-100 km apart). Oval-shaped basement highs that have been emplaced on the flanks of the rift are aligned parallel to the trend of the Molloy Transform Fault. These may either be remnant slices of continental crust or may be once-active volcanic centers that were rafted off the spreading center with plate motion. Further geophysical investigation is needed to clarify their origin.

Off-axial faults are not parallel to the overall trend of the spreading center. Instead, the farther north the fault, the closer its position to the axis of spreading. Conjugate pairs of flanking faults make a V-shaped pattern about the rise axis, with the point of the V intersecting with the Molloy Transform Fault.

The neotectonic expression of the Molloy Transform Fault is dramatic because sediments have everywhere buried older basement topography. Two parallel transcurrent fault traces make up the transform itself, but a broader belt of deformed lineations striking 30-45 degrees with respect to the transform trend extends up to 10-30 km southwest from the transform axis. These structures curve gradually into the northern Knipovich Ridge (Tiles 16, 17, 18; Plates 30, 31, 32). The Molloy Ridge, a pull-apart basin within the Spitsbergen Fracture Zone, has little conspicuous neovolcanic expression, as its dramatic relief (1,500-5,500 m) is dominated by mass wasting (Tiles 16, 22, 23; Plates 30, 36, 37).

The topographic and bathymetric maps produced by the SeaMARC II system provide additional evidence that the Knipovich Ridge is propagating northward. If this model is correct for the opening of the Norwegian-Greenland Sea, and if the analysis of the heat flow data is reasonable, then it can be suggested that the Fram Strait began to separate approximately 40 Ma, allowing exchange of water masses between the Arctic and the Atlantic oceans. Propagation of the ridge suggests that faulting and volcanic activity will continue to occur with greater magnitude on and north of Svalbard for millions of years to come.

Acknowledgements

The authors would like to thank the crew of *Håkon Mosby* of the University of Bergen for their important contributions to the success of this project. Without their astute seamanship, imagery as far north as 82°N would never have been collected. The authors would also like to thank the Naval Research Laboratory, the Office of Naval Research, and the University of Bergen for funding support, the Hawaii Institute of Geophysics for supplying computational and staff support for the processing of the data and the subsequent production of these SeaMARC II images. In particular, we would like to thank Bruce Appelgate, Clyde Nishamura, and Karen Sender, who greatly facilitated the map production. We also gratefully acknowledge the other individuals who assisted in the data collection efforts: Chris Jones, Christian deMoustier, Hany Doss, Nilgün Okay, Mark Rognstad, Joel Erickson, Dan Chayes, Gail Yamada, Steve Dang, Dan Johnson and Doug Bergerson.

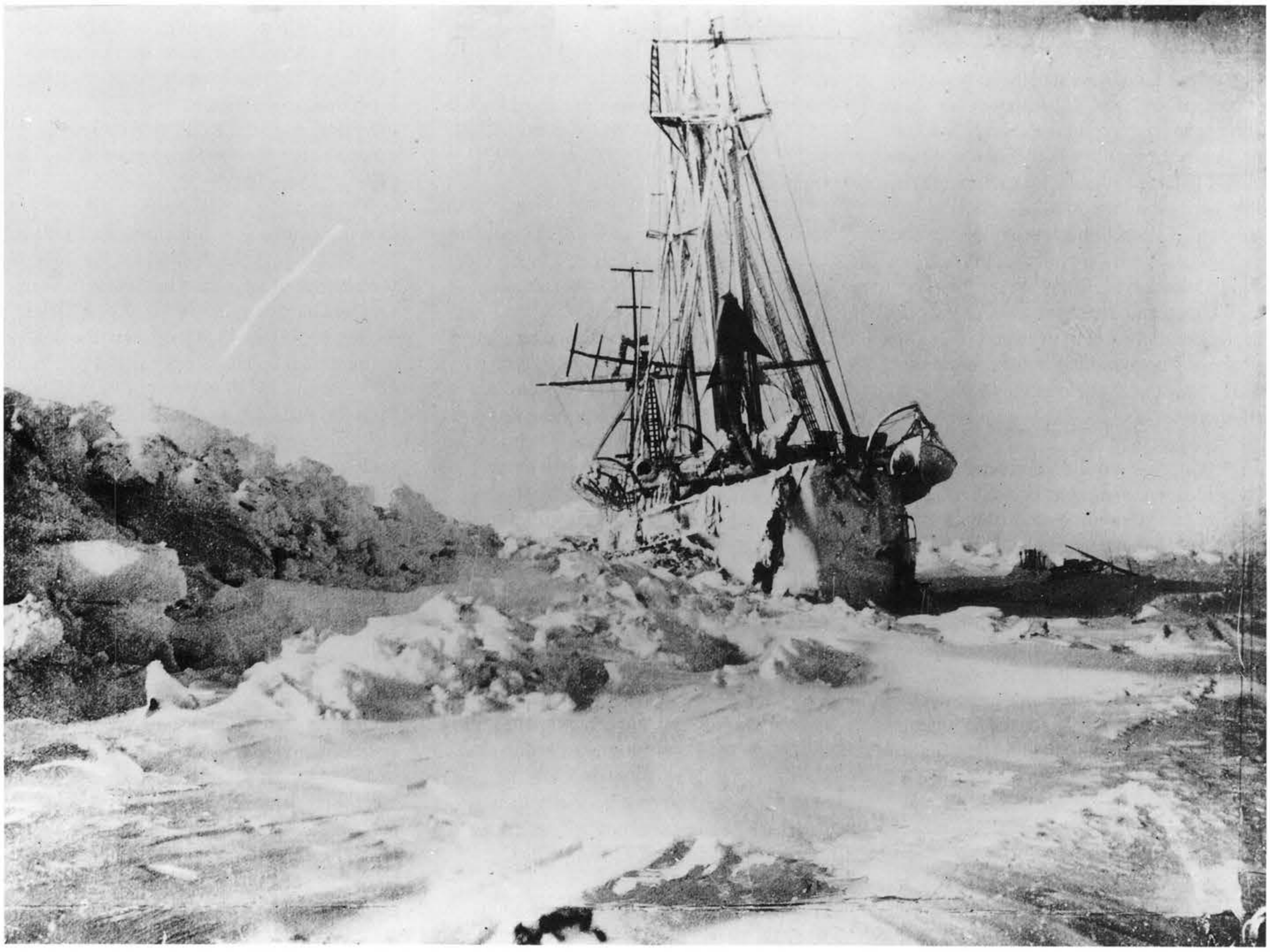

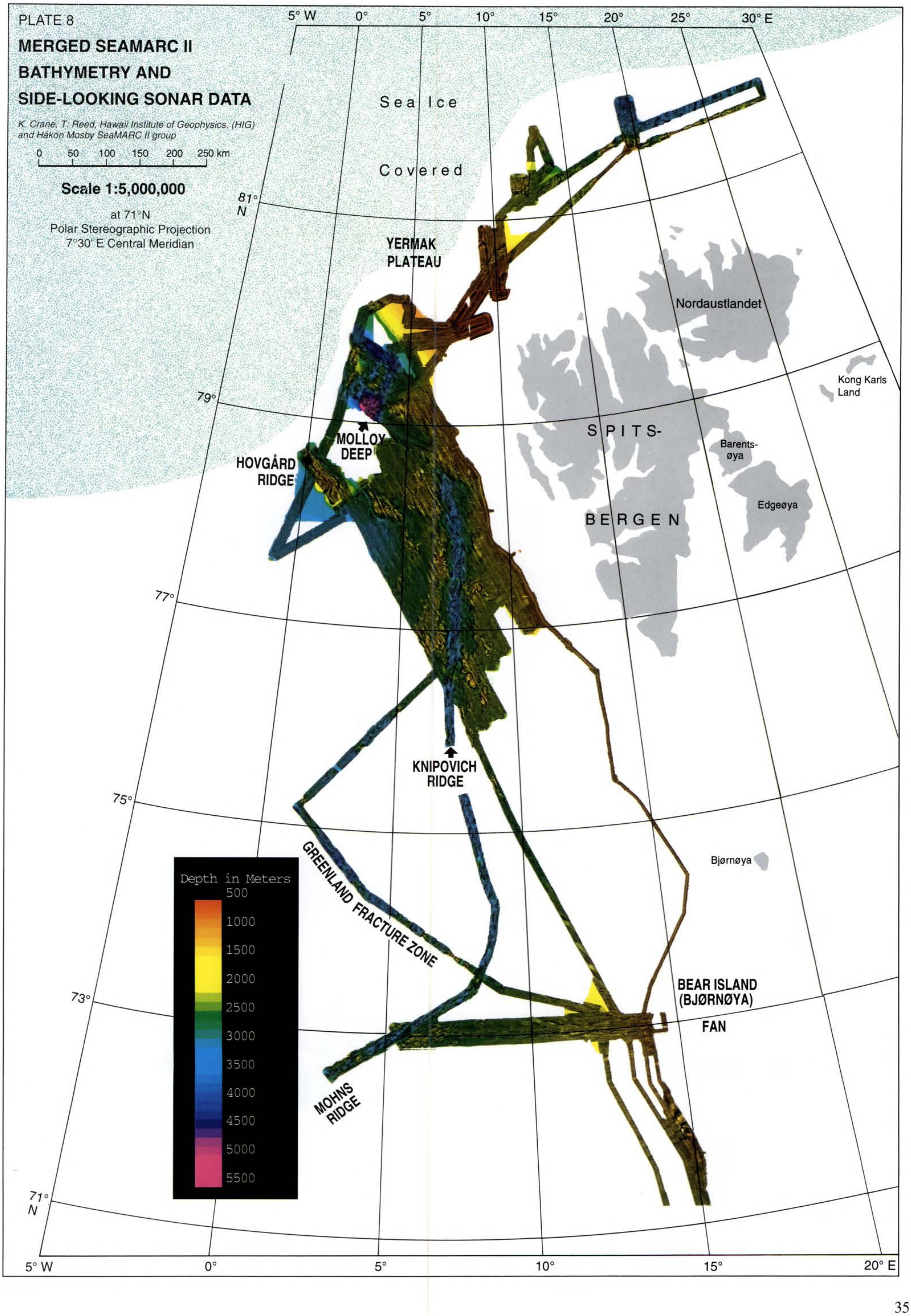

PLATE 8
MERGED SEAMARC II BATHYMETRY AND SIDE-LOOKING SONAR DATA
K. Crane, T. Reed, Hawaii Institute of Geophysics, (HIG) and Håkon Mosby SeaMARC II group
0 50 100 150 200 250 km
Scale 1:5,000,000
at 71°N
Polar Stereographic Projection
7°30' E Central Meridian
Sea Ice
Covered
YERMAK PLATEAU
Nordaustlandet
Kong Karls Land
MOLLOY DEEP
HOVGÅRD RIDGE
SPITS-
BERGEN
Barents-øya
Edgeøya
KNIPOVICH RIDGE
GREENLAND FRACTURE ZONE
Bjørnøya
BEAR ISLAND (BJØRNØYA)
FAN
MOHNS RIDGE
Depth in Meters
500
1000
1500
2000
2500
3000
3500
4000
4500
5000
5500
5° W 0° 5° 10° 15° 20° 25° 30° E
81° N
79°
77°
75°
73°
71° N
5° W 0° 5° 10° 15° 20° E

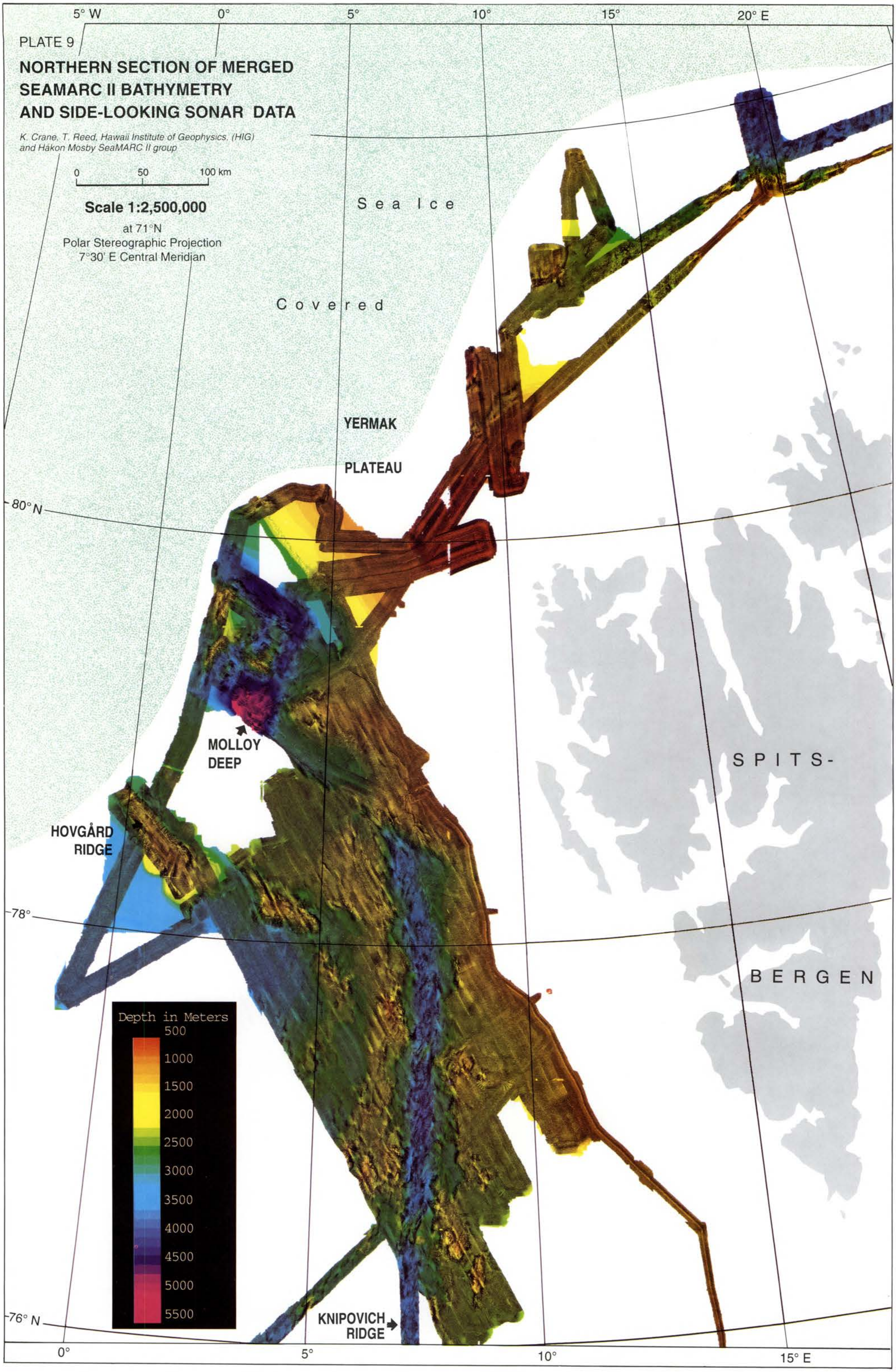
PLATE 9
NORTHERN SECTION OF MERGED SEAMARC II BATHYMETRY AND SIDE-LOOKING SONAR DATA
K. Crane, T. Reed, Hawaii Institute of Geophysics, (HIG) and Håkon Mosby SeaMARC II group
0
50
100 km
Scale 1:2,500,000
at 71°N
Polar Stereographic Projection
7°30' E Central Meridian
5° W
0°
5°
10°
15°
20° E
Sea Ice
Covered
YERMAK
PLATEAU
80° N
78°
76° N
MOLLOY
DEEP
HOVGÅRD
RIDGE
KNIPOVICH
RIDGE
SPITS-
BERGEN
Depth in Meters
500
1000
1500
2000
2500
3000
3500
4000
4500
5000
5500
0°
5°
10°
15° E

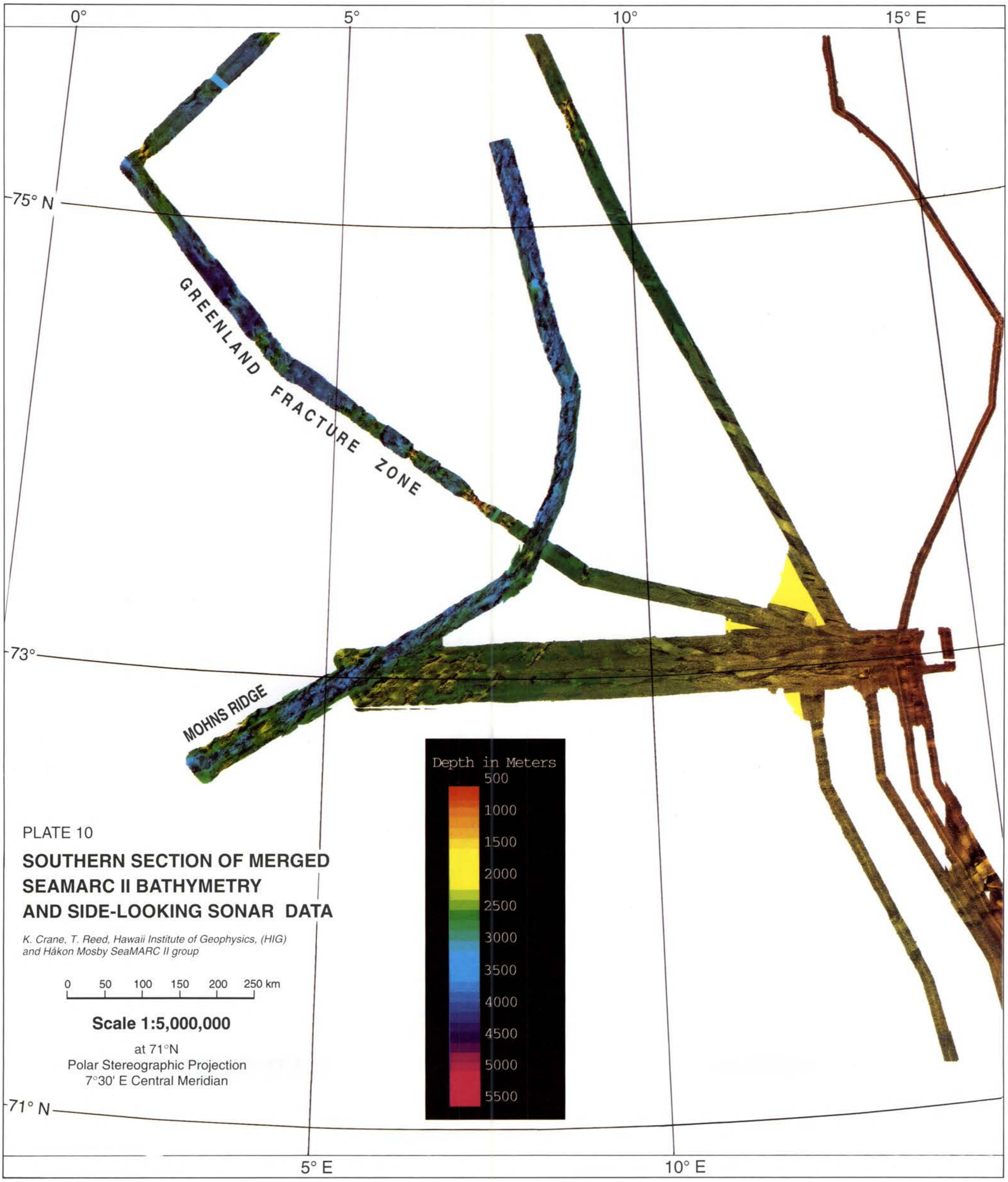

0°
5°
10°
15° E
75° N
73°
71° N
5° E
10° E
GREENLAND FRACTURE ZONE
MOHNS RIDGE
Depth in Meters
500
1000
1500
2000
2500
3000
3500
4000
4500
5000
5500
PLATE 10
SOUTHERN SECTION OF MERGED SEAMARC II BATHYMETRY AND SIDE-LOOKING SONAR DATA
K. Crane, T. Reed, Hawaii Institute of Geophysics, (HIG) and Håkon Mosby SeaMARC II group
0 50 100 150 200 250 km
Scale 1:5,000,000
at 71°N
Polar Stereographic Projection
7°30' E Central Meridian

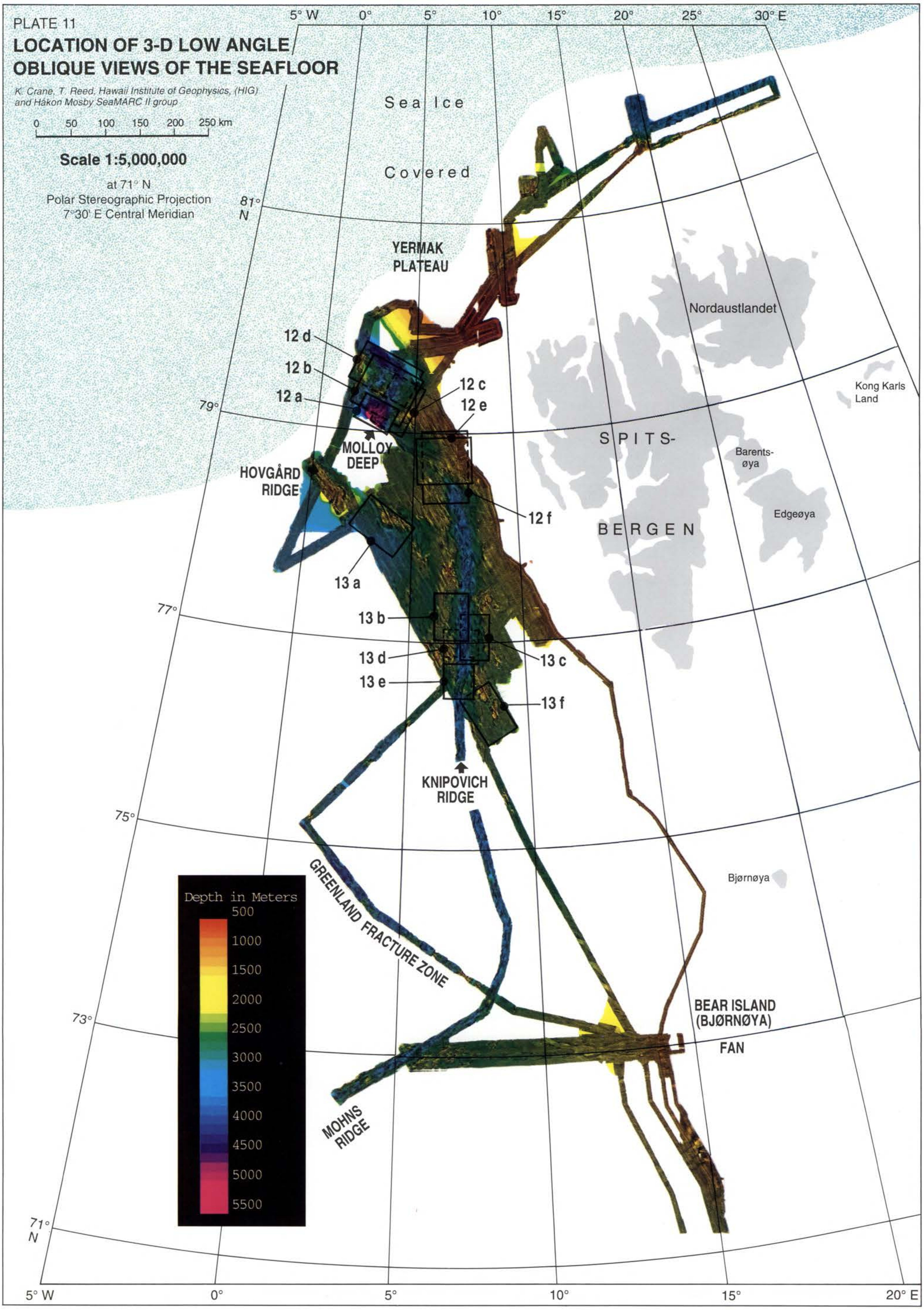
PLATE 11
LOCATION OF 3-D LOW ANGLE OBLIQUE VIEWS OF THE SEAFLOOR
K. Crane, T. Reed, Hawaii Institute of Geophysics, (HIG) and Håkon Mosby SeaMARC II group
0 50 100 150 200 250 km
Scale 1:5,000,000
at 71° N
Polar Stereographic Projection
7°30' E Central Meridian
Sea Ice Covered
YERMAK PLATEAU
Nordaustlandet
Kong Karls Land
SPITS-BERGEN
Barents-øya
Edgeøya
12 a
12 b
12 c
12 d
12 e
12 f
MOLLOY DEEP
HOVGÅRD RIDGE
13 a
13 b
13 c
13 d
13 e
13 f
KNIPOVICH RIDGE
GREENLAND FRACTURE ZONE
Bjørnøya
BEAR ISLAND (BJØRNØYA) FAN
MOHNS RIDGE
Depth in Meters
500
1000
1500
2000
2500
3000
3500
4000
4500
5000
5500
5° W
0°
5°
10°
15°
20°
25°
30° E
81° N
79°
77°
75°
73°
71° N
5° W
0°
5°
10°
15°
20° E

PLATE 12

3-D LOW ANGLE OBLIQUE VIEWS OF THE SEAFLOOR (Locations in Plate 11)

*K. Crane, T. Reed, Hawaii Institute of Geophysics, (HIG)
and Håkon Mosby SeaMARC II group*

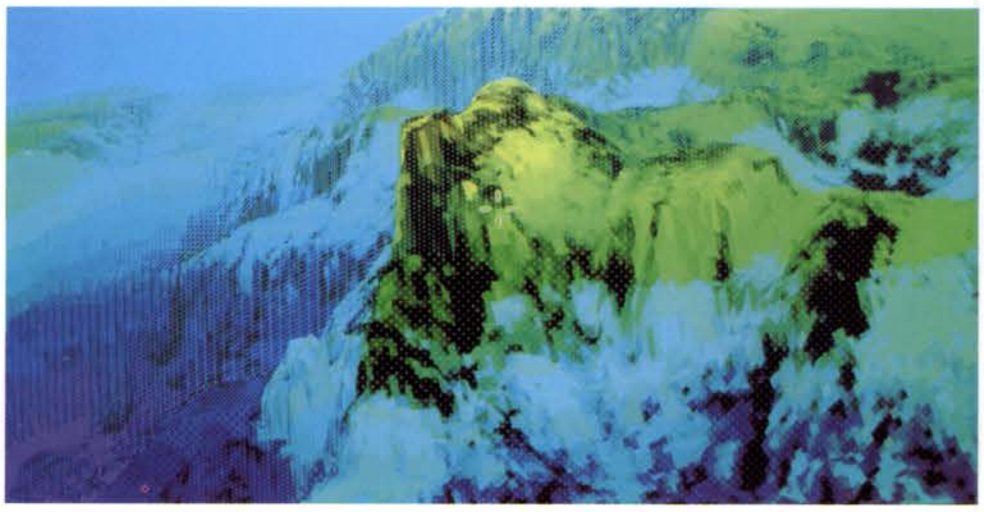

12 a
Low angle oblique view from Vestnesa westwards towards the Molloy Ridge (center), the Molloy Deep (left) and the Molloy Ridge rift valley (front). Colors represent depth in meters (see color bar on plate 11).

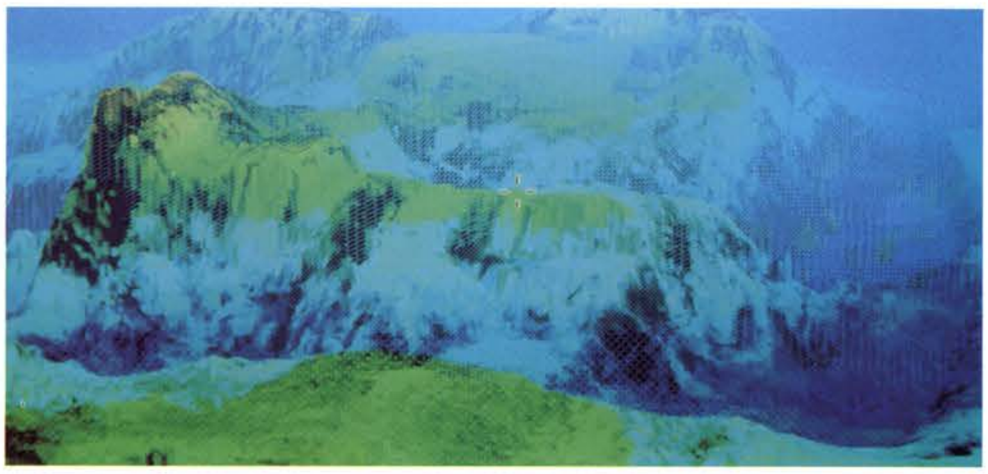

12 b
Low angle oblique view looking westwards towards the Molloy Ridge (left), the Molloy Ridge rift valley (from left to right near foreground) and the Spitsbergen Transform Fault (right).

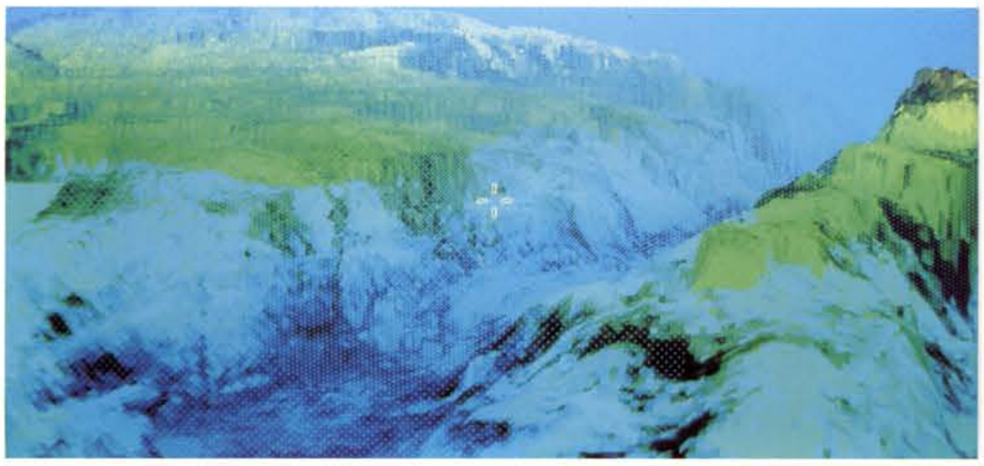

12 c
Low angle oblique view looking south by southeast down the Molloy Ridge rift valley. Molloy Ridge on right (background) and Vestnesa (Svalbard continental margin) on left.

12 d
Low angle oblique, north-northwesterly view of the Molloy Ridge rift valley (foreground) and the Spitsbergen Transform Fault (background).

12 e
Low angle oblique, west, northwesterly view of the northern tip of the Knipovich Ridge (foreground) where it intersects the Molloy Transform Fault (background, center). Note faults on the Svalbard continental margin (right). These may represent the early stages of rift propagation northwards.

12 f
Southerly, low angle oblique view of the Knipovich Ridge and the Molloy Transform Fault intersection. The Molloy Transform Fault is in the foreground, the Knipovich Ridge rift valley occupies the center, and remanent transform faults are located between the active Molly Transform Fault and the more southerly Hovgård Ridge.

PLATE 13

3-D LOW ANGLE OBLIQUE VIEWS OF THE SEAFLOOR (Locations in Plate 11)

*K. Crane, T. Reed, Hawaii Institute of Geophysics, (HIG)
and Håkon Mosby SeaMARC II group*

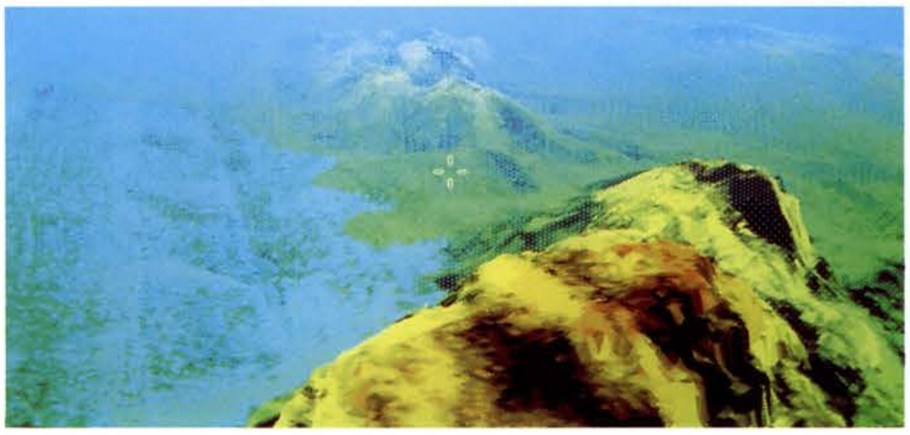

13 a
Southwesterly, low angle oblique view of the Hovgård chain of seamounts on the western flank of the Knipovich Ridge.

13b
Low angle oblique view of the western flank of the Knipovich Ridge looking northwards and centered at 77° 20' N. Western rift mountains in center and Knipovich rift valley on right.

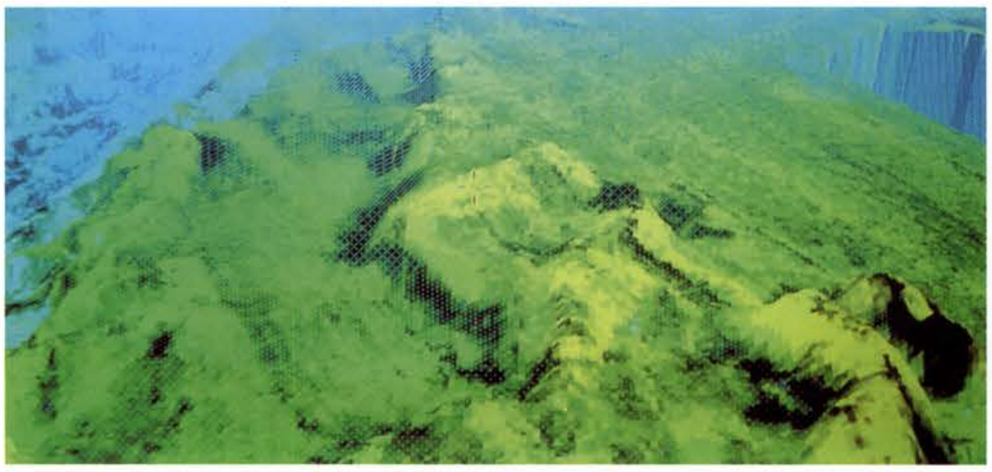

13 c
Low angle oblique view of the eastern flank of the Knipovich Ridge looking northwards and centered at 77° 05' N. Eastern rift mountains in center and Knipovich Ridge rift valley on left.

13 d
Low angle oblique view of the Knipovich Ridge rift valley looking southwards centered at 77° N. Note the dark, highly reflective seafloor in the center of the rift valley. This is interpreted to be a fresh lava flow.

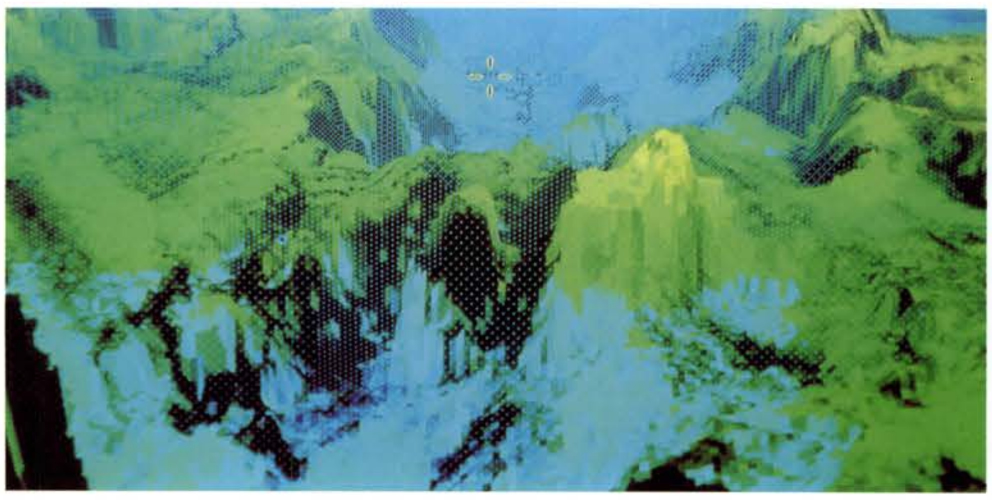

13 e
Low angle oblique view of the Knipovich Ridge rift valley looking northwards, centered at 76° 40' N. The shallow axial valley high is bound by faults which cut obliquely across the rift valley. This is typical for many of the Knipovich Ridge rift valley central highs. Suggesting that their origins are not strictly volcanic.

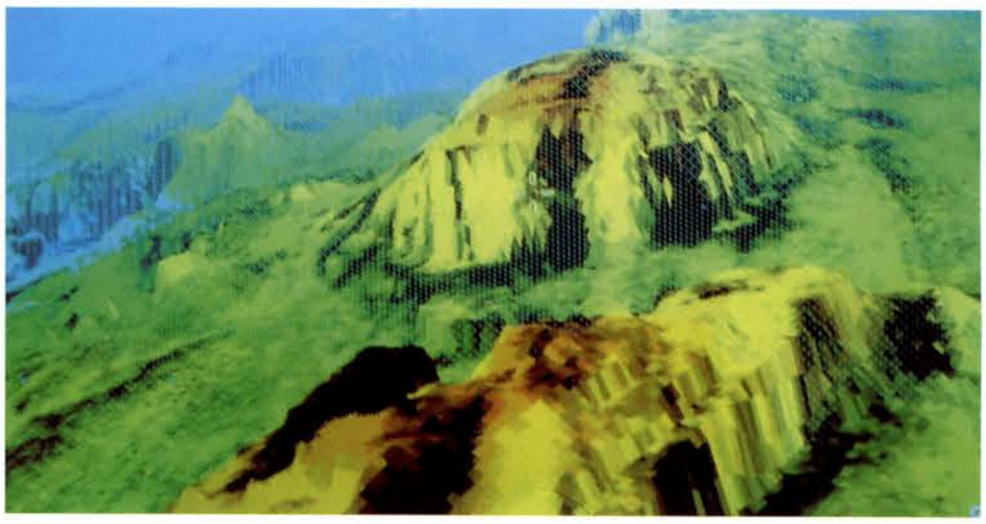

13 f
Low angle oblique, northwesterly view of a chain of off-axial seamounts on the eastern flank of the Knipovich Ridge centered at 76° 20' N and 8° E.

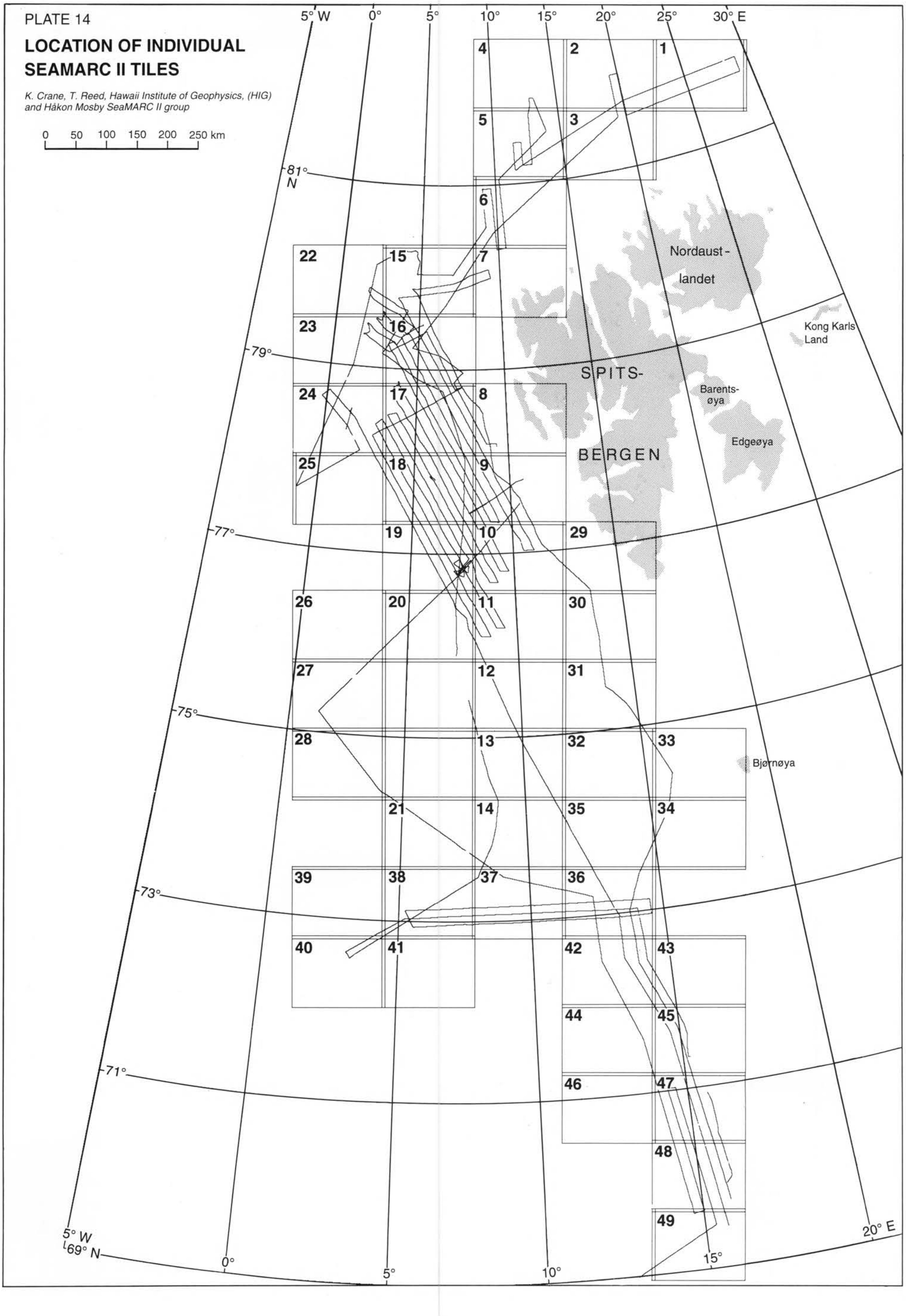

PLATE 14
LOCATION OF INDIVIDUAL SEAMARC II TILES
K. Crane, T. Reed, Hawaii Institute of Geophysics, (HIG) and Håkon Mosby SeaMARC II group
0 50 100 150 200 250 km
5° W
0°
5°
10°
15°
20°
25°
30° E
81° N
79°
77°
75°
73°
71°
5° W
69° N
0°
5°
10°
15°
20° E
Nordaust-landet
Kong Karls Land
SPITS-BERGEN
Barents-øya
Edgeøya
Bjørnøya
1
2
3
4
5
6
7
8
9
10
11
12
13
14
15
16
17
18
19
20
21
22
23
24
25
26
27
28
29
30
31
32
33
34
35
36
37
38
39
40
41
42
43
44
45
46
47
48
49

PLATE 15A

TILE 1A: SEAMARC II SIDE-LOOKING SONAR DATA

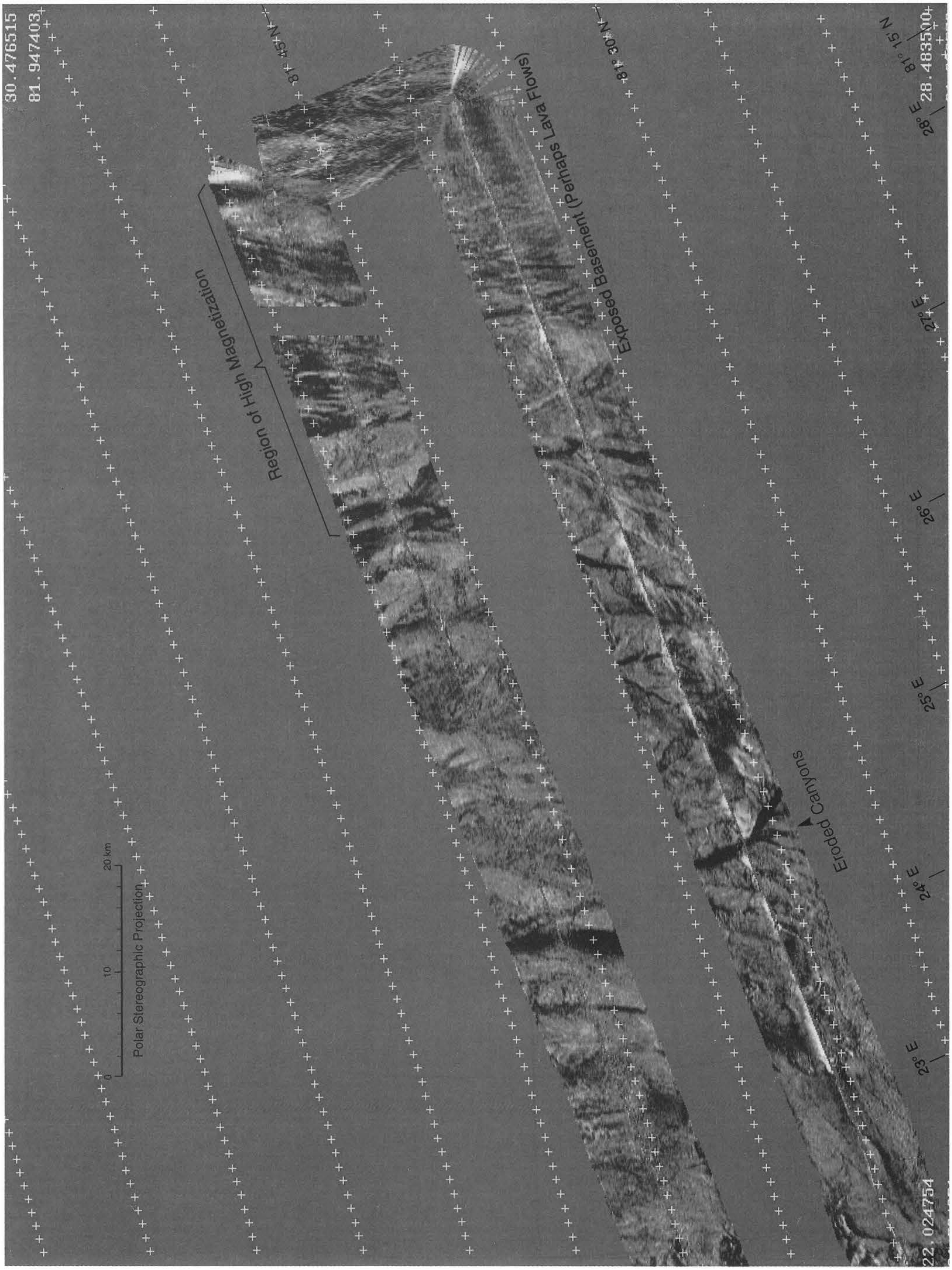

TILE 1B: SEAMARC II MERGED BATHYMETRIC AND SIDE-LOOKING SONAR DATA

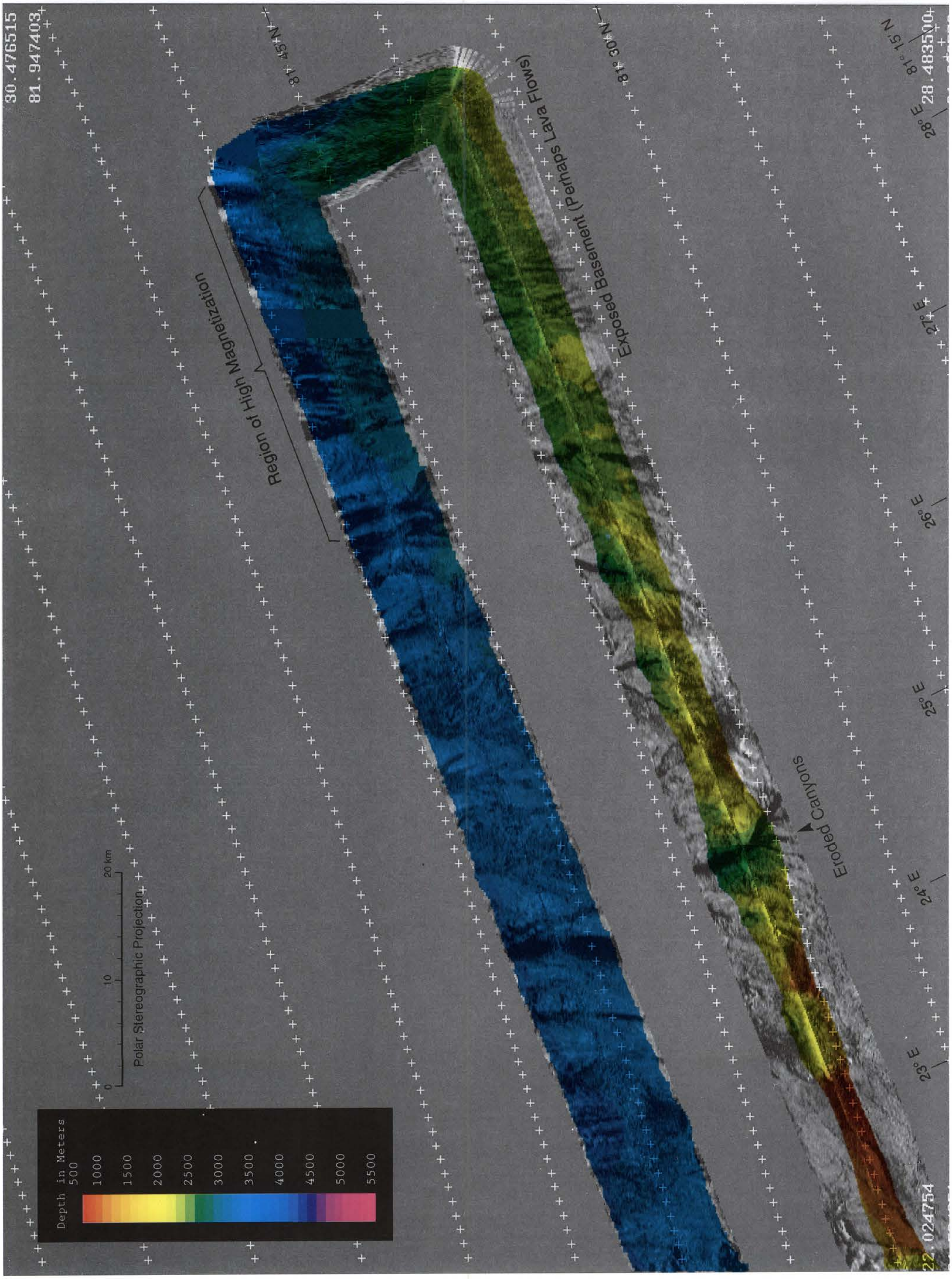

TILE 2A: SEAMARC II SIDE-LOOKING SONAR DATA

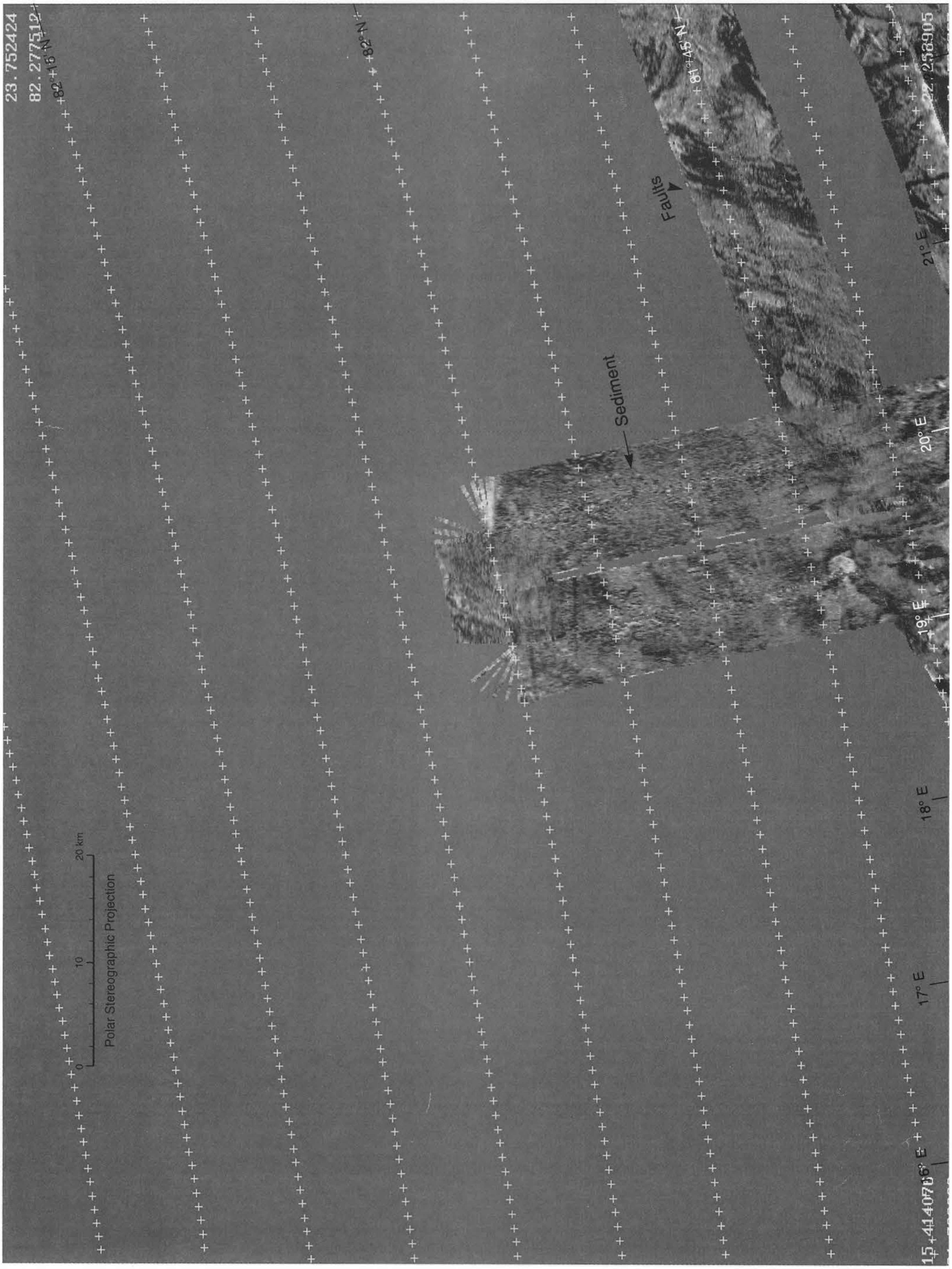

PLATE 16B TILE 2B: SEAMARC II MERGED BATHYMETRIC AND SIDE-LOOKING SONAR DATA

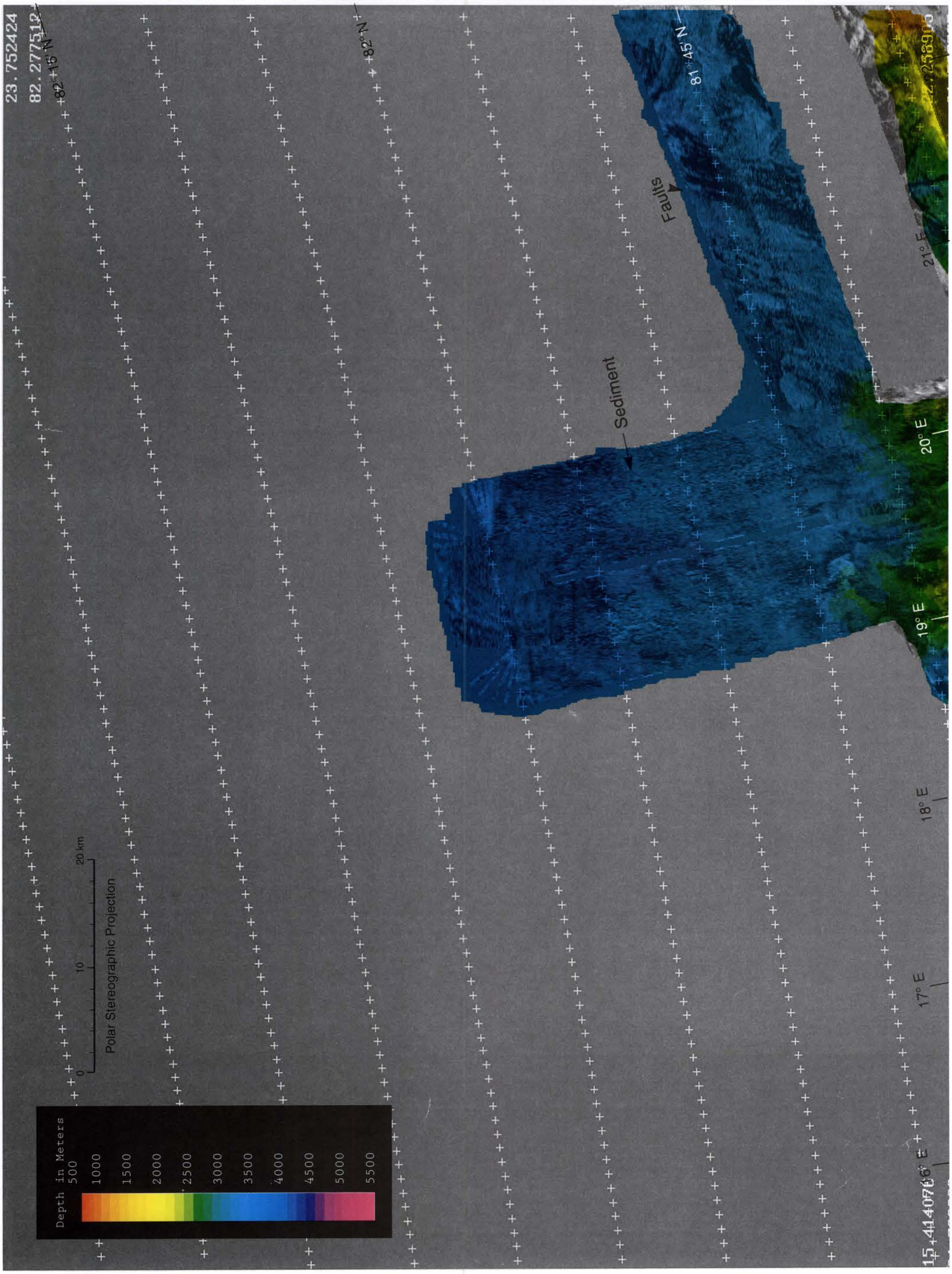

TILE 3A: SEAMARC II SIDE-LOOKING SONAR DATA

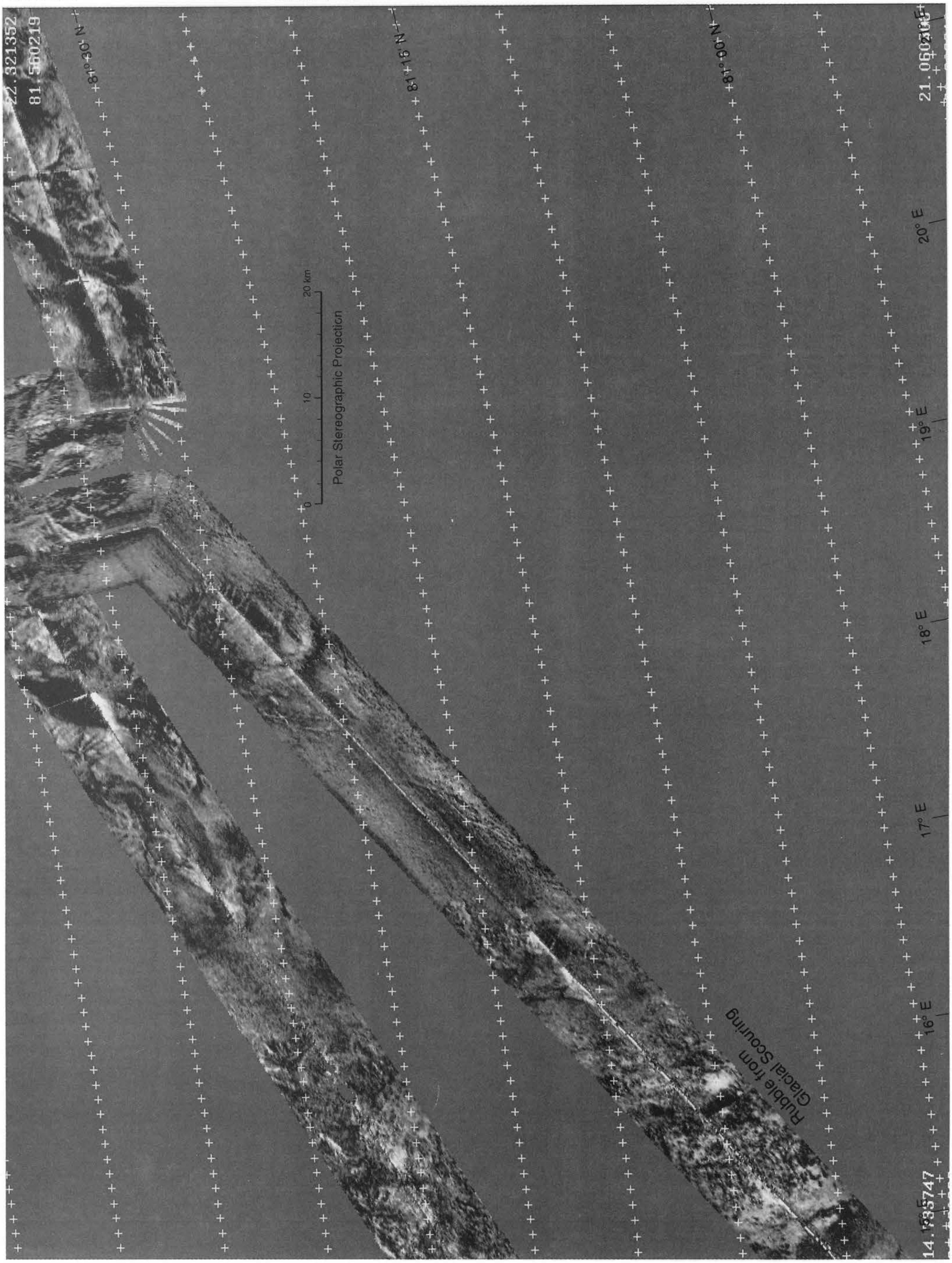

PLATE 17B TILE 3B: SEAMARC II MERGED BATHYMETRIC AND SIDE-LOOKING SONAR DATA

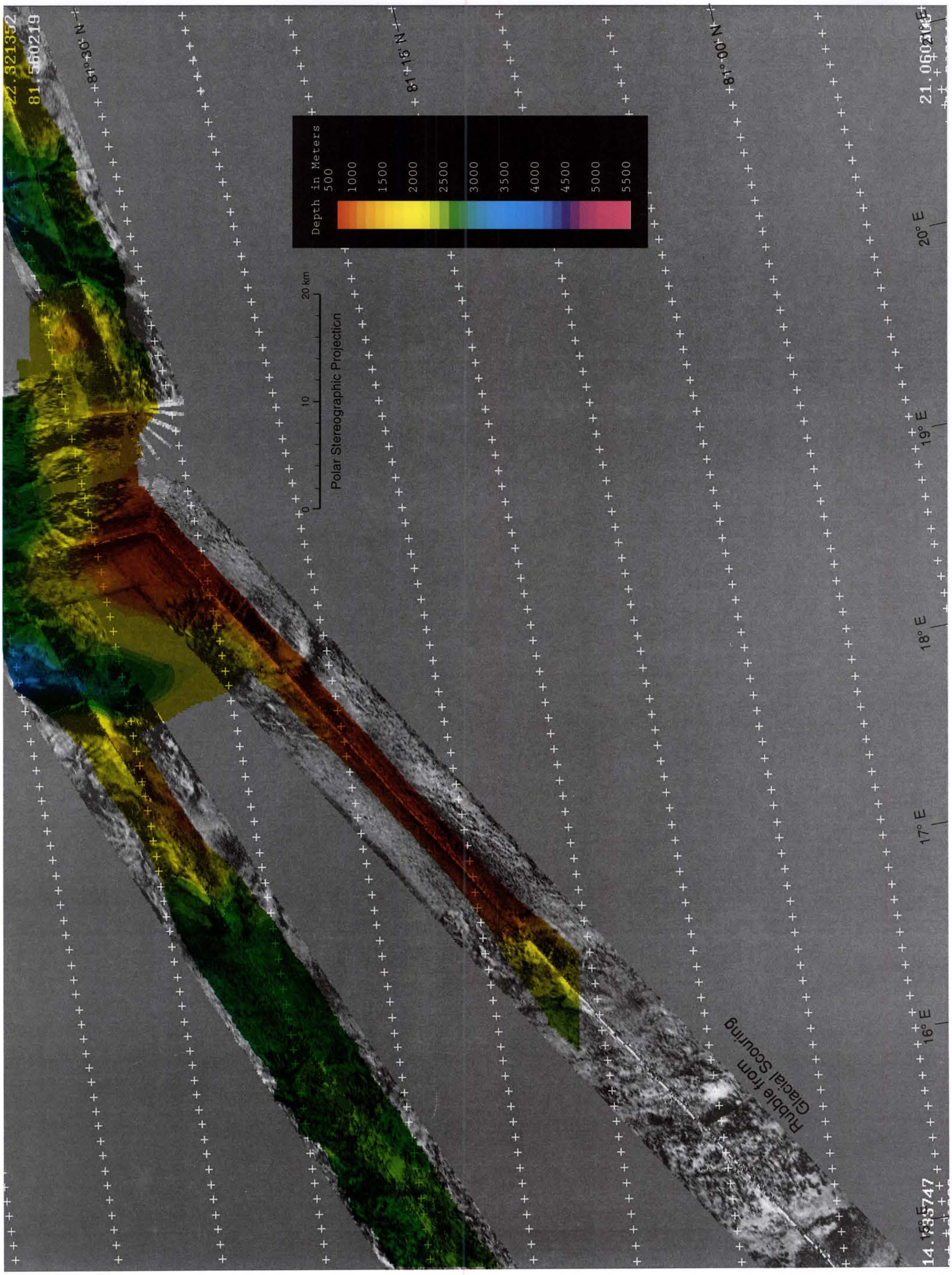

TILE 4A: SEAMARC II SIDE-LOOKING SONAR DATA

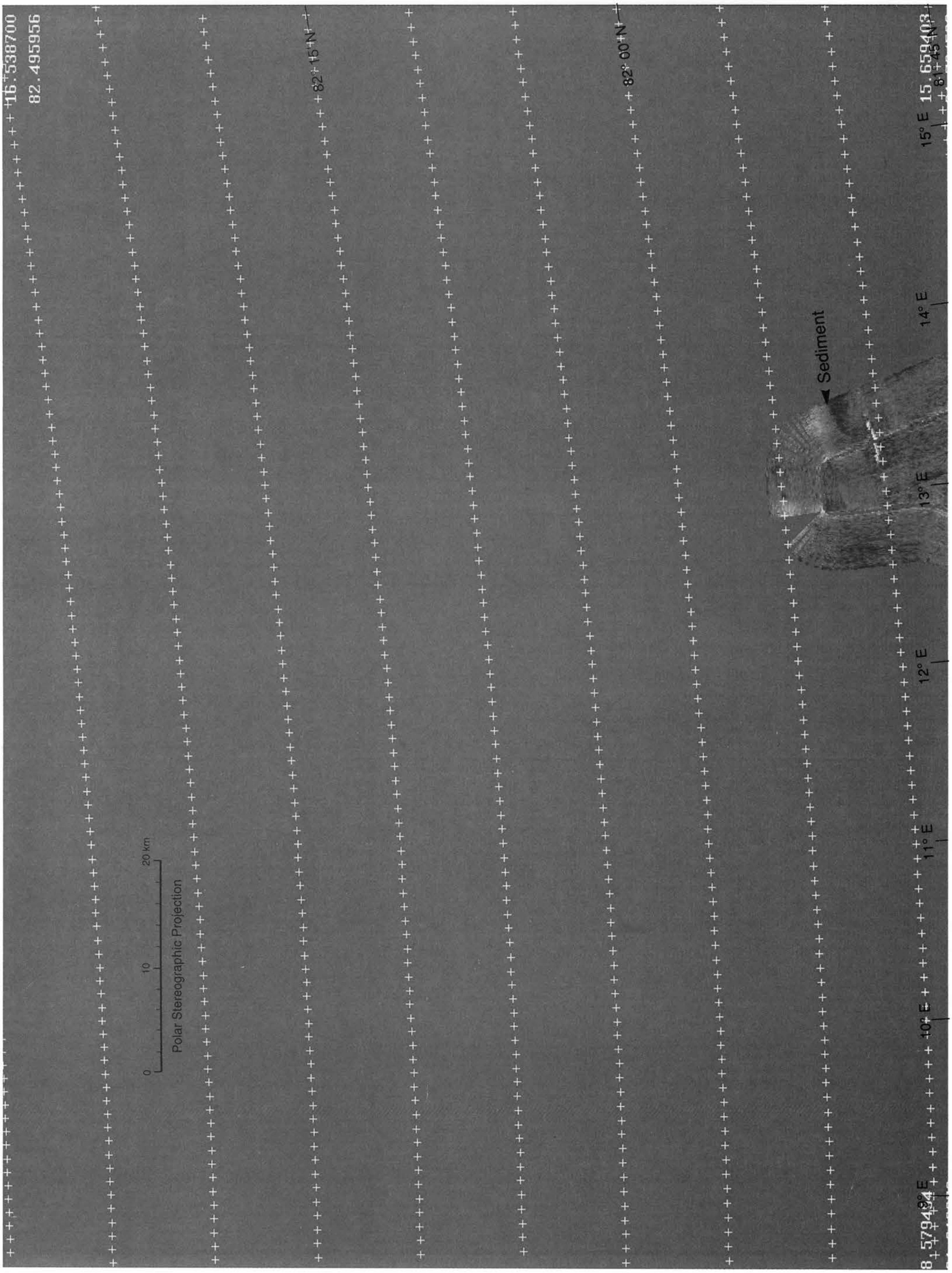

PLATE 18B TILE 4B: SEAMARC II MERGED BATHYMETRIC AND SIDE-LOOKING SONAR DATA

PLATE 19A

TILE 5A: SEAMARC II SIDE-LOOKING SONAR DATA

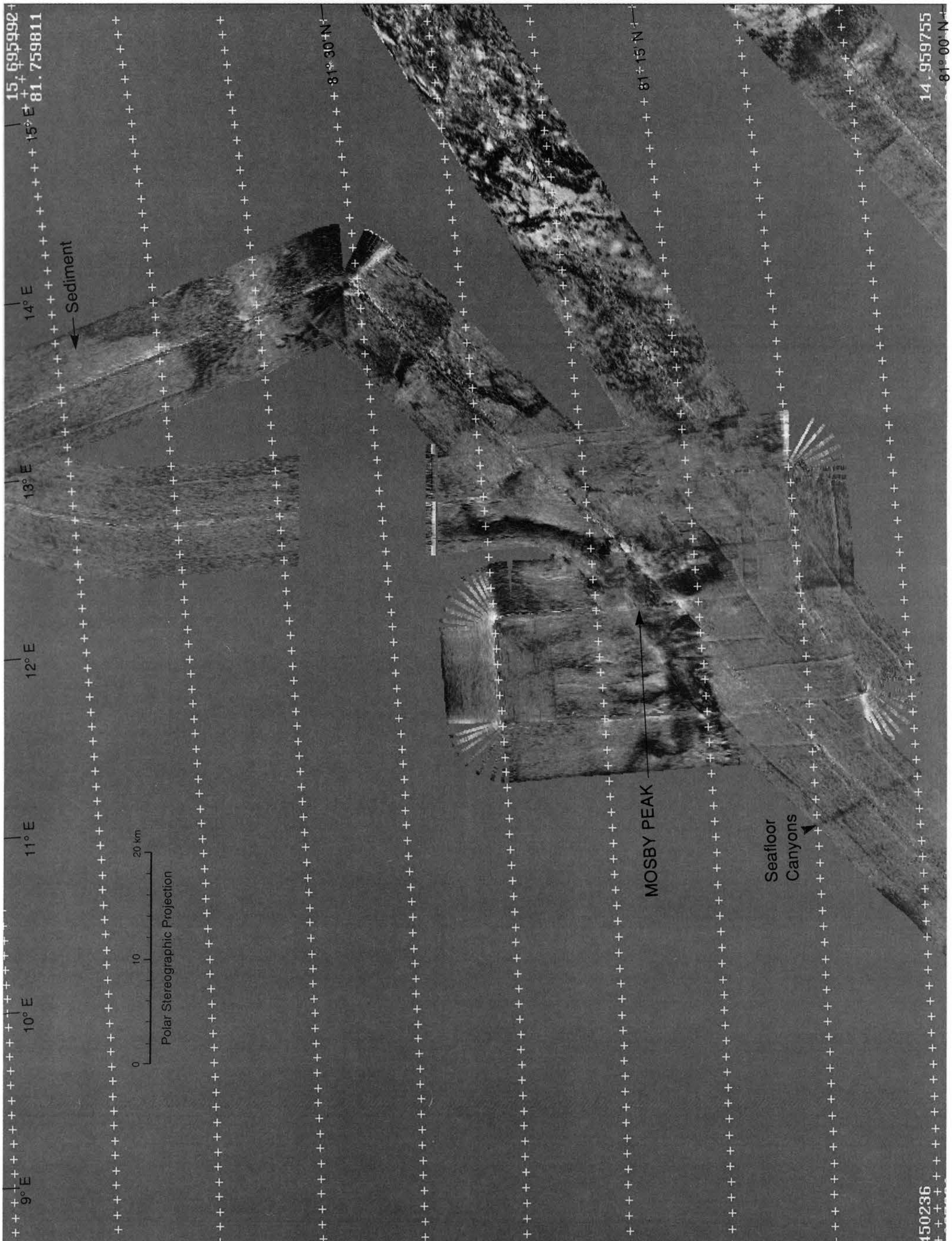

TILE 5B: SEAMARC II MERGED BATHYMETRIC AND SIDE-LOOKING SONAR DATA

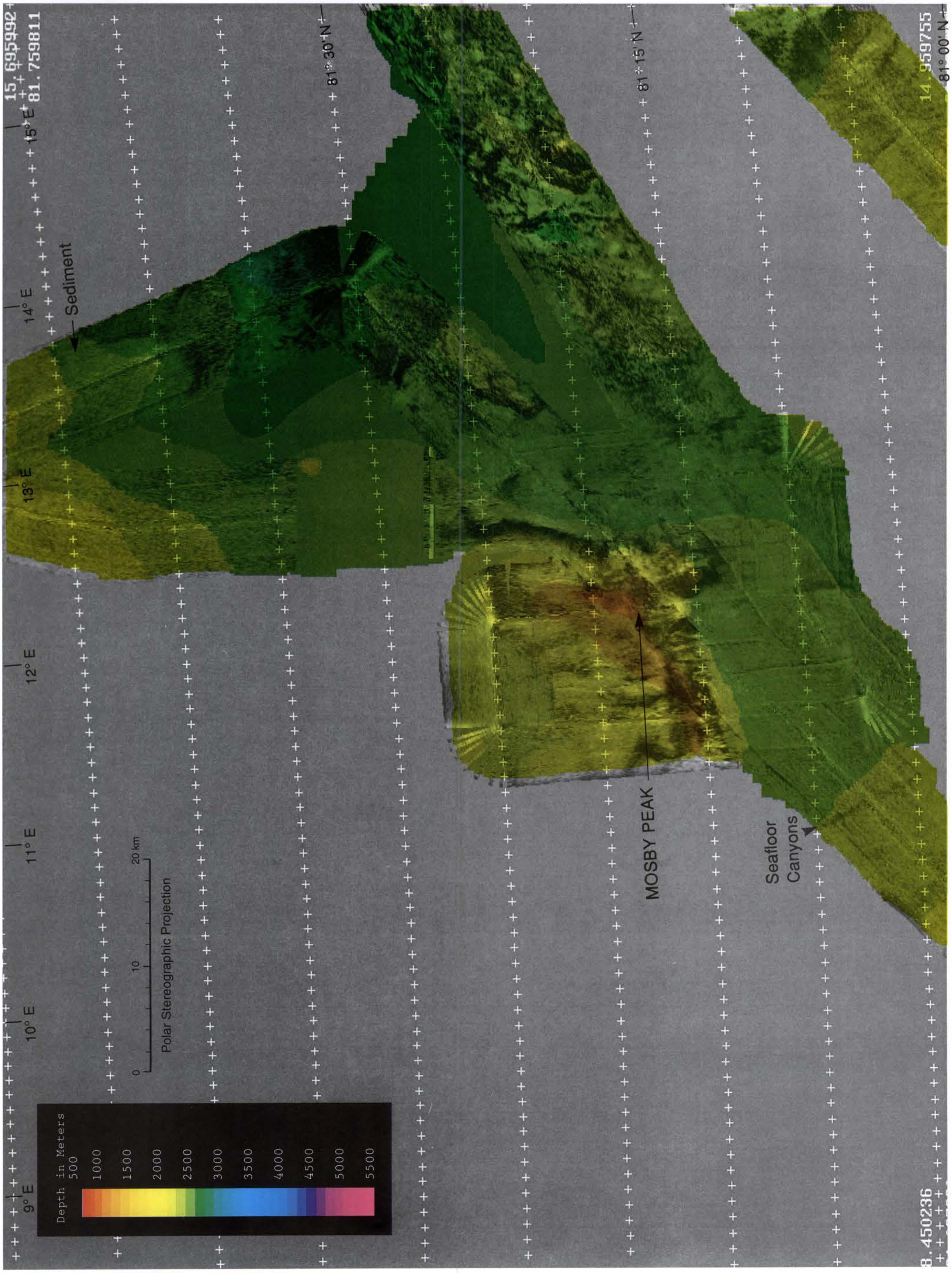

TILE 6A: SEAMARC II SIDE-LOOKING SONAR DATA

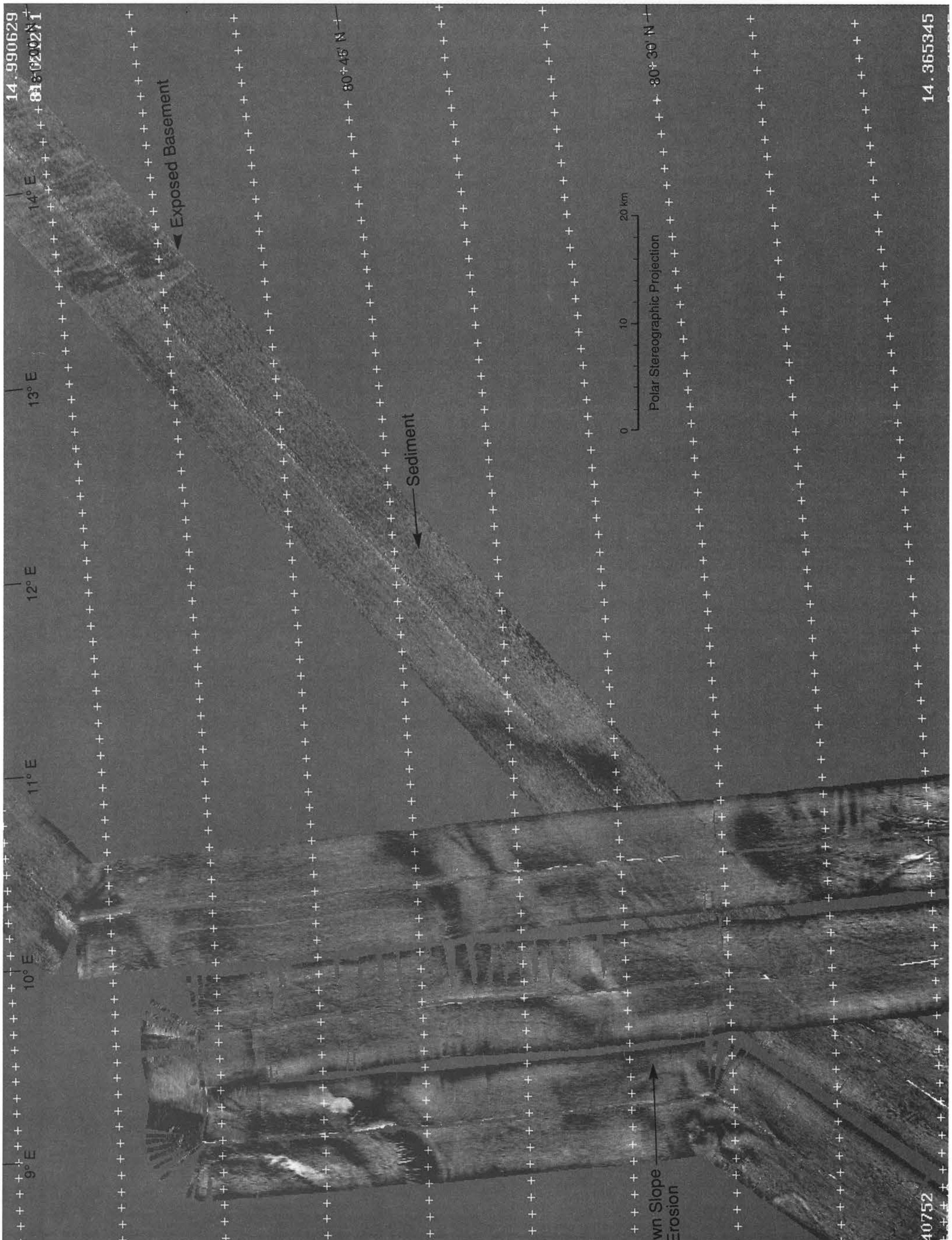

PLATE 20B TILE 6B: SEAMARC II MERGED BATHYMETRIC AND SIDE-LOOKING SONAR DATA

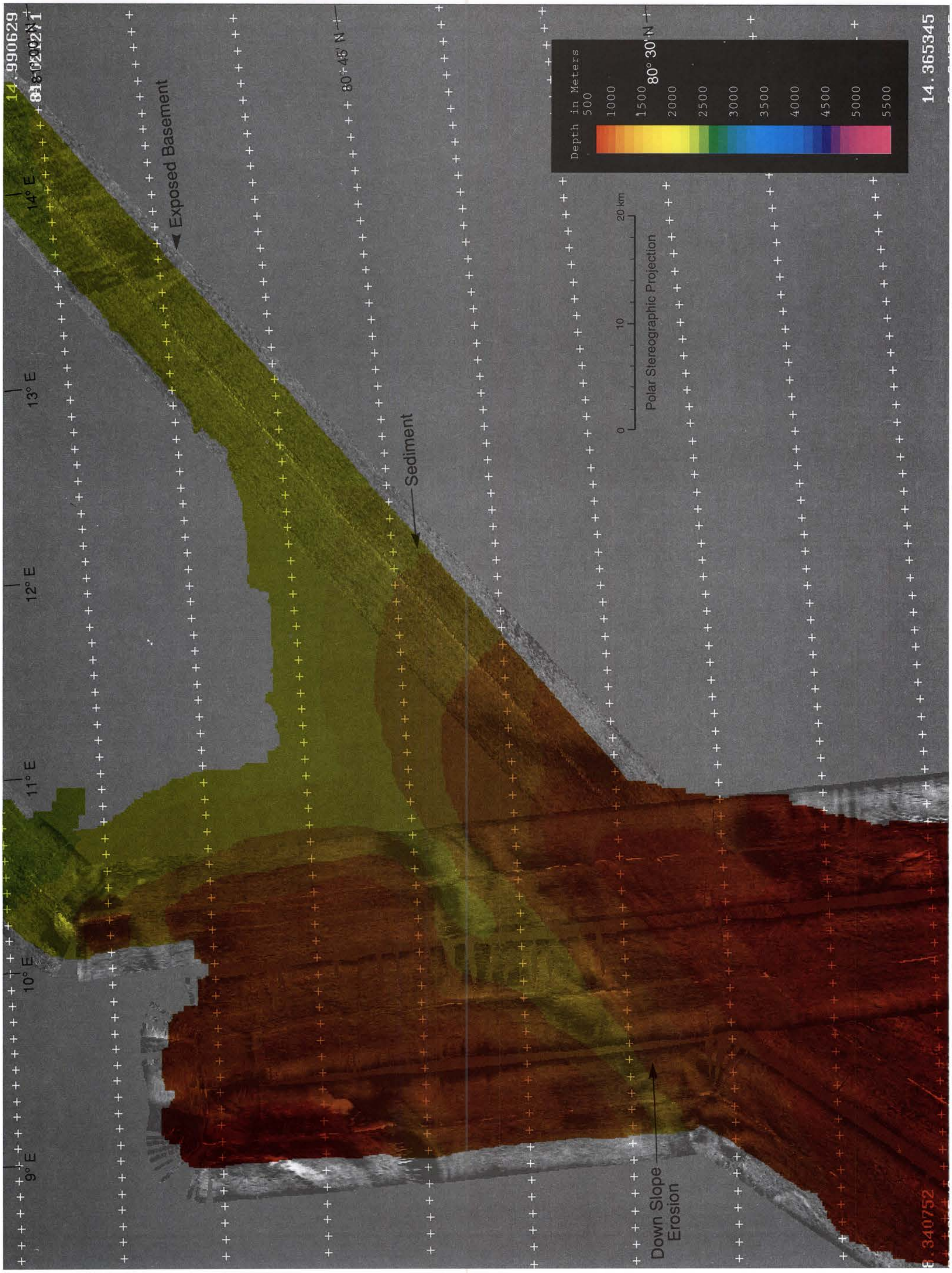

TILE 7A: SEAMARC II SIDE-LOOKING SONAR DATA

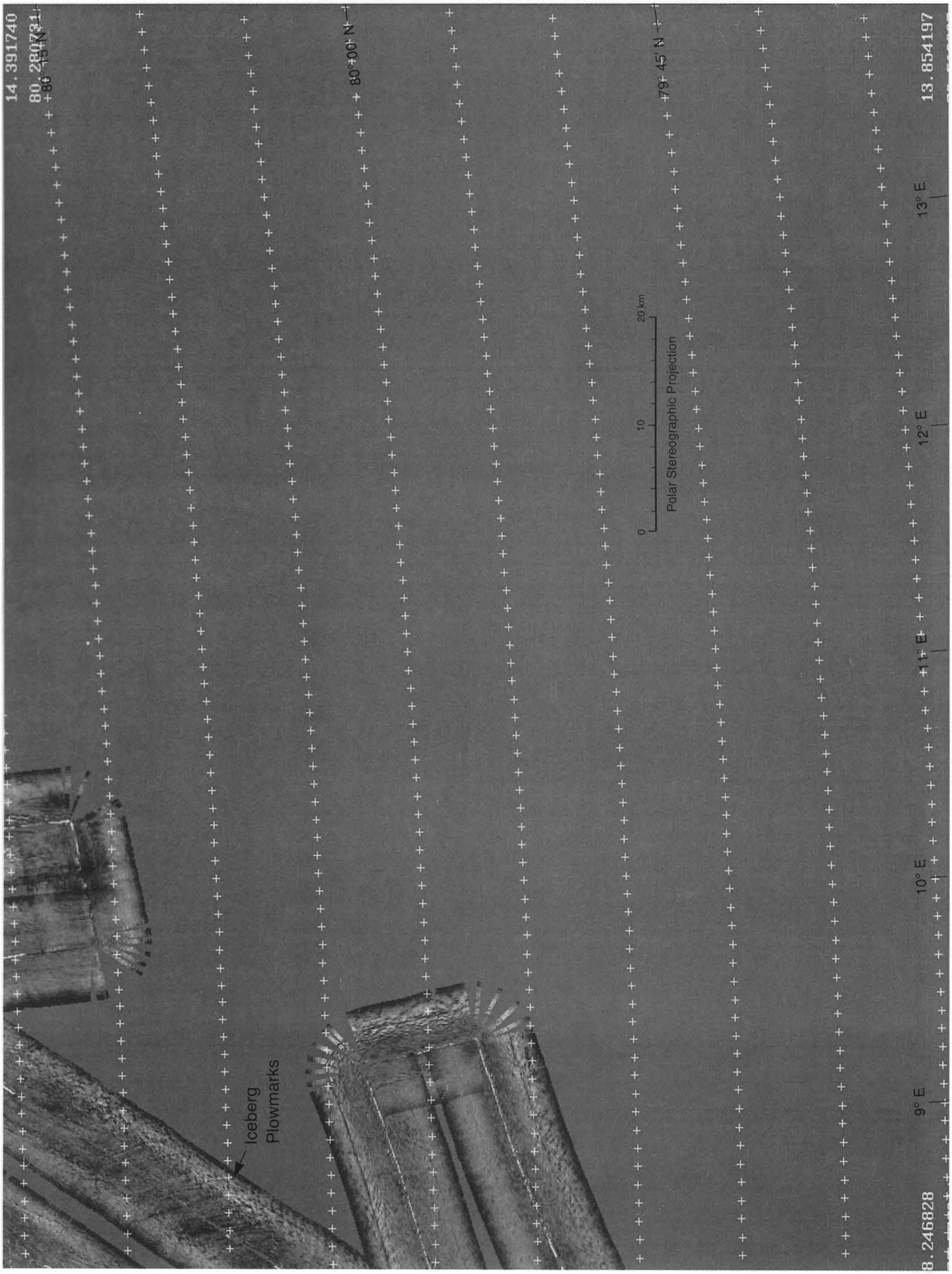

PLATE 21B TILE 7B: SEAMARC II MERGED BATHYMETRIC AND SIDE-LOOKING SONAR DATA

TILE 8A: SEAMARC II SIDE-LOOKING SONAR DATA

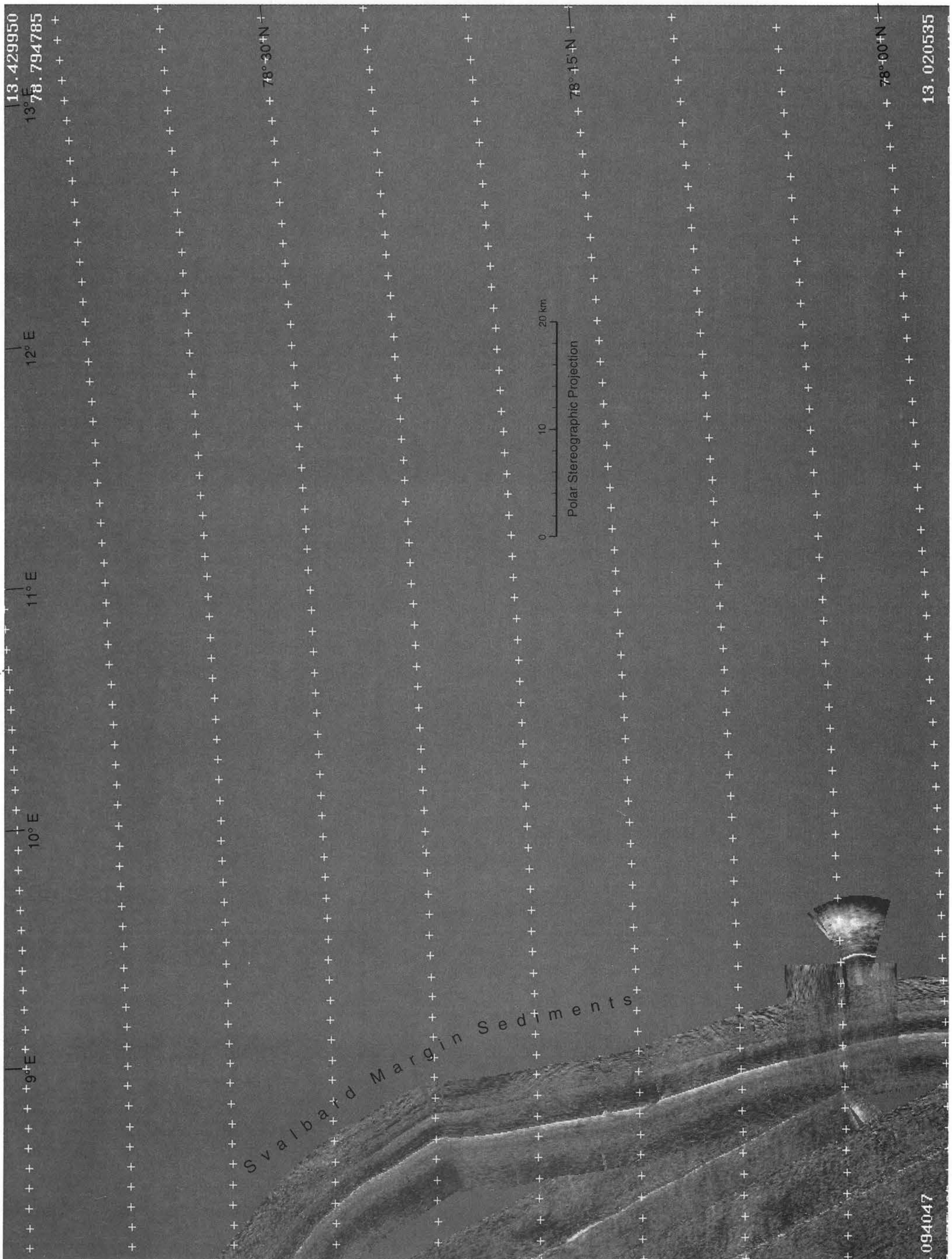

TILE 8B: SEAMARC II MERGED BATHYMETRIC AND SIDE-LOOKING SONAR DATA

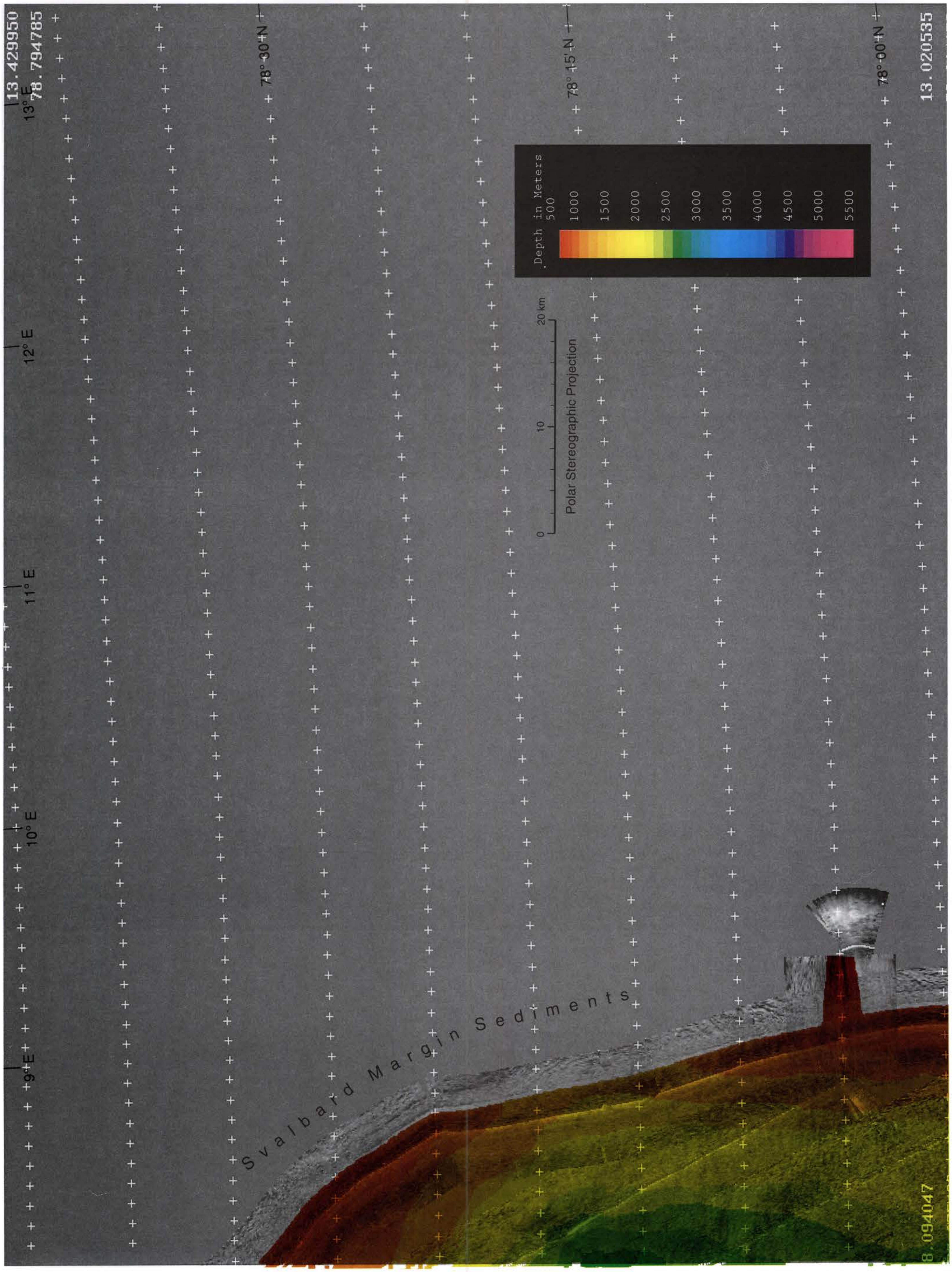

TILE 9A: SEAMARC II SIDE-LOOKING SONAR DATA

PLATE 23B TILE 9B: SEAMARC II MERGED BATHYMETRIC AND SIDE-LOOKING SONAR DATA

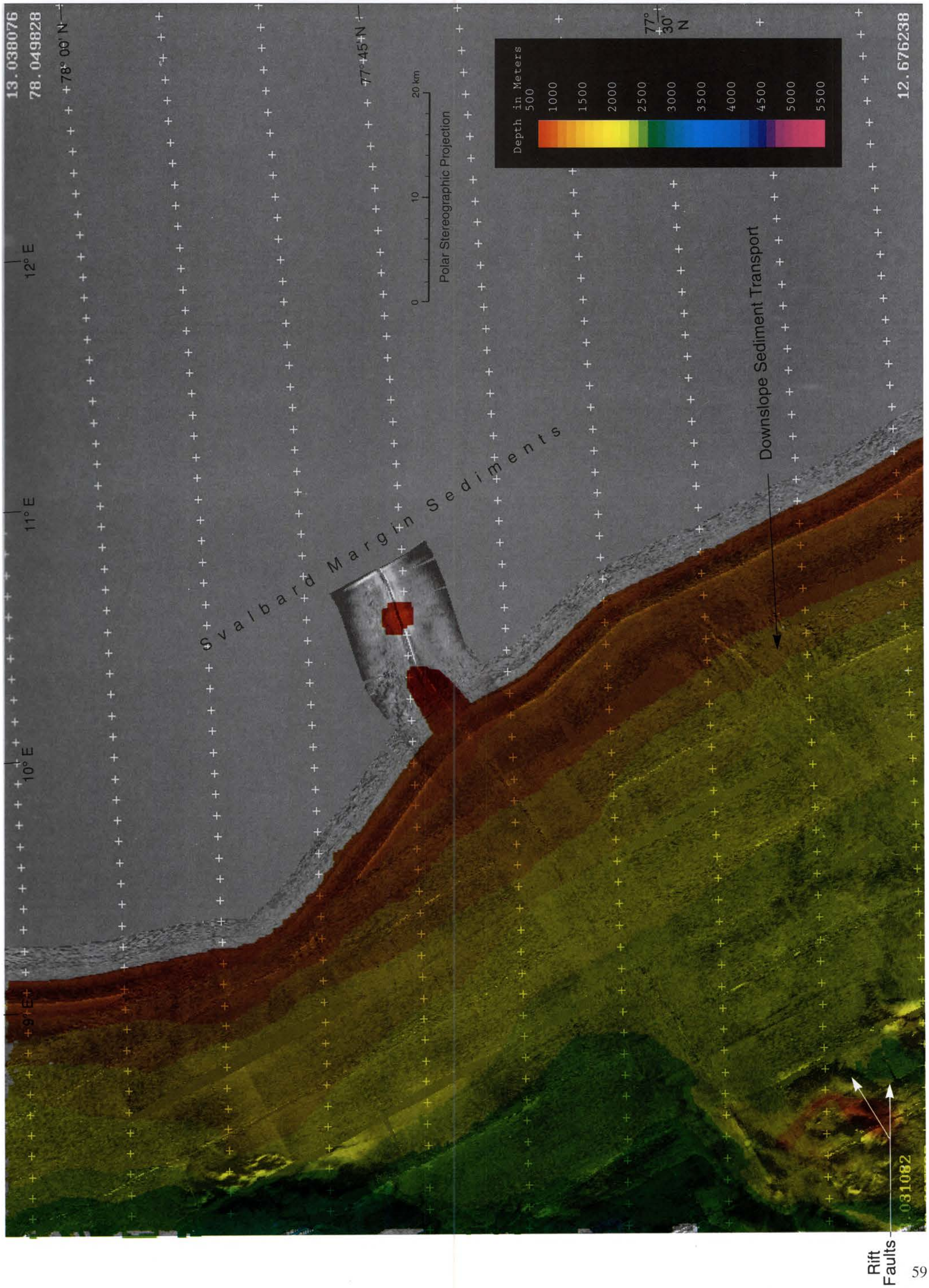

TILE 10A: SEAMARC II SIDE-LOOKING SONAR DATA

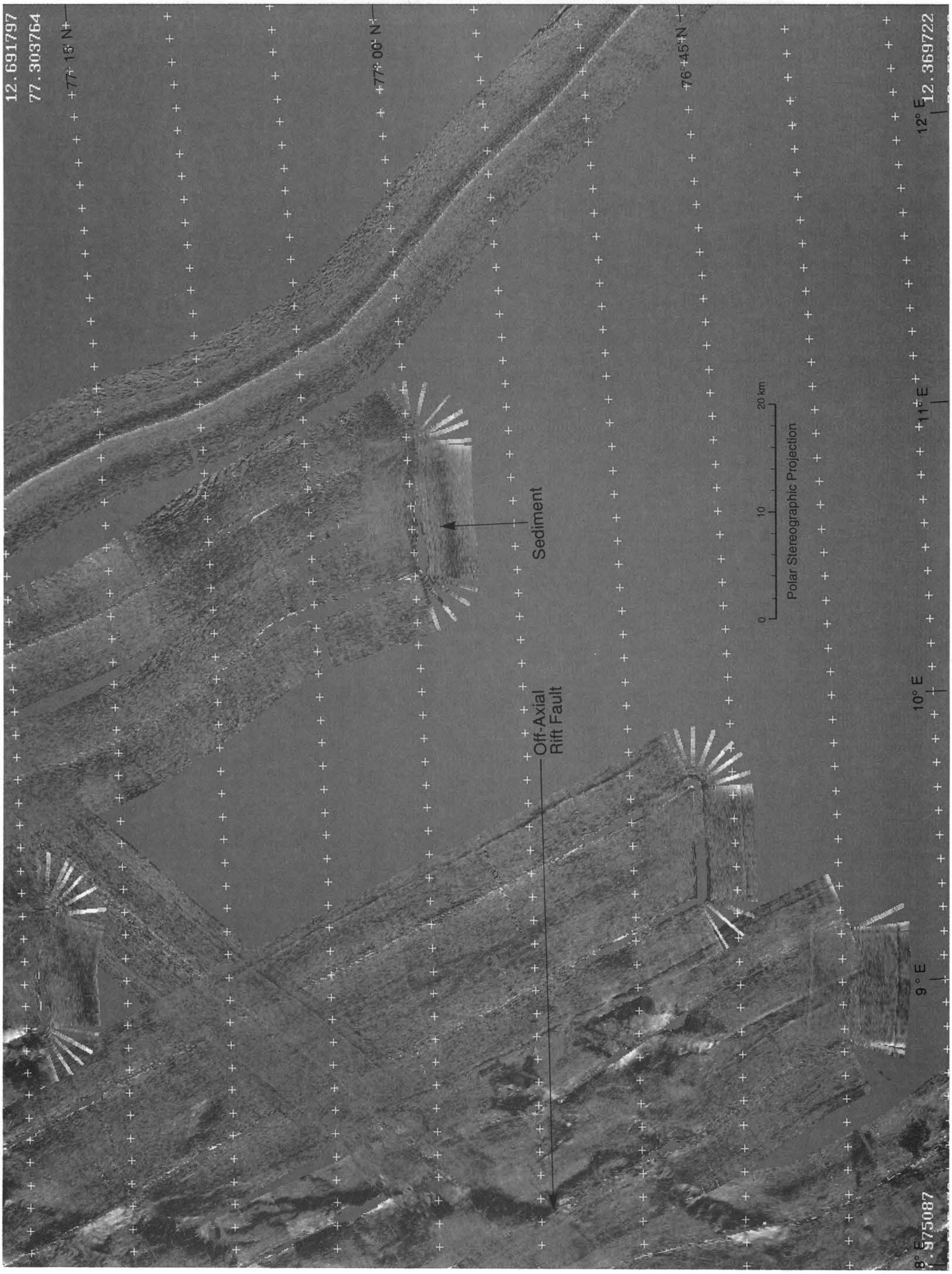

PLATE 24B TILE 10B: SEAMARC II MERGED BATHYMETRIC AND SIDE-LOOKING SONAR DATA

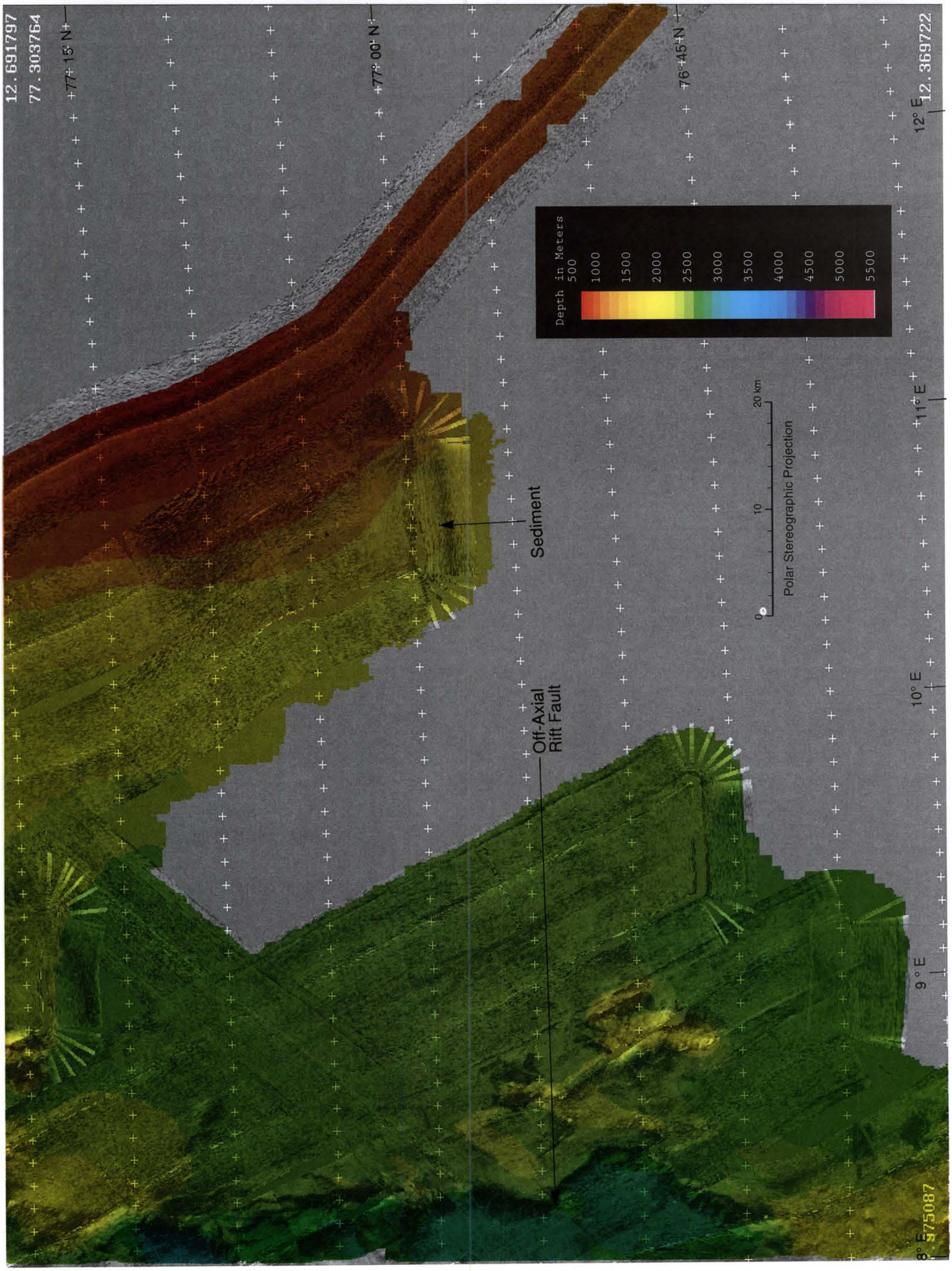

TILE 11A: SEAMARC II SIDE-LOOKING SONAR DATA

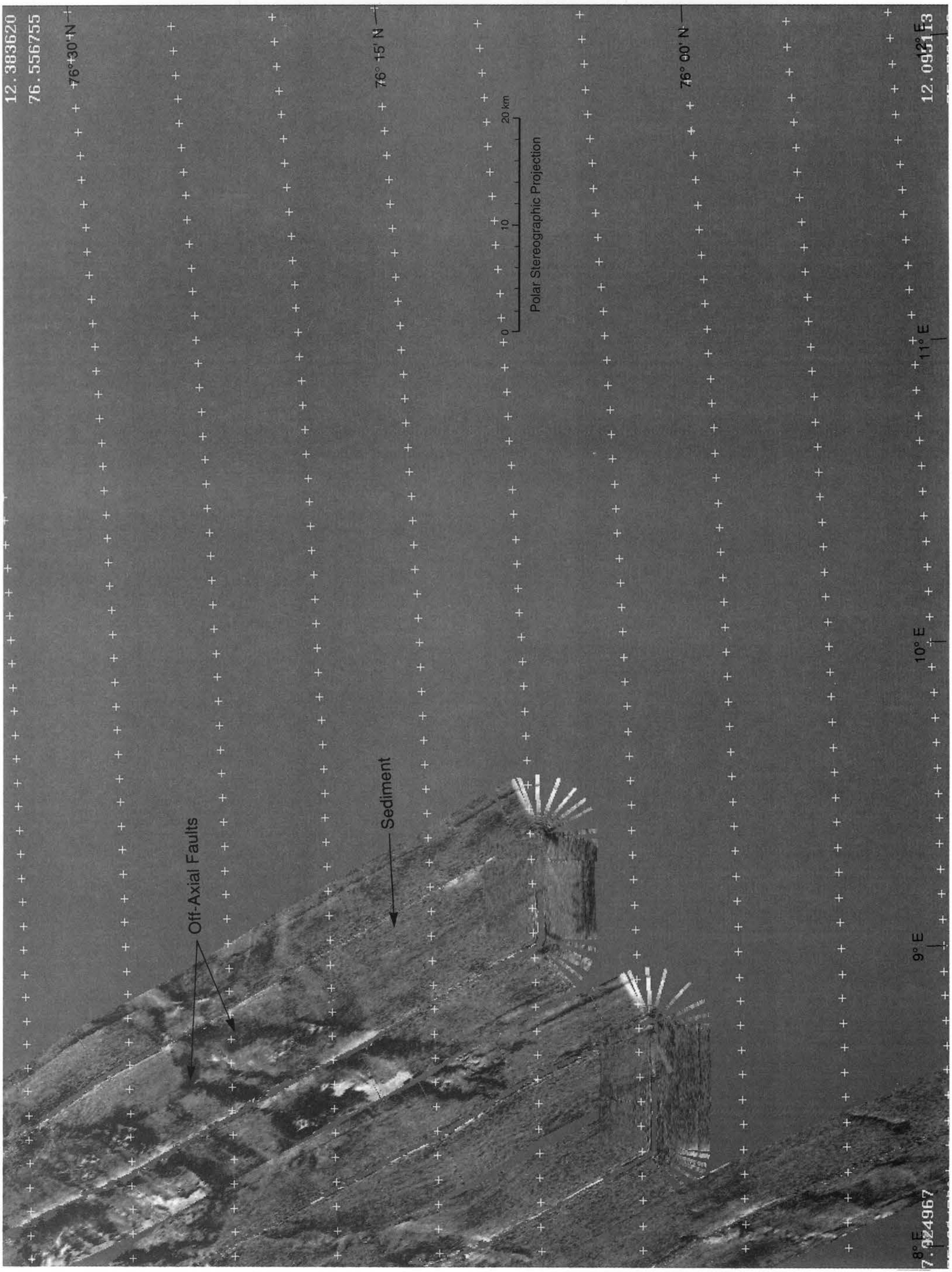

PLATE 25B TILE 11B: SEAMARC II MERGED BATHYMETRIC AND SIDE-LOOKING SONAR DATA

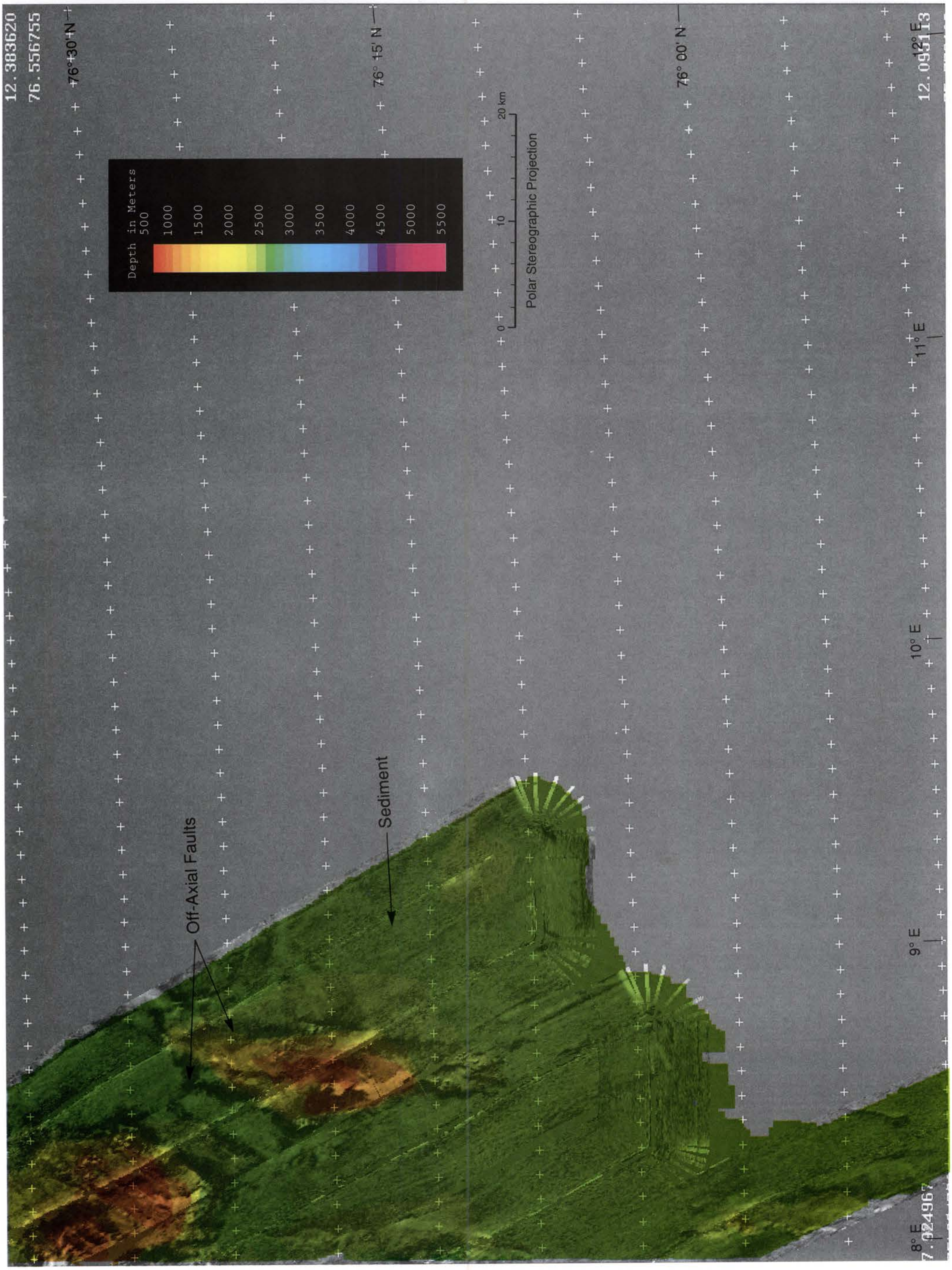

TILE 12A: SEAMARC II SIDE-LOOKING SONAR DATA

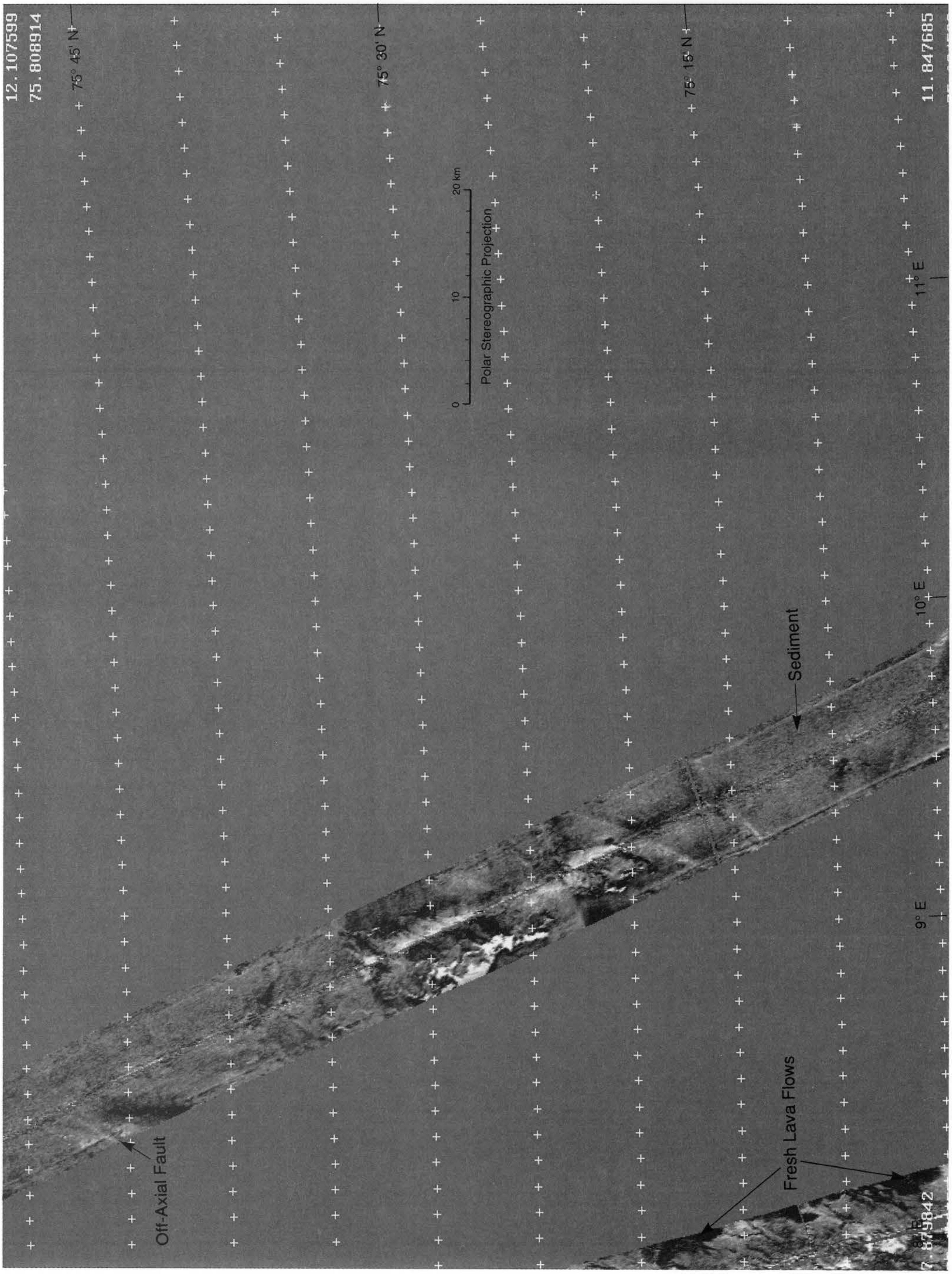

PLATE 26B TILE 12B: SEAMARC II MERGED BATHYMETRIC AND SIDE-LOOKING SONAR DATA

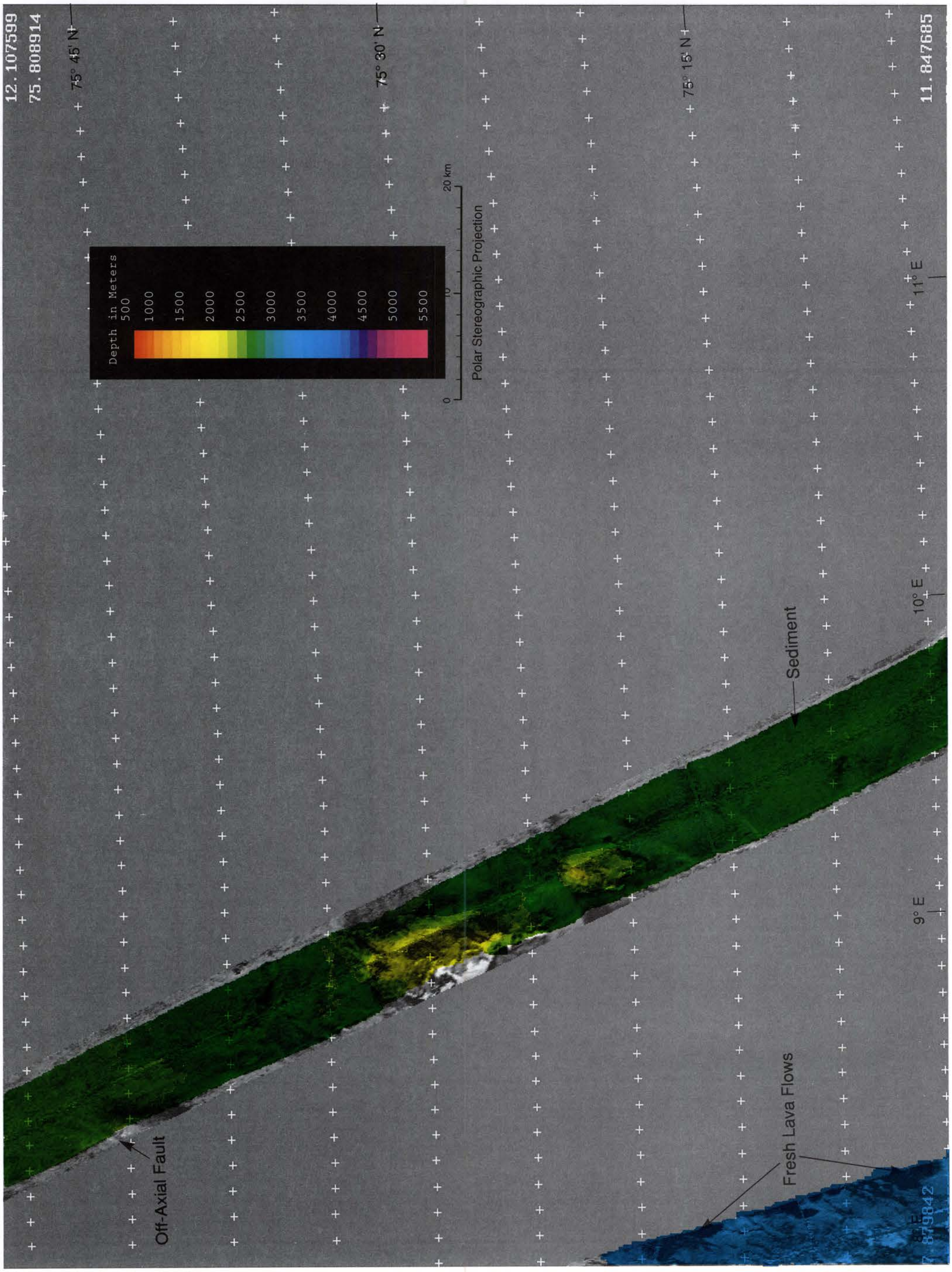

PLATE 27A

TILE 13A: SEAMARC II SIDE-LOOKING SONAR DATA

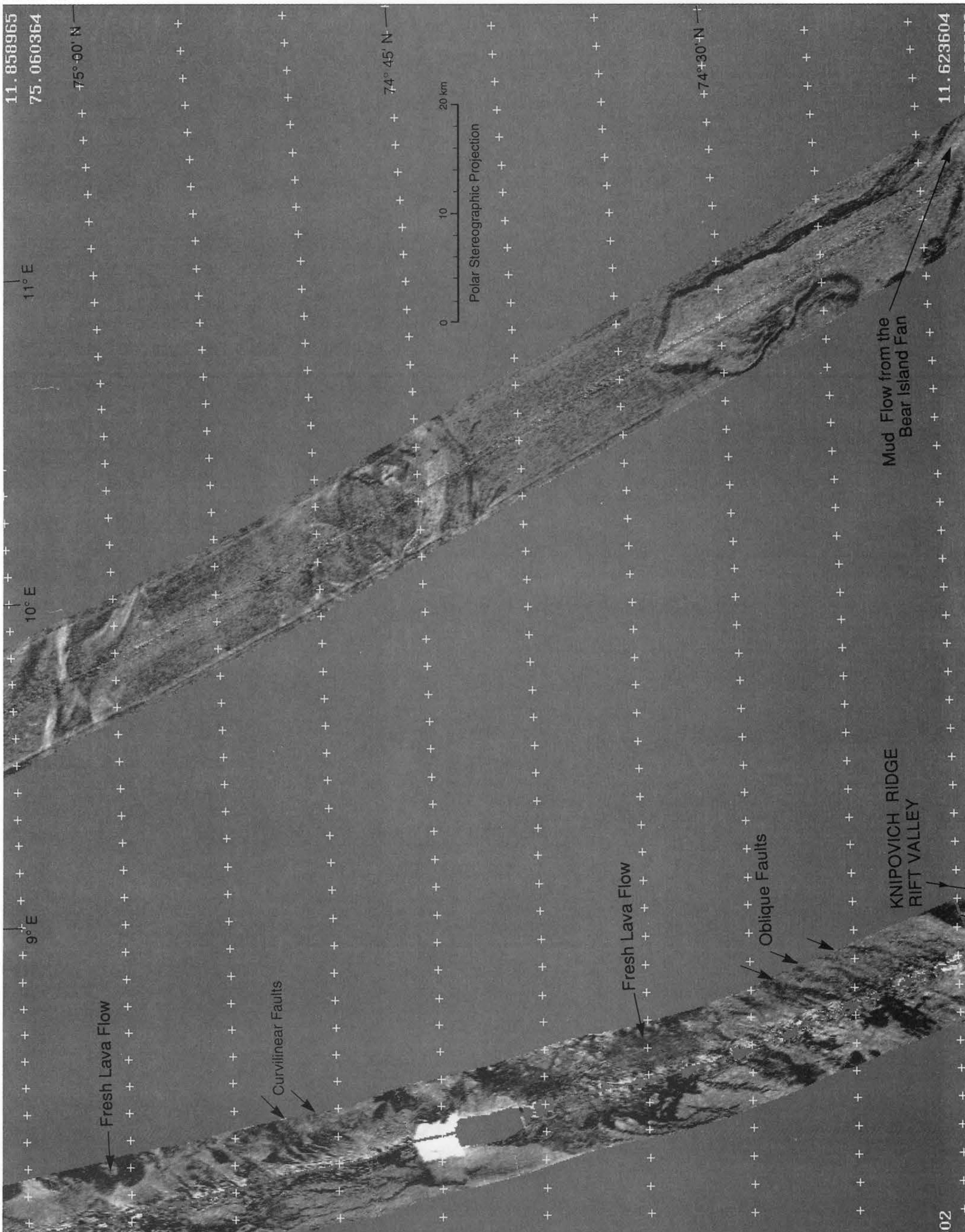

PLATE 27B TILE 13B: SEAMARC II MERGED BATHYMETRIC AND SIDE-LOOKING SONAR DATA

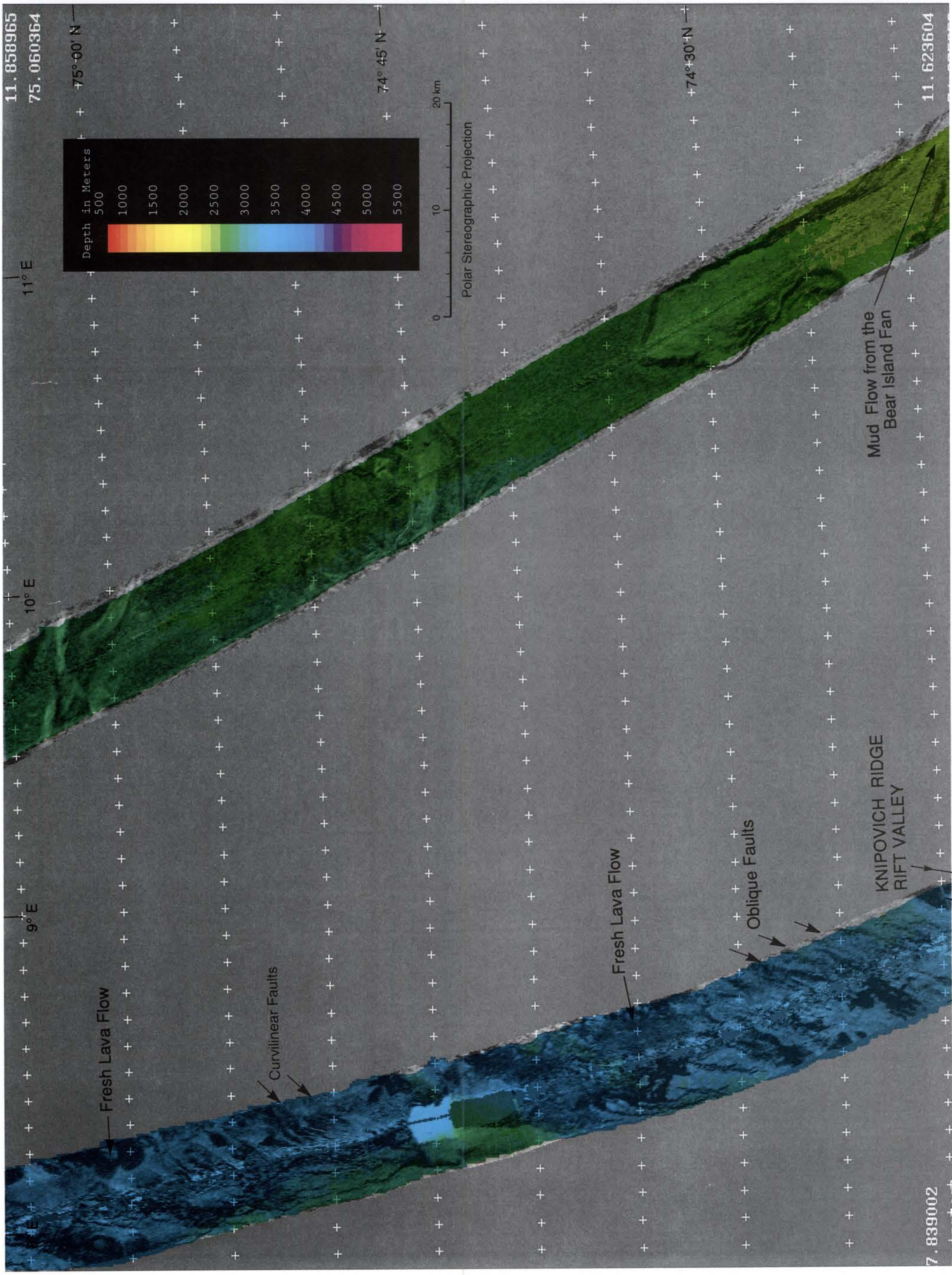

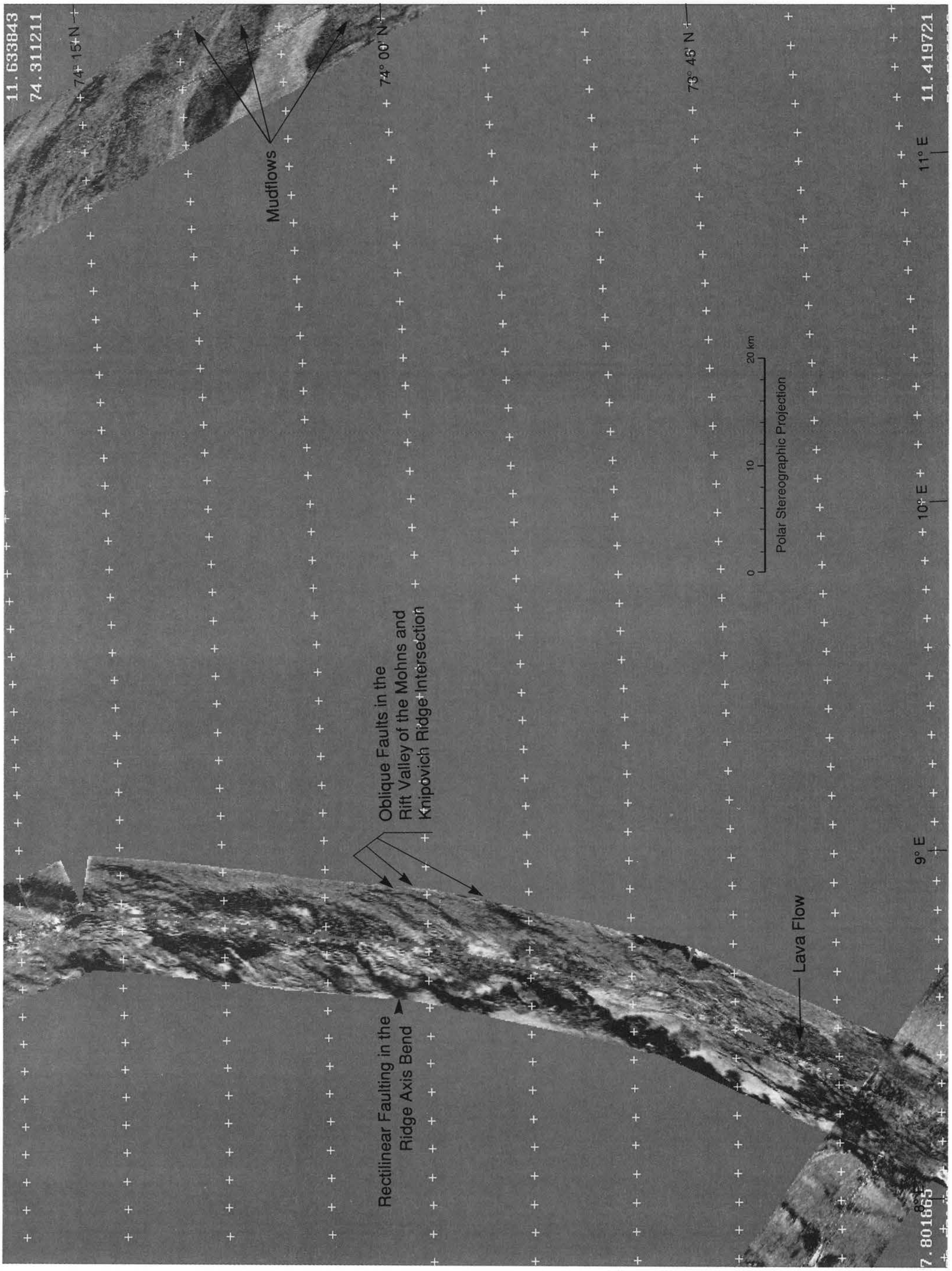
11.633843
74.311211
74° 15' N
74° 00' N
73° 45' N
11.419721
11° E
10° E
9° E
8° E
7.801665
Mudflows
0
10
20 km
Polar Stereographic Projection
Oblique Faults in the
Rift Valley of the Mohns and
Knipovich Ridge Intersection
Rectilinear Faulting in the
Ridge Axis Bend
Lava Flow

TILE 14B: SEAMARC II MERGED BATHYMETRIC AND SIDE-LOOKING SONAR DATA

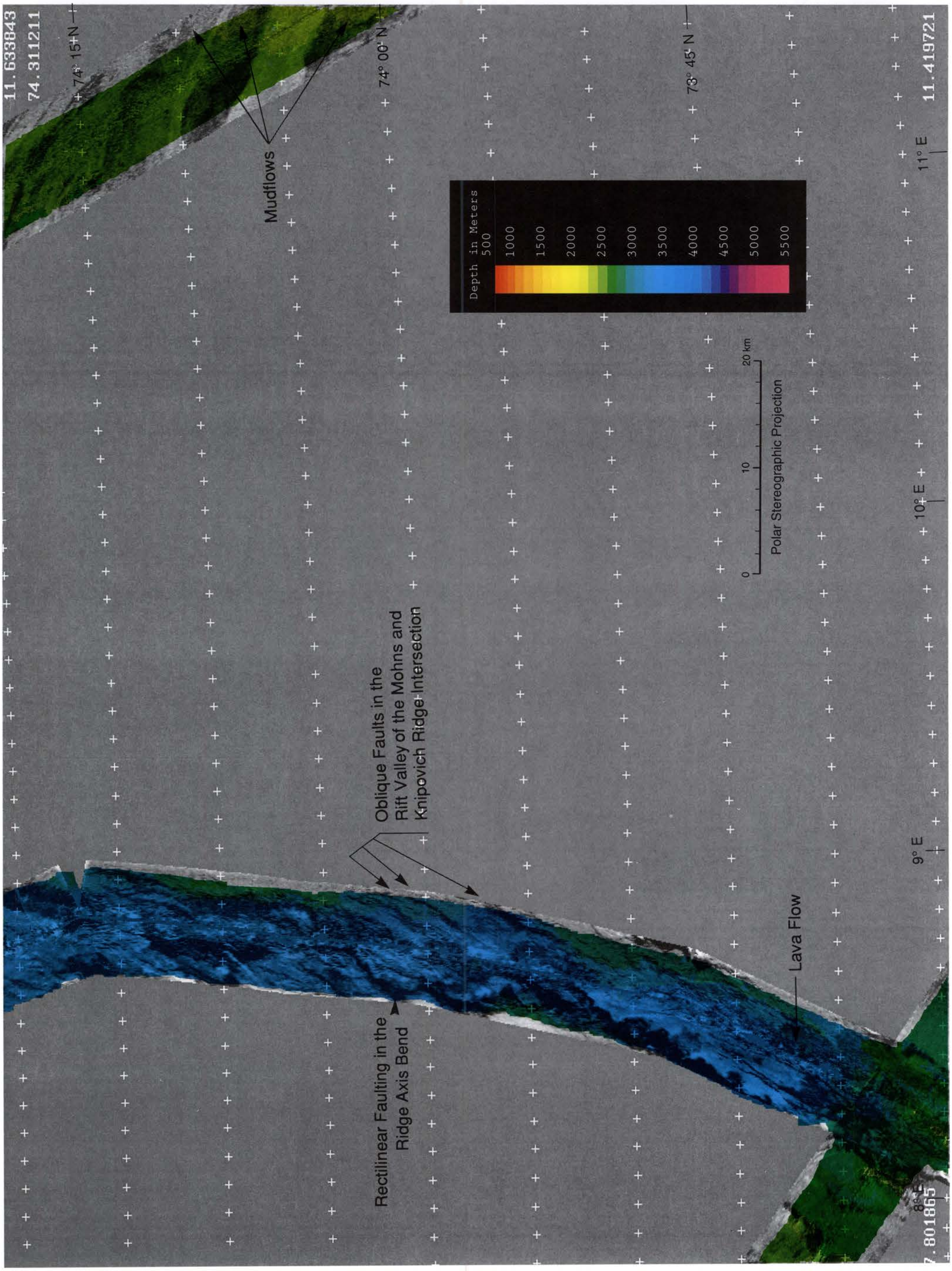

TILE 15A: SEAMARC II SIDE-LOOKING SONAR DATA

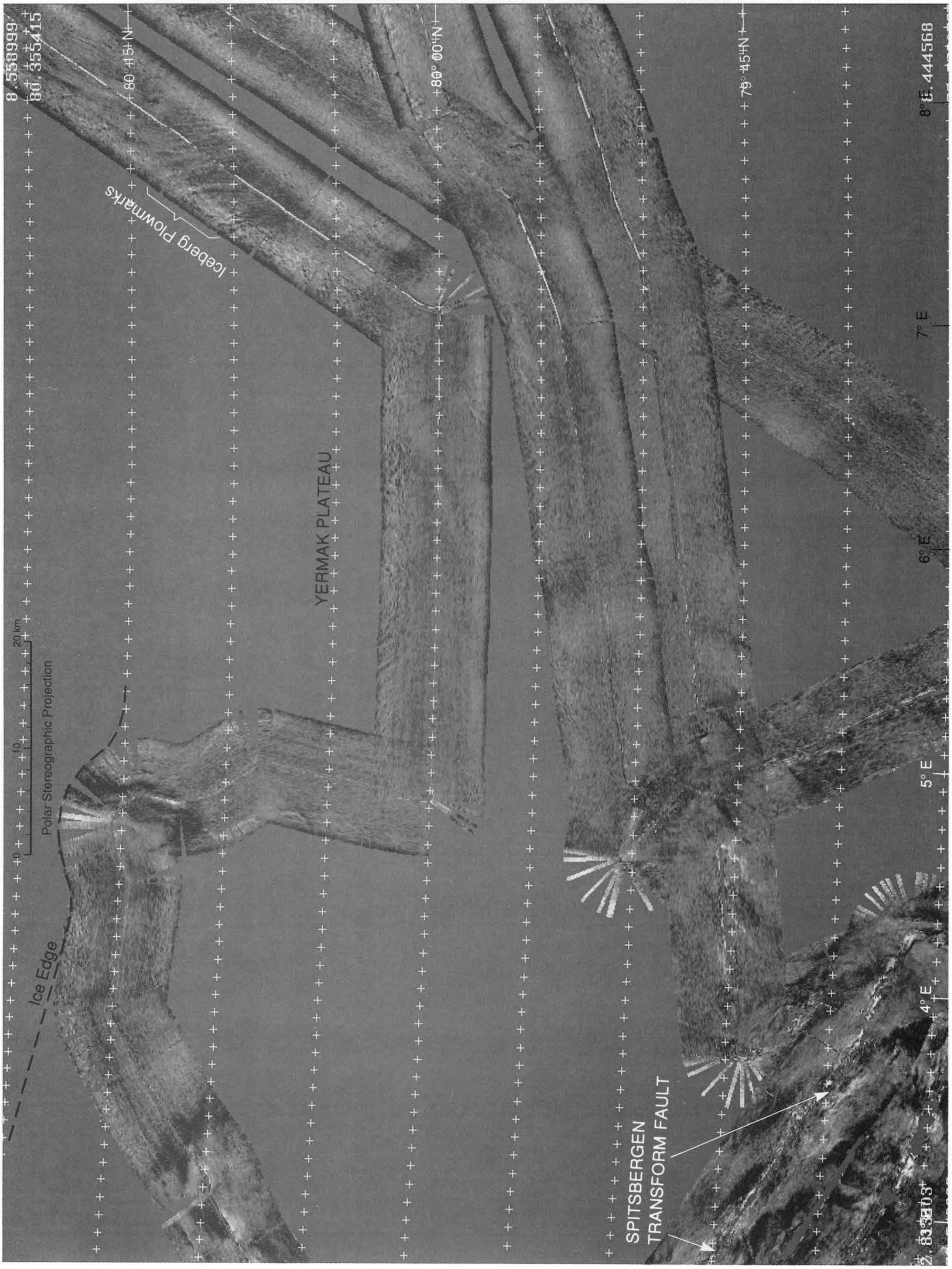

PLATE 29B TILE 15B: SEAMARC II MERGED BATHYMETRIC AND SIDE-LOOKING SONAR DATA

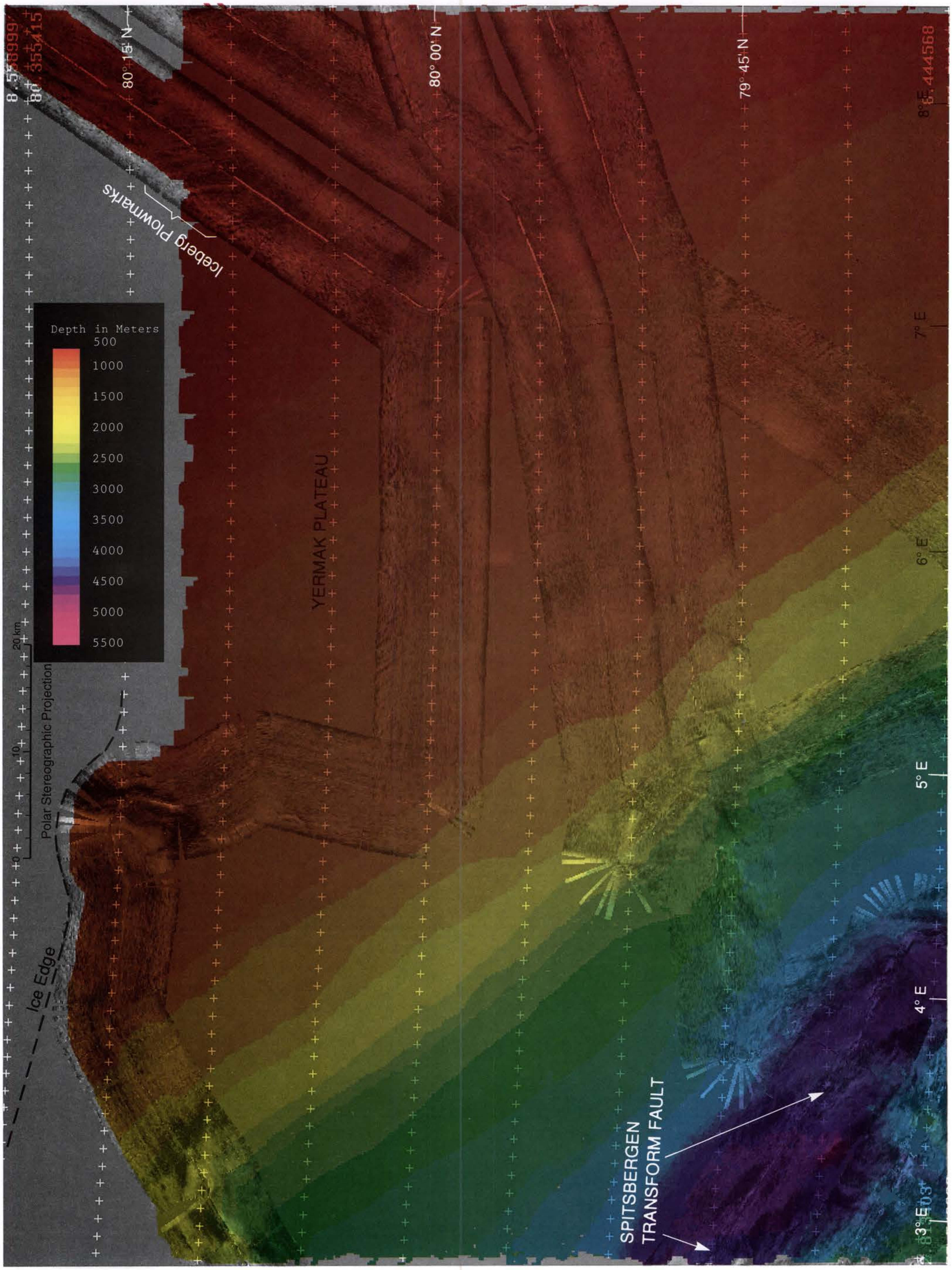

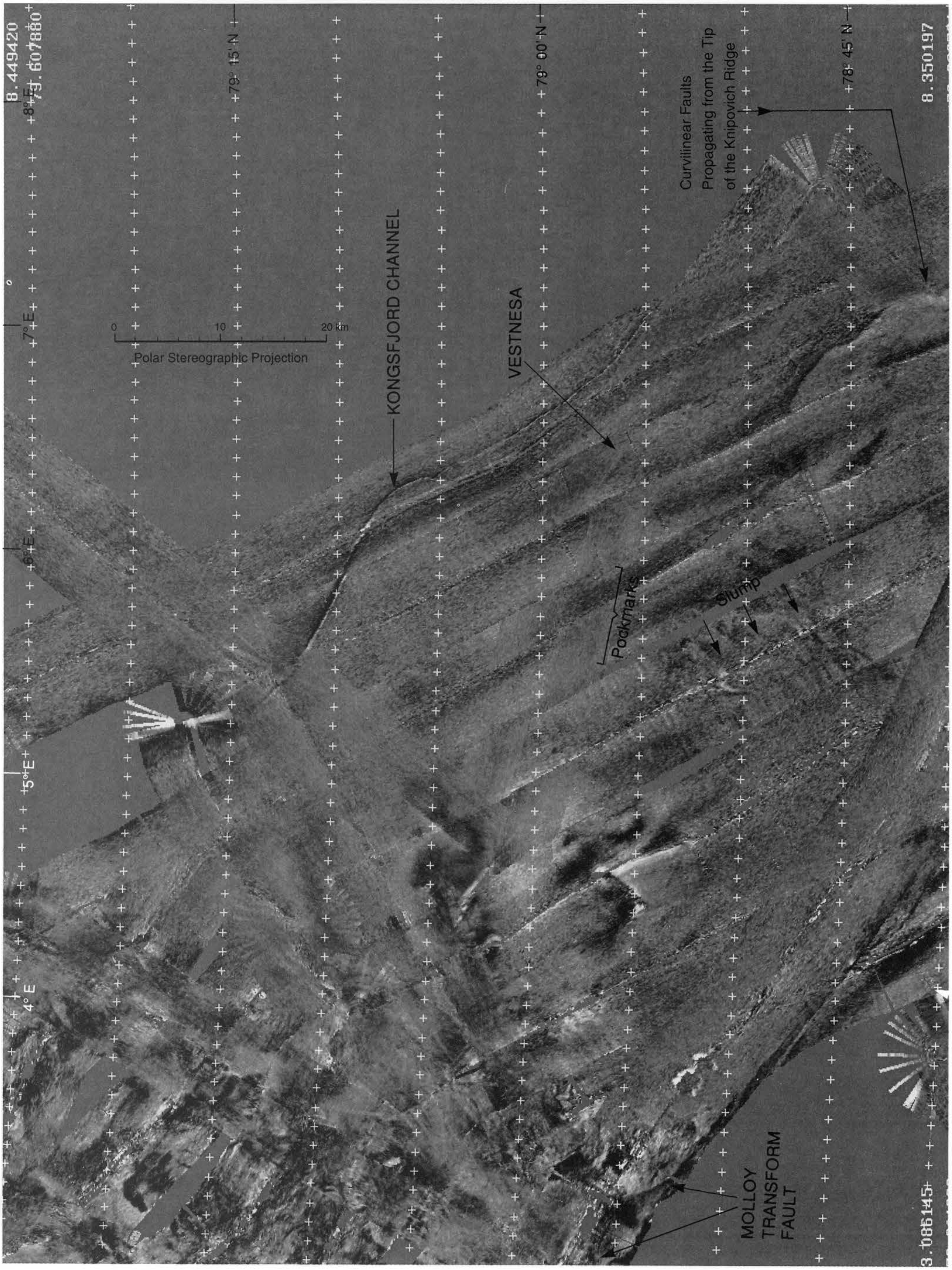
8.449420
73.607880
8° E
7° E
6° E
5° E
4° E
79° 15' N
79° 00' N
78° 45' N
8.350197
3.086145
0
10
20 km
Polar Stereographic Projection
KONGSFJORD CHANNEL
VESTNESA
Curvilinear Faults
Propagating from the Tip
of the Knipovich Ridge
Pockmarks
Slump
MOLLOY
TRANSFORM
FAULT

TILE 16B: SEAMARC II MERGED BATHYMETRIC AND SIDE-LOOKING SONAR DATA

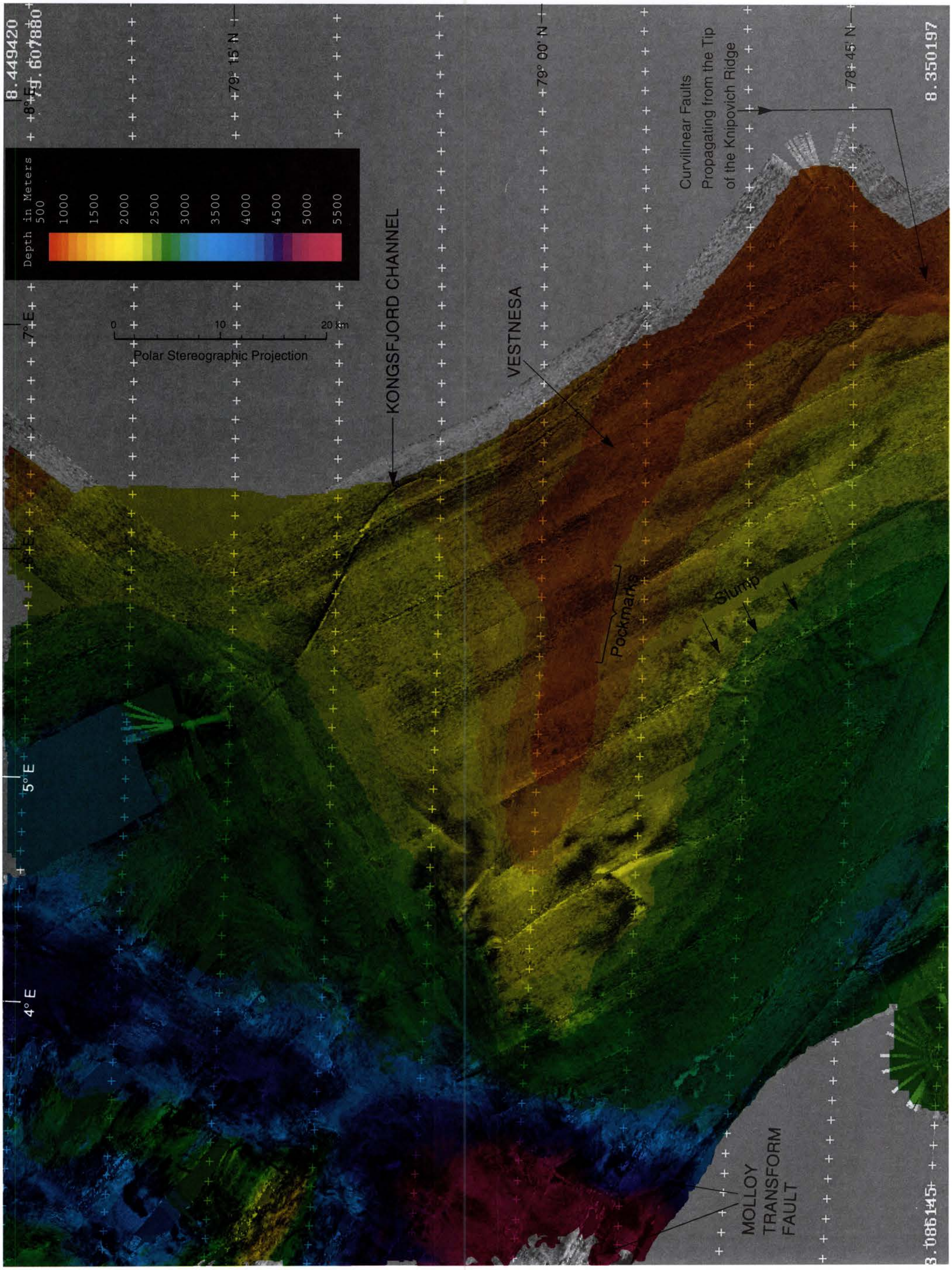

TILE 17A: SEAMARC II SIDE-LOOKING SONAR DATA

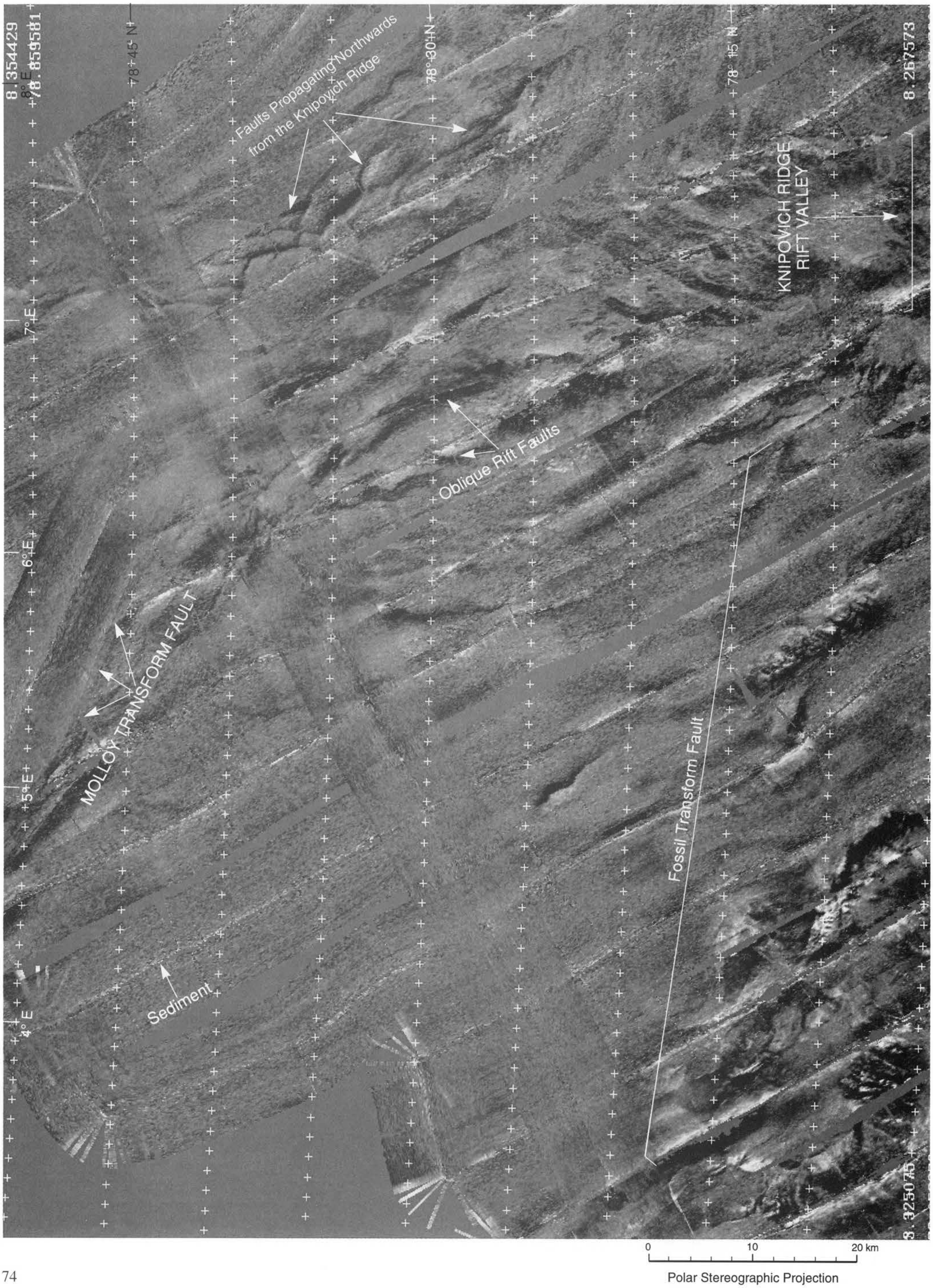

TILE 17B: SEAMARC II MERGED BATHYMETRIC AND SIDE-LOOKING SONAR DATA

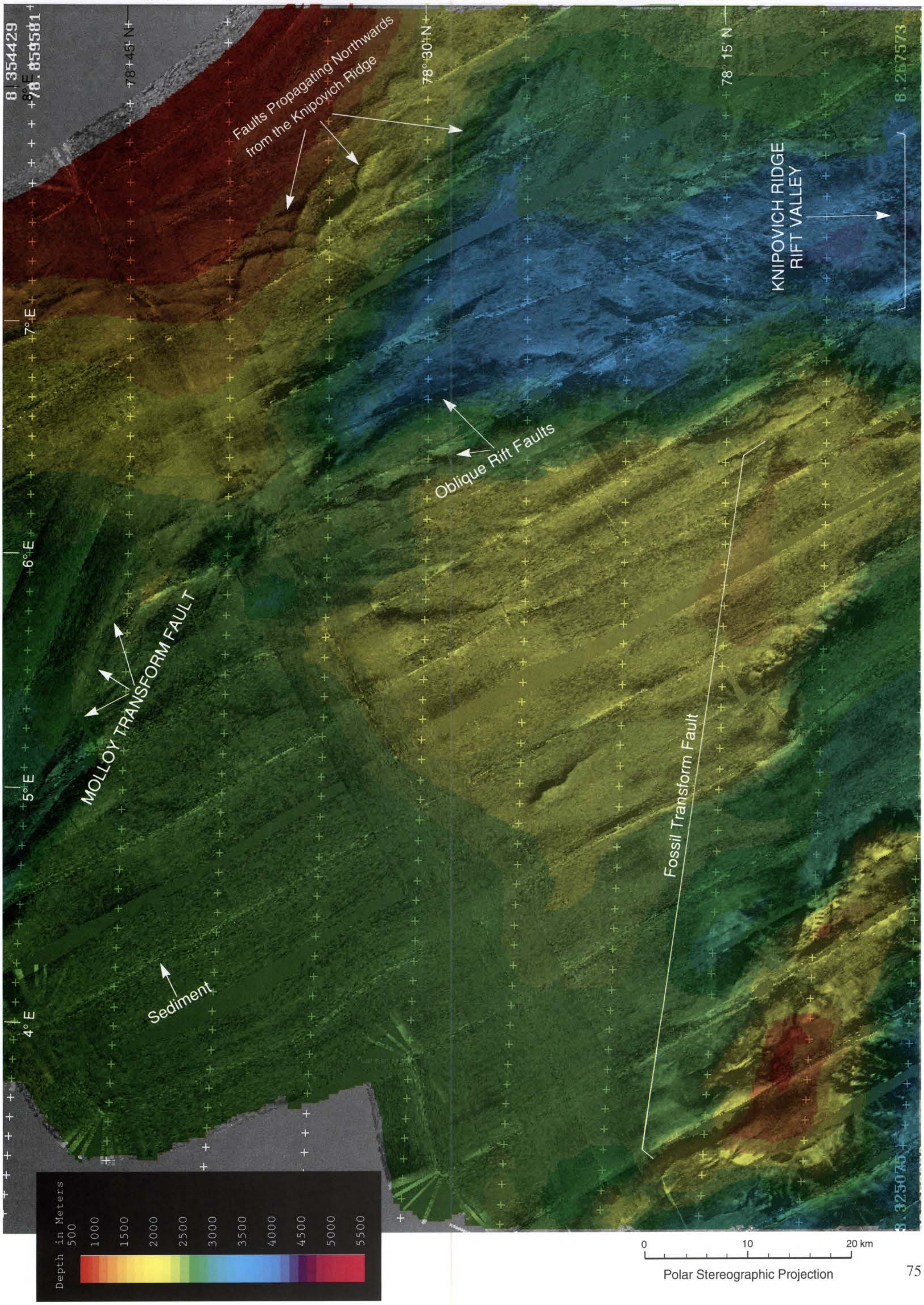

TILE 18A: SEAMARC II SIDE-LOOKING SONAR DATA

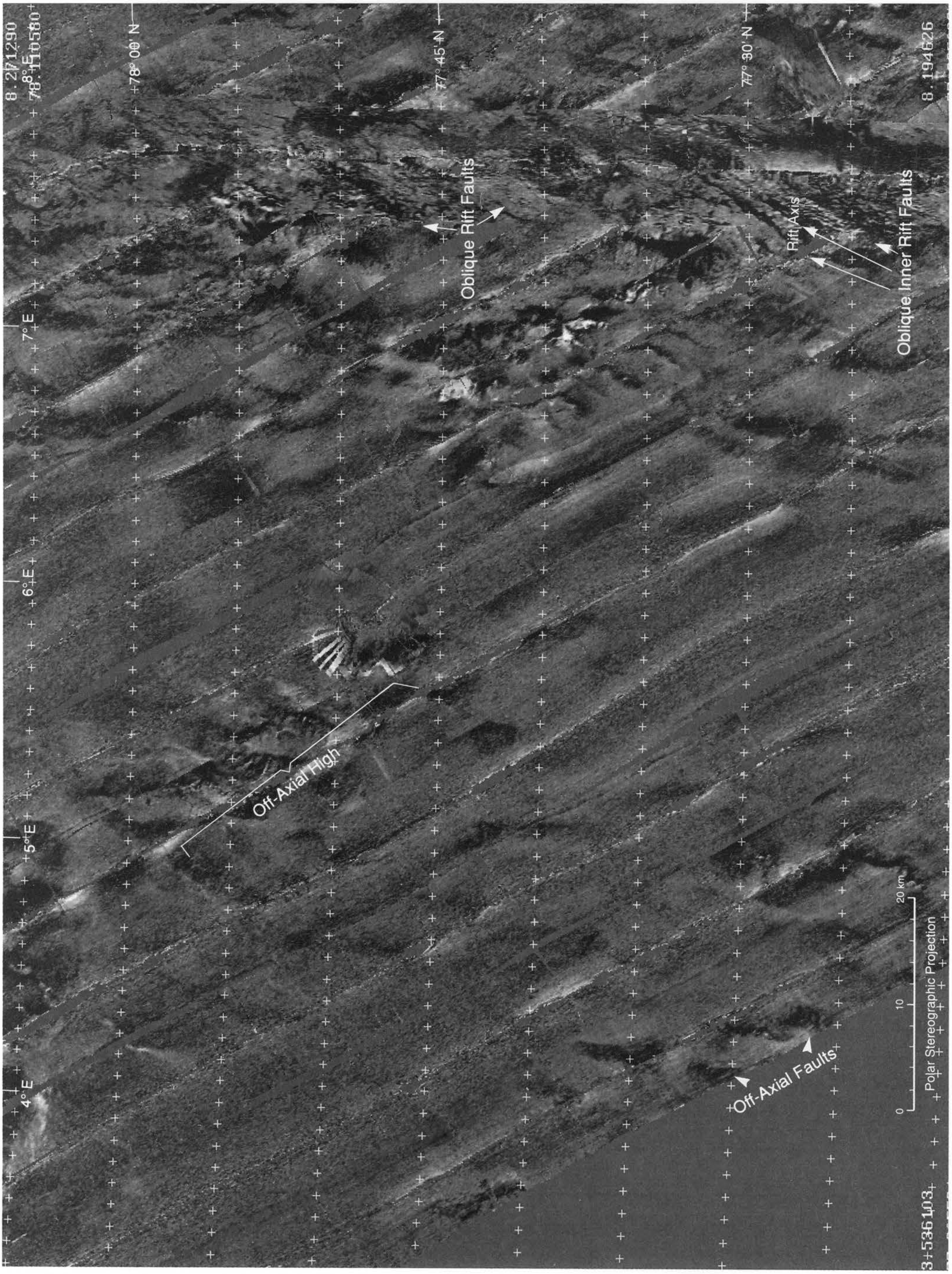

TILE 18B: SEAMARC II MERGED BATHYMETRIC AND SIDE-LOOKING SONAR DATA

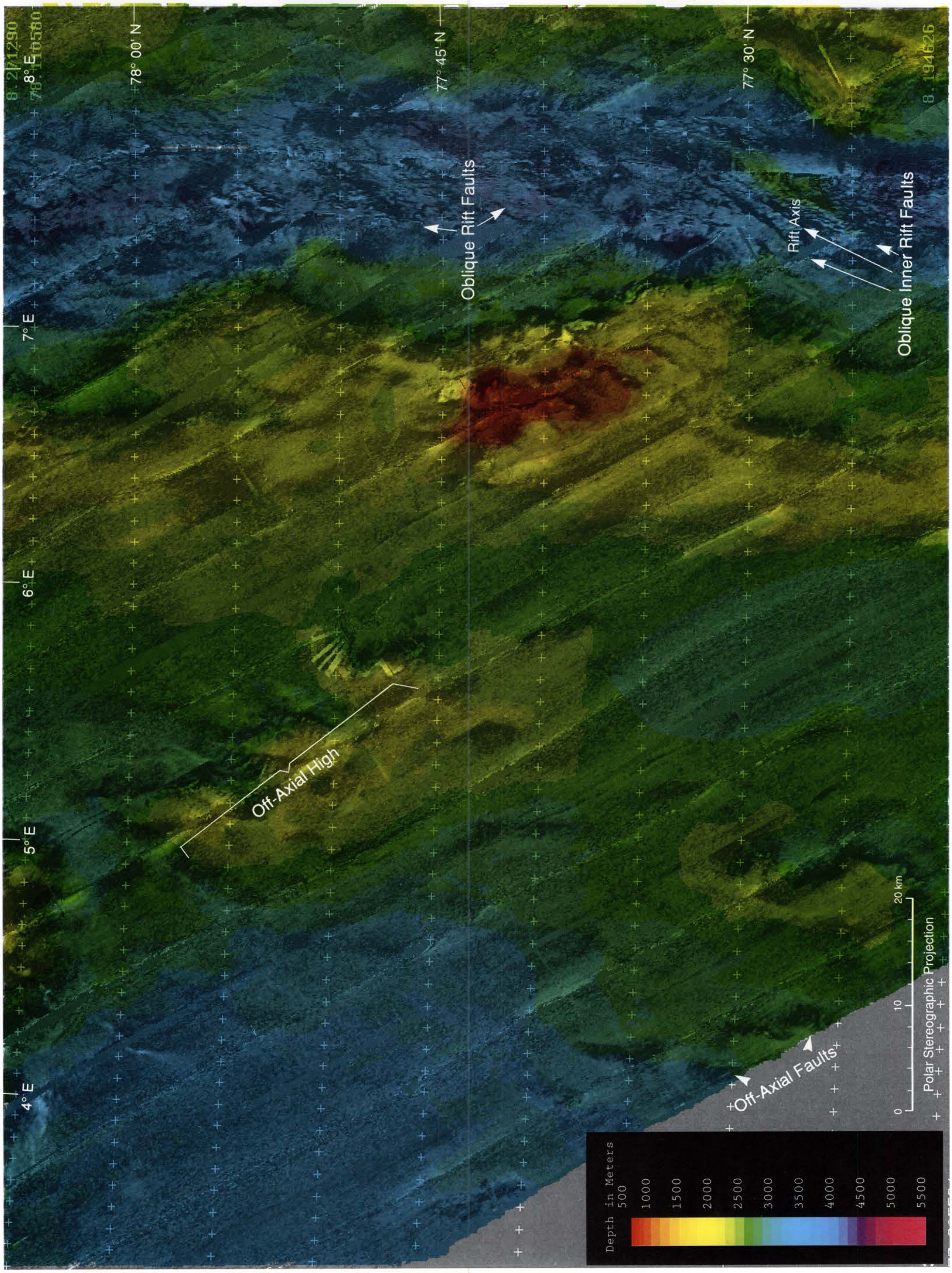

TILE 19A: SEAMARC II SIDE-LOOKING SONAR DATA

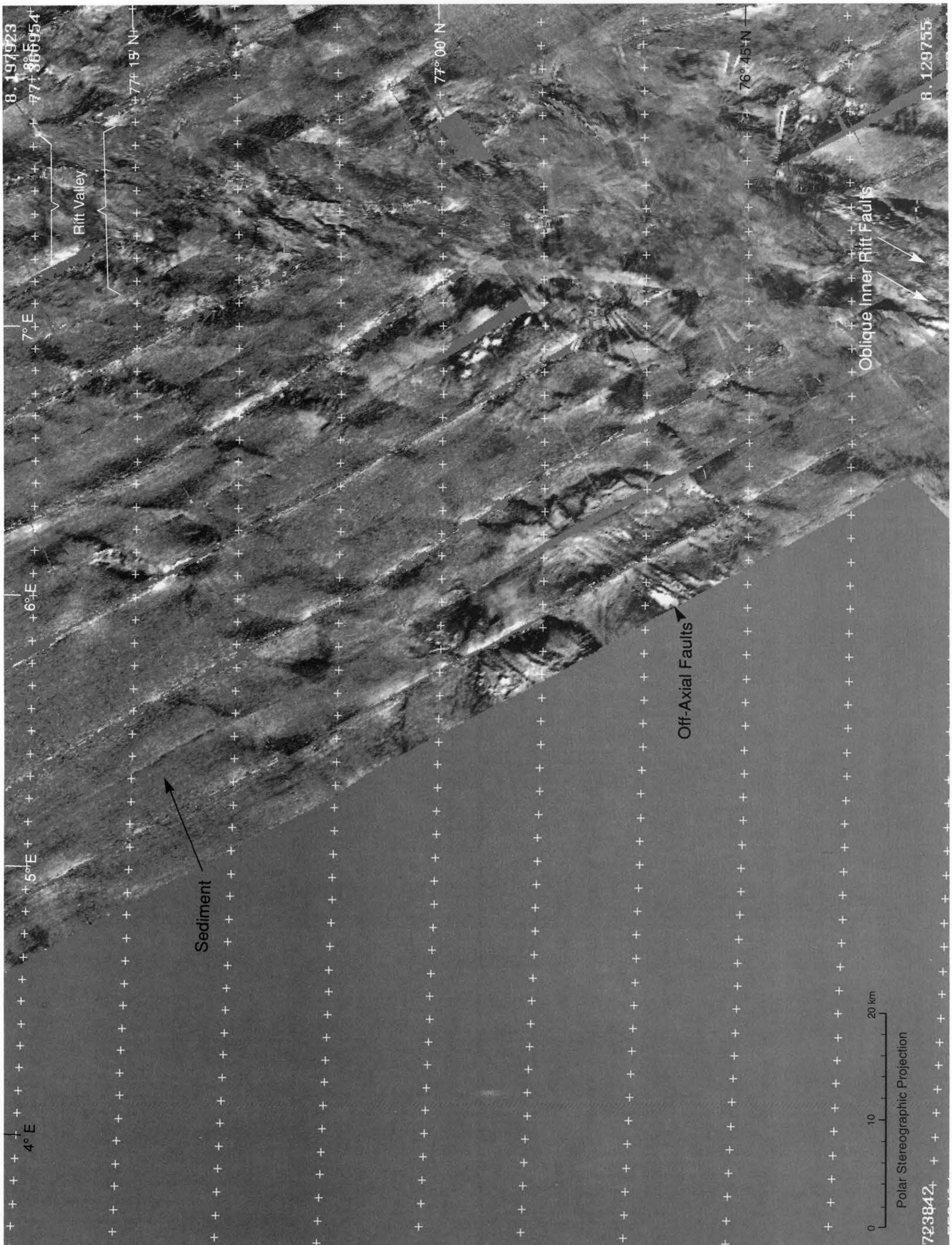

PLATE 33B TILE 19B: SEAMARC II MERGED BATHYMETRIC AND SIDE-LOOKING SONAR DATA

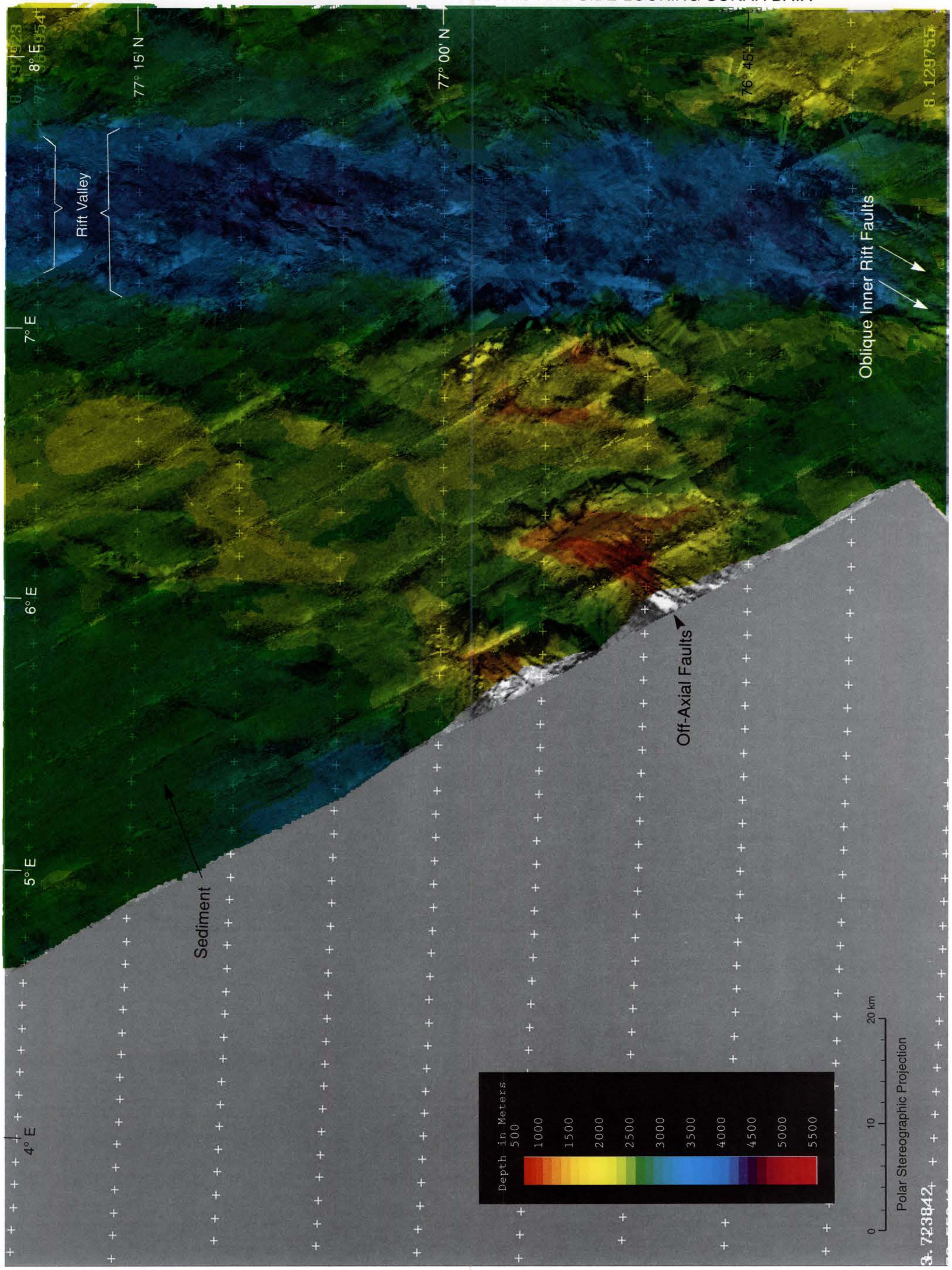

TILE 20A: SEAMARC II SIDE-LOOKING SONAR DATA

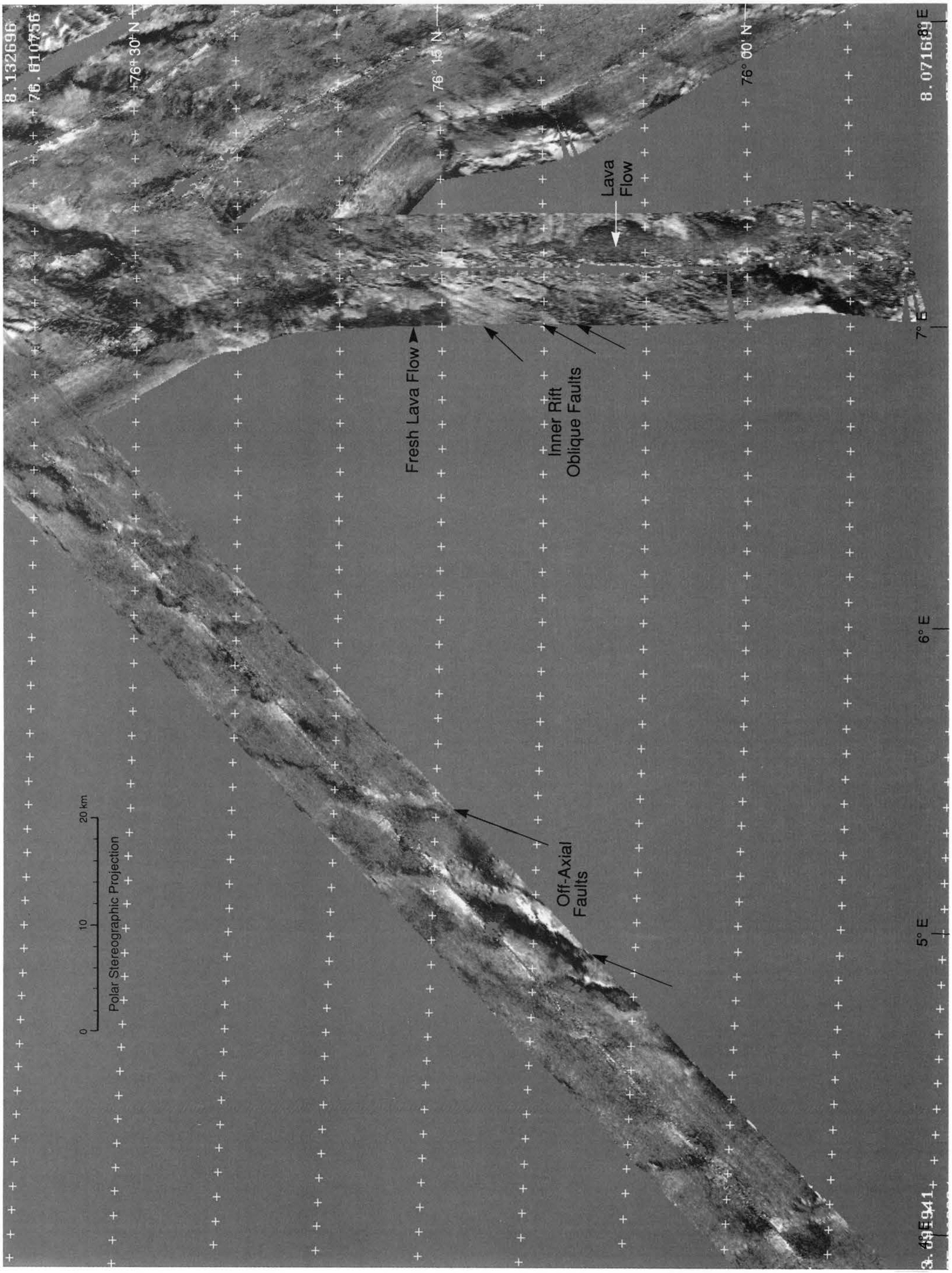

TILE 20B: SEAMARC II MERGED BATHYMETRIC AND SIDE-LOOKING SONAR DATA

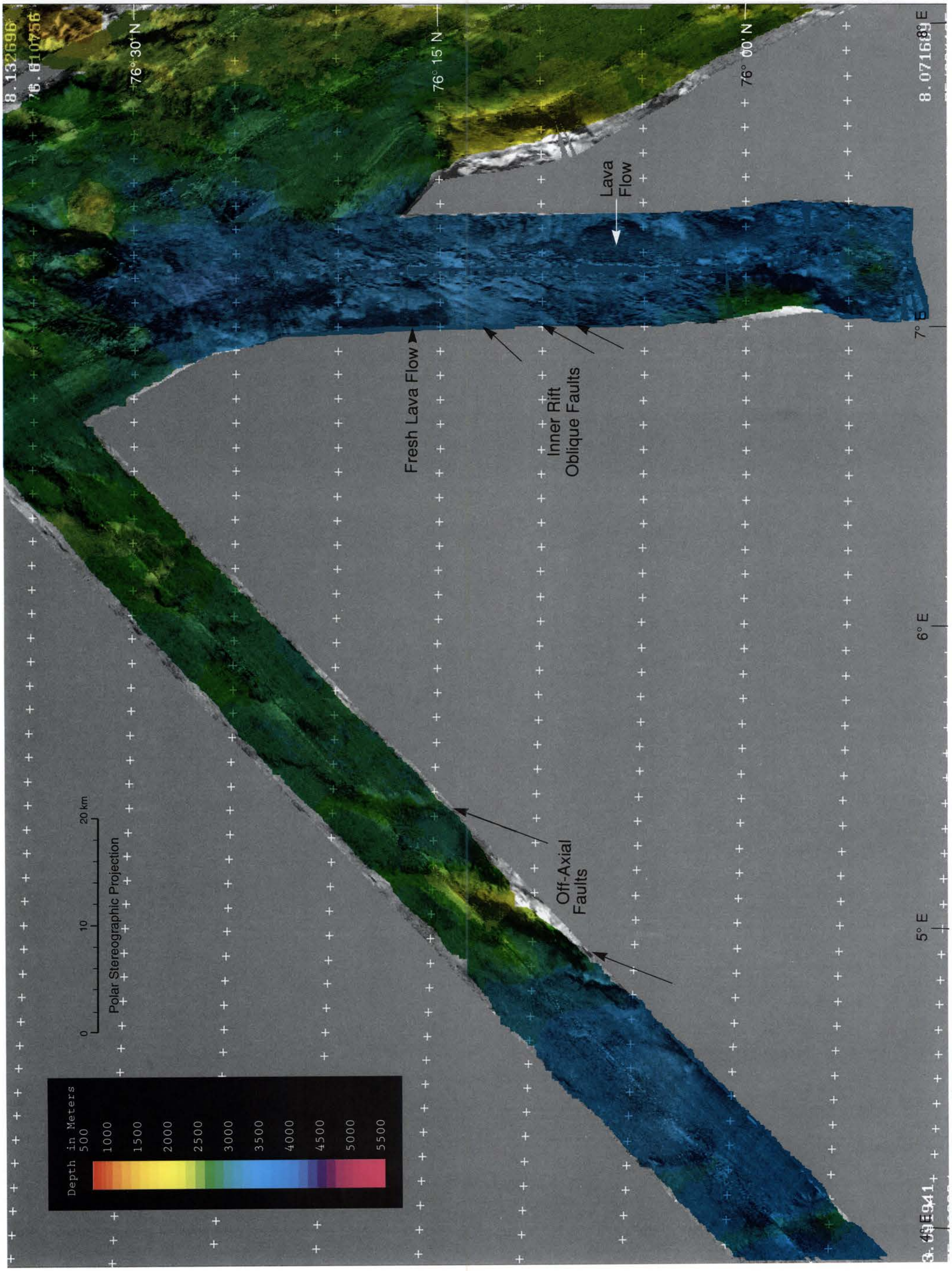

TILE 21A: SEAMARC II SIDE-LOOKING SONAR DATA

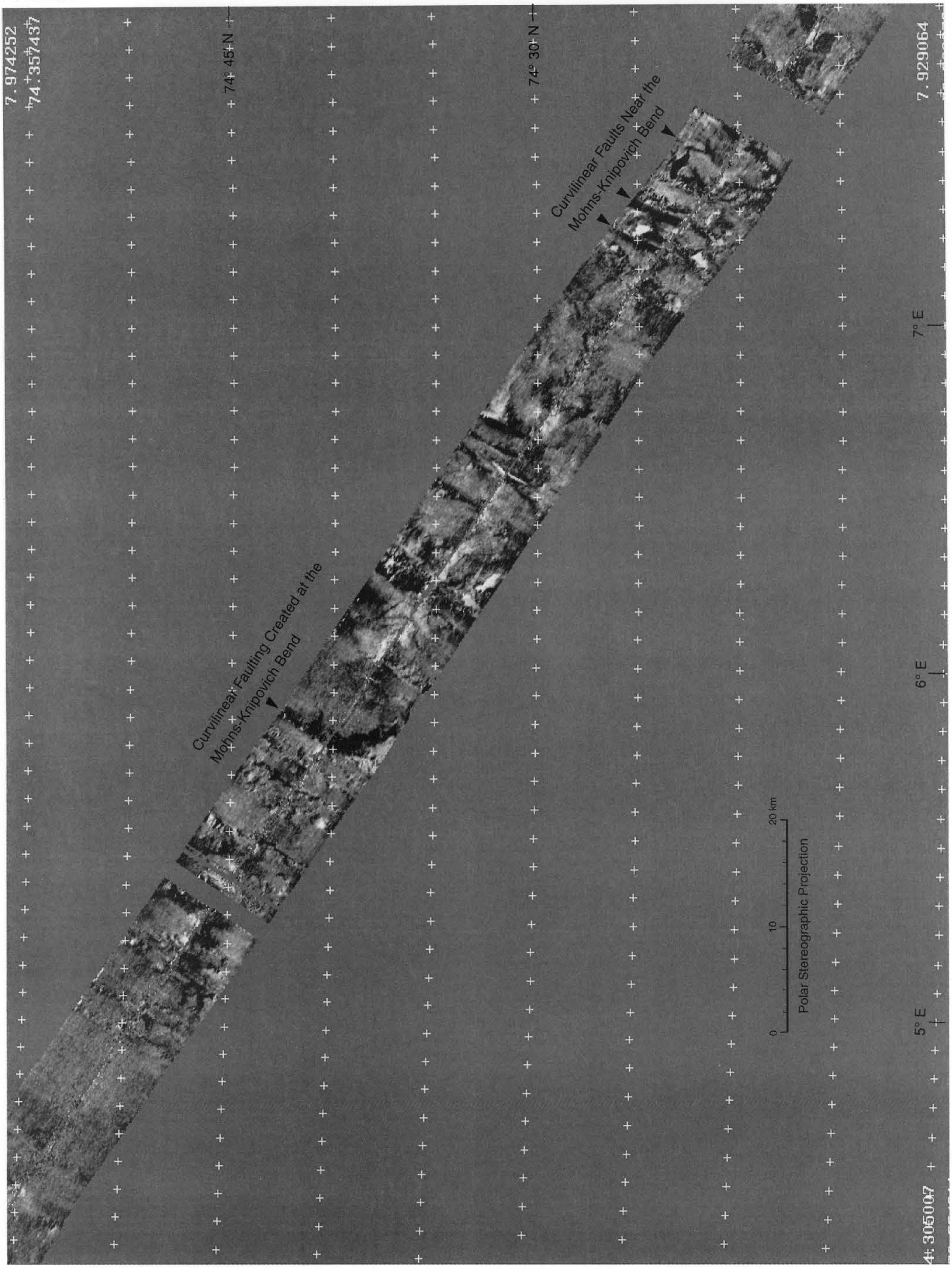

TILE 21B: SEAMARC II MERGED BATHYMETRIC AND SIDE-LOOKING SONAR DATA

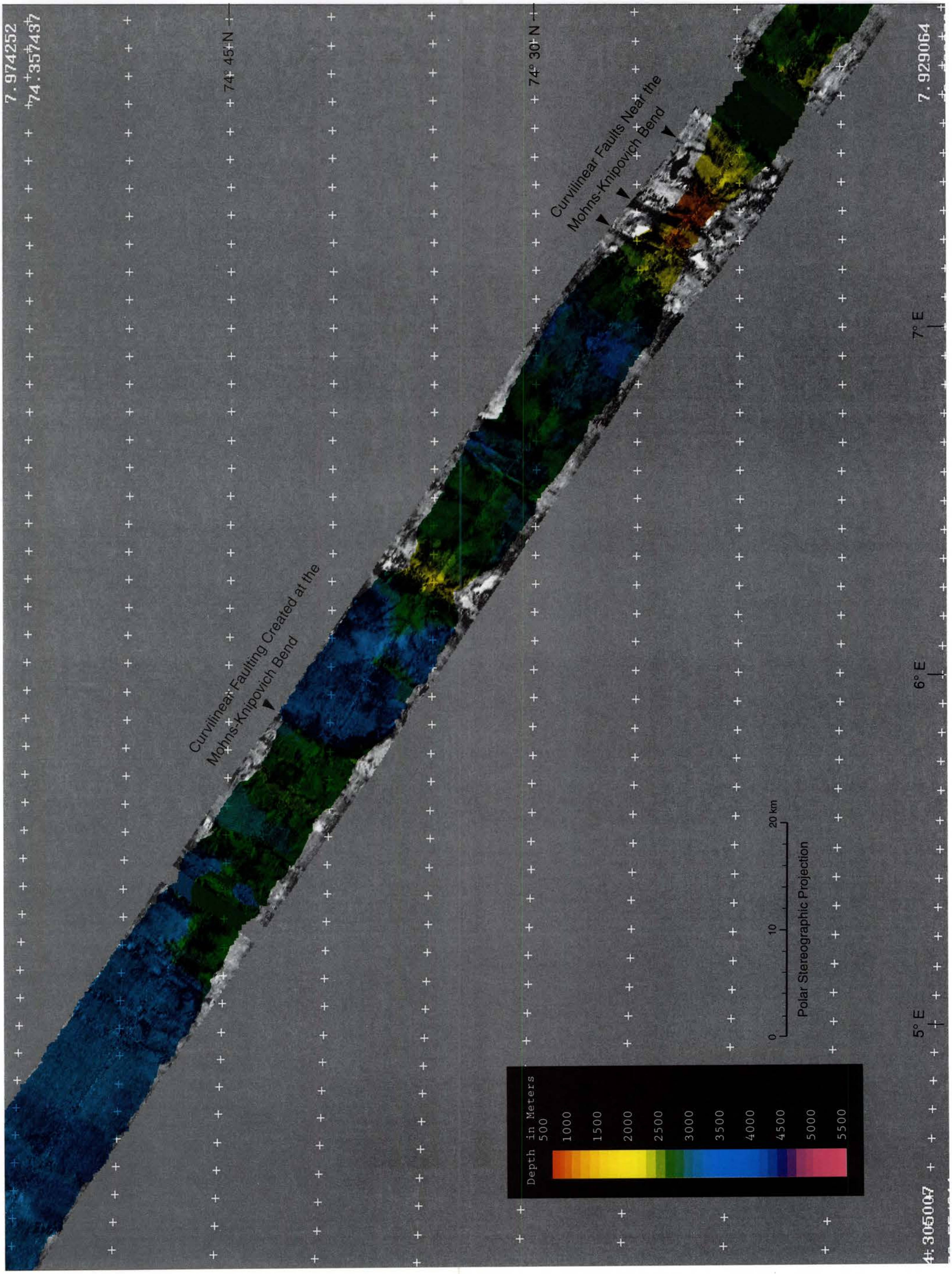

TILE 22A: SEAMARC II SIDE-LOOKING SONAR DATA

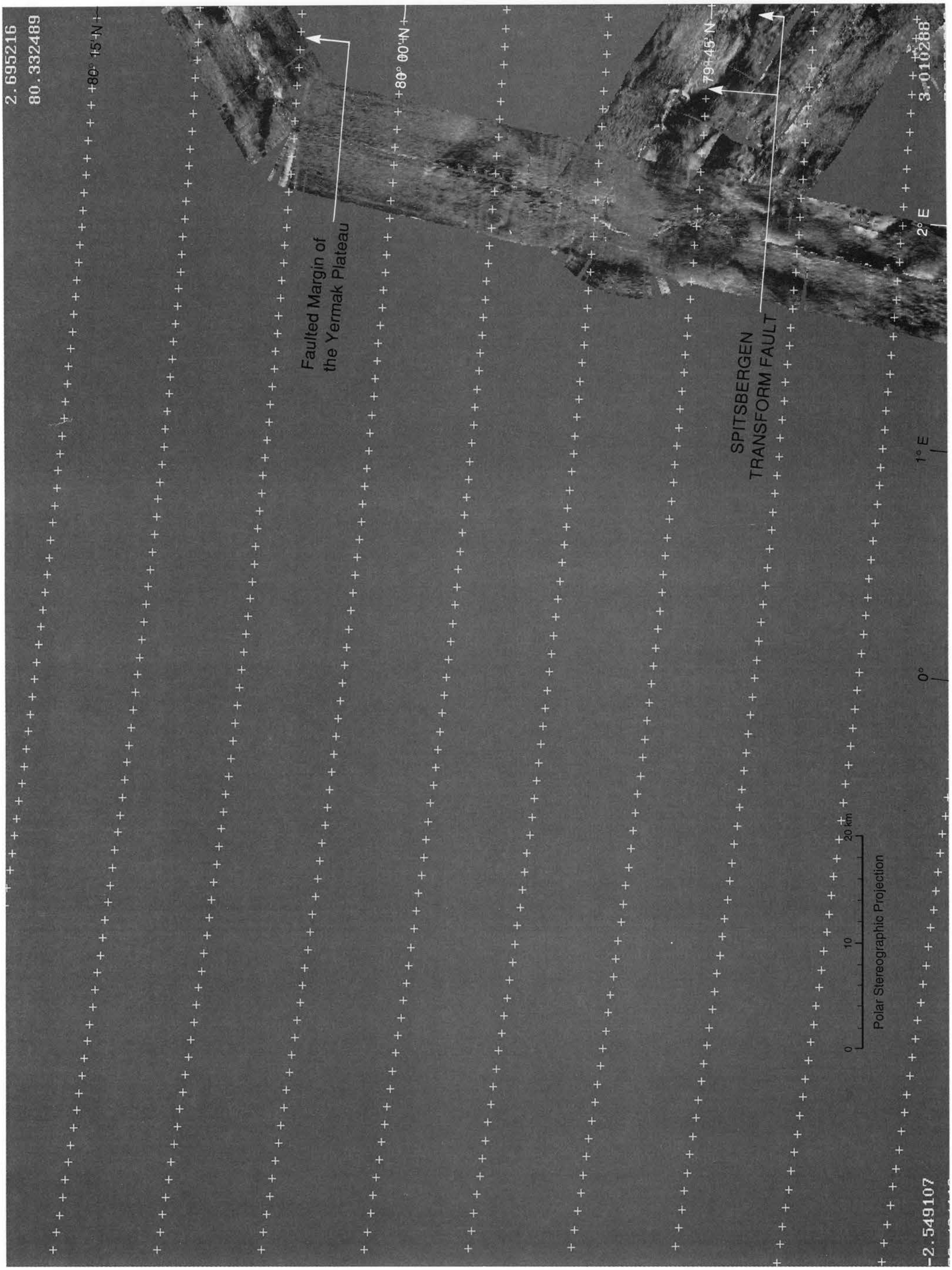

TILE 22B: SEAMARC II MERGED BATHYMETRIC AND SIDE-LOOKING SONAR DATA

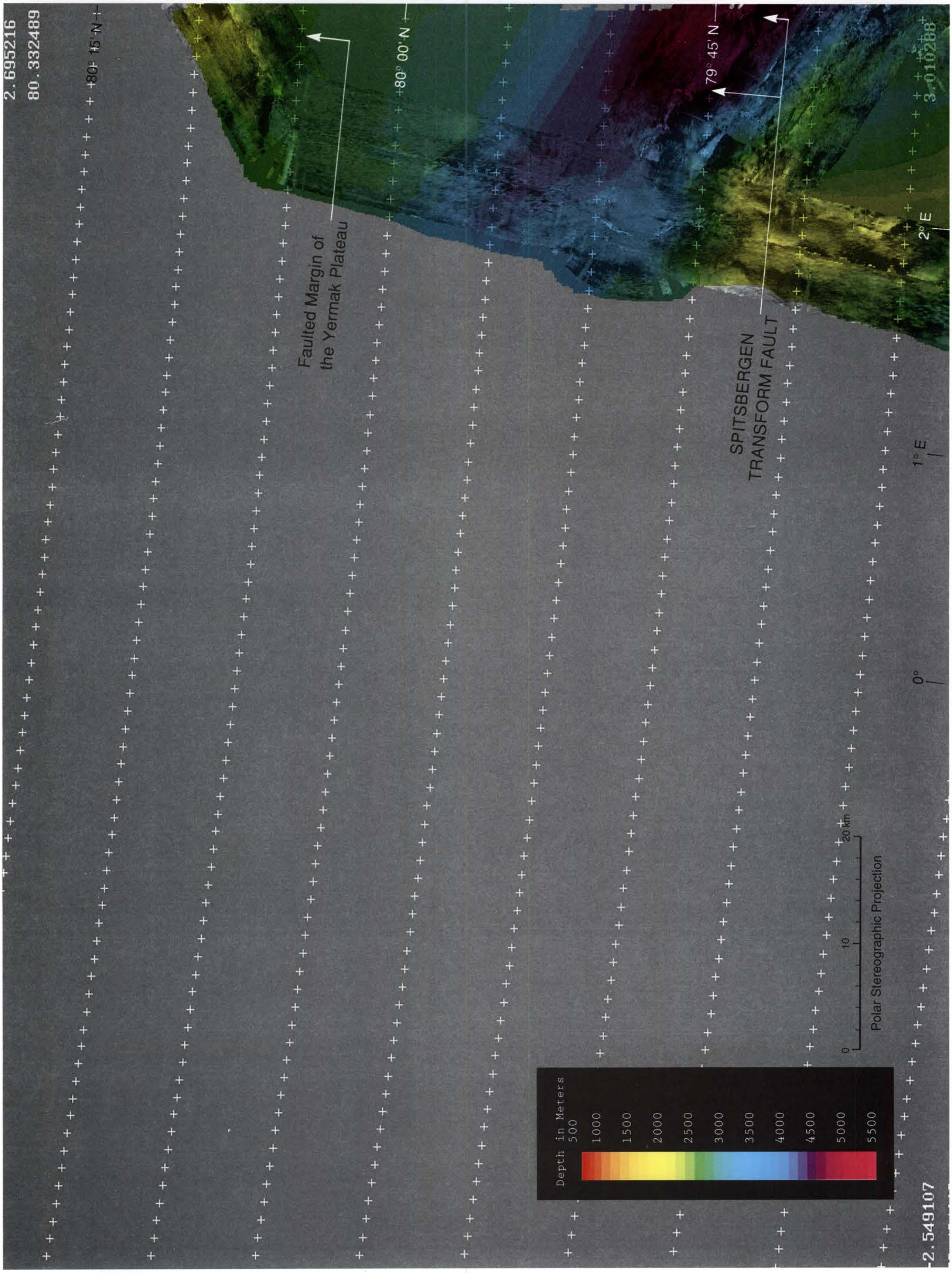

TILE 23A: SEAMARC II SIDE-LOOKING SONAR DATA

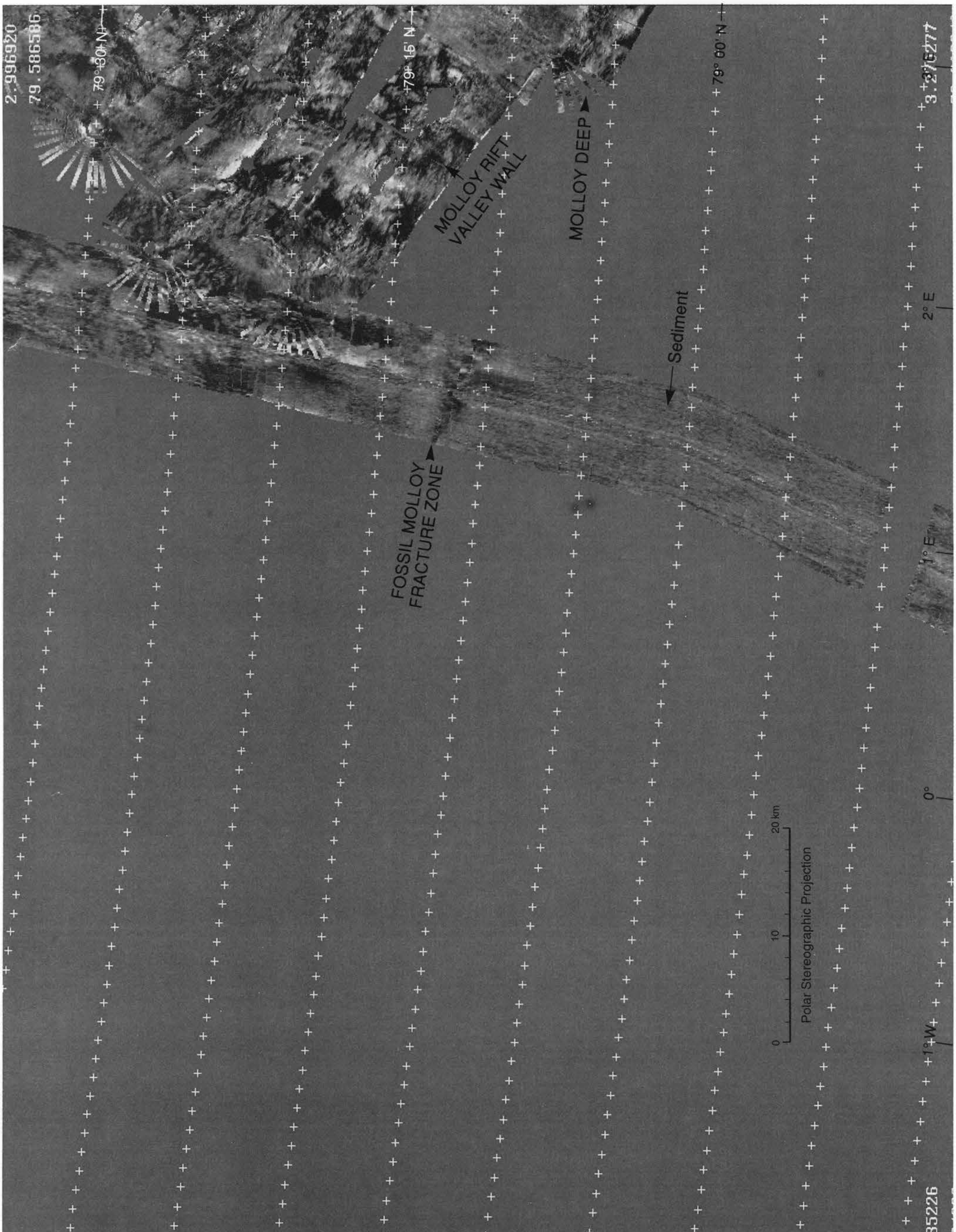

TILE 23B: SEAMARC II MERGED BATHYMETRIC AND SIDE-LOOKING SONAR DATA

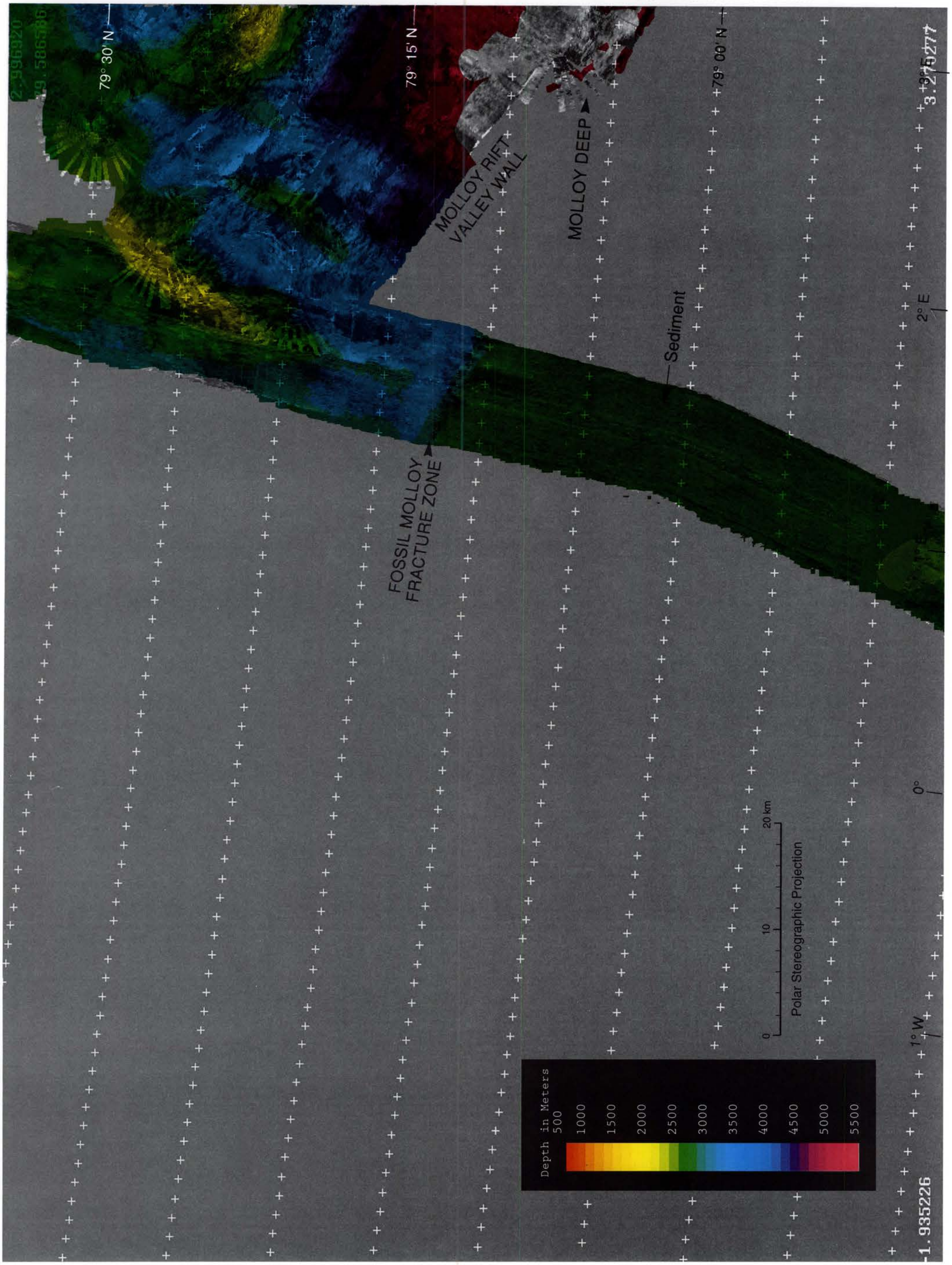

TILE 24A: SEAMARC II SIDE-LOOKING SONAR DATA

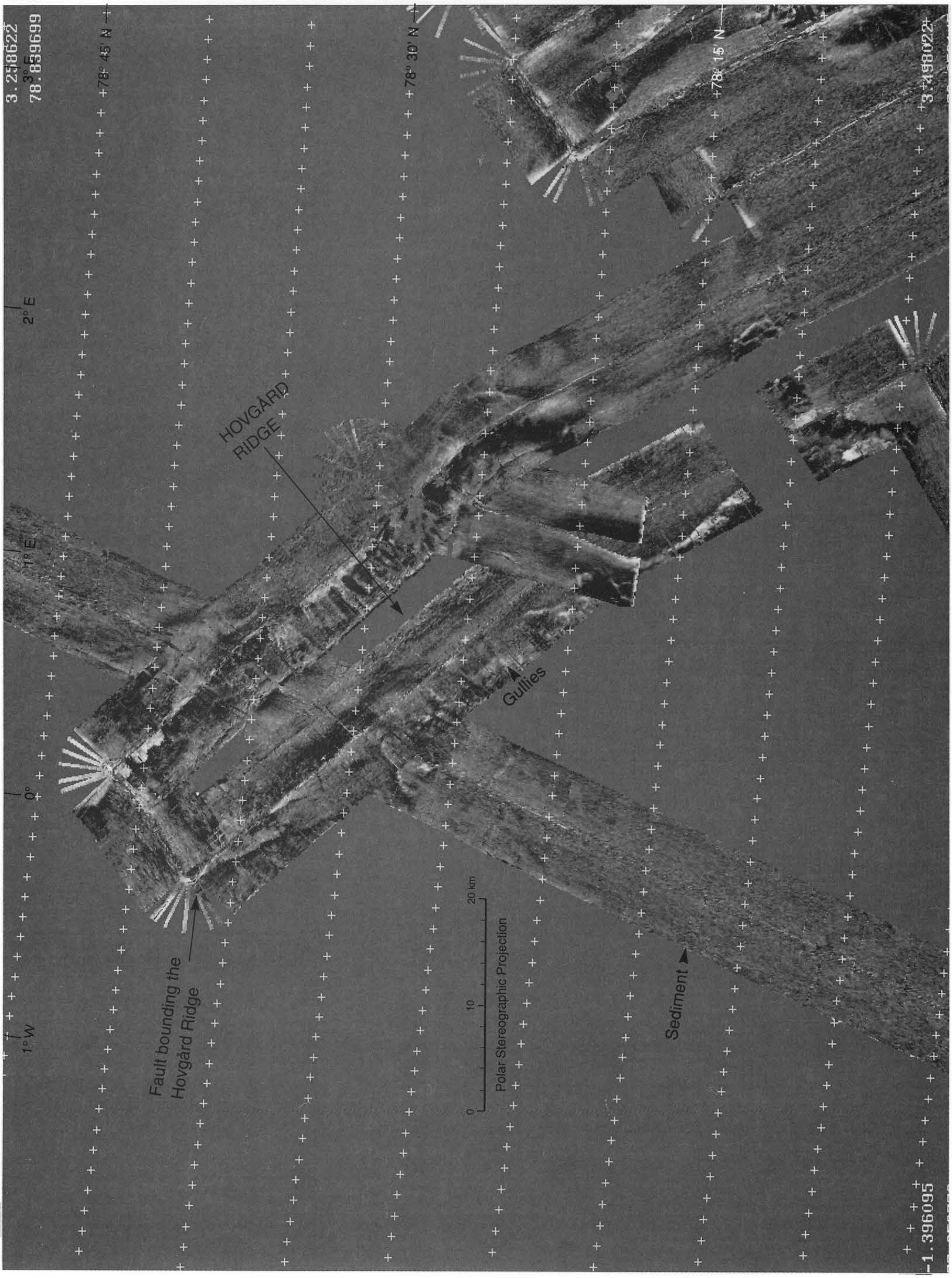

TILE 24B: SEAMARC II MERGED BATHYMETRIC AND SIDE-LOOKING SONAR DATA

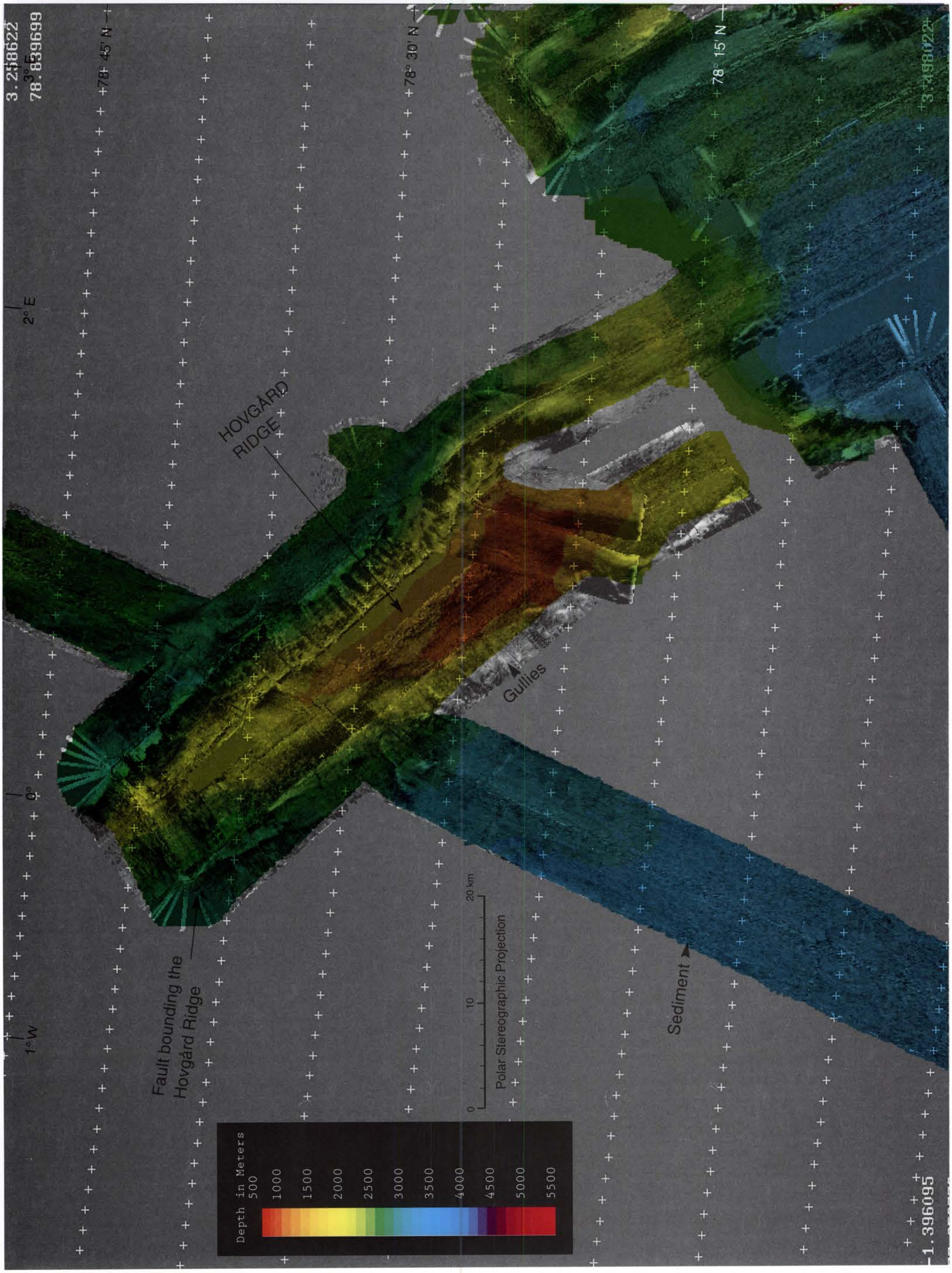

TILE 25A: SEAMARC II SIDE-LOOKING SONAR DATA

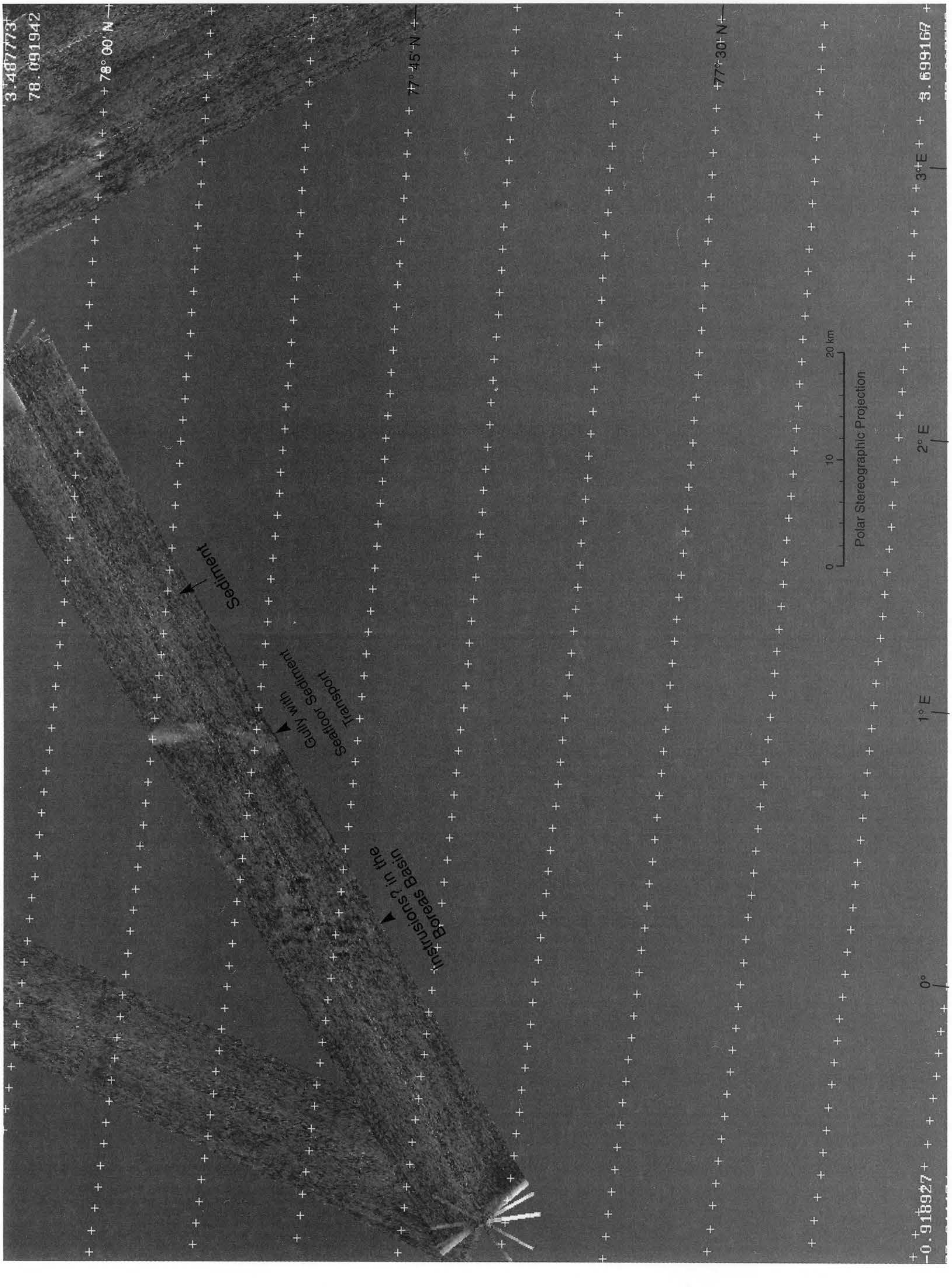

TILE 25B: SEAMARC II MERGED BATHYMETRIC AND SIDE-LOOKING SONAR DATA

TILE 26A: SEAMARC II SIDE-LOOKING SONAR DATA

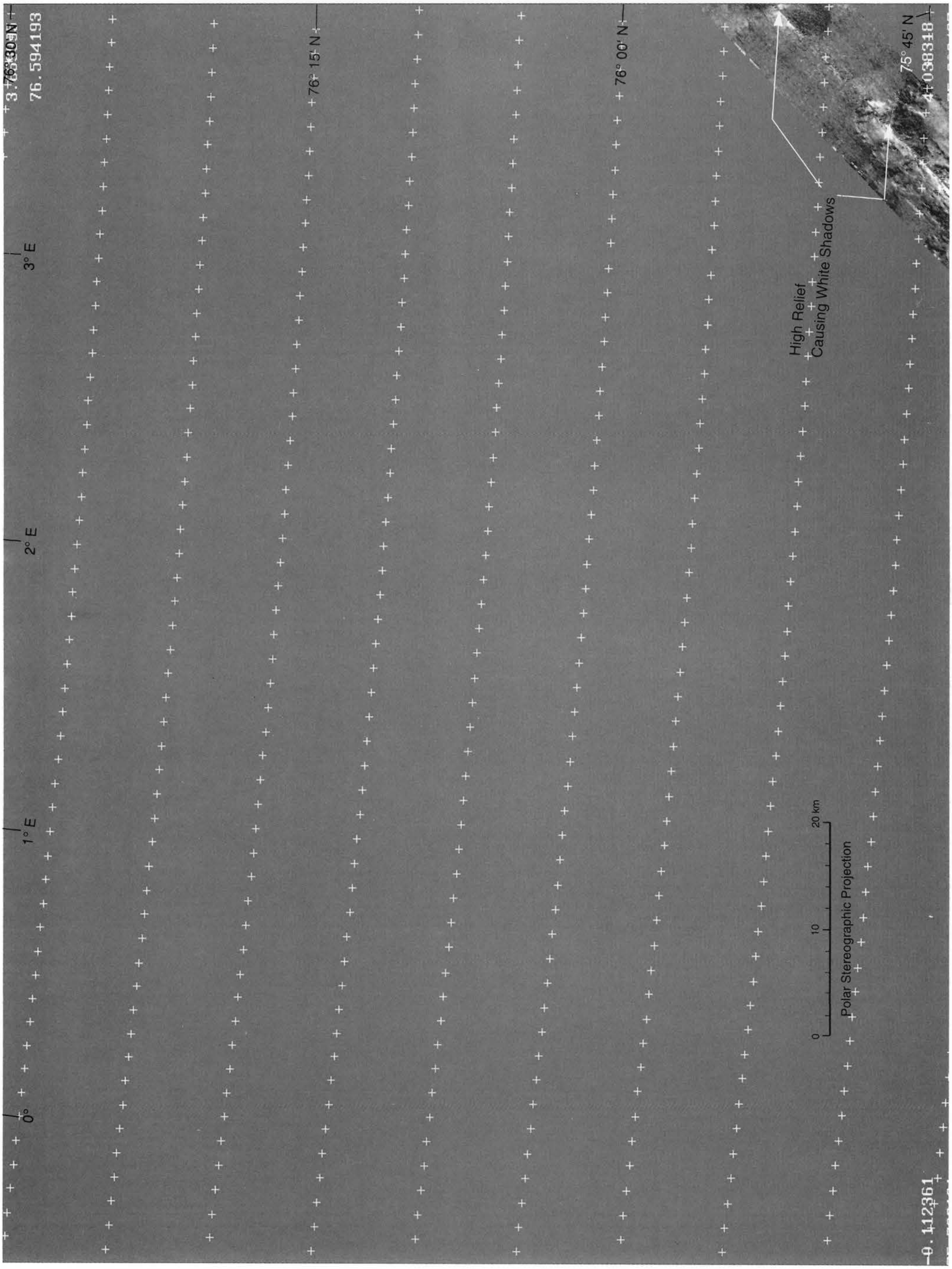

TILE 26B: SEAMARC II MERGED BATHYMETRIC AND SIDE-LOOKING SONAR DATA

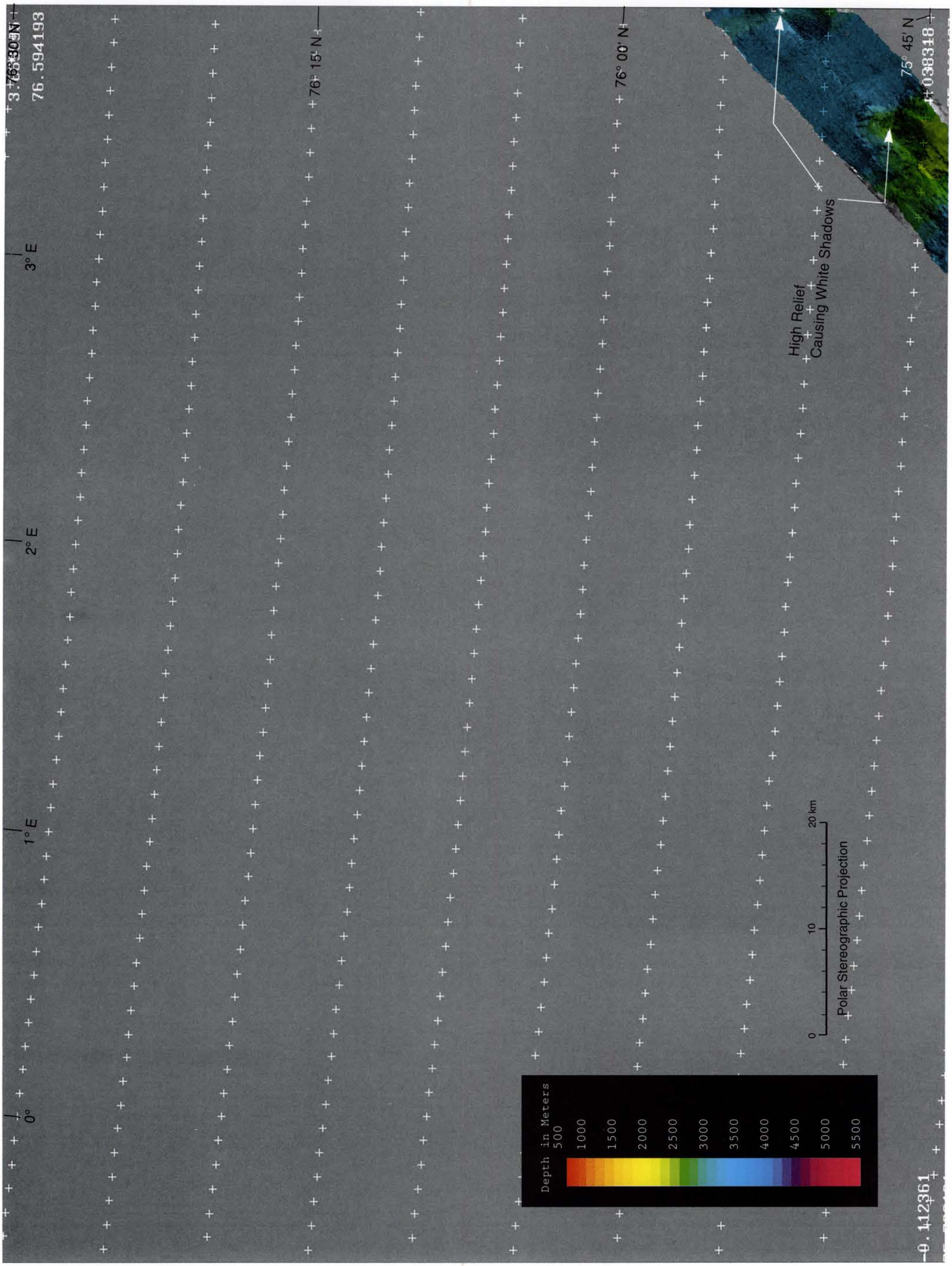

TILE 27A: SEAMARC II SIDE-LOOKING SONAR DATA

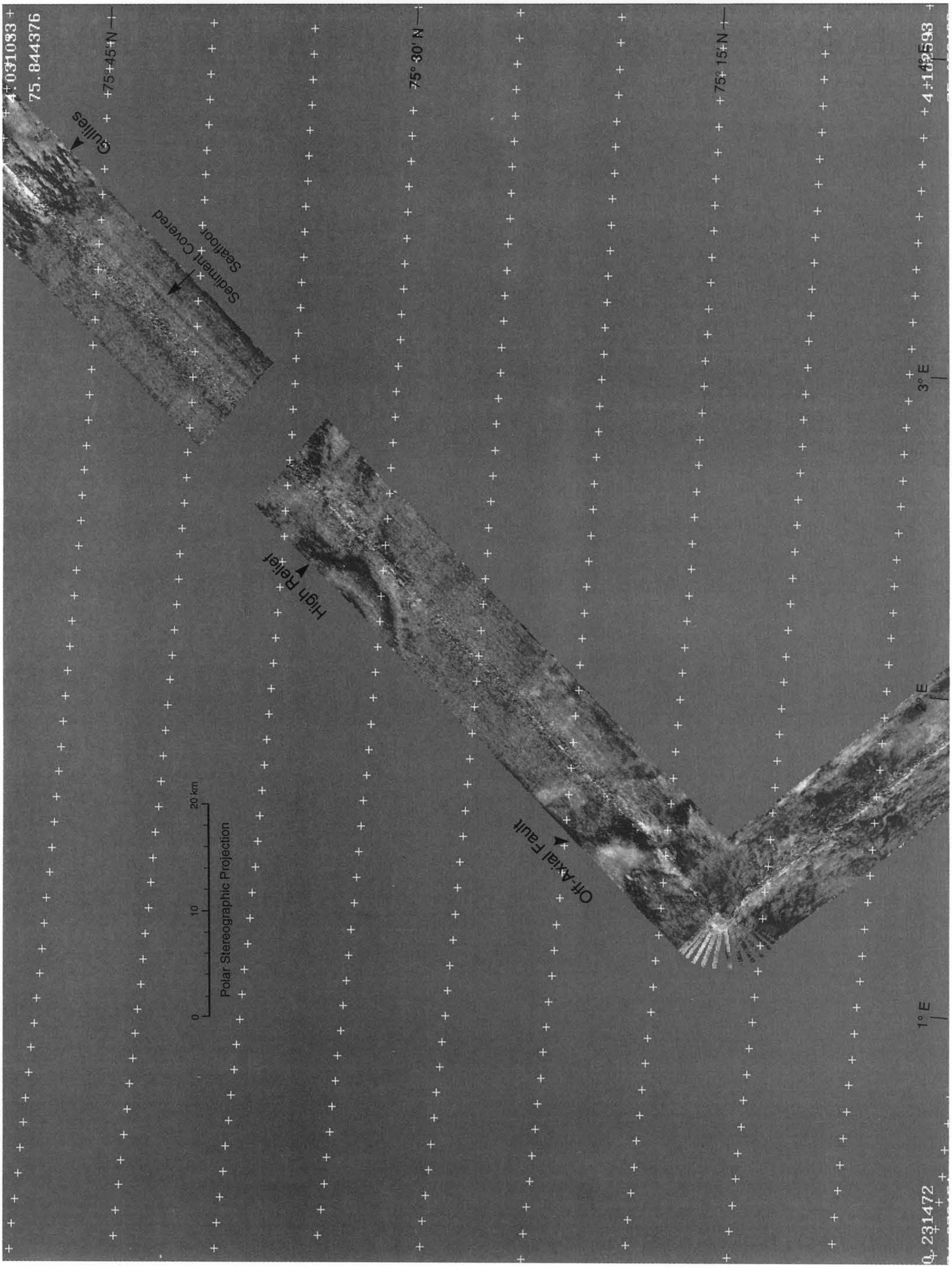

TILE 27B: SEAMARC II MERGED BATHYMETRIC AND SIDE-LOOKING SONAR DATA

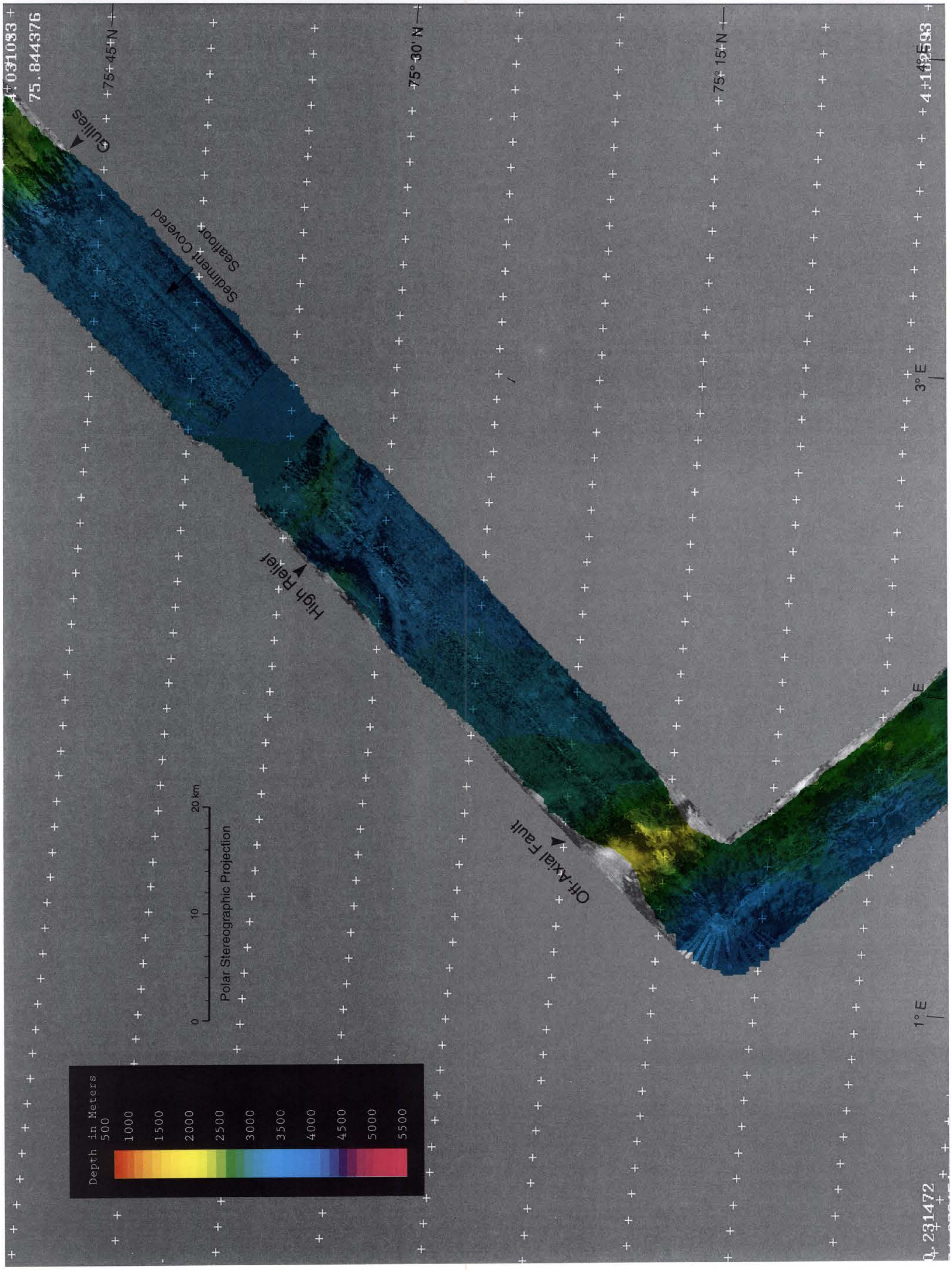

TILE 28A: SEAMARC II SIDE-LOOKING SONAR DATA

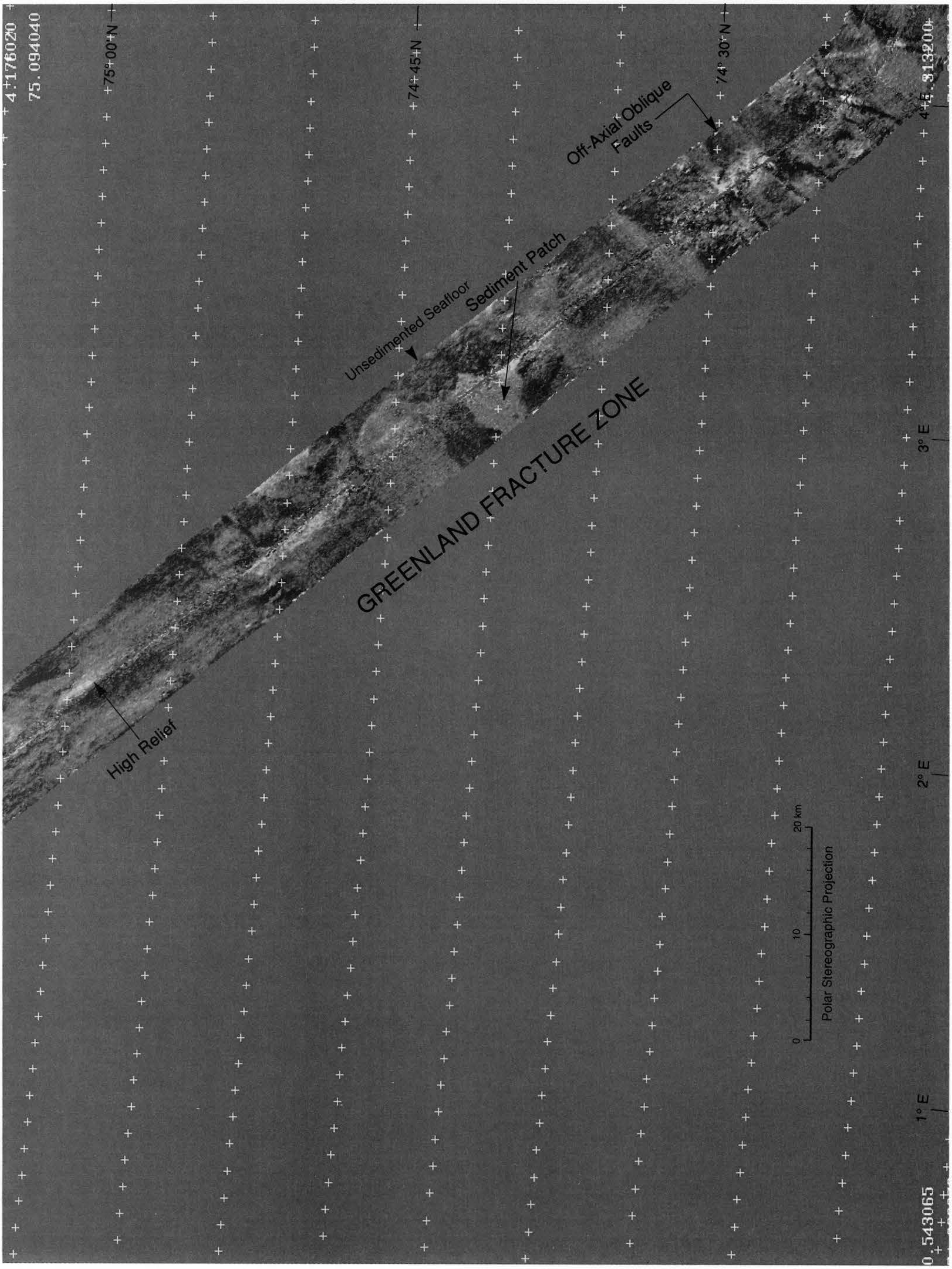

PLATE 42B TILE 28B: SEAMARC II MERGED BATHYMETRIC AND SIDE-LOOKING SONAR DATA

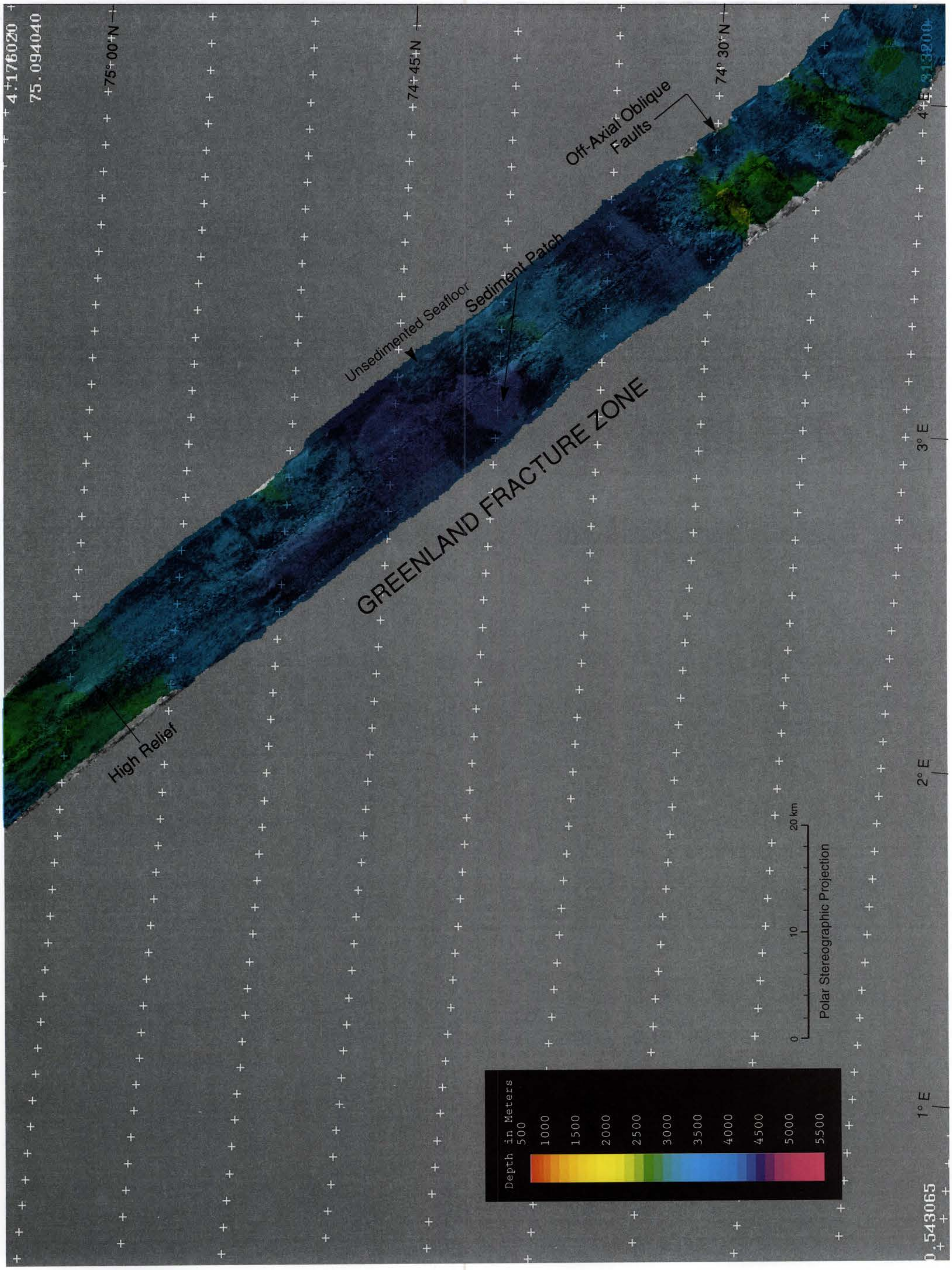

TILE 29A: SEAMARC II SIDE-LOOKING SONAR DATA

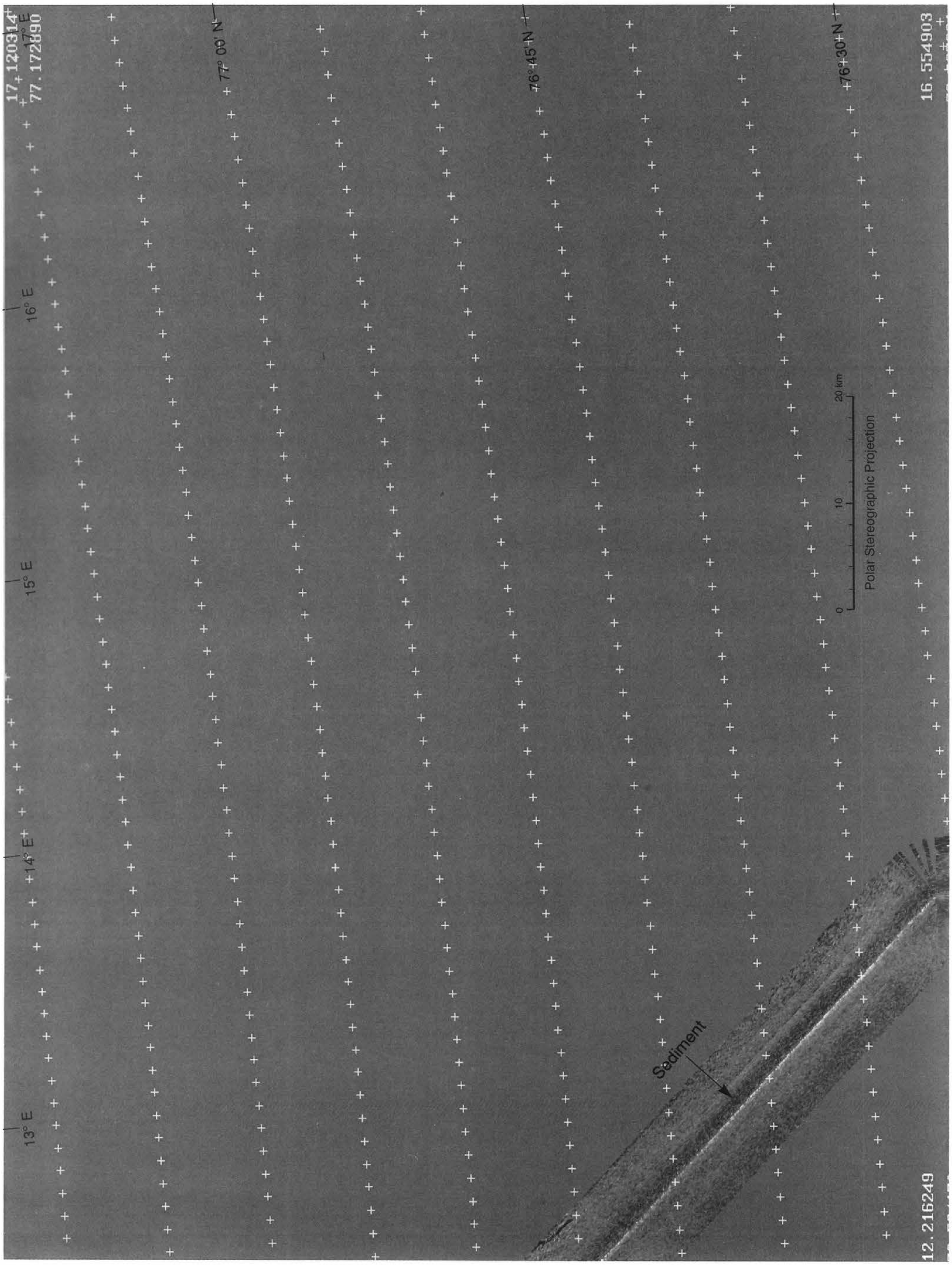

TILE 29B: SEAMARC II MERGED BATHYMETRIC AND SIDE-LOOKING SONAR DATA

TILE 30A: SEAMARC II SIDE-LOOKING SONAR DATA

TILE 30B: SEAMARC II MERGED BATHYMETRIC AND SIDE-LOOKING SONAR DATA

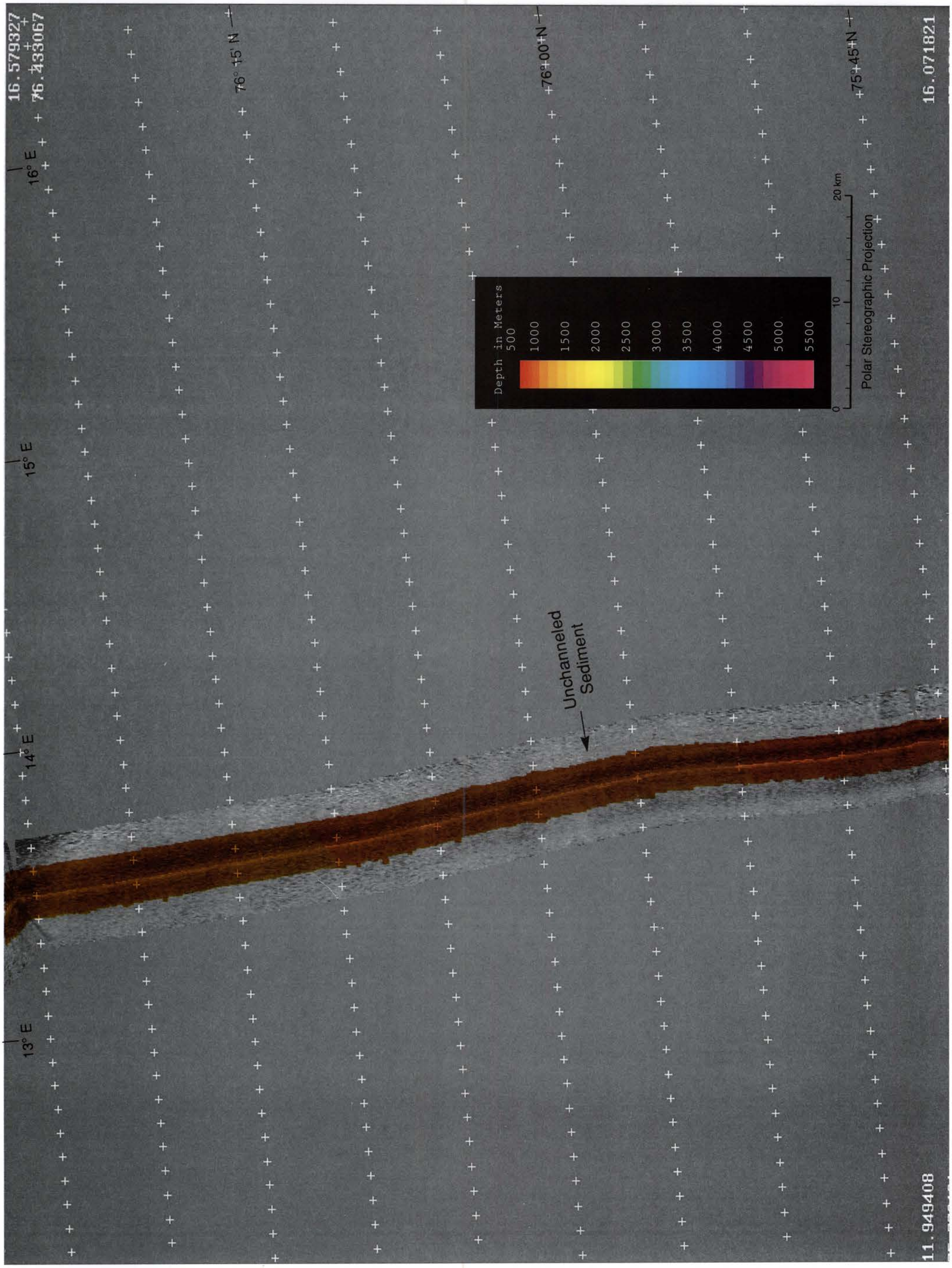

TILE 31A: SEAMARC II SIDE-LOOKING SONAR DATA

TILE 31B: SEAMARC II MERGED BATHYMETRIC AND SIDE-LOOKING SONAR DATA

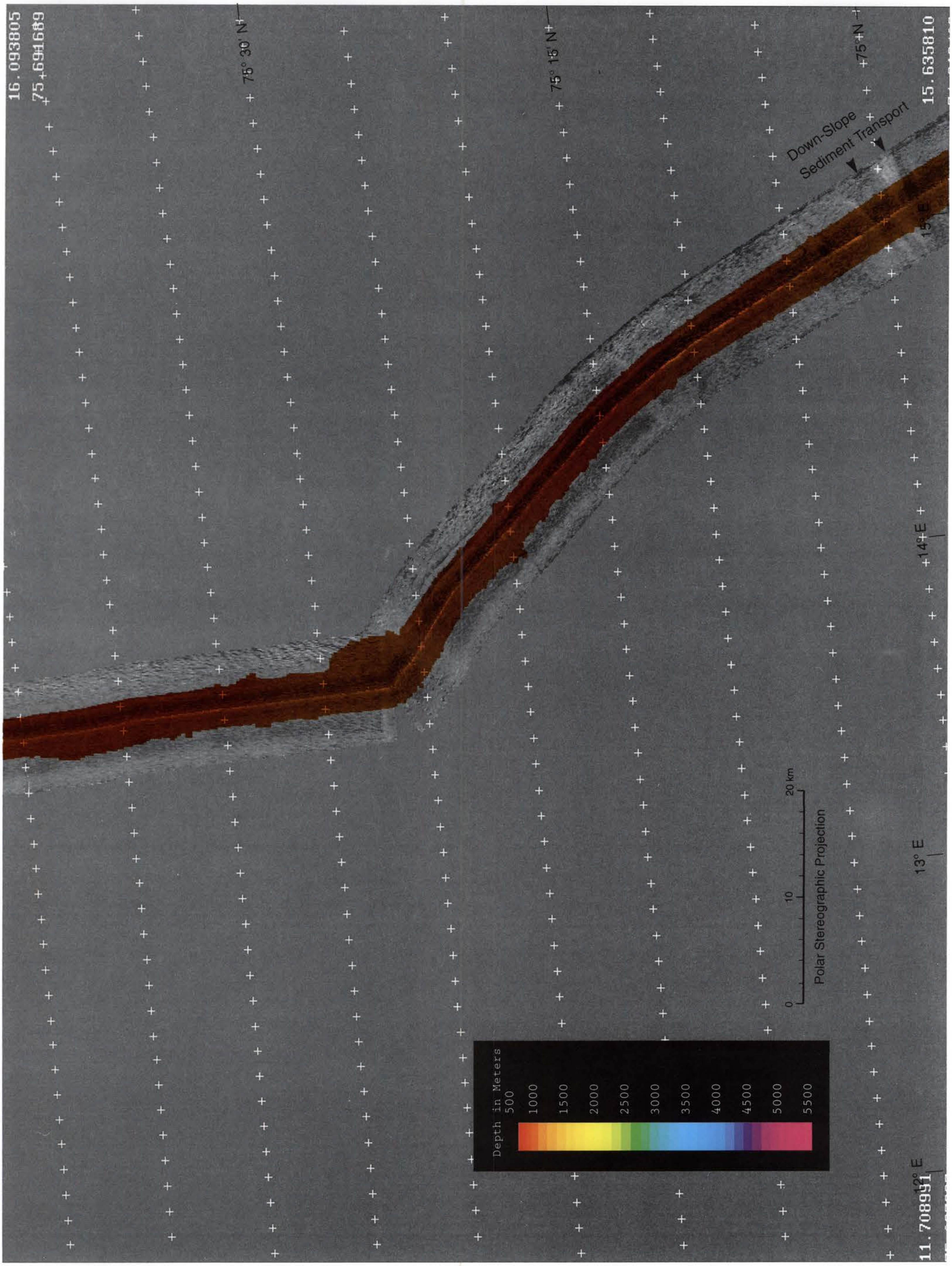

TILE 32A: SEAMARC II SIDE-LOOKING SONAR DATA

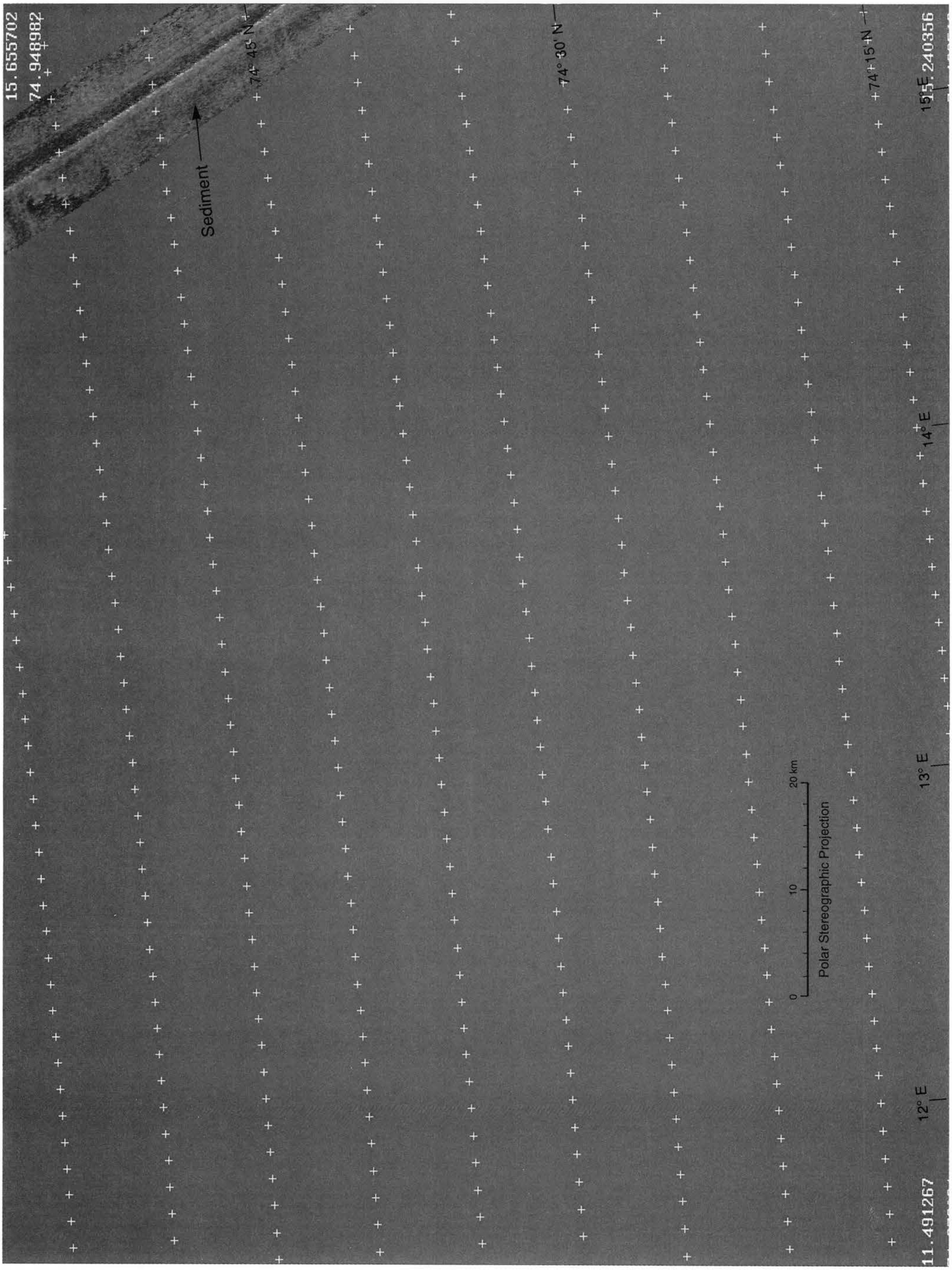

PLATE 46B

TILE 32B: SEAMARC II MERGED BATHYMETRIC AND SIDE-LOOKING SONAR DATA

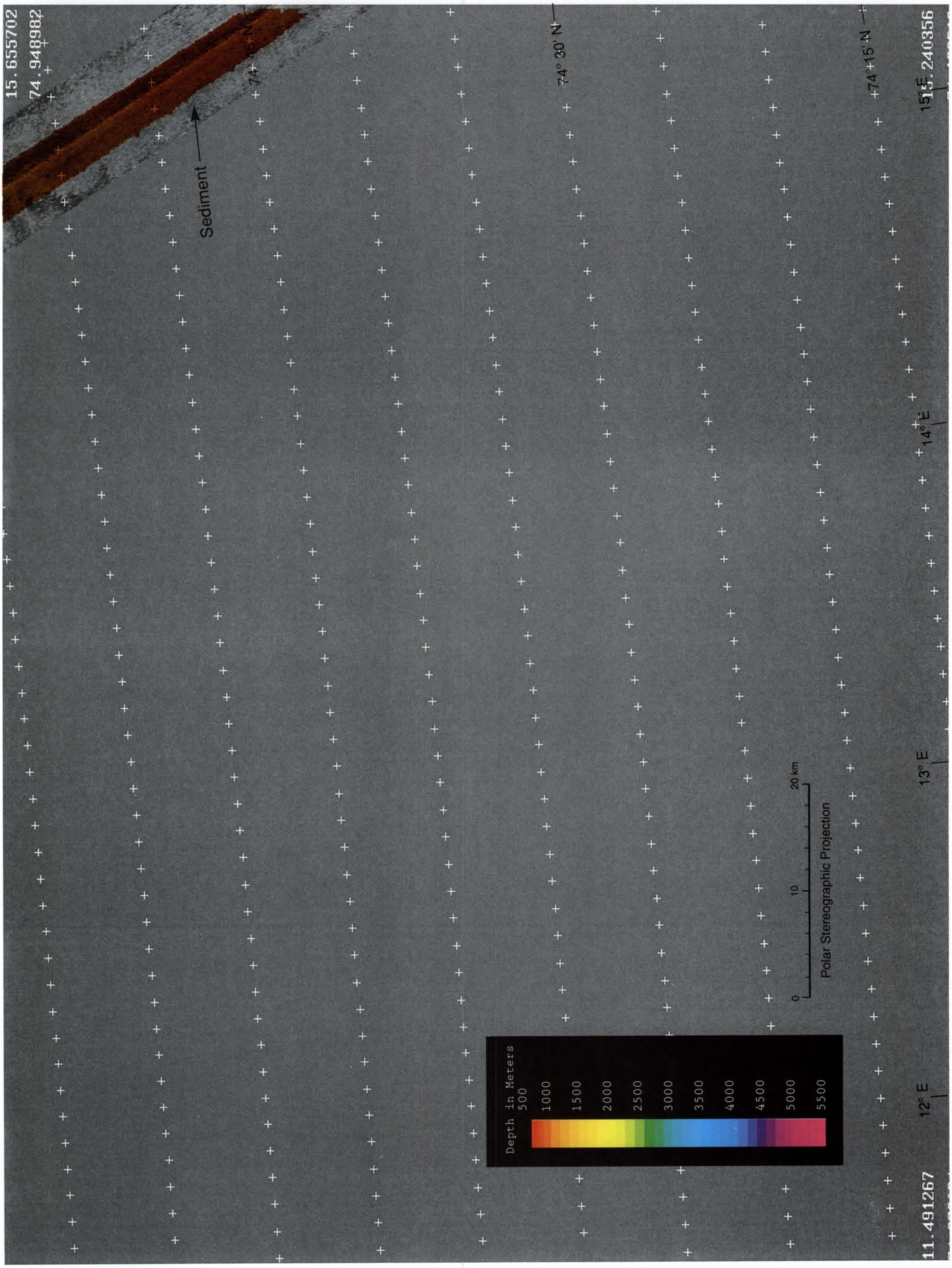

TILE 33A: SEAMARC II SIDE-LOOKING SONAR DATA

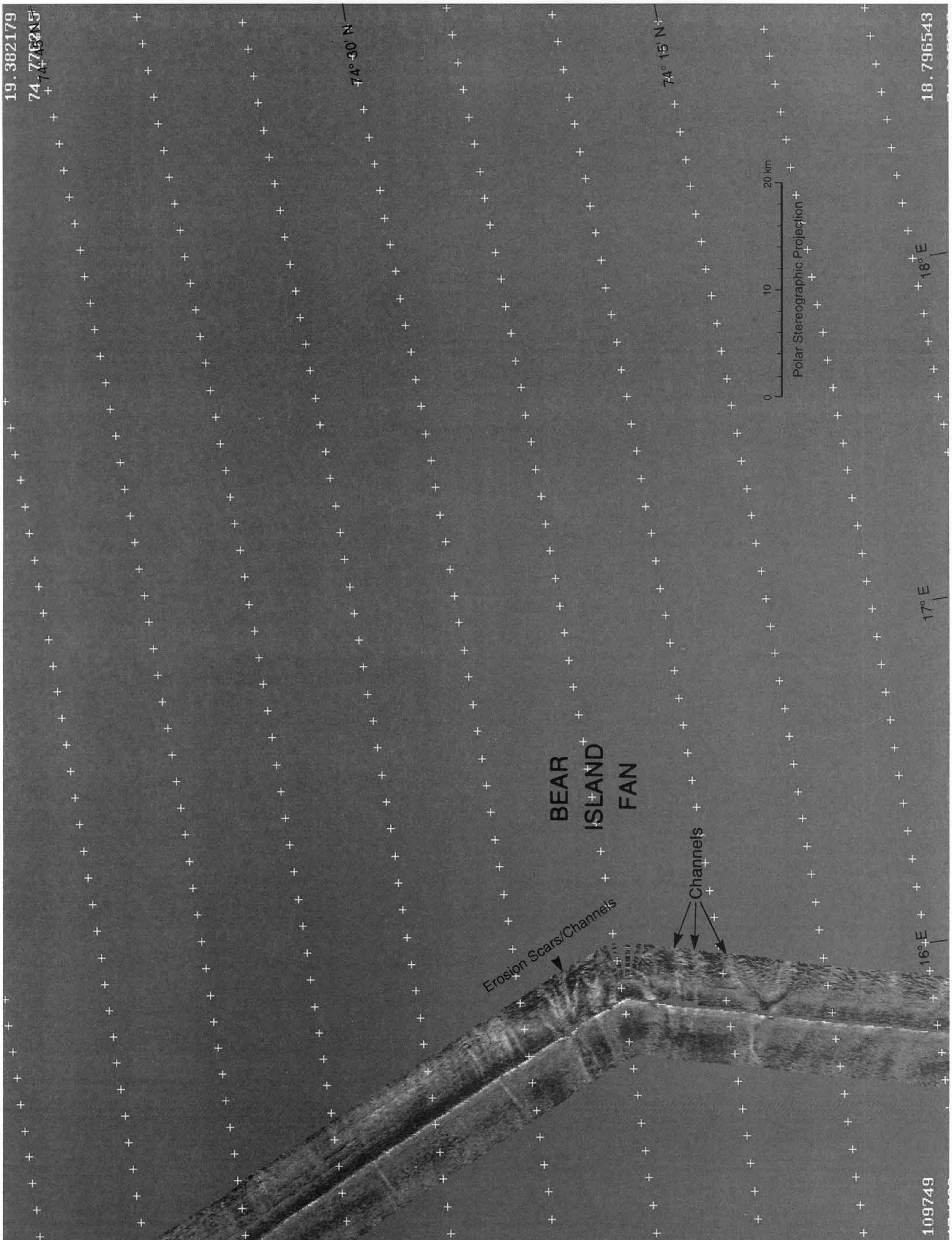

TILE 33B: SEAMARC II MERGED BATHYMETRIC AND SIDE-LOOKING SONAR DATA

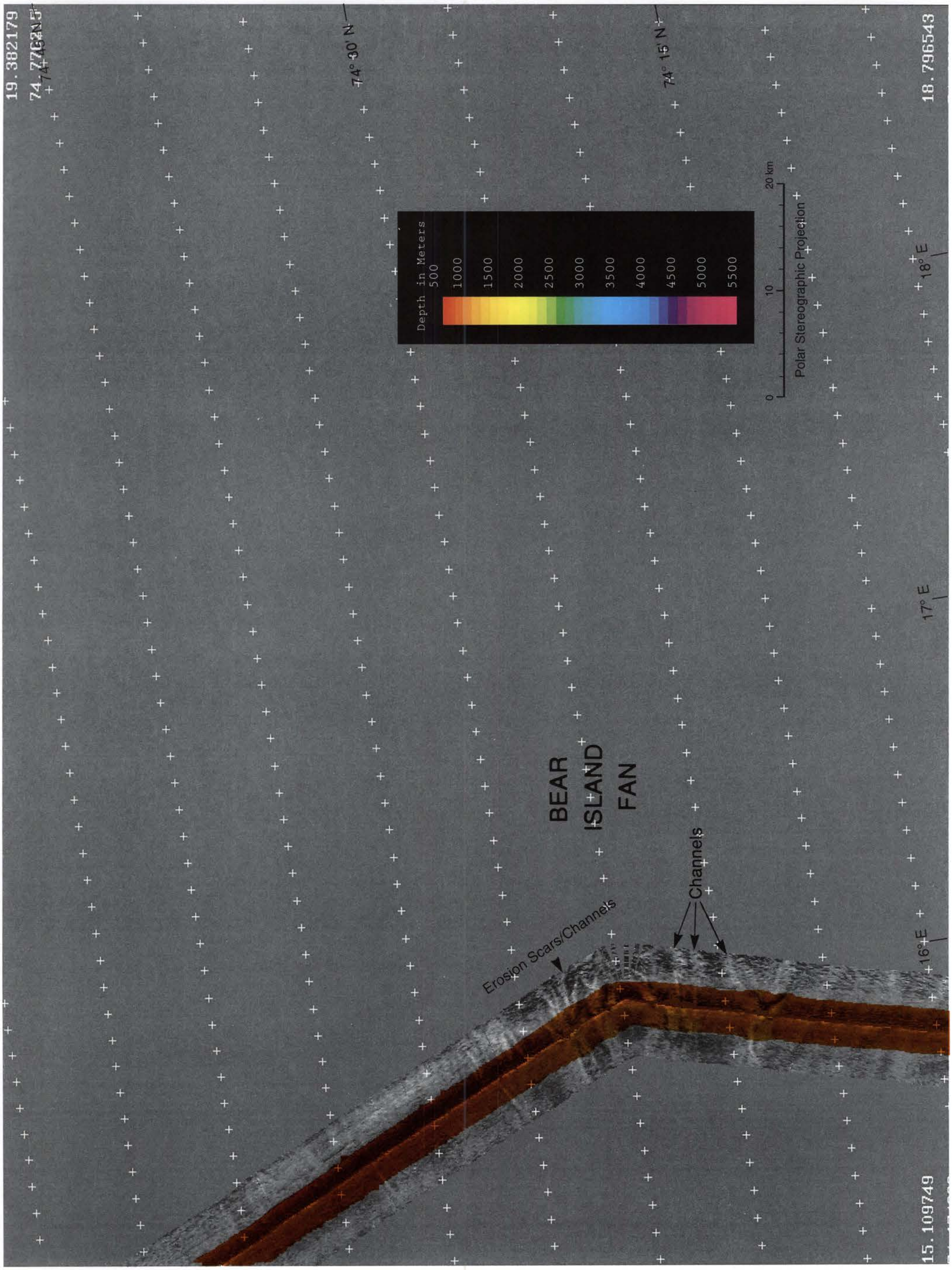

TILE 34A: SEAMARC II SIDE-LOOKING SONAR DATA

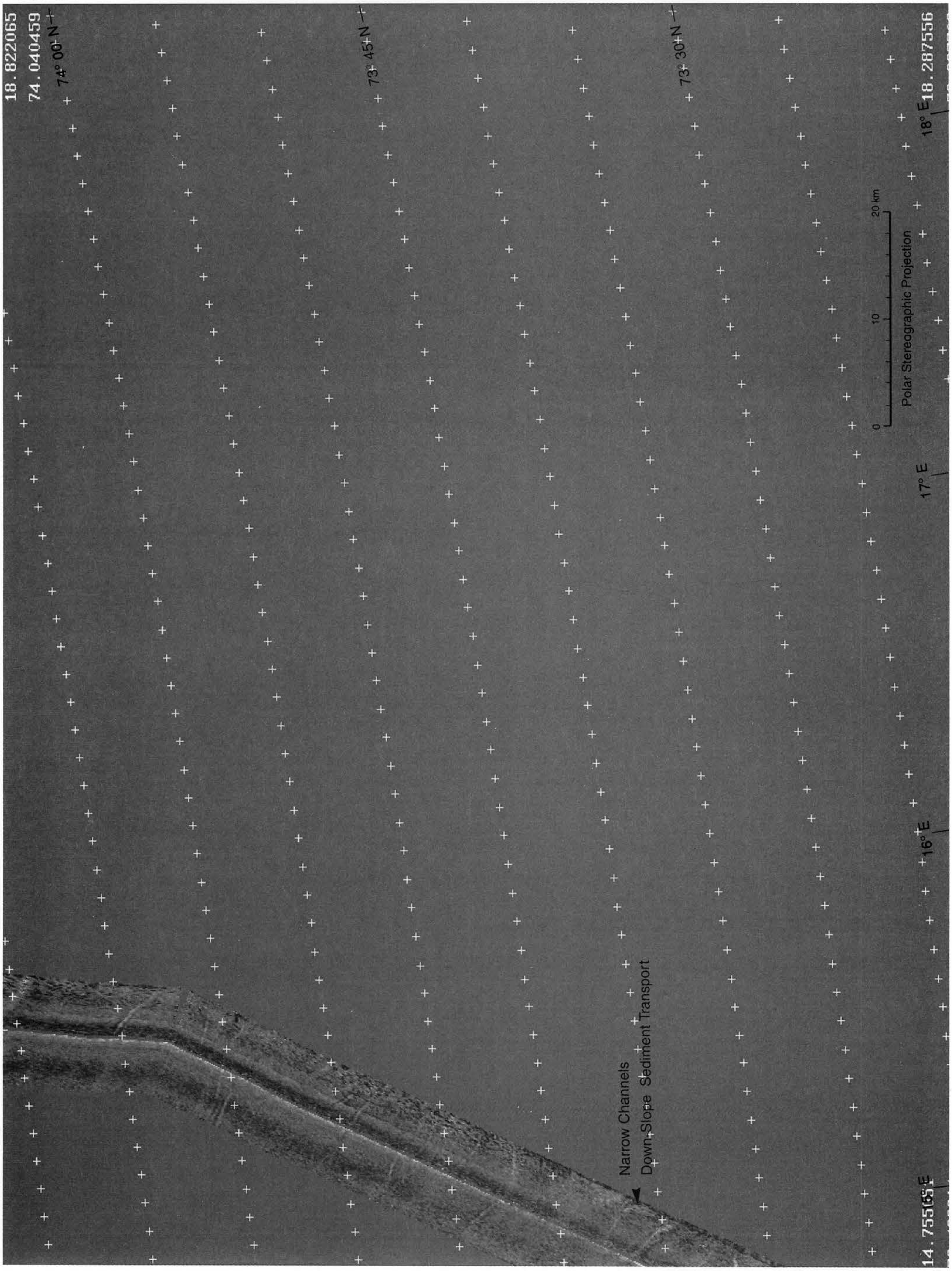

PLATE 48B TILE 34B: SEAMARC II MERGED BATHYMETRIC AND SIDE-LOOKING SONAR DATA

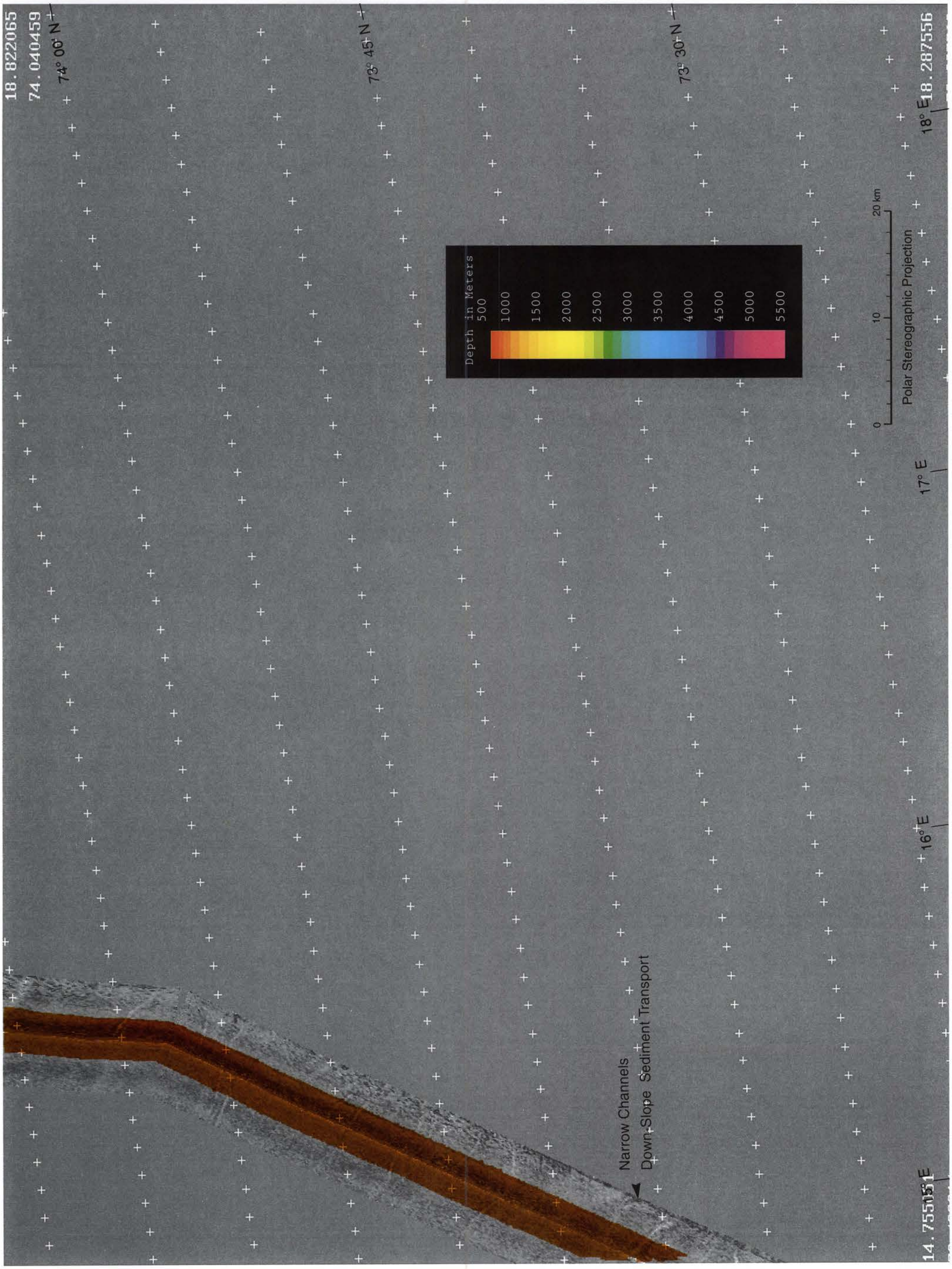

TILE 35A: SEAMARC II SIDE-LOOKING SONAR DATA

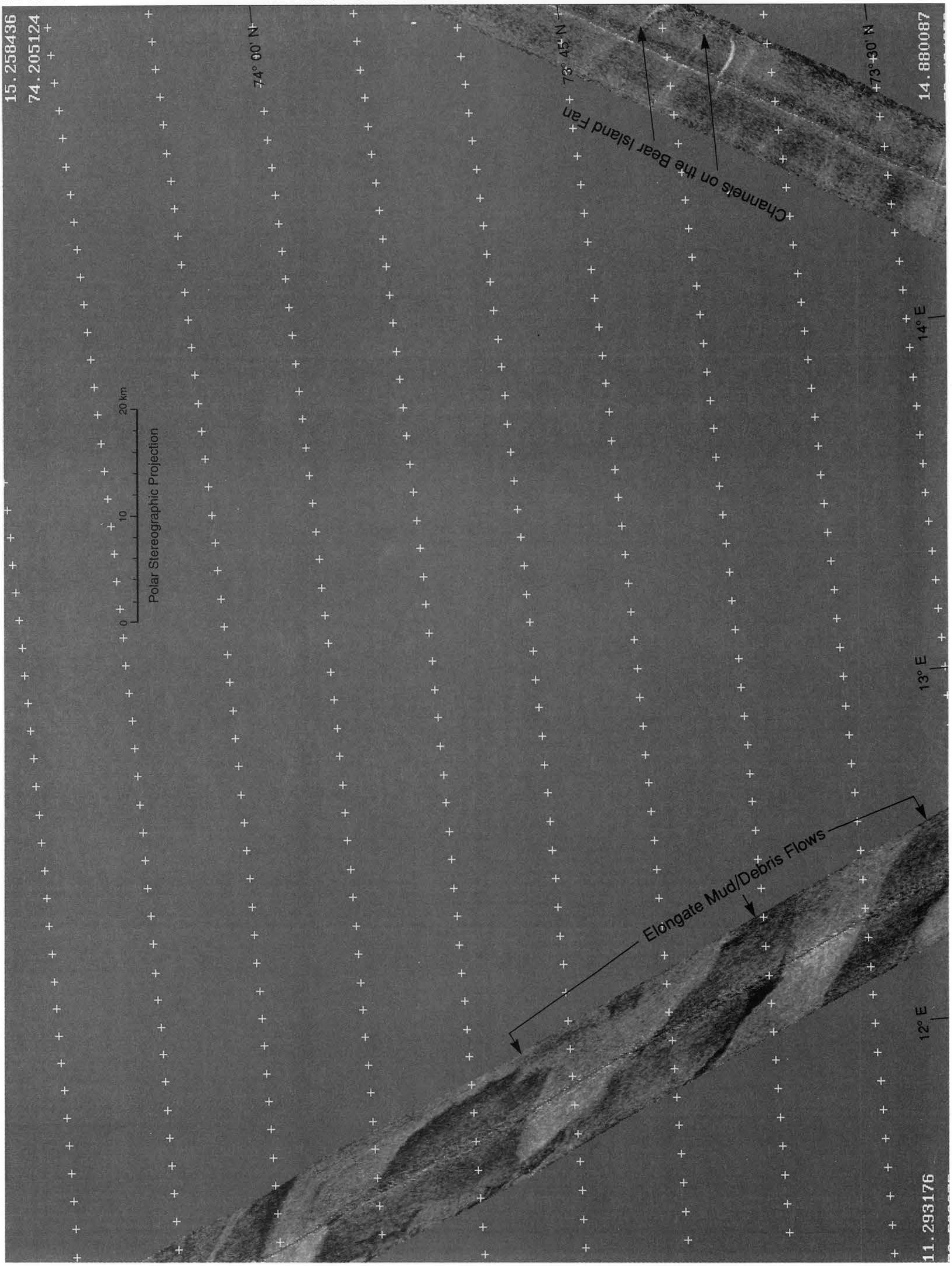

PLATE 49B TILE 35B: SEAMARC II MERGED BATHYMETRIC AND SIDE-LOOKING SONAR DATA

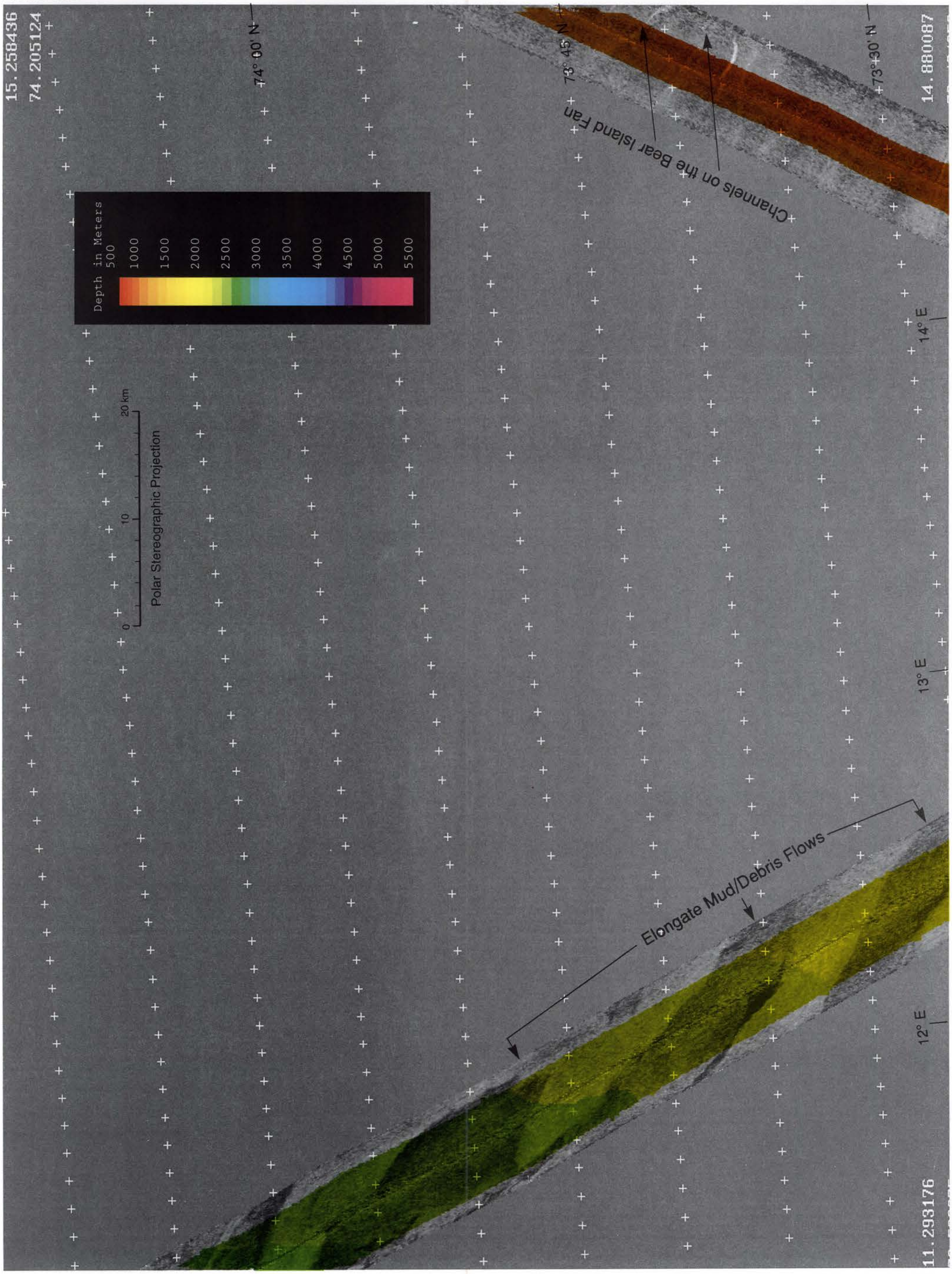

PLATE 50A

TILE 36A: SEAMARC II SIDE-LOOKING SONAR DATA

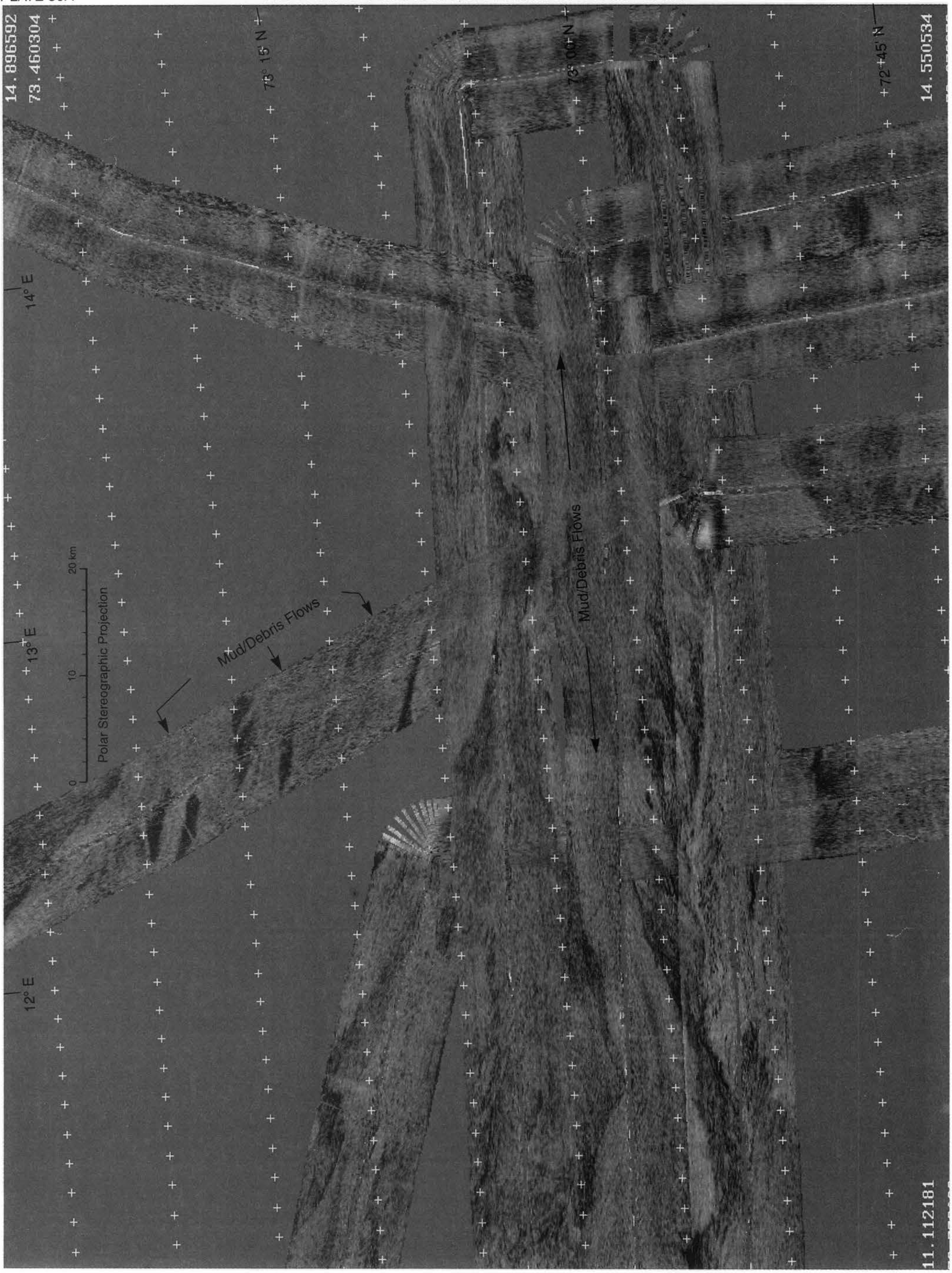

TILE 36B: SEAMARC II MERGED BATHYMETRIC AND SIDE-LOOKING SONAR DATA

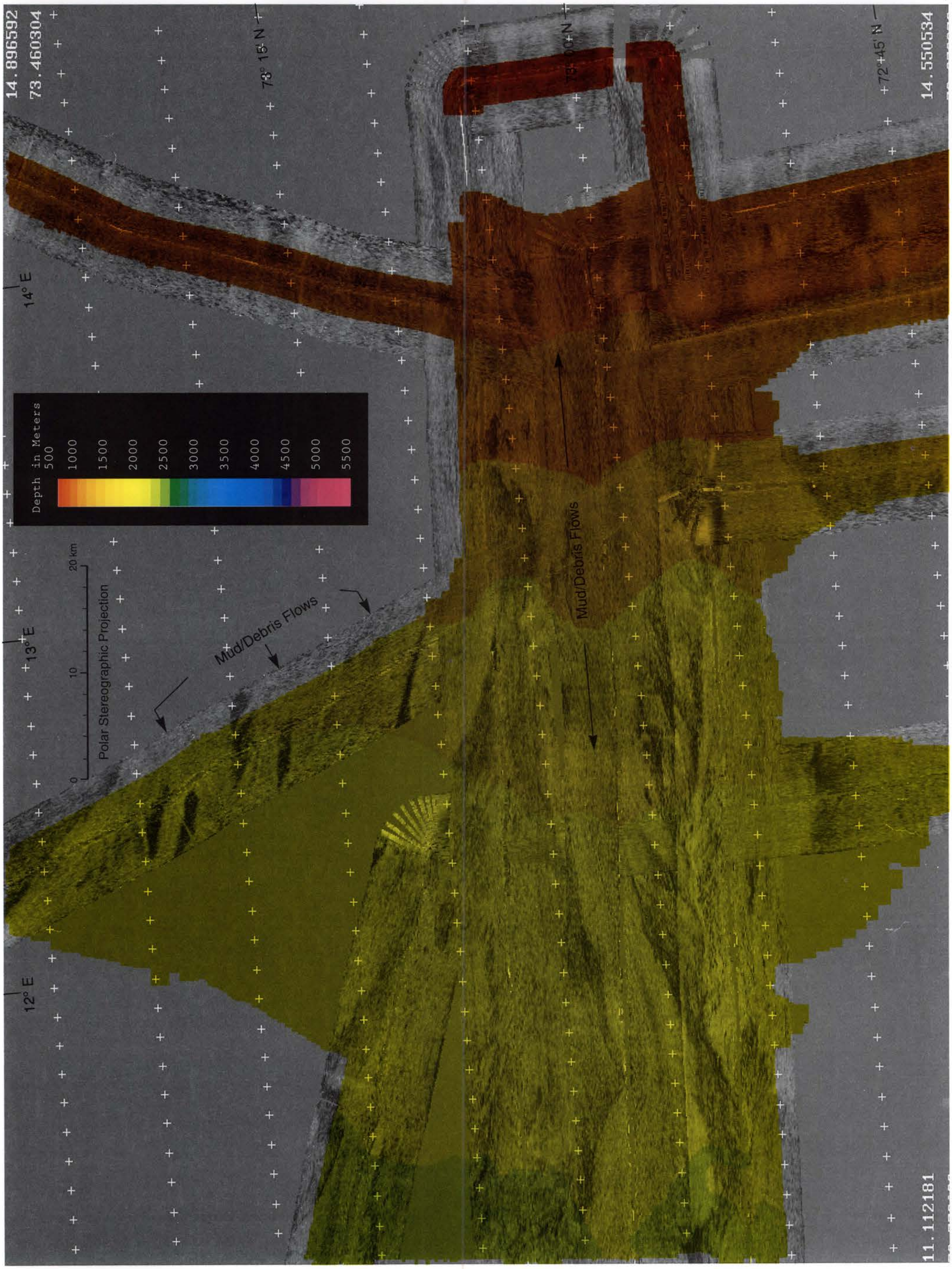

PLATE 51A

TILE 37A: SEAMARC II SIDE-LOOKING SONAR DATA

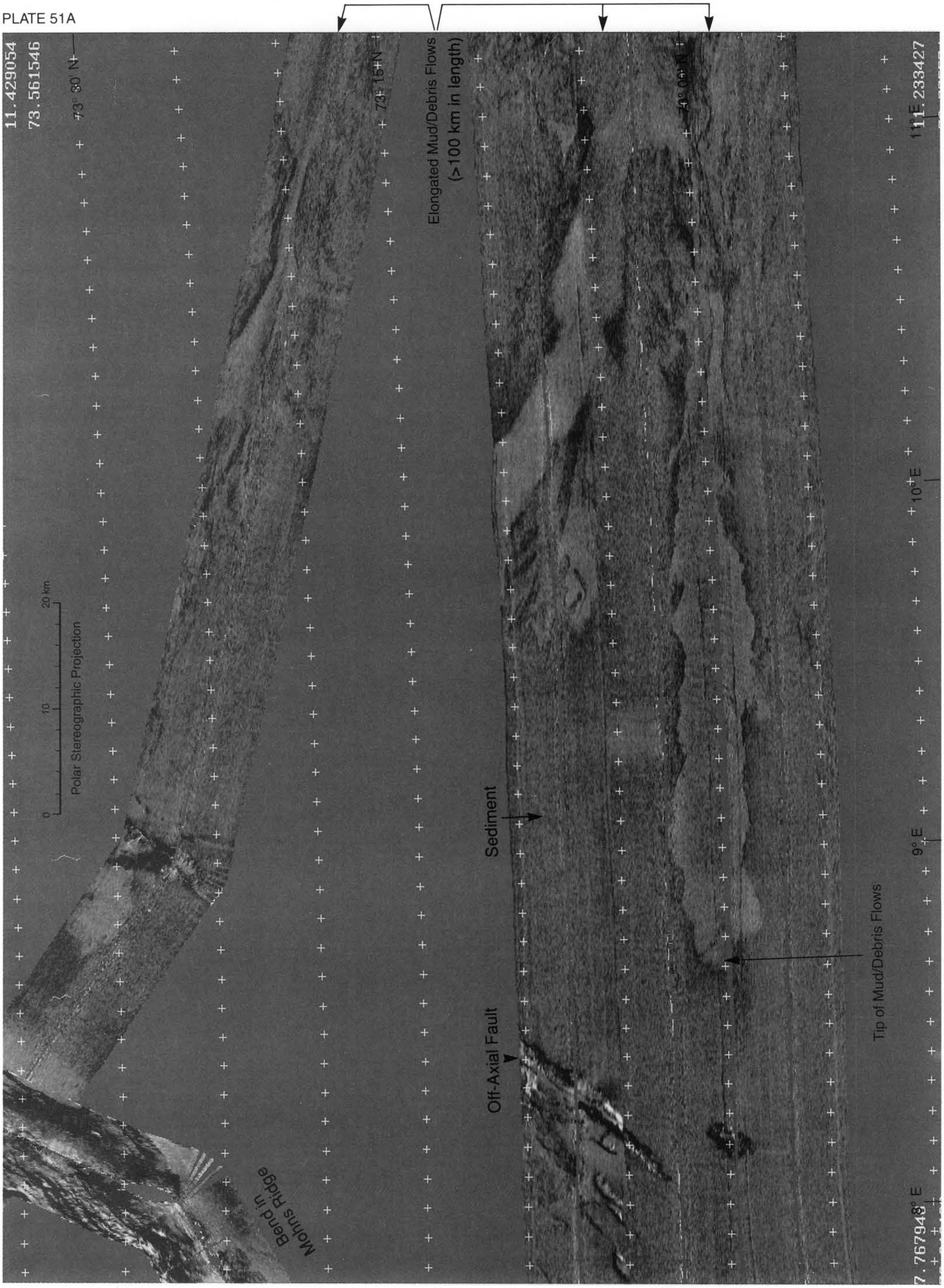

TILE 37B: SEAMARC II MERGED BATHYMETRIC AND SIDE-LOOKING SONAR DATA

PLATE 51B

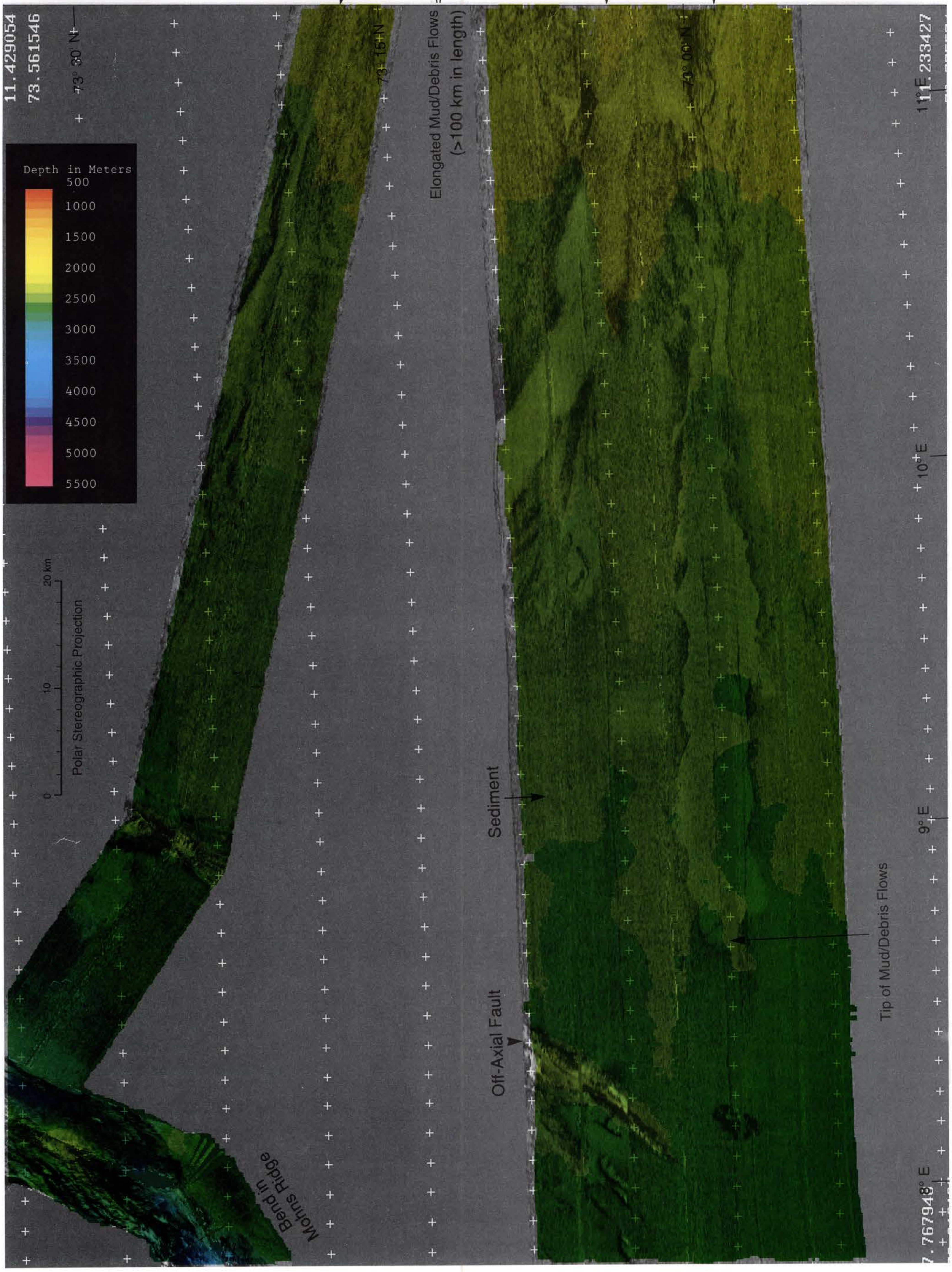

TILE 38A: SEAMARC II SIDE-LOOKING SONAR DATA

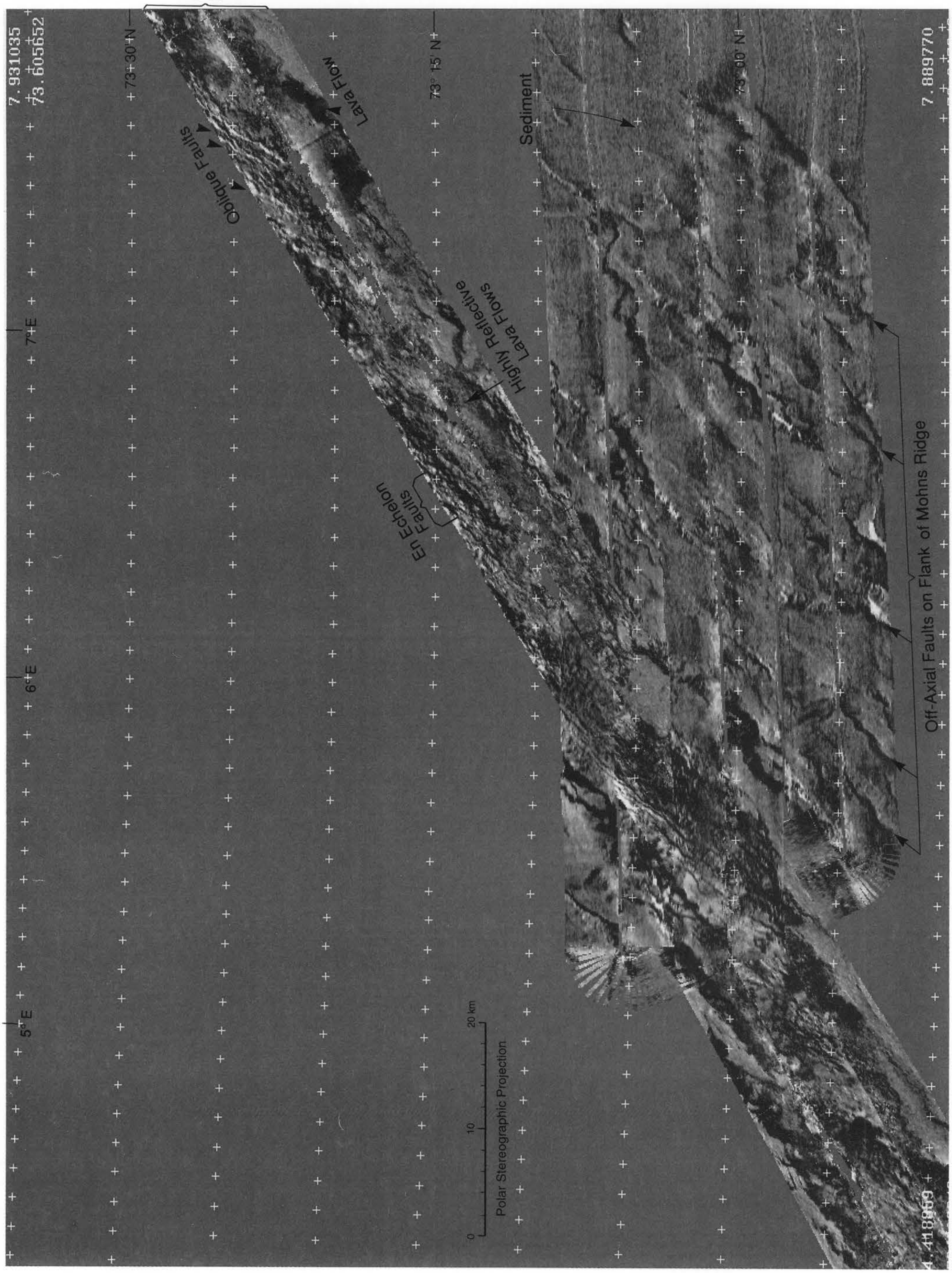

TILE 38B: SEAMARC II MERGED BATHYMETRIC AND SIDE-LOOKING SONAR DATA

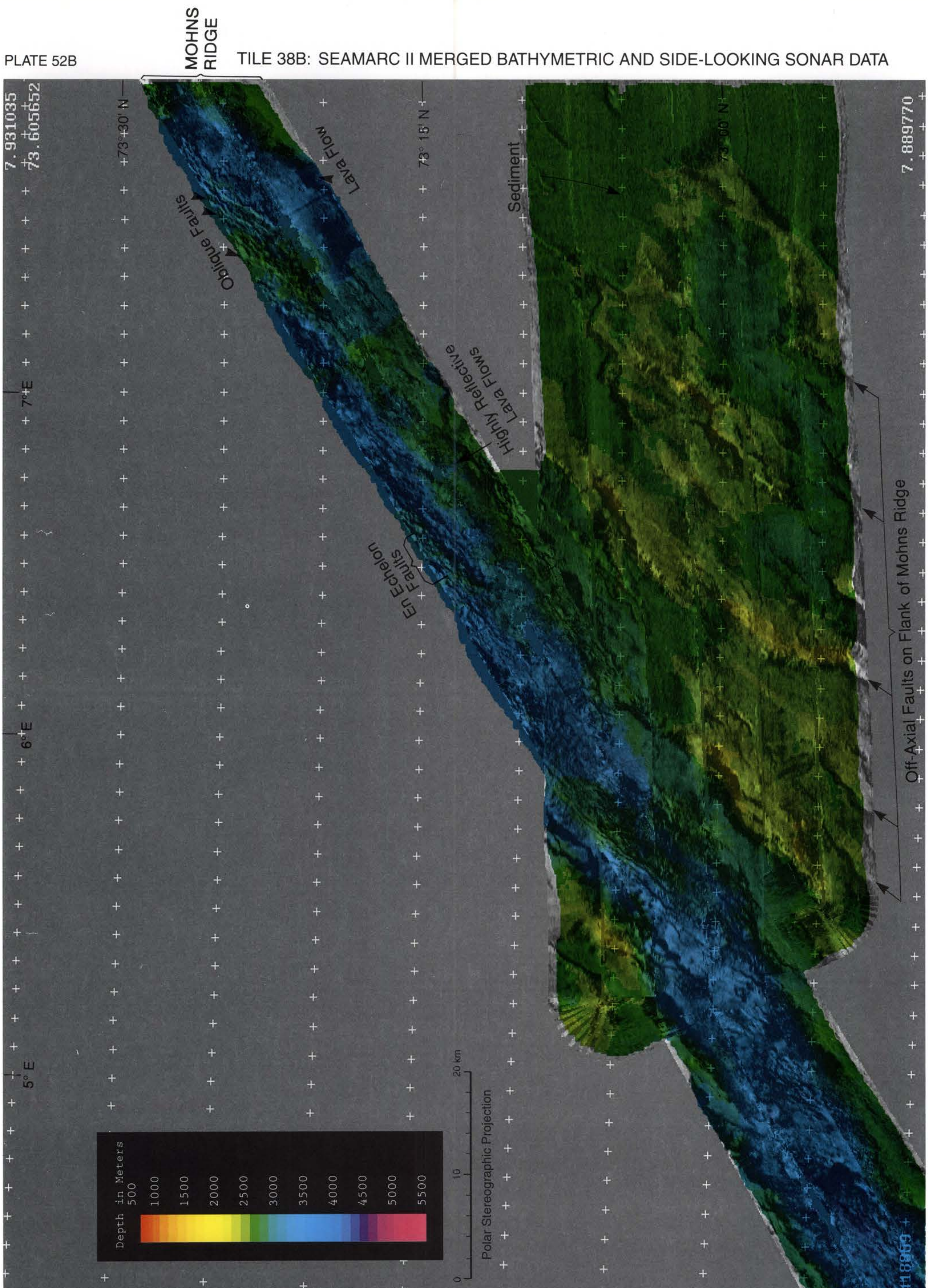

TILE 39A: SEAMARC II SIDE-LOOKING SONAR DATA

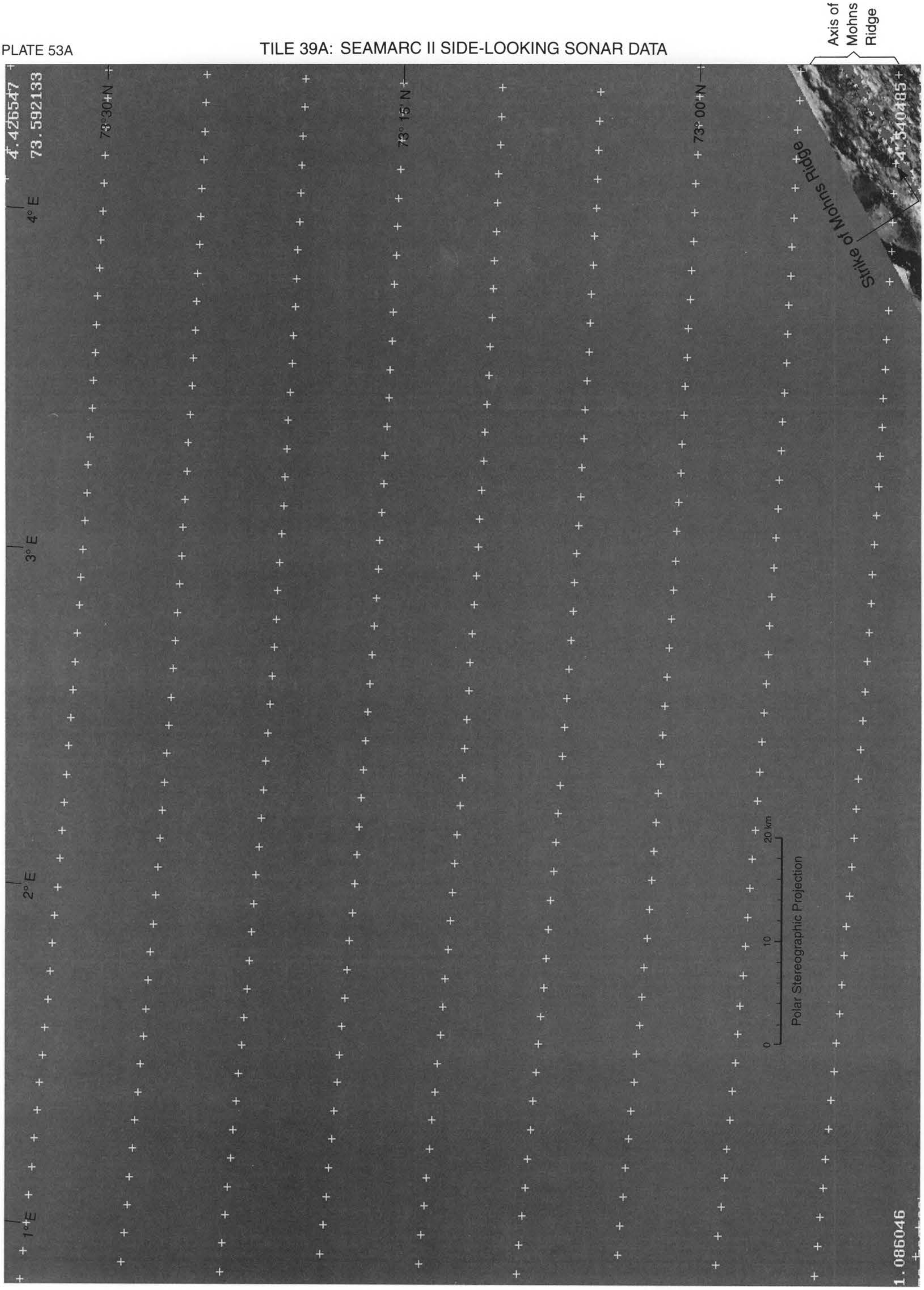

PLATE 53B

TILE 39B: SEAMARC II MERGED BATHYMETRIC AND SIDE-LOOKING SONAR DATA

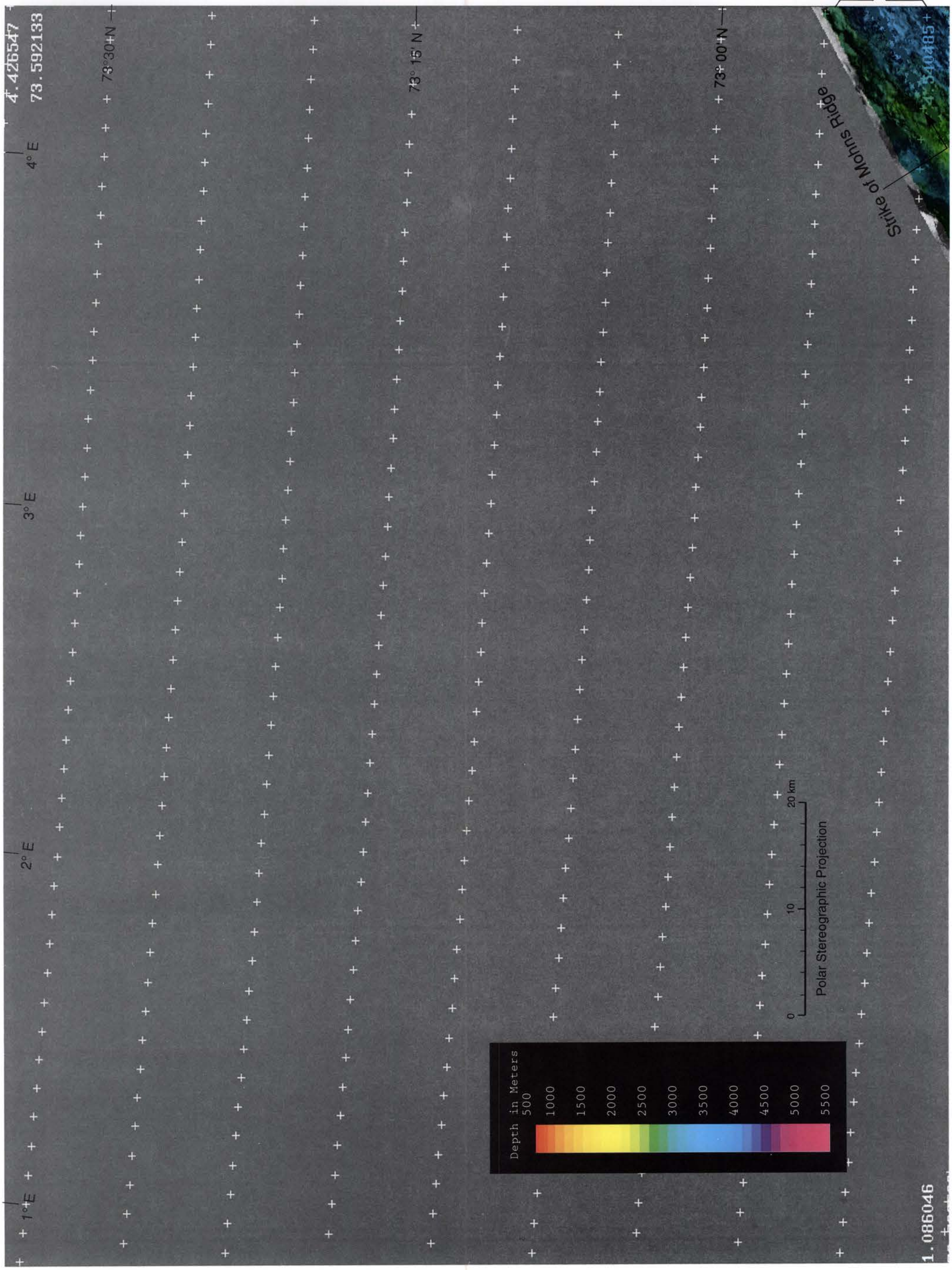

TILE 40A: SEAMARC II SIDE-LOOKING SONAR DATA

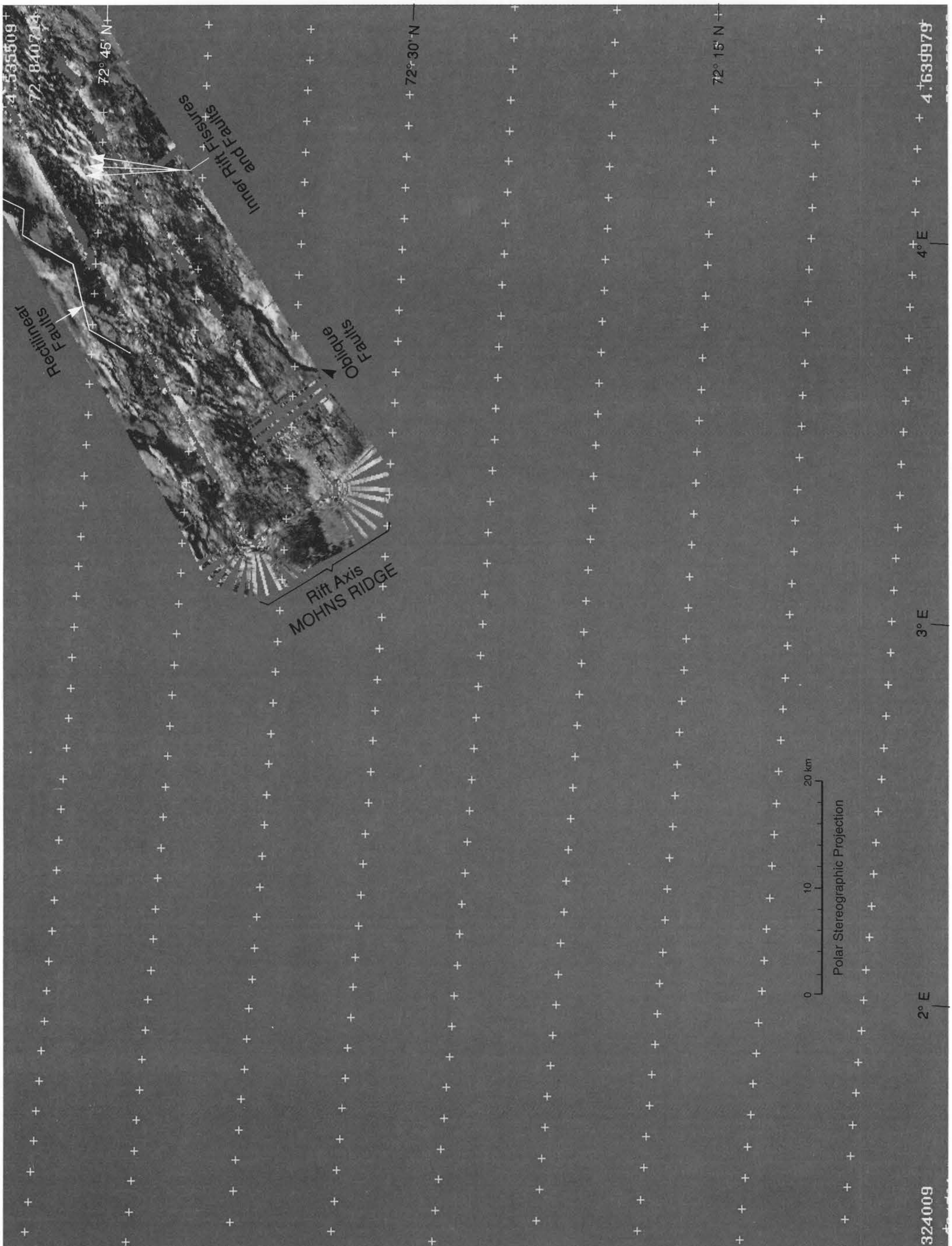

TILE 40B: SEAMARC II MERGED BATHYMETRIC AND SIDE-LOOKING SONAR DATA

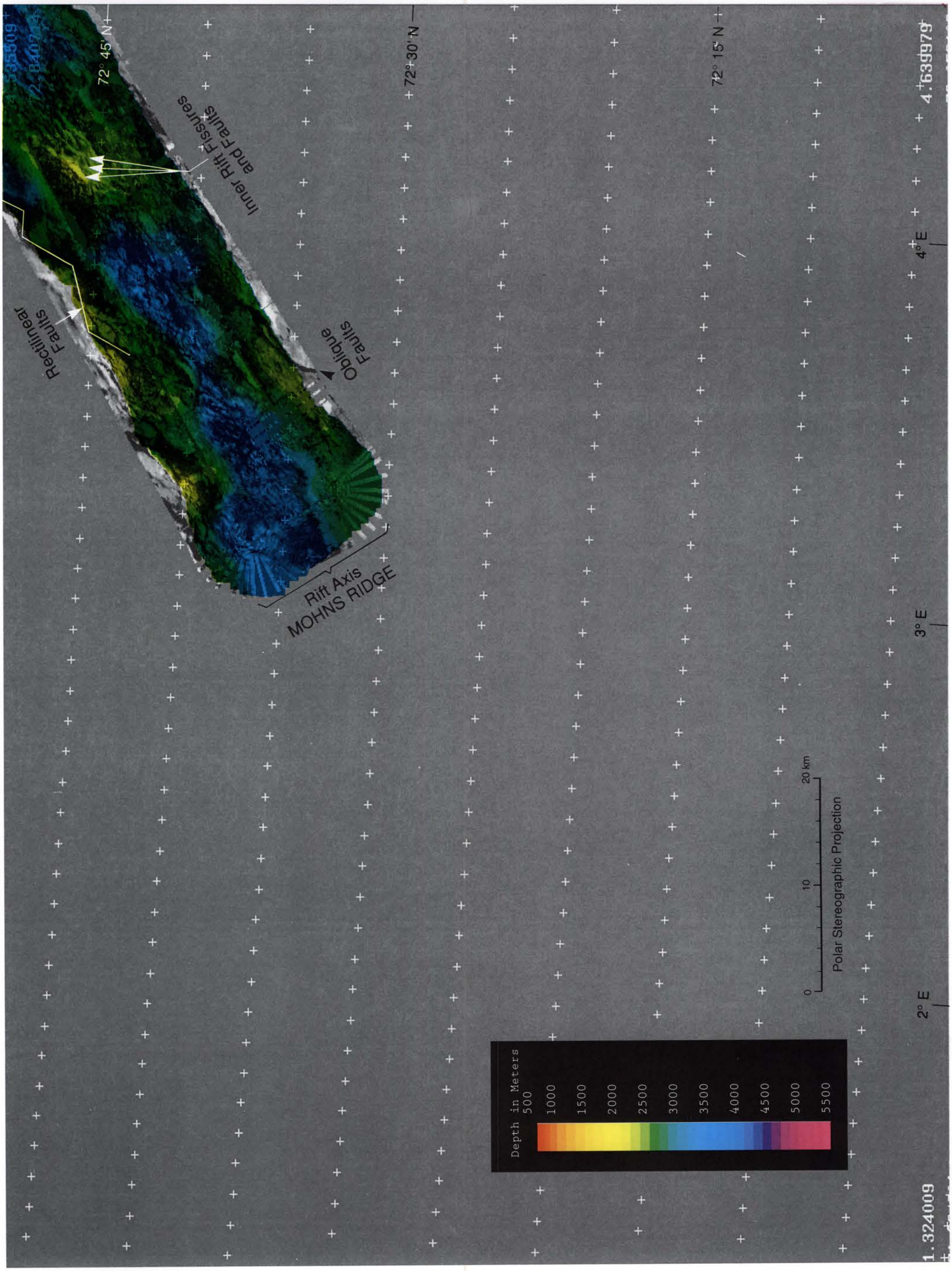

TILE 41A: SEAMARC II SIDE-LOOKING SONAR DATA

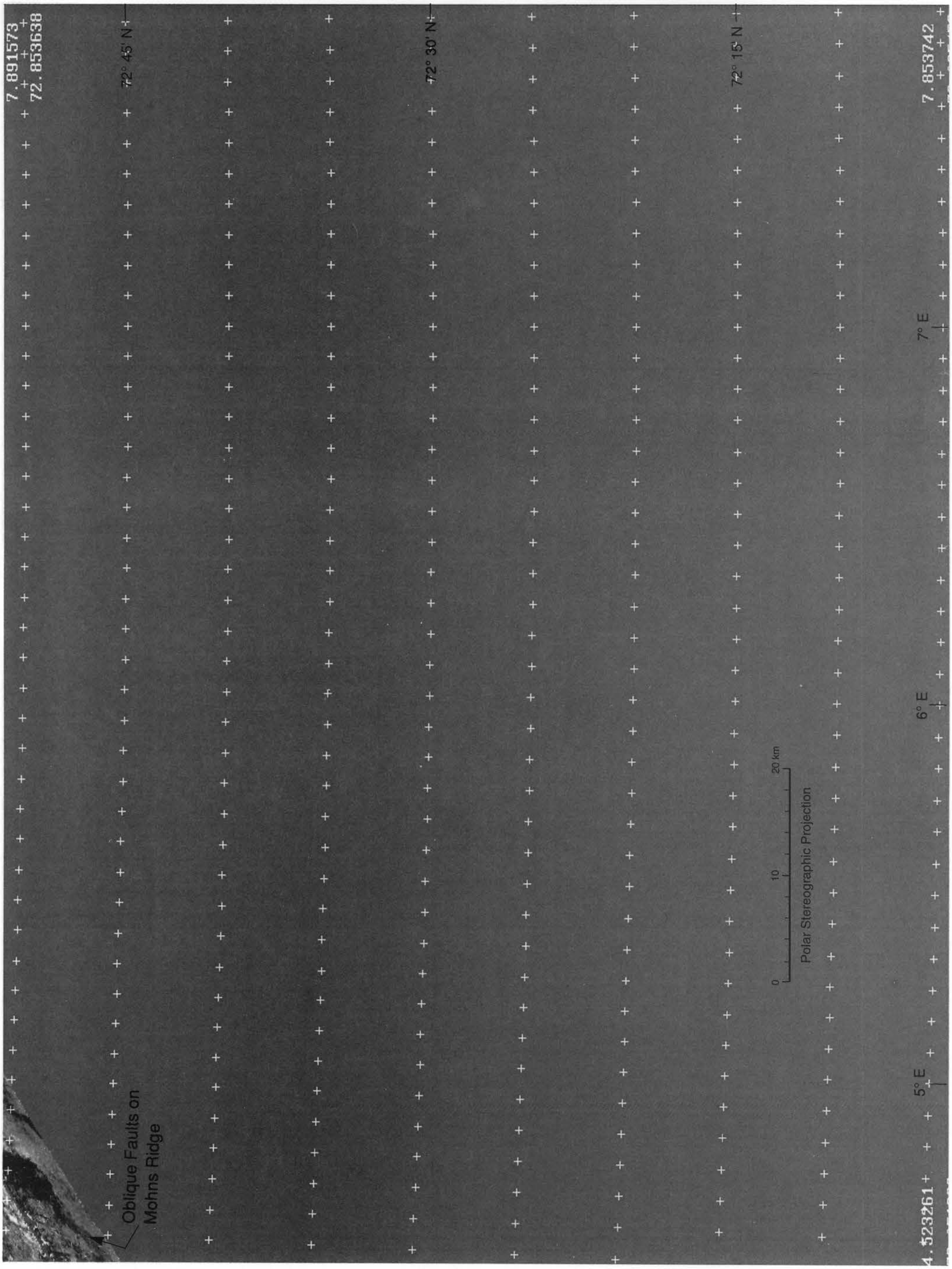

TILE 41B: SEAMARC II MERGED BATHYMETRIC AND SIDE-LOOKING SONAR DATA

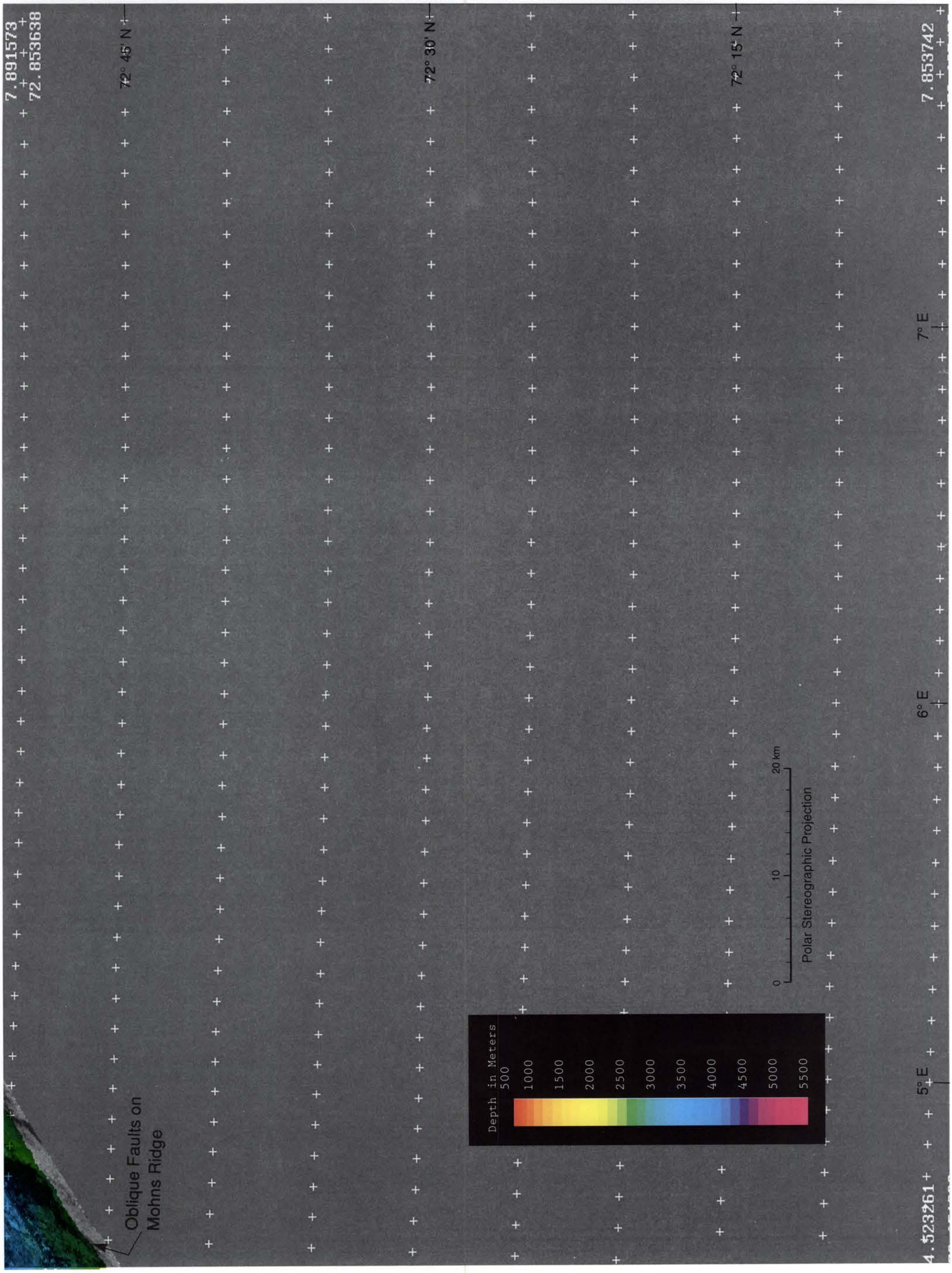

TILE 42A: SEAMARC II SIDE-LOOKING SONAR DATA

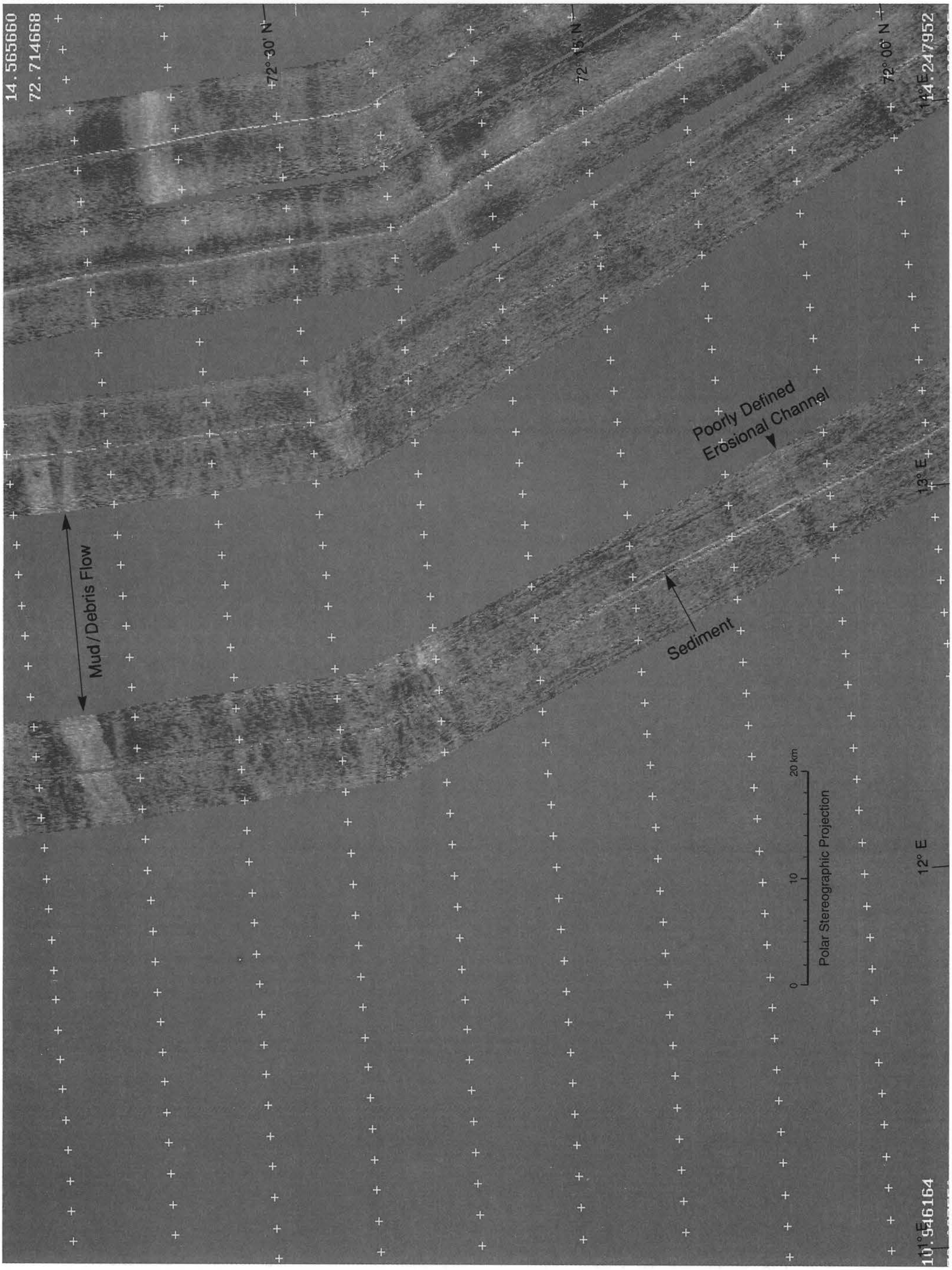

PLATE 56B TILE 42B: SEAMARC II MERGED BATHYMETRIC AND SIDE-LOOKING SONAR DATA

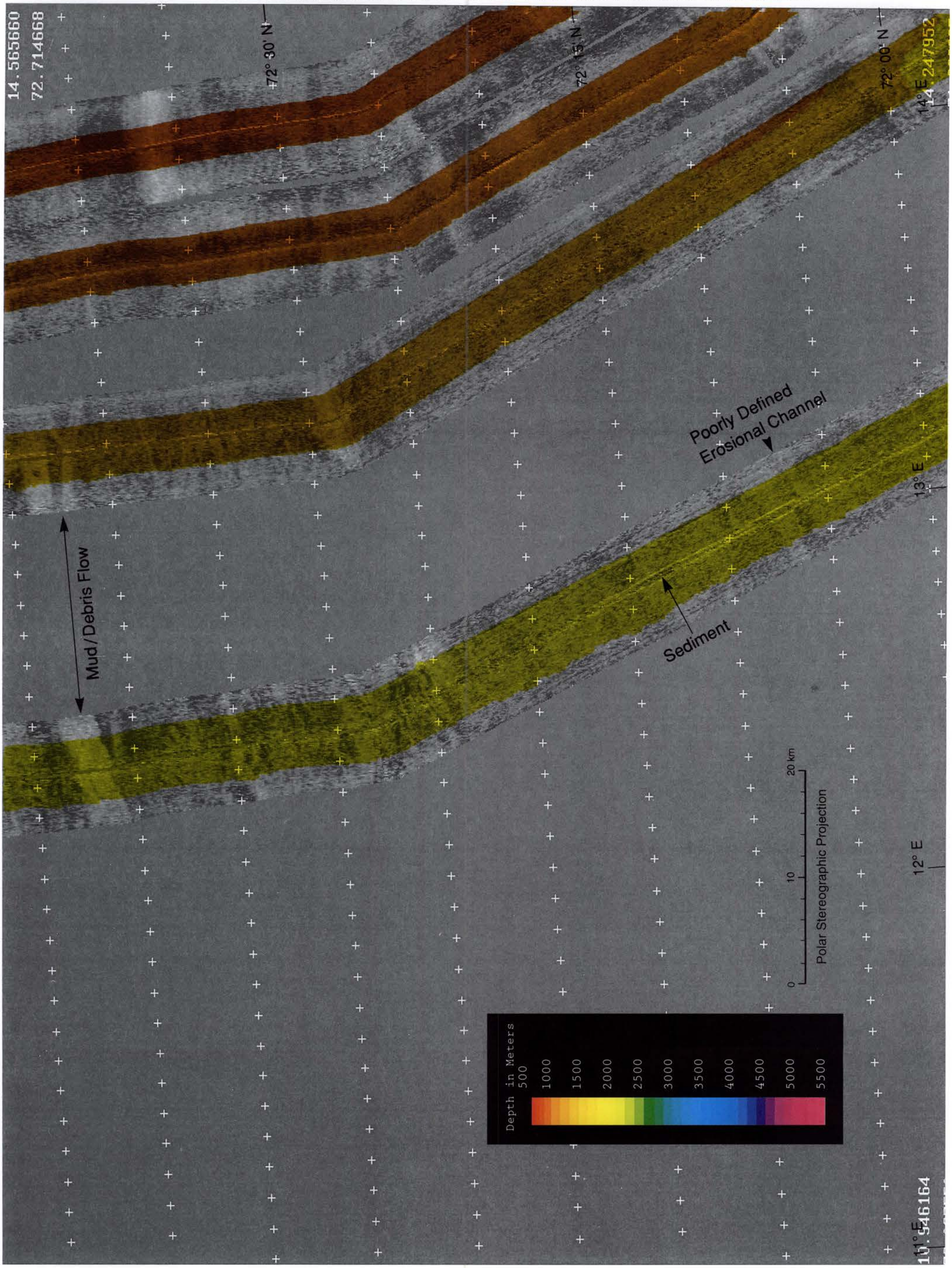

TILE 43A: SEAMARC II SIDE-LOOKING SONAR DATA

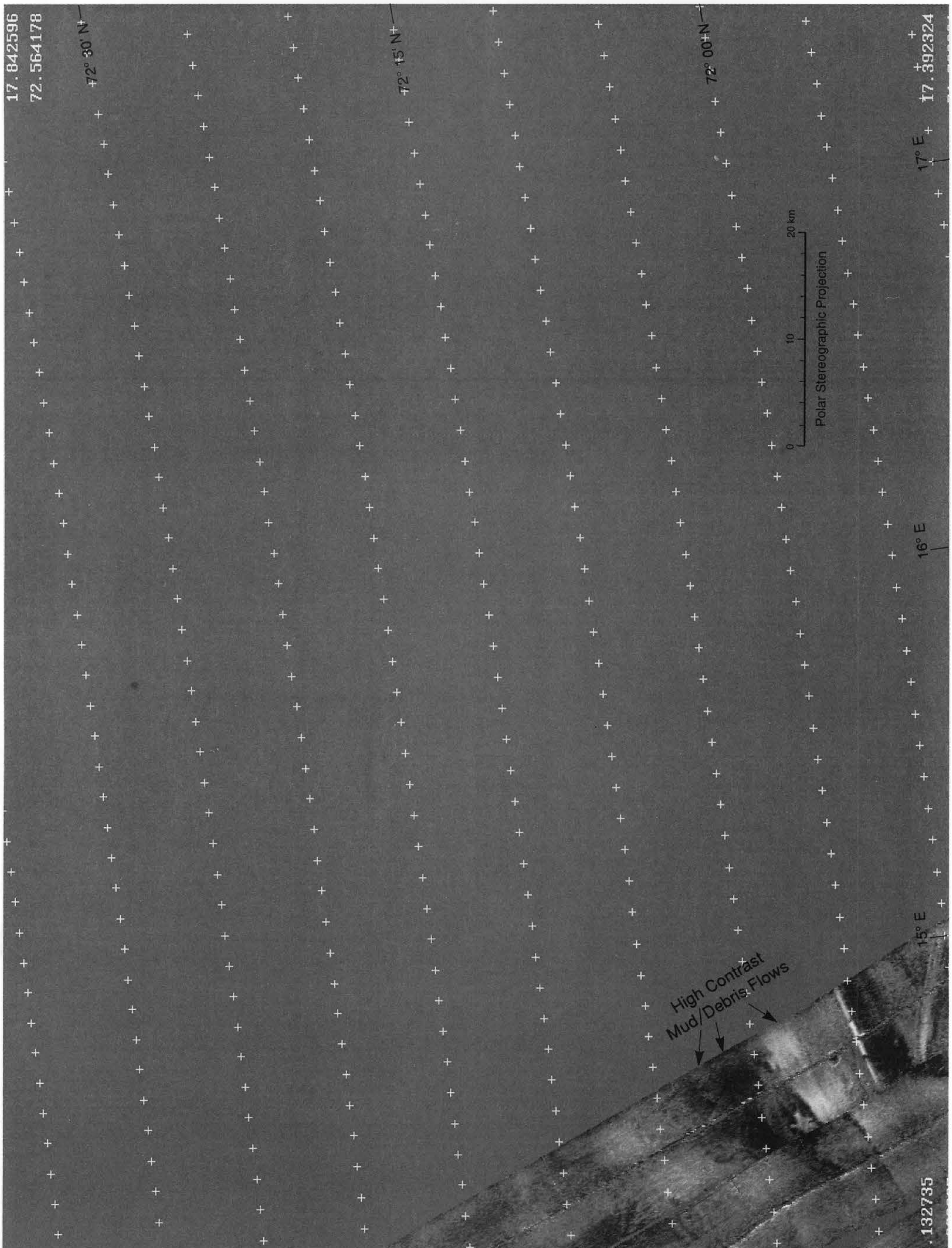

TILE 43B: SEAMARC II MERGED BATHYMETRIC AND SIDE-LOOKING SONAR DATA

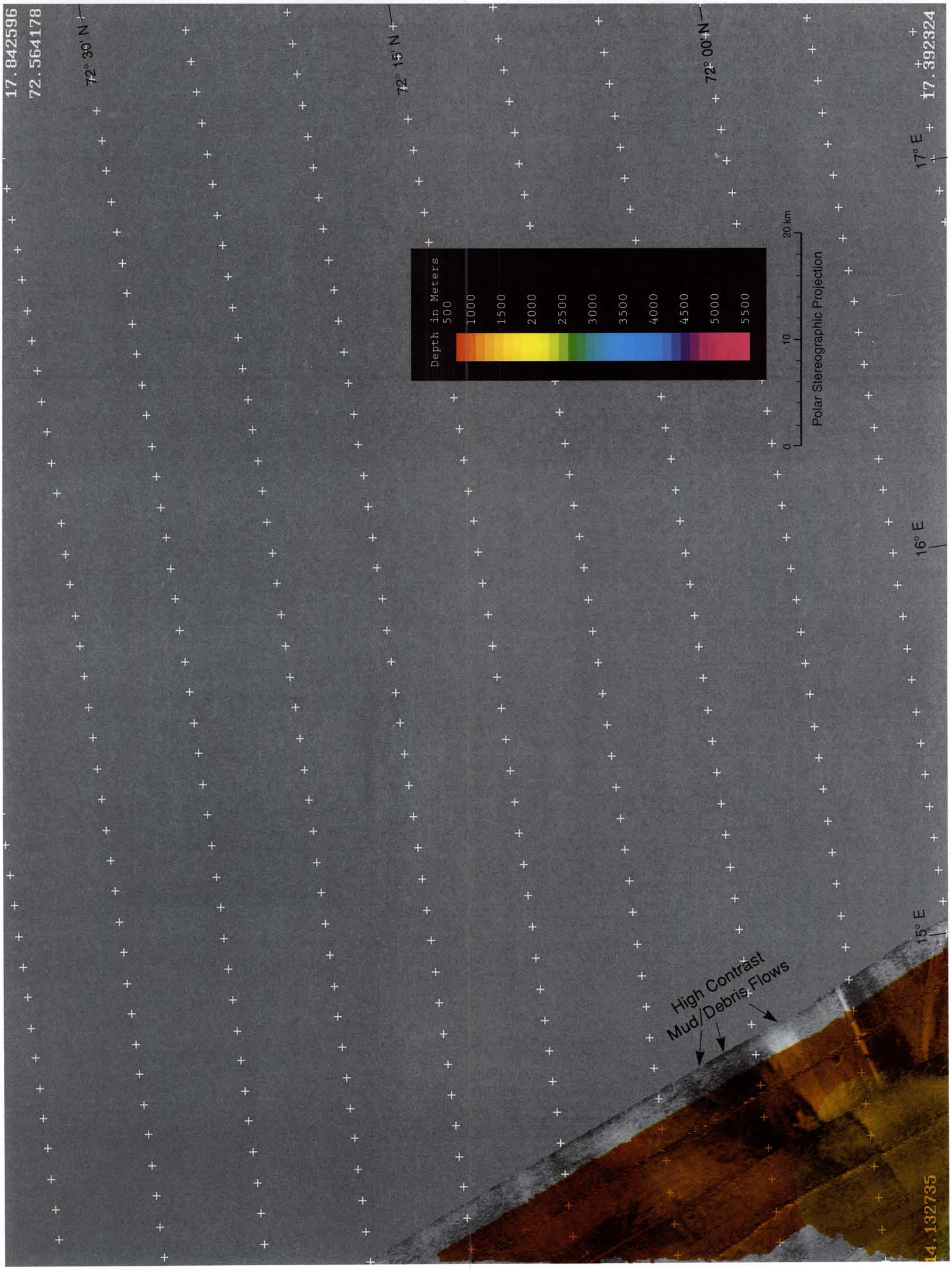

TILE 44A: SEAMARC II SIDE-LOOKING SONAR DATA

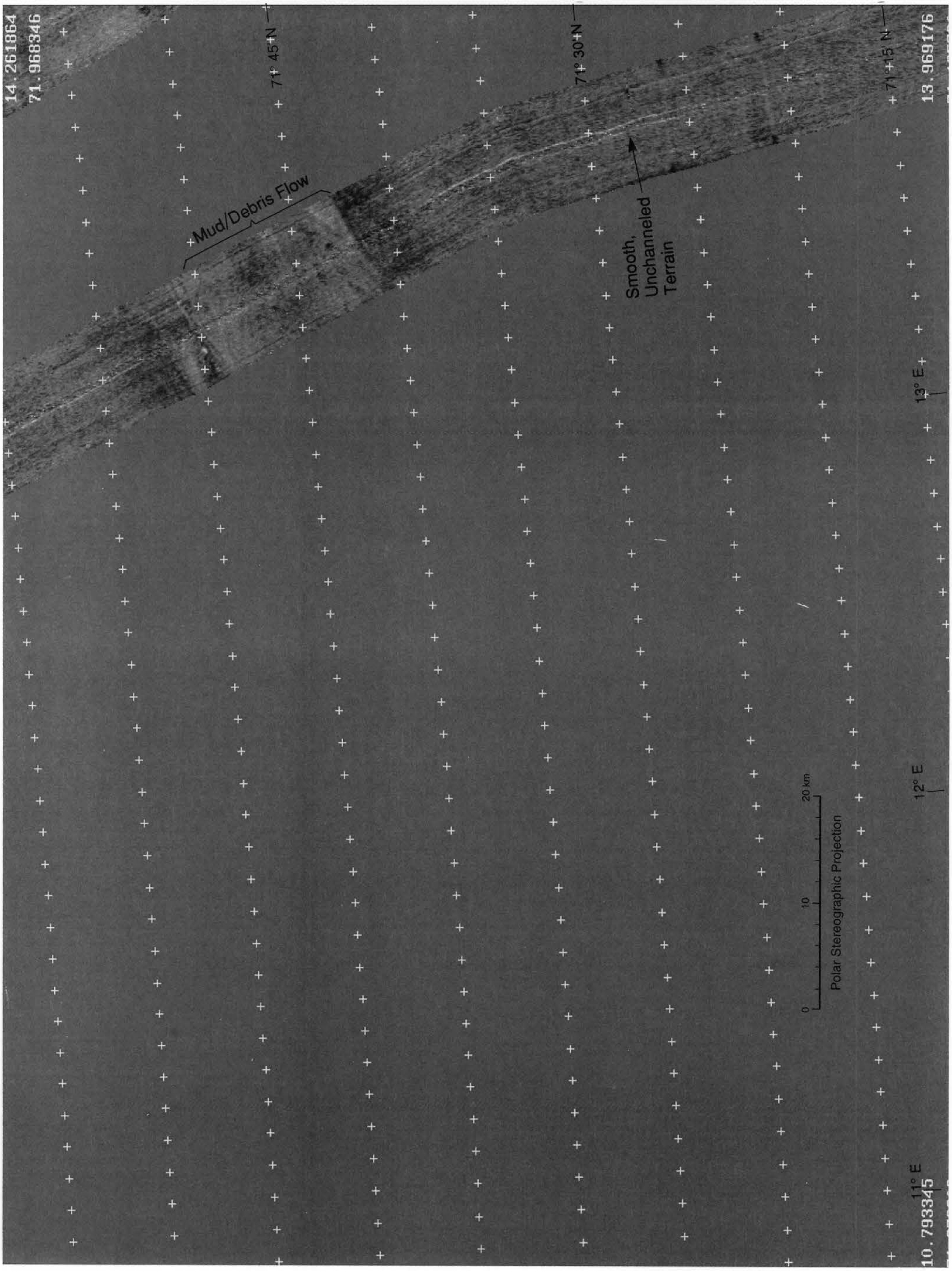

TILE 44B: SEAMARC II MERGED BATHYMETRIC AND SIDE-LOOKING SONAR DATA

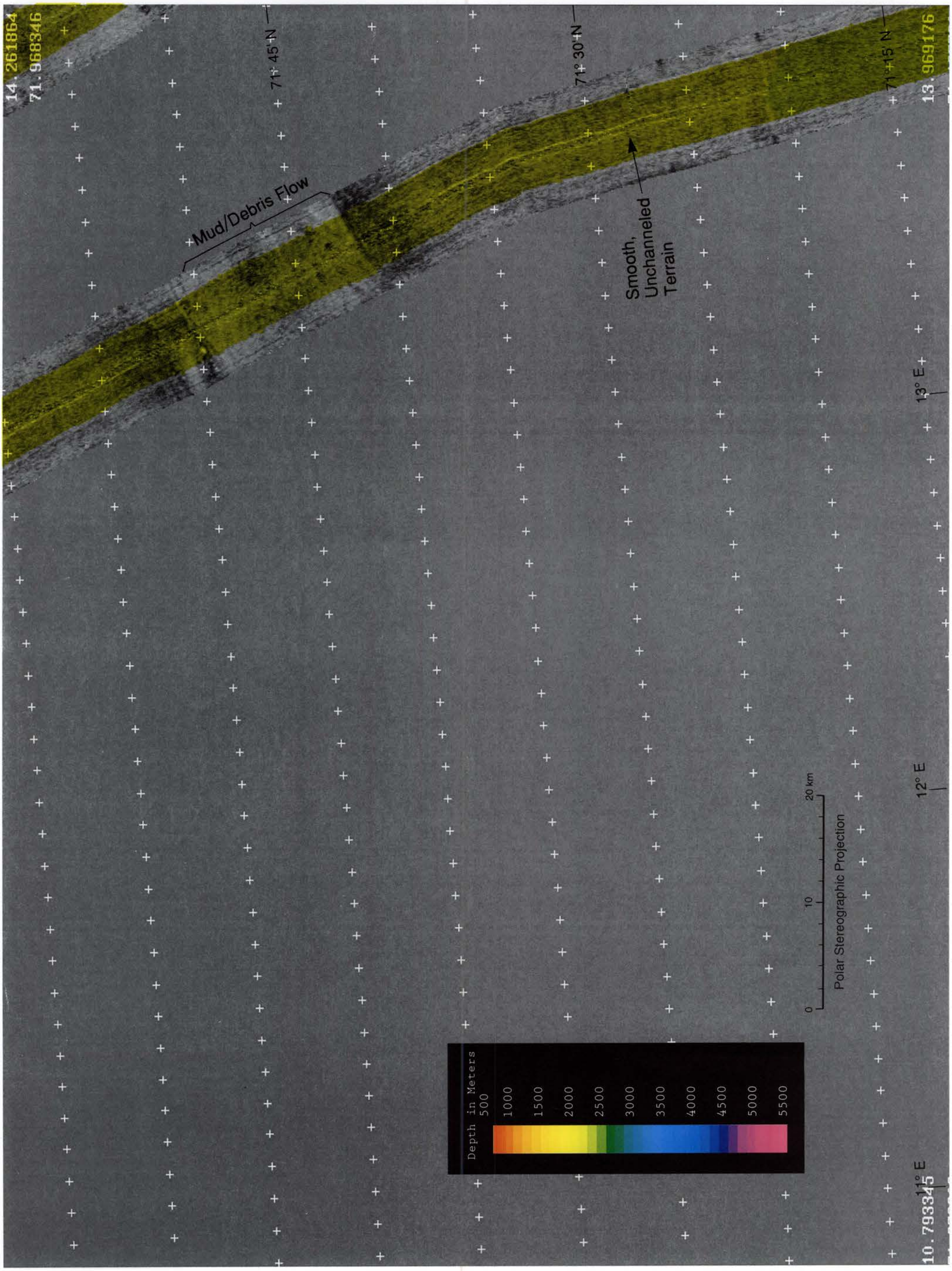

TILE 45A: SEAMARC II SIDE-LOOKING SONAR DATA

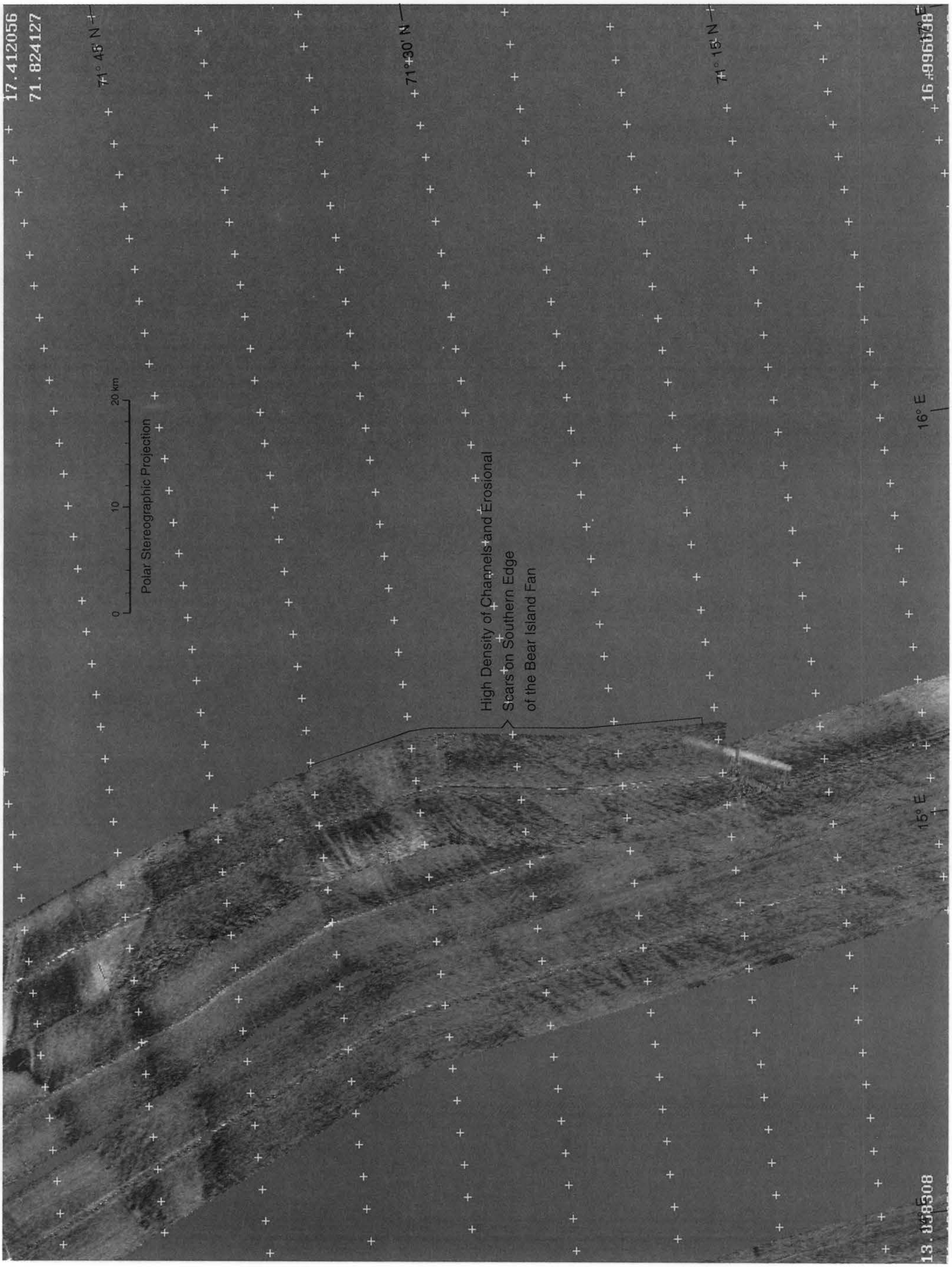

TILE 45B: SEAMARC II MERGED BATHYMETRIC AND SIDE-LOOKING SONAR DATA

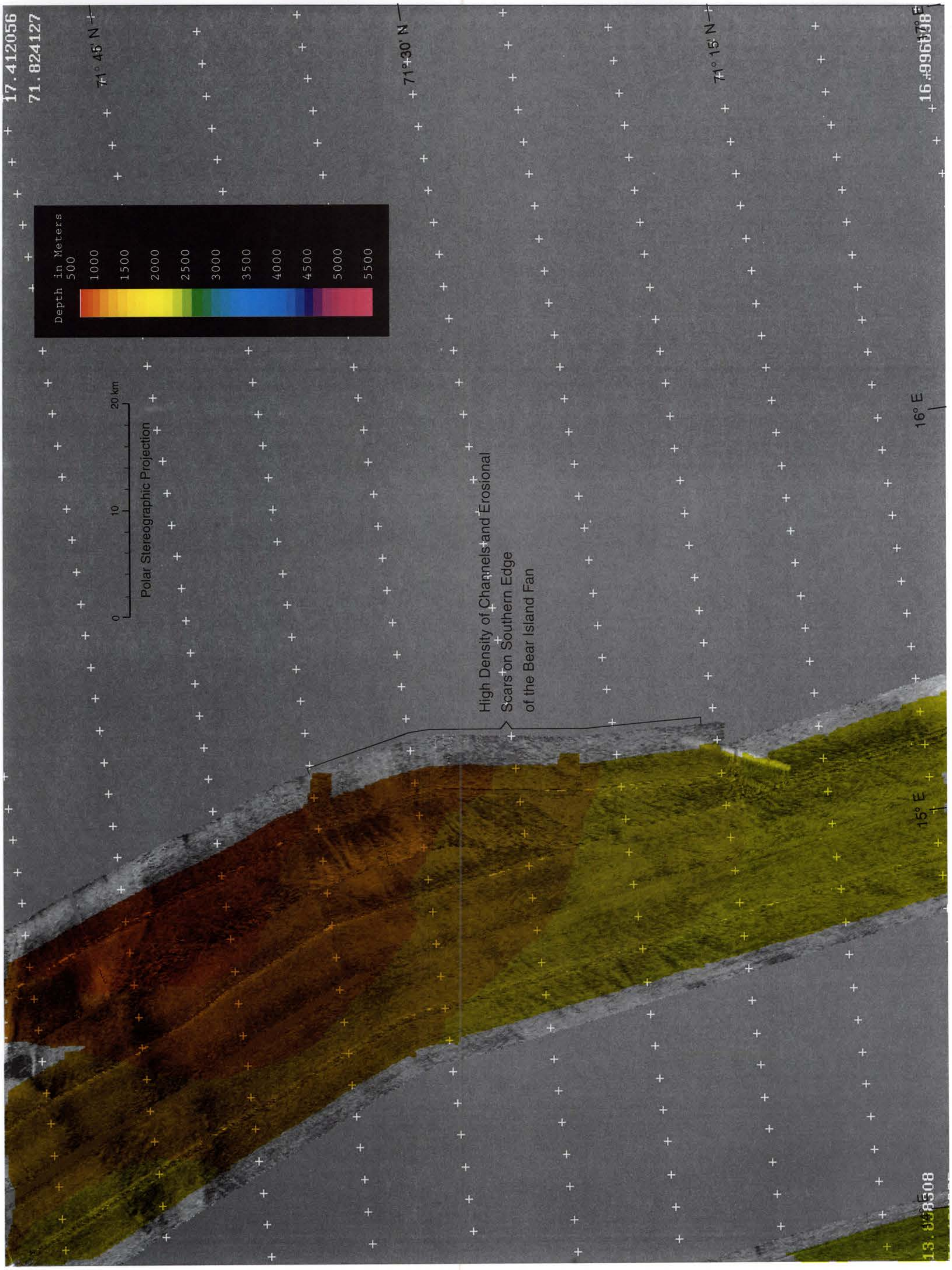

TILE 46A: SEAMARC II SIDE-LOOKING SONAR DATA

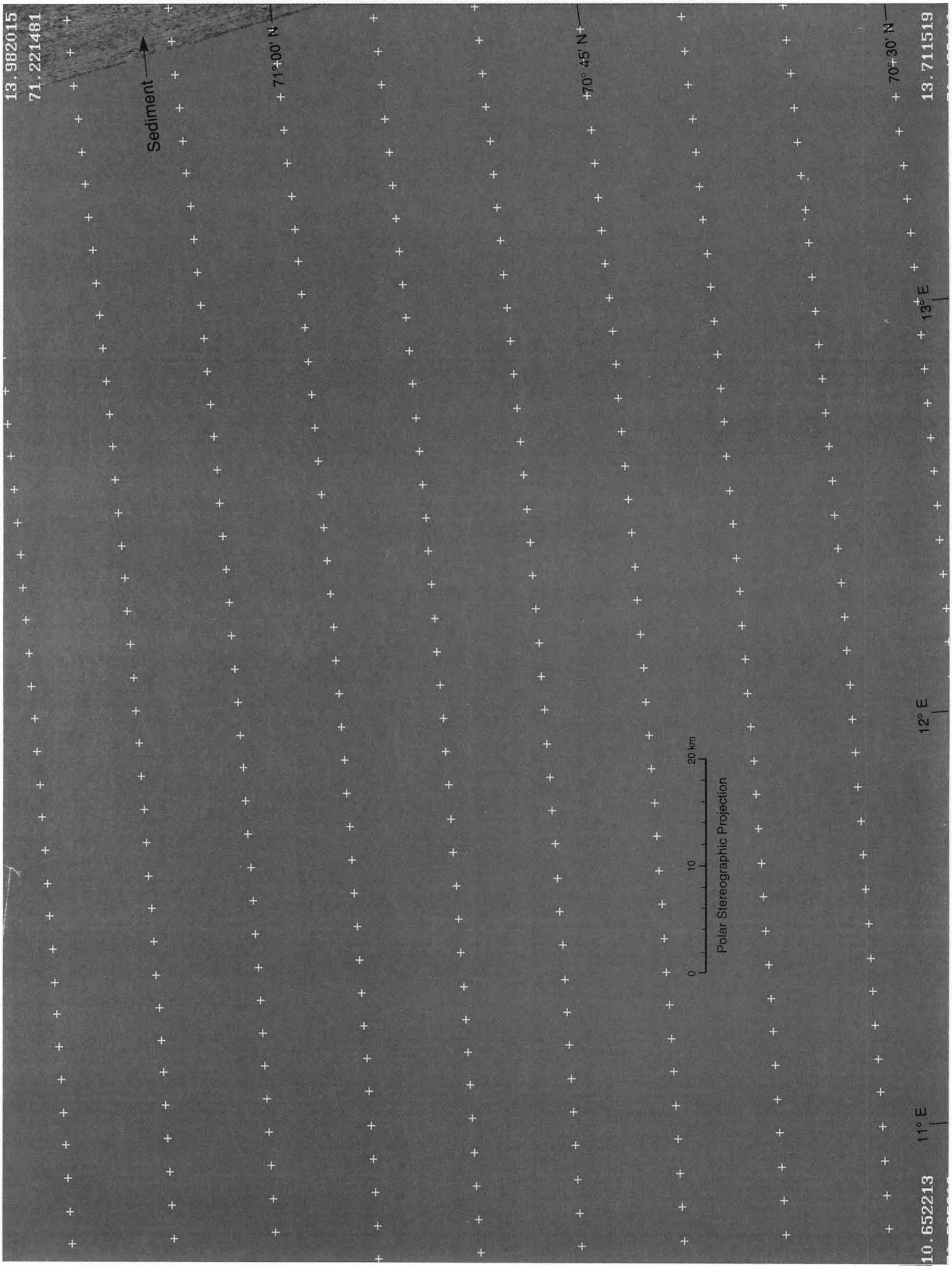

TILE 46B: SEAMARC II MERGED BATHYMETRIC AND SIDE-LOOKING SONAR DATA

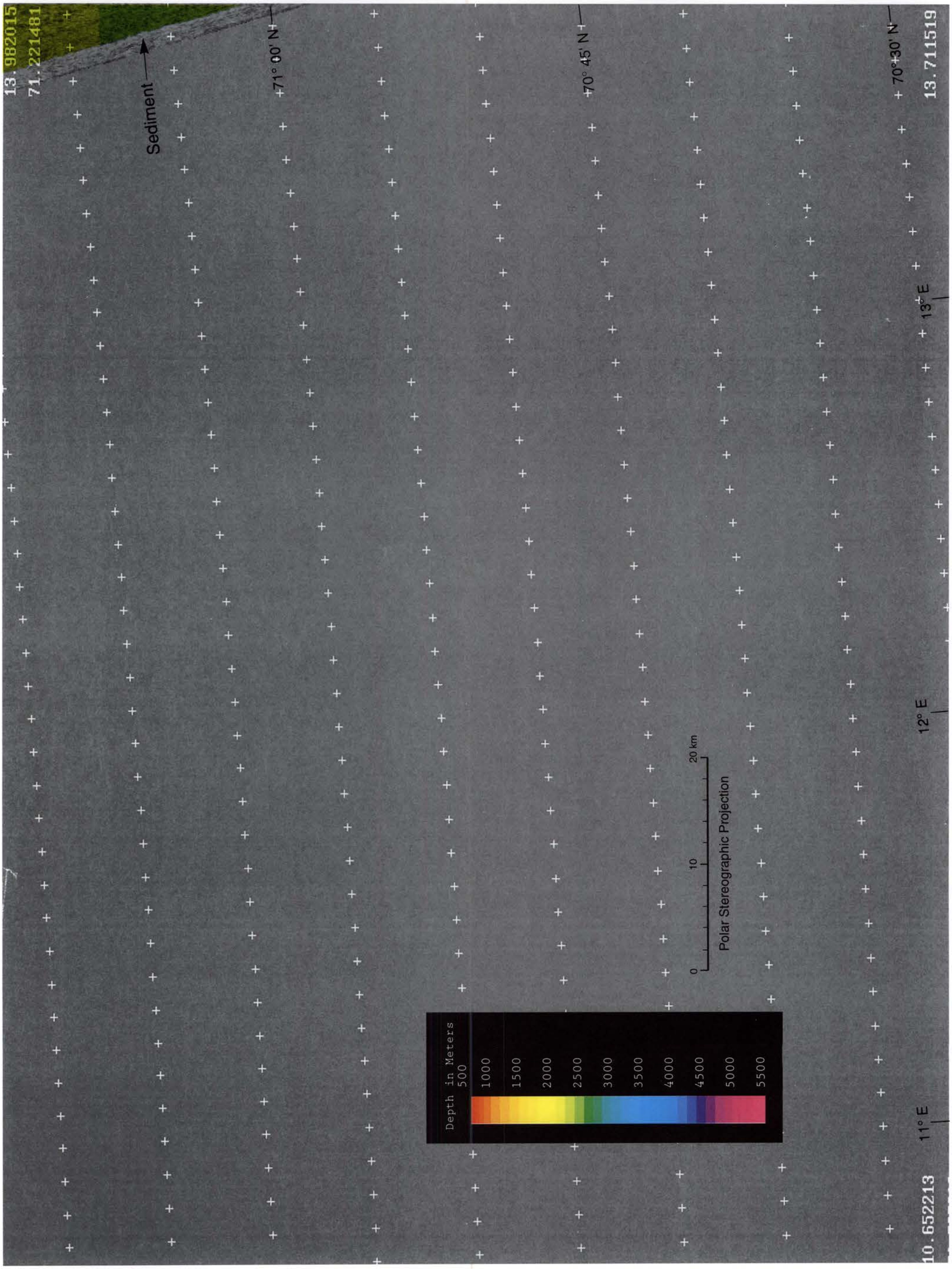

PLATE 61A

TILE 47A: SEAMARC II SIDE-LOOKING SONAR DATA

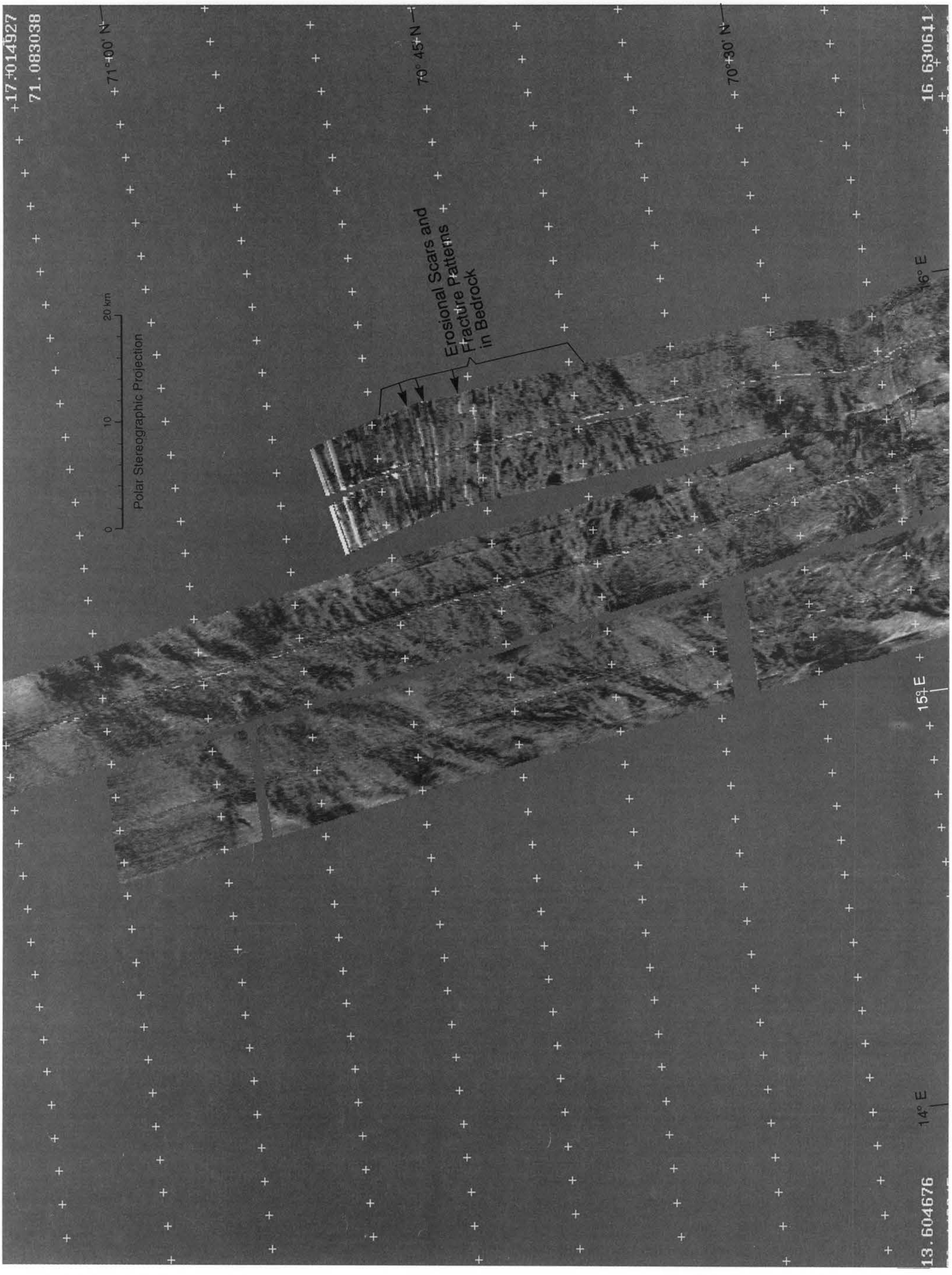

TILE 47B: SEAMARC II MERGED BATHYMETRIC AND SIDE-LOOKING SONAR DATA

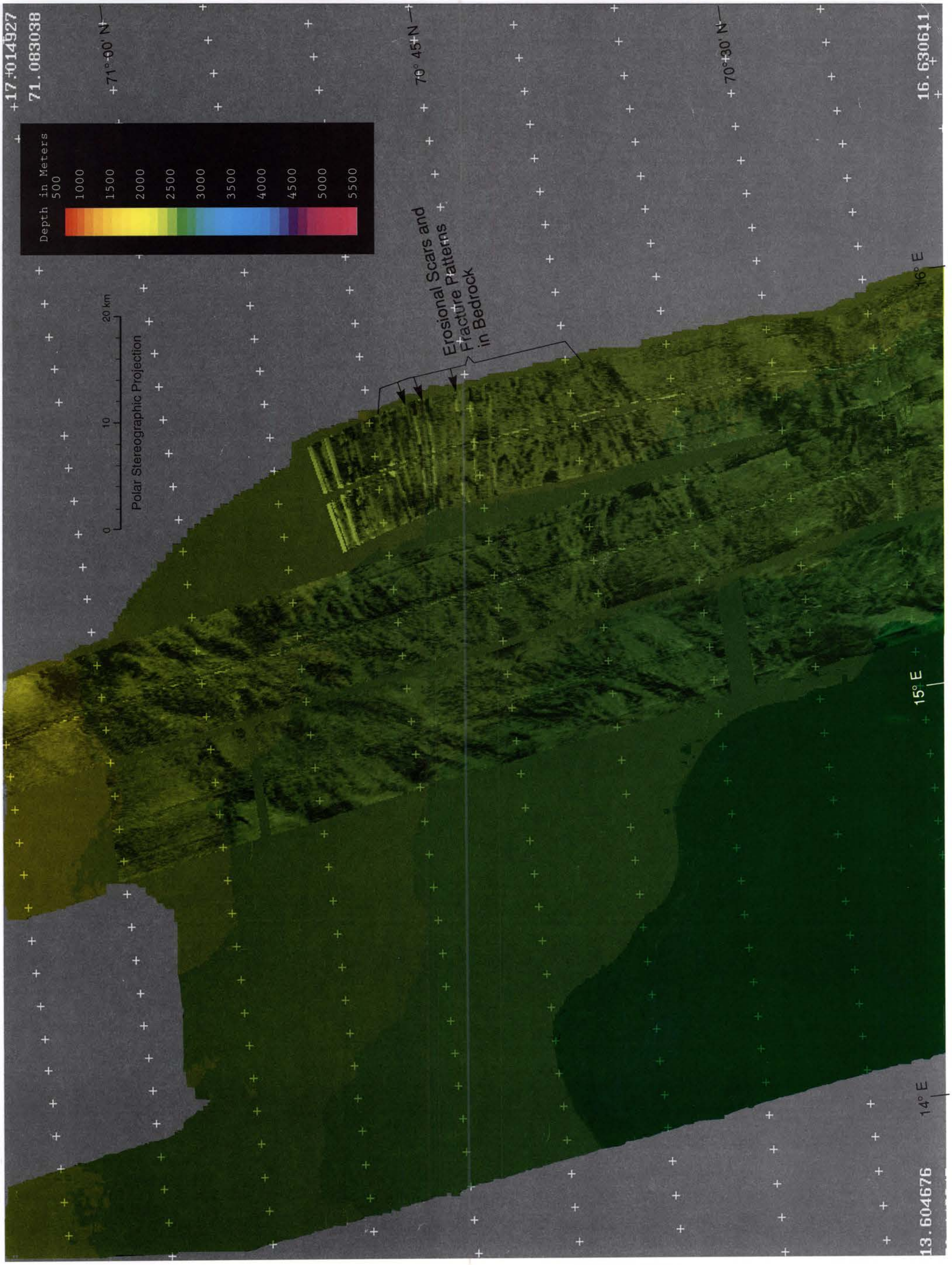

TILE 48A: SEAMARC II SIDE-LOOKING SONAR DATA

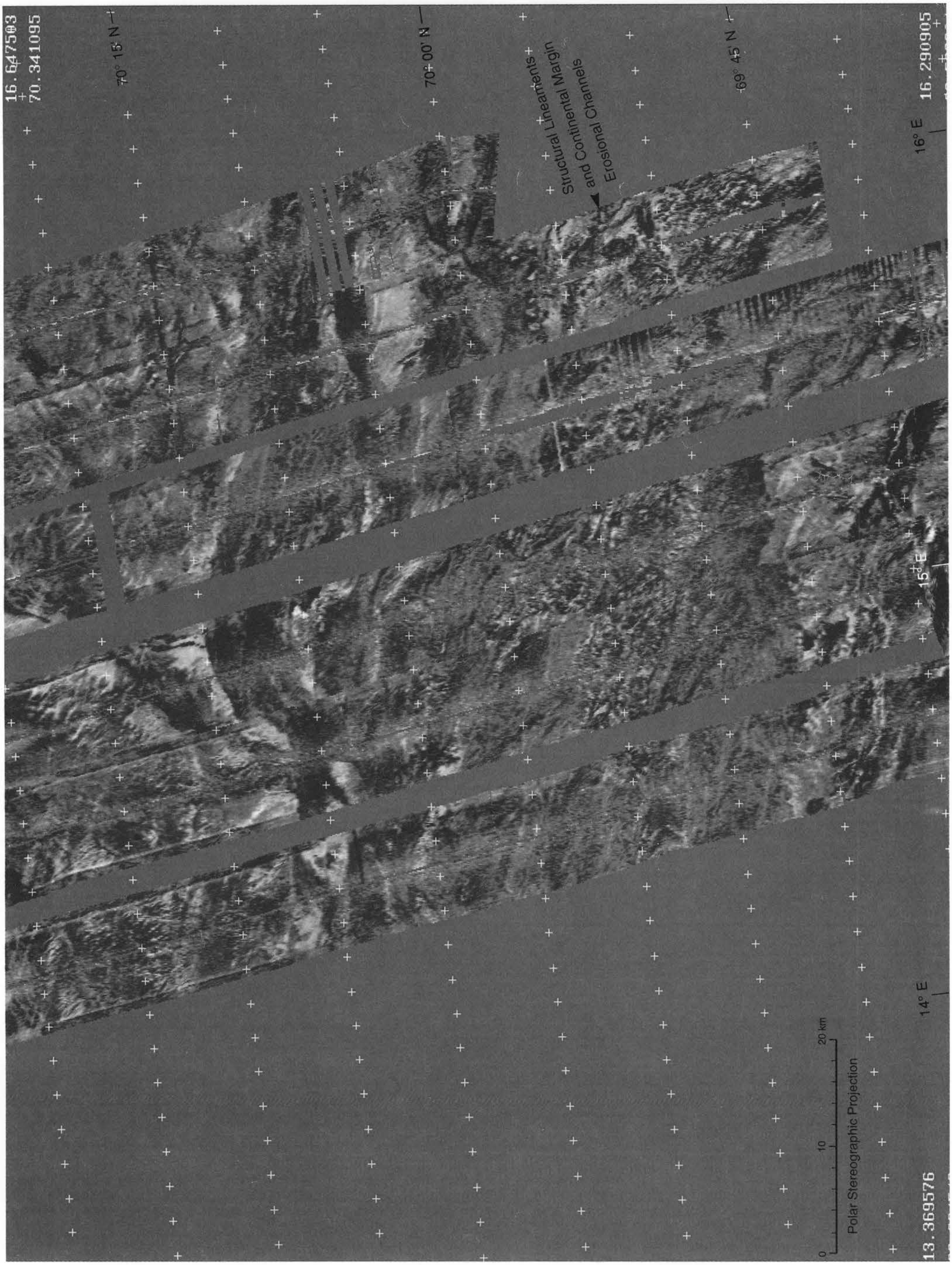

TILE 48B: SEAMARC II MERGED BATHYMETRIC AND SIDE-LOOKING SONAR DATA

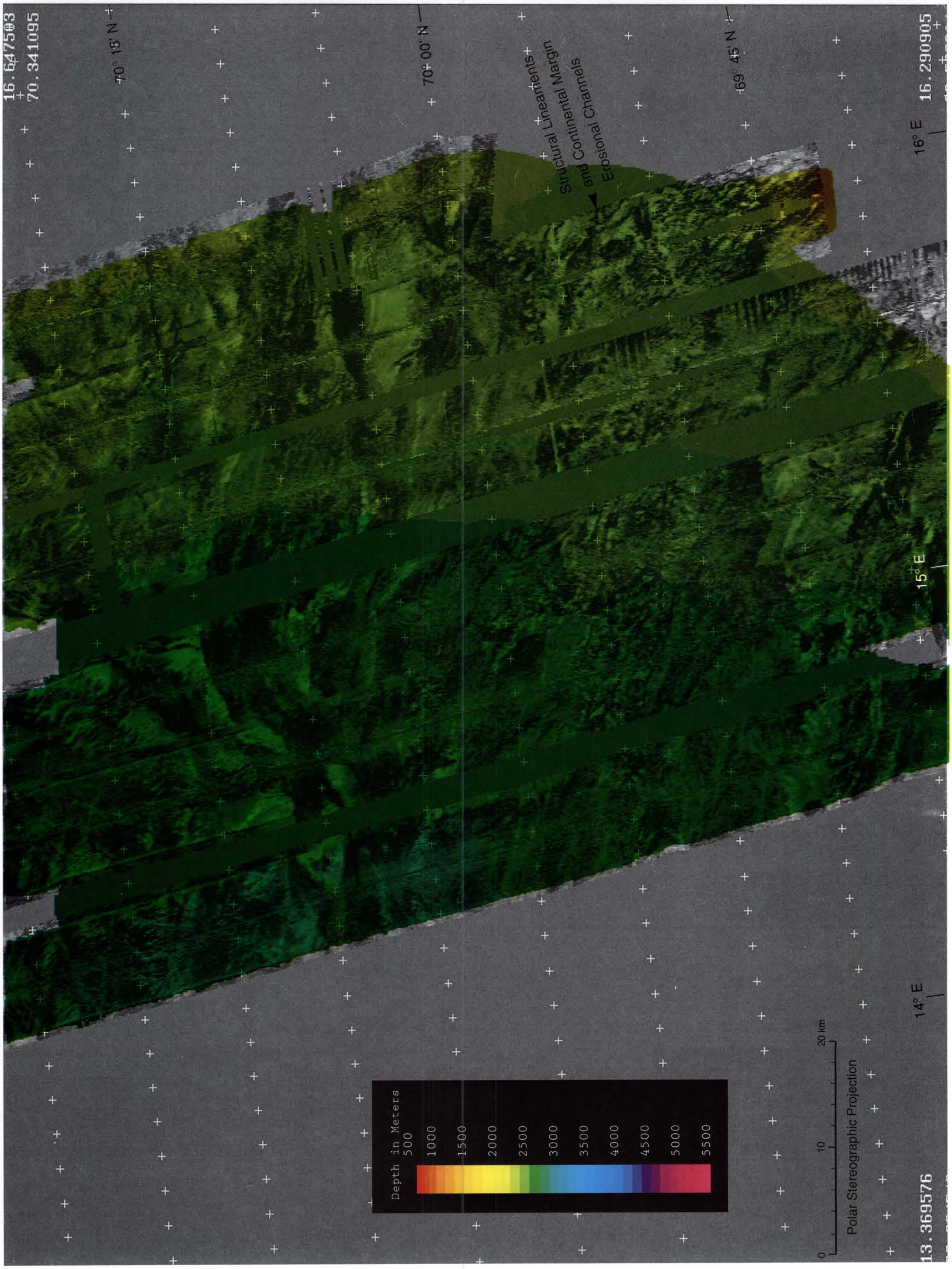

TILE 49A: SEAMARC II SIDE-LOOKING SONAR DATA

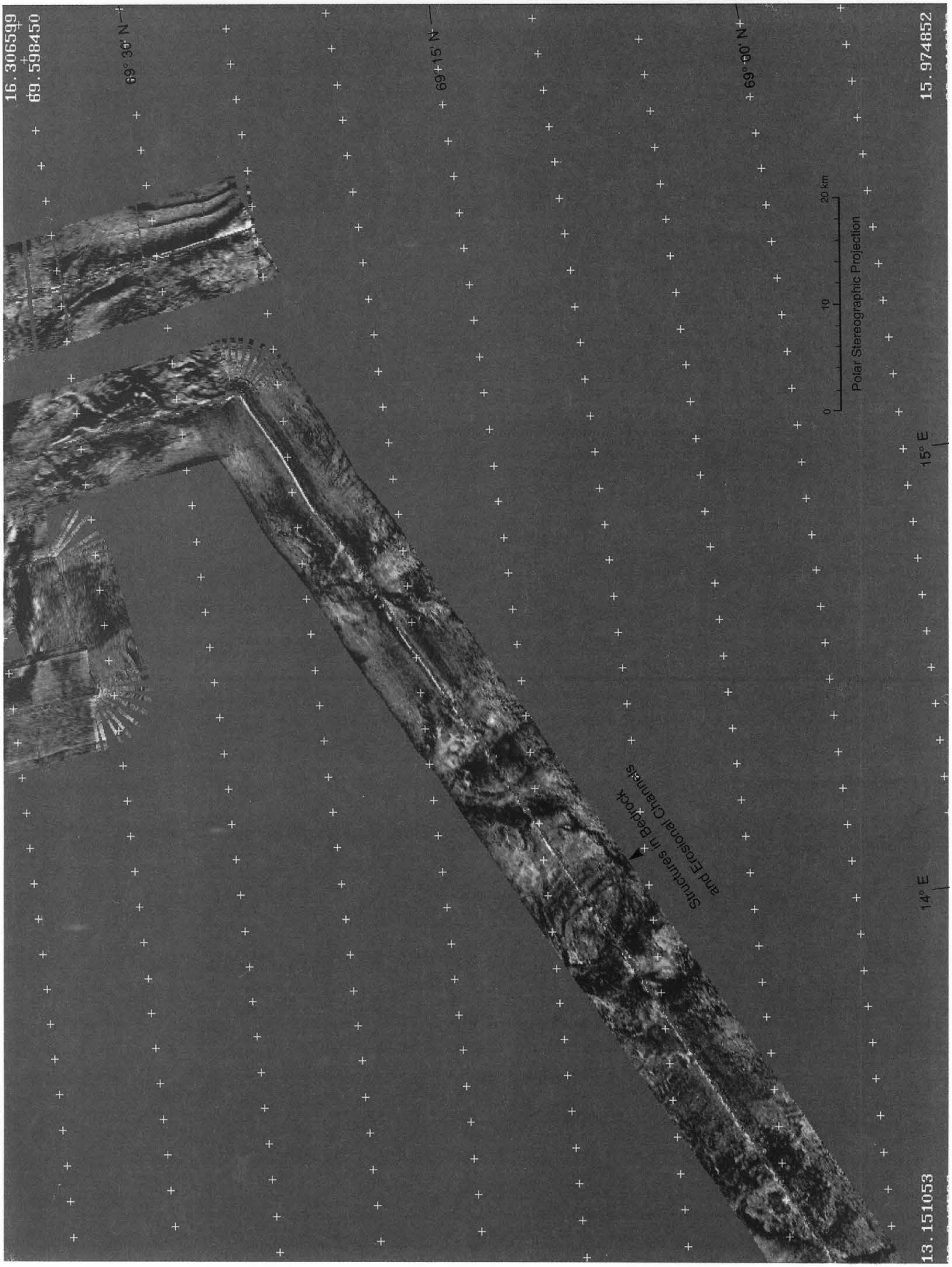

TILE 49B: SEAMARC II MERGED BATHYMETRIC AND SIDE-LOOKING SONAR DATA

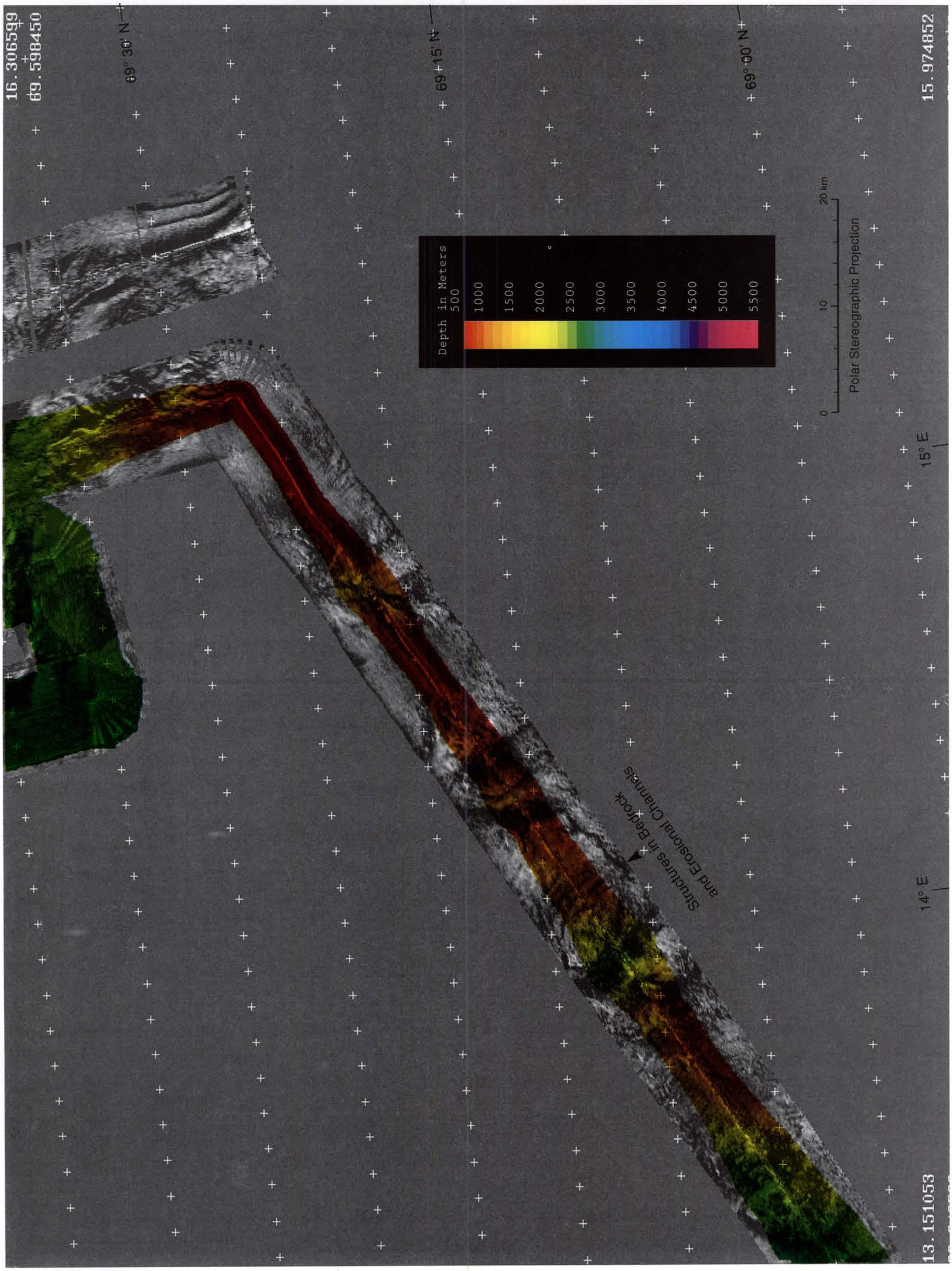

PLATE 64

VOLCANIC/TECTONIC INTERPRETATION OF THE KNIPOVICH RIDGE

K. Crane

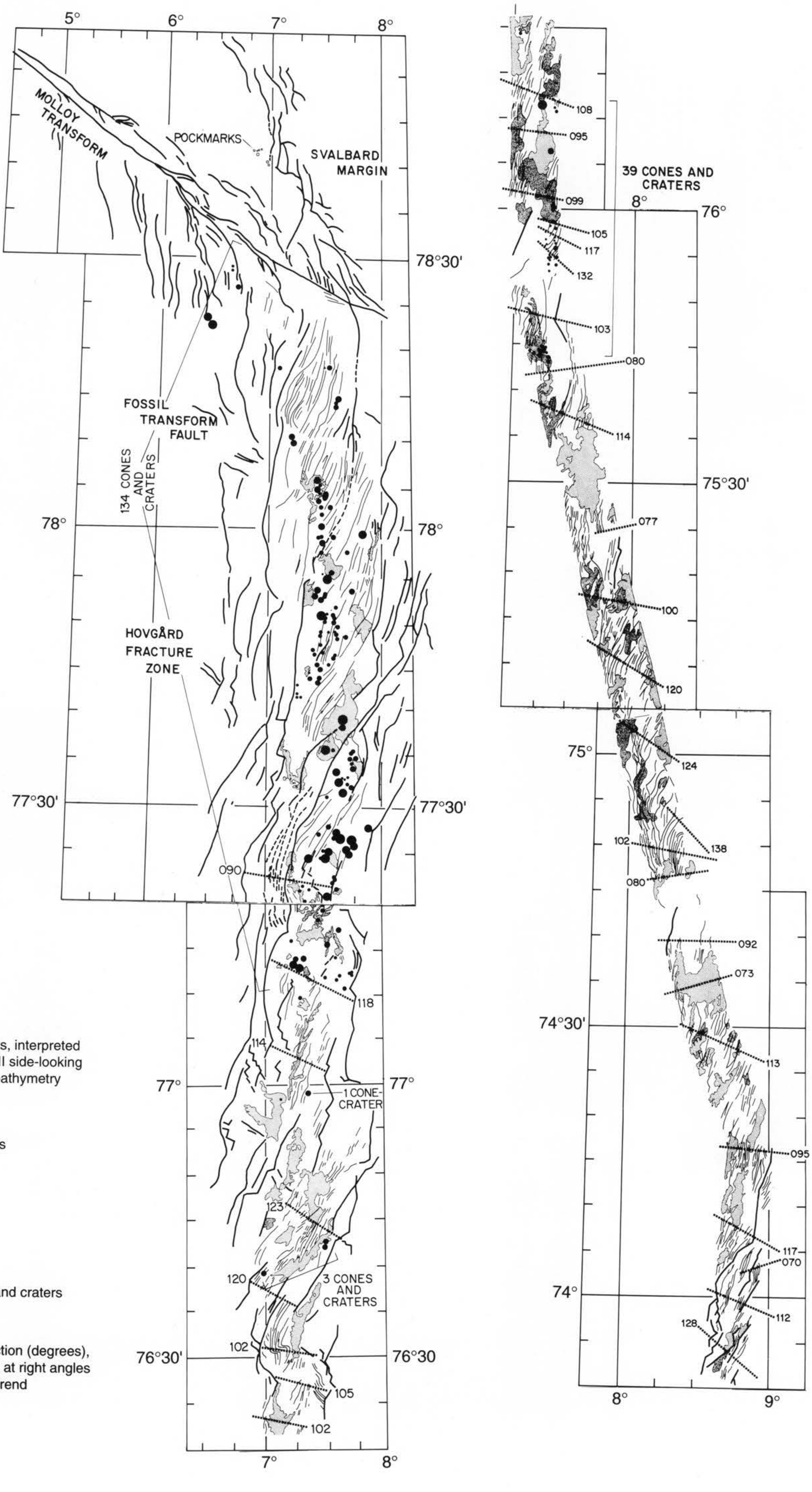

Legend:

Large offset faults, interpreted from SeaMARC II side-looking sonar data and bathymetry

Small offset faults

Lava flows

Volcanic cones and craters

Extensional direction (degrees), interpreted to be at right angles to the local fault trend

III. SEABEAM, HYDROSWEEP AND GLORIA SURVEYS

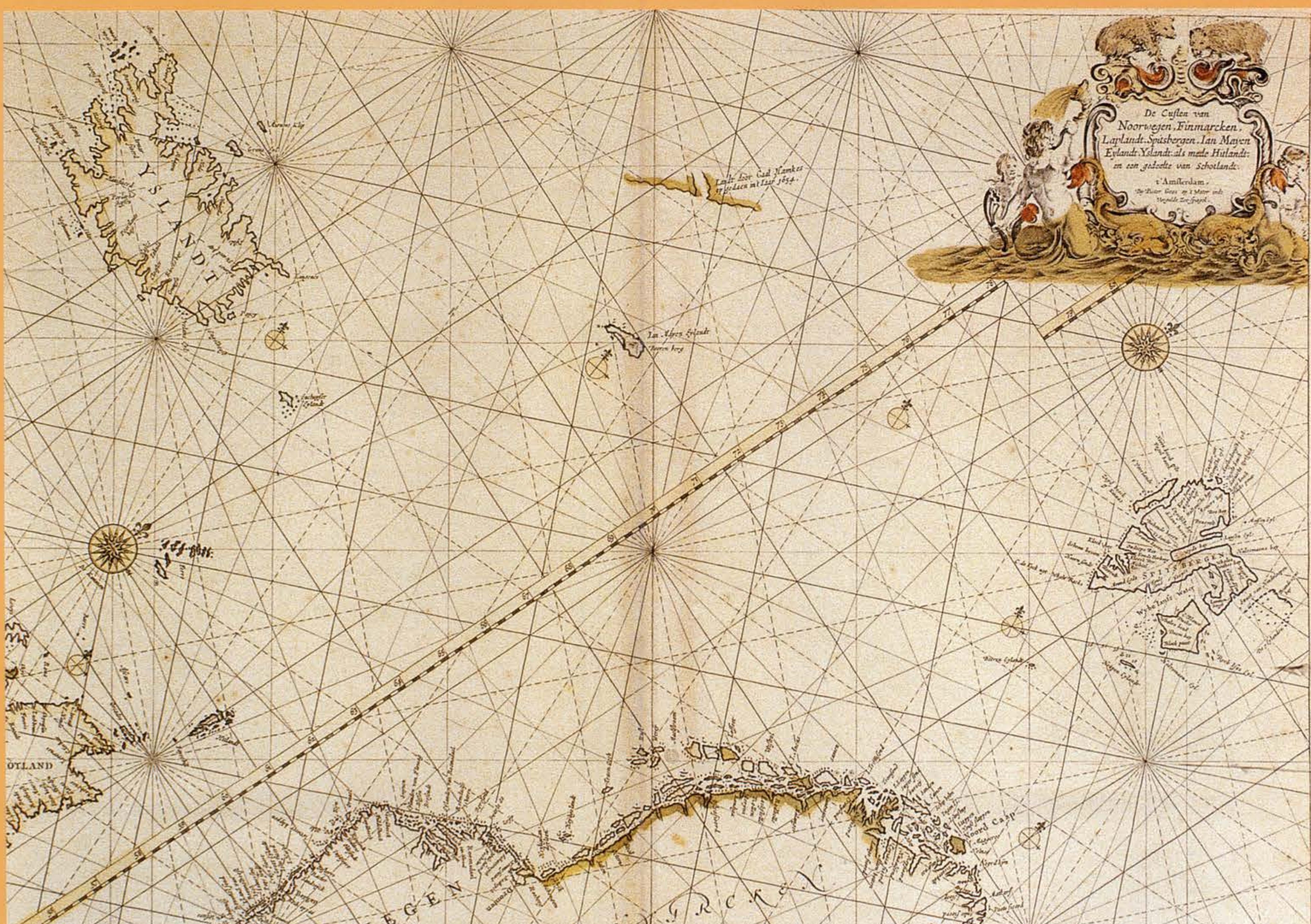

PLATE 65

SEABEAM AND SEAMARC II-DERIVED IMAGERY FROM THE MOHNS RIDGE

VINCENT RENARD, LOUIS GELI AND KATHLEEN CRANE

A two-cruise geophysical program conducted during the summer of 1988 by the Marine Geosciences Department of IFREMER collected SeaBeam data acquired by the *R/V Jean Charcot* multibeam facilities. The data indicate that the rift valley floor is broken into an en-echelon system of fault bounded basins oriented N30°, 30° oblique to the average strike of the Mohns Ridge axis (N60°). Within the en-echelon fault bounded basins lie volcanic ridges with large positive magnetic anomalies in excess of 1,000 gammas (Renard et al. 1989) (See Plate 5 for a regional perspective).

By comparison, SeaMARC II side-looking sonar data collected in 1989 and 1990 (H. Doss et al. pers. comm. 1994), reveal not only the en-echelon orientation of rift valley fissures and faults, but also the non-uniform spacing of volcanic cones, craters and large area lava flows. Cones and craters are most concentrated near 72°40'N and between 73°N and 73°20'N.

If inner rift fault strikes are consequences of local spreading directions, then seafloor extension across the Mohns Ridge is highly variable ranging from an orientation of 110° to 175°. More likely, the large variation in fault trend is a response of thin-skin faulting to the stress fields developed both at the locations where basins overlap as well as within the region of oblique transition between the Mohns and Knipovich Ridges. That no transform faults can be found in this bend linking the two spreading centers, may explain why fault orientations within the rift valleys are so oblique to the large scale trend of the plate boundaries.

SEABEAM AND SEAMARC II DERIVED IMAGERY FROM THE MOHNS RIDGE

(See PLATE 2 for Location and 64 for Legend)

V. Renard, L. Geli and K. Crane

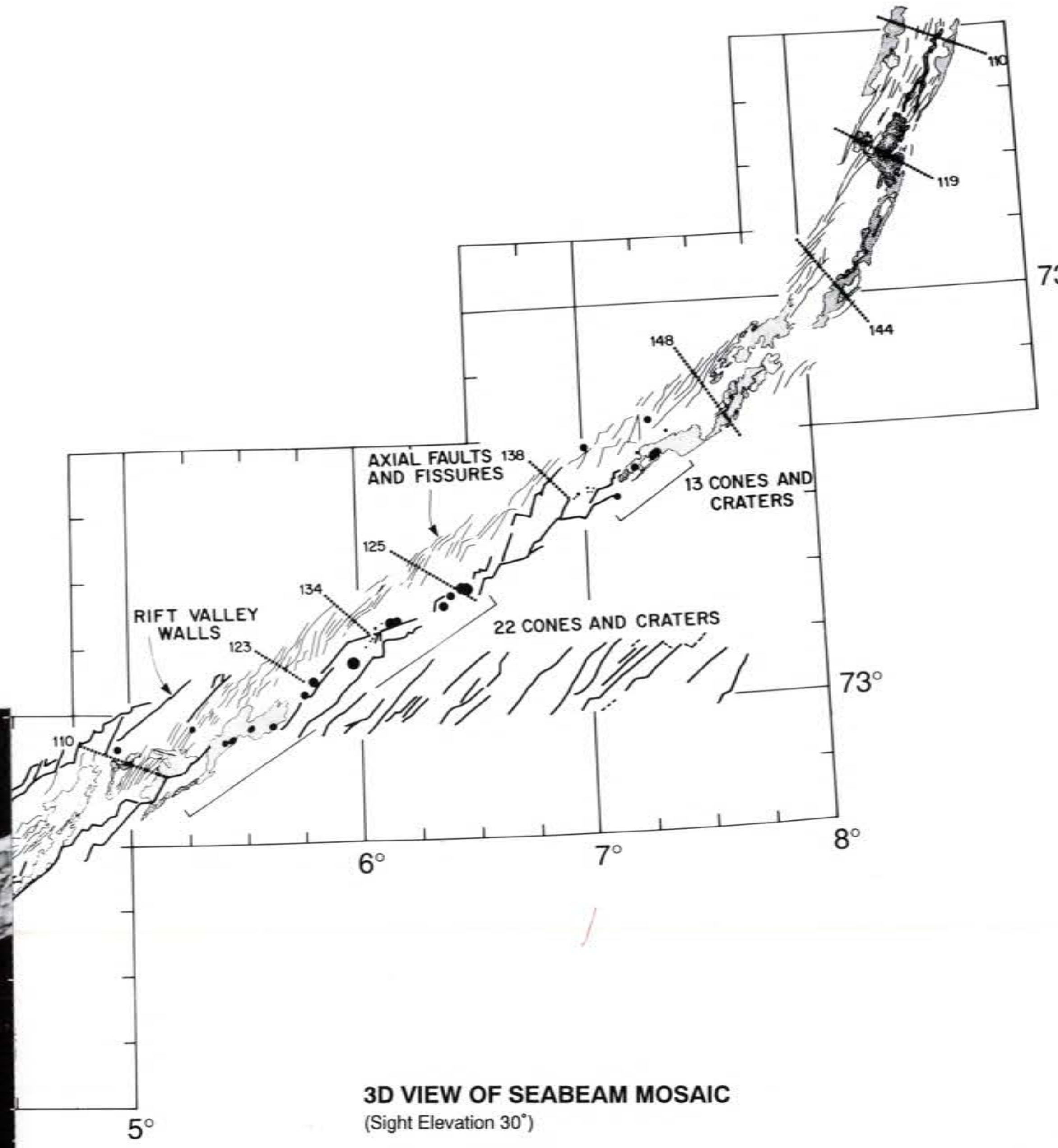

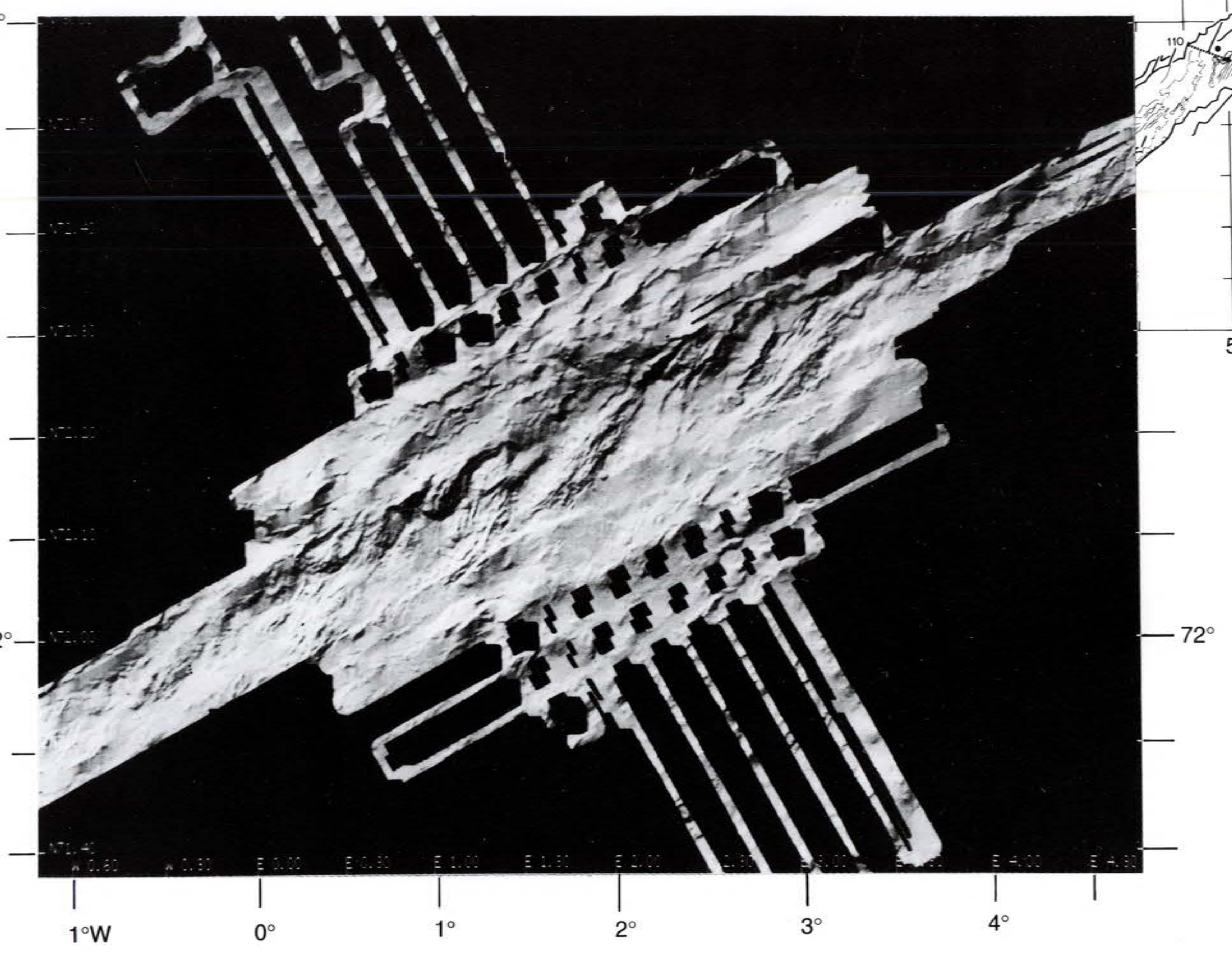

3D VIEW OF SEABEAM MOSAIC
(Sight Elevation 30°)

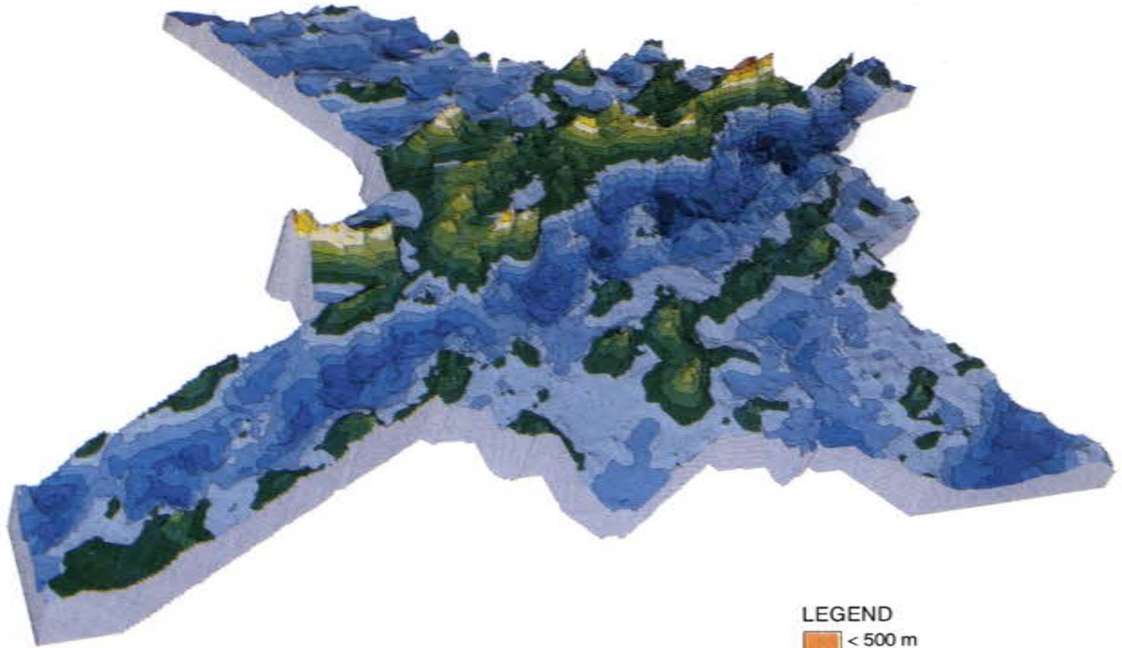

PLATES 66-70

MULTIBEAM BATHYMETRIC DATA OF THE MOLLOY DEEP, HOVGÅRD RIDGE AND VESTERISBANKEN

Klemens Heidland, Heinrich Hinze, Jürgen Monk, Fred Niederjasper, Hans-Werner Schenke and Telo Schöne

This compilation of bathymetry is based on marine surveys carried out during several *R/V Polarstern* expeditions between 1984 and 1991 (Cherkis et al. 1994, Döscher & Schöne 1992, Heidland 1989, Hempel et al. 1991, IGH 1984, and Niederjasper & Focke 1989). Two multibeam sonar systems (SeaBeam and Hydrosweep) were used to map a wide strip of the seafloor directly beneath the ship's track. The width of each swath is approximately 75% of the local depth ensonified by the SeaBeam sonar system and 200% of the local depth ensonified by the Hydrosweep sonar system. The combined surveys took over ten million bathymetric soundings and positions which were used to create the digital terrain model upon which the plates 66-70 are based. All bathymetric contours are determined using a standard sound velocity of 1,500 m/s in sea water.

Both SeaBeam and Hydrosweep data are compiled to create the 3-D low angle-oblique views of the Molloy Deep and Hovgård Ridge regions. The results show clearly the complexity of the Molloy Deep area which is comprised of two transform faults: (the Spitsbergen and Molloy) and a pull-apart spreading center of punctiform highs and one large depression (the Molloy Deep; the deepest spot in the Norwegian-Greenland Sea (>5,200 m)). In contrast, the Hovgård Ridge, which is thought to be a part of the Hovgård Fracture Zone, is an elongate high with a sheer southern wall and a V-shaped northern wall. That the geometry of this ridge is profoundly different from highs or ridges located in the Molloy and Spitsbergen Transform Fault regions, suggests different volcanic/tectonic provenances for these features.

In contrast to the Molloy Deep and Hovgård Ridge (regions which are associated with recent or ancient plate boundaries) is the punctiform shaped seamount called Vesterisbanken at 73°30'N and 9°W, thought to be an ancient volcanic feature located in mid-plate. Although no heat flow data have been collected close to Vesterisbanken, relatively high heat flow has been detected somewhat to the north (and also in mid-plate, see Plate 6) suggesting that the region may be undergoing either thermal rejuvenation or has been a continuous source of high heat flux throughout its history.

Acknowledgements

The authors would like to thank the responsible scientists who provided data and the individuals who participated in the following expeditions:

ARK II/4	W. Reil, Dr. H. W. Schenke
ARK III/2	K. Heidland, C. Jahnke, B. M. Powitz
ARK III/3	N. Cherkis, K. Heidland, C. Jahnke, B. M. Powitz
ARK IV/1	J. Focke, V. Meier, F. Niederjasper
ARK IV/3	K. Heidland
ARK VII/1	N. Cherkis, S. Steinmetz, J. Theiner
ARK VII/3a	J. Dreyer, R. Laing, J. Monk, F. Niederjasper, Dr. H. W. Schenke, K. Völker
ARK VIII/3	T. Döscher, T. Schöne

PLATE 66

SEABEAM AND HYDROSWEEP BATHYMETRY FROM THE MOLLOY AND HOVGÅRD RIDGES

K. Heidland, H. Hinze, J. Monk, F. Niederjasper, H-W. Schenke, and T. Schöne

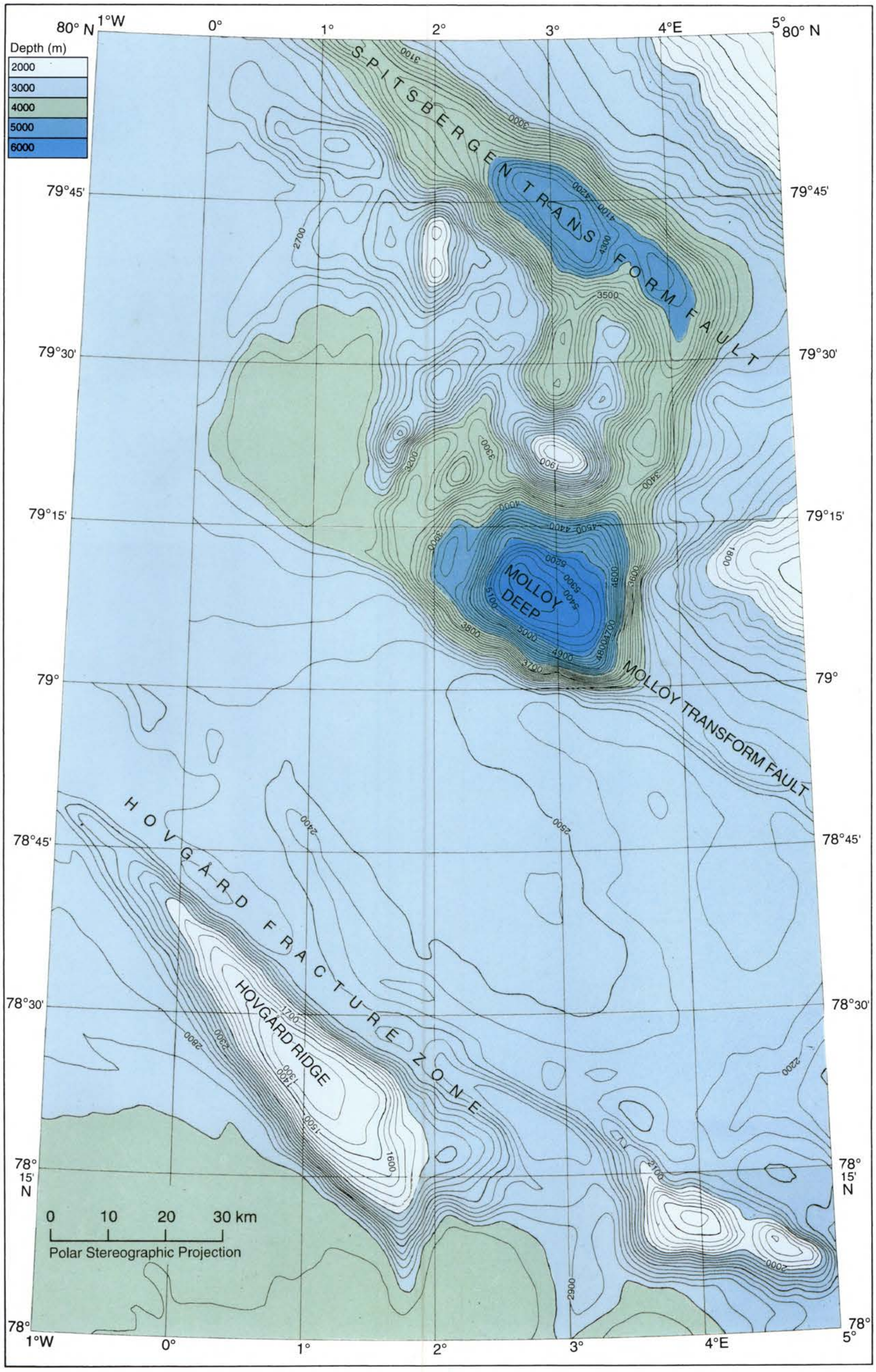

PLATE 67

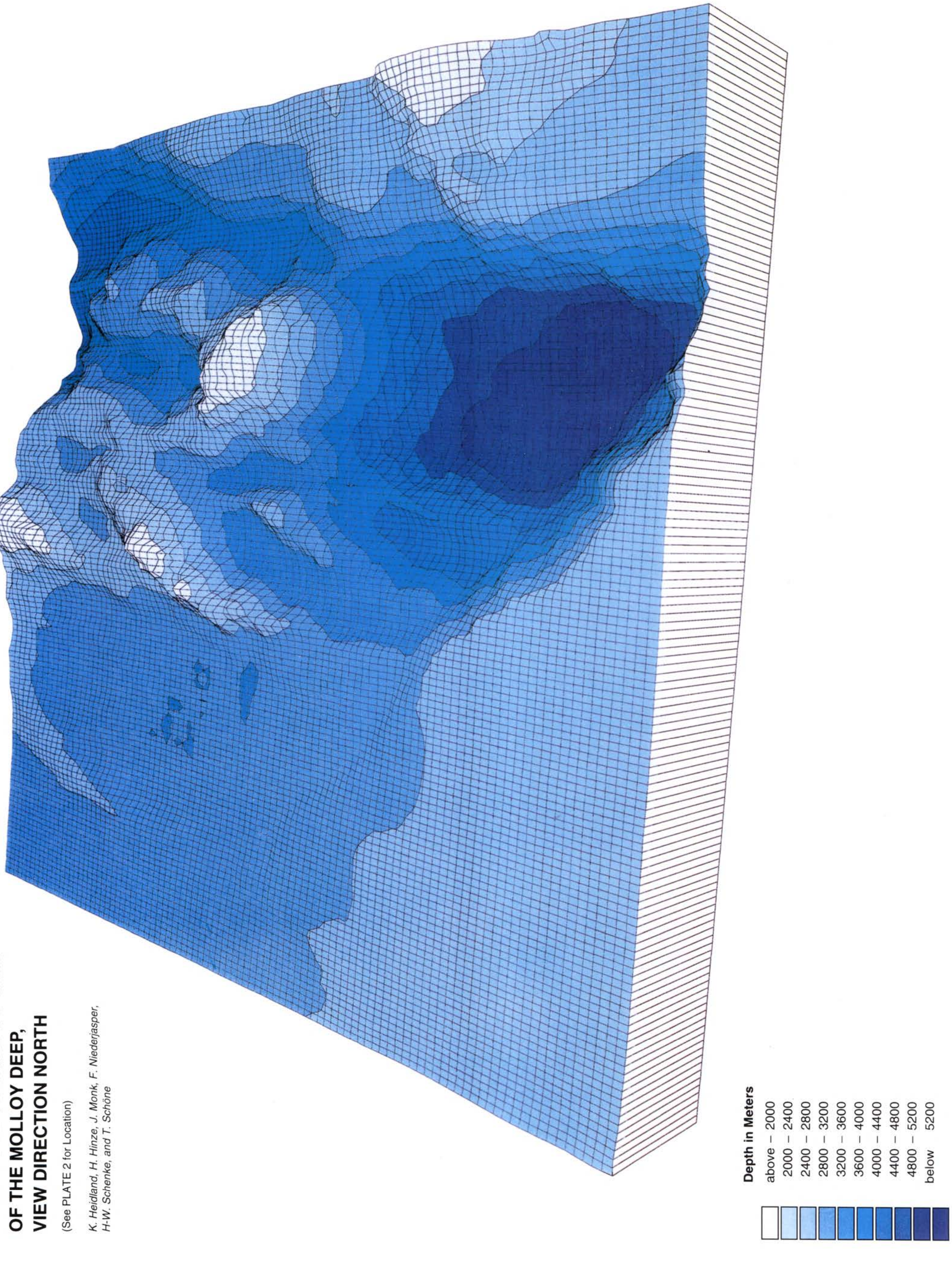

LOW ANGLE OBLIQUE 3-D VIEW OF THE MOLLOY DEEP, VIEW DIRECTION NORTH

(See PLATE 2 for Location)

K. Heidland, H. Hinze, J. Monk, F. Niederjasper, H-W. Schenke, and T. Schöne

LOW ANGLE OBLIQUE 3-D VIEW OF THE HOVGÅRD RIDGE, VIEW DIRECTION NORTH

(See PLATE 2 for Location)

K. Heidland, H. Hinze, J. Monk, F. Niederjasper, H-W. Schenke, and T. Schöne

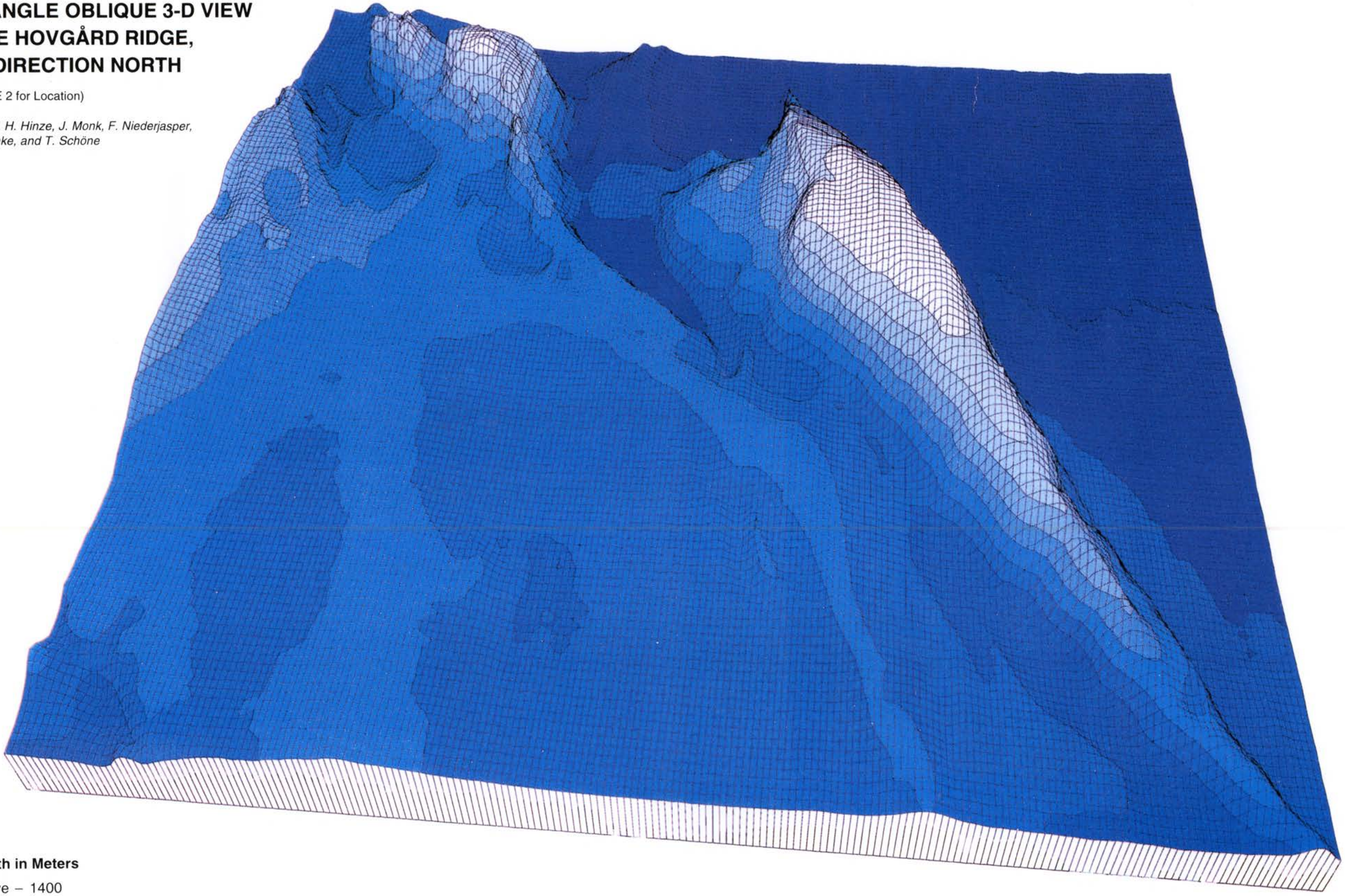

Depth in Meters

	above – 1400
	1400 – 1600
	1600 – 1800
	1800 – 2000
	2000 – 2200
	2200 – 2400
	2400 – 2600
	2600 – 2800
	2800 – 3000
	below 3000

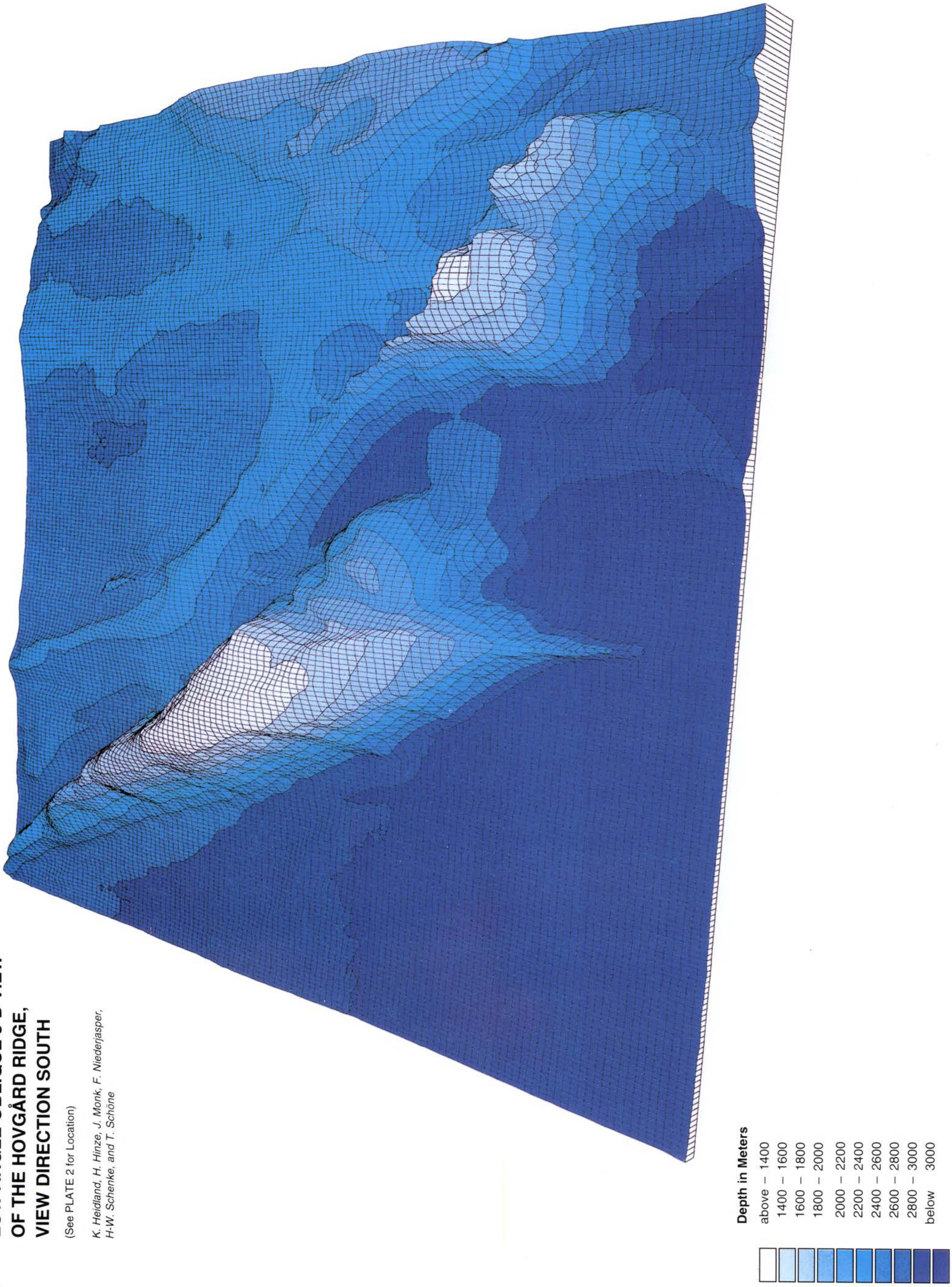

LOW ANGLE OBLIQUE 3-D VIEW OF THE HOVGÅRD RIDGE, VIEW DIRECTION SOUTH

(See PLATE 2 for Location)

K. Heidland, H. Hinze, J. Monk, F. Niederjasper, H-W. Schenke, and T. Schöne

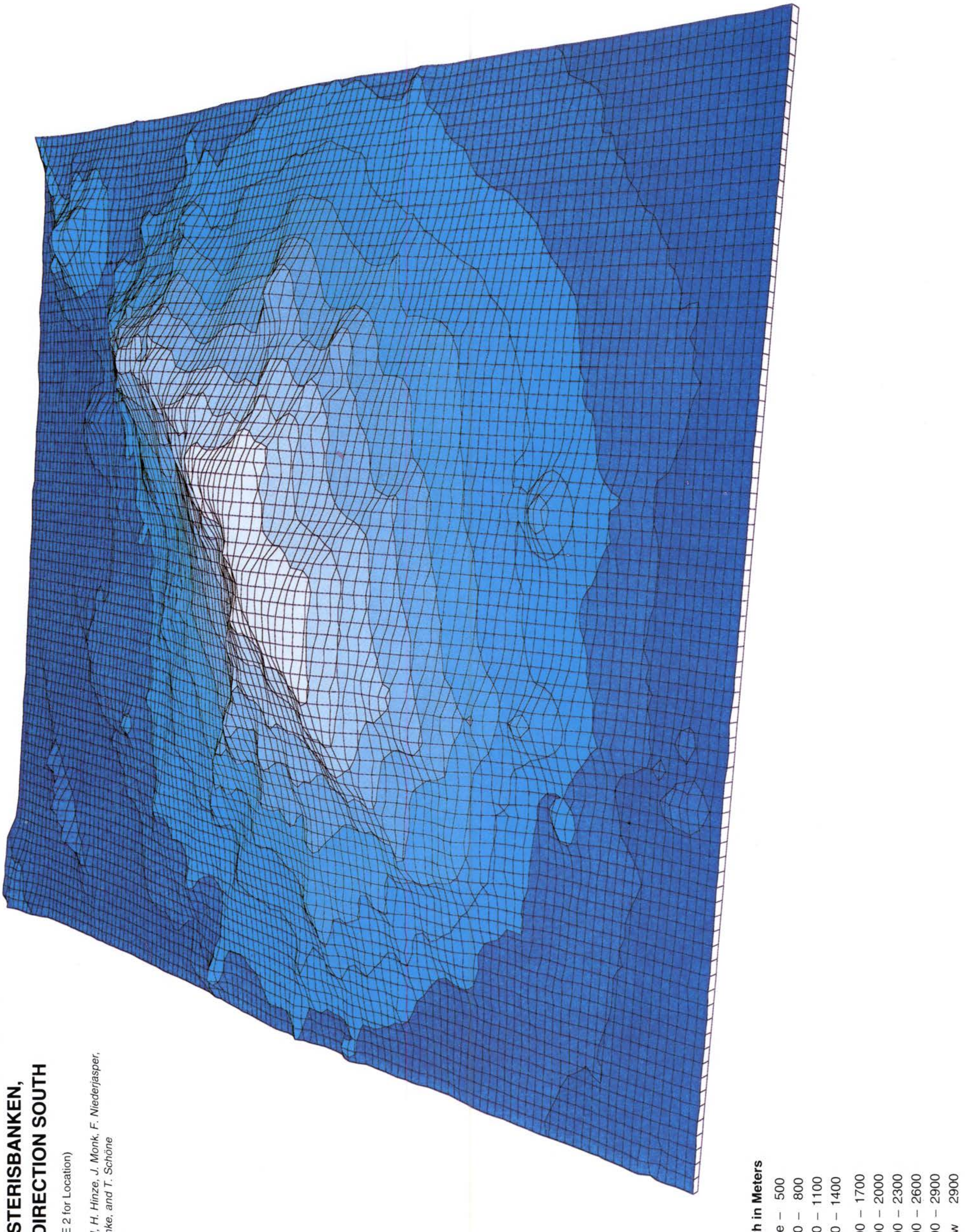

LOW ANGLE OBLIQUE 3-D VIEW OF VESTERISBANKEN, VIEW DIRECTION SOUTH

(See PLATE 2 for Location)

K. Heidland, H. Hinze, J. Monk, F. Niederjasper, H-W. Schenke, and T. Schöne

PLATE 71

GLORIA SURVEY OF THE EAST GREENLAND MARGIN: 70°N TO 80°N

JÜRGEN MIENERT, FRANZ-JOSEF HOLLENDER AND NEIL H. KENYON

The GLORIA System

The technique and interpretation of long-range sidescan sonar were pioneered at IOS (Institute of Oceanographic Sciences, Deacon Laboratory, Wormley, U.K.) (Somers et al. 1978).The GLORIA system has two rows of transducers with 30 elements, each emitting a beam swath with a horizontal angular width of 2.5° and a peak vertical angular beam width of 30°. The operating frequency is 6.2 to 6.8 kHz, with a peak electrical power of 12 kW per side and a peak power into the water of 10.5 kW per side. The seafloor coverage ranges from 7 km to 30 km on each side. GLORIA is 7.75 meters long, has a diameter of 0.66 meters (the length of the active part is 5.33 meters), the total weight of the vehicle in air is 2.04 tonnes, and the overall weight including cable, power pack, etc. is 13 tonnes. It is towed 400 meters behind the survey ship at a speed of up to 10 knots and a nominal depth of 50 meters. The output of GLORIA data are stored on magnetic tape in a digital format and on-line on analog images from which the sidescan sonar mosaic shown in this atlas (Plate 71) is produced.

Sedimentary Processes

During the cruise with the *R/V Livonia* in 1992, GLORIA was used to map large scale changes in sedimentary pattern along the east Greenland continental margin (Plate 2). The goal of the cruise was to determine the variety of large scale sea floor processes in order to improve our understanding of the interaction between ice sheets, current regimes and sedimentary processes. The working area encompassed the Fram Strait, the Boreas Basin, the Greenland Basin and a small basin just north of the Jan Mayen fracture zone. The area is normally heavily covered by sea ice except during August and September when the sea ice front often retreats towards the shelf edge.

The Boreas Basin has a very uniform medium to low level backscatter with the exception of a single lineated weakly-backscattered feature that appears to be a channel cut into the seafloor at 78°N and 1°E. This channel is discontinuous and is thus believed to be inactive and perhaps filled by fine grained abandoned sediment facies (Mienert et al. 1993). In all of the sonograph images of this area, one notices an acoustic artifact, which is believed to be the result of interference fringes caused by multiple paths taken through the uppermost layers of soft sediment. This implies that the sea floor sedimentary layers are fine grained but with differing acoustic properties. Patches of high backscatter, some of which have a positive relief, are also seen at 77°50'N and 2°W. The patches are equidimensional and up to half a kilometer across. They may be indicative of gas venting because pockmarks and hard grounds are located in the region.

Backscatter Provinces

Backscatter provinces in the Greenland Basin are variable but the overall backscatter level is much higher than that of the Boreas Basin. In the south, four deep sea channel systems are observed, whereas the northern basin remains relatively uncut by channels. In the north, the shelf is at its widest and is believed to have been built out over a long period by sedimentation from glaciers that possibly covered the cross shelf trough. On the continental slope changes from very high backscatter at the upper slope to intermediate backscatter at a possible sediment wave field (75°40'N, 6°W) to low backscatter at the base of the slope are observed. Superimposed on the steeper slope are lineations which resemble scoured channels (75°40'N, 7°W) (Mienert et al. 1993). The lineations are similar in size to the downslope trending scours found on the Norwegian margin, attributed to cold water cascades (Vorren et al. 1989). The uppermost part on the slope was not observable because the range of the sonar was limited by sea ice cover and the density structure in the water column which distorted the acoustic pathway. Adjacent to this region are regularly spaced bands of contrasting backscatter that are believed to be sediment waves with a wavelength of 2-3 km. This feature is common in deep sea channelised systems and is usually attributed to the molding of the muddy overbank sediments by near-bottom currents which remove the upper layer of the turbidity flow (Mienert et al. 1993). The basin north of the Jan Mayen Fracture Zone (71°40'N, 10°-12°W) is not cut by channels nor is there any evidence for the transport of sediment from the shelf into the basin.

A first conclusion based on the interpretation of the analog sonographs of the long-range sidescan sonar GLORIA is: There is little direct evidence for along slope transport of sediments adjacent to the east Greenland margin and basins (Sommerhoff 1973). In contrast, strong evidence exists for down slope transport of sediment from the Greenland shelf into the Greenland Basin. The existence of sediment wave fields may indicate bottom water or turbidity current activity at specific locations. Circular patches with a high level of backscatter hints at areas of gas venting. All of these interpretations need to be ground truthed by direct sampling or the use of alternative imaging techniques.

PLATE 71

GLORIA SURVEY OF THE EAST GREENLAND MARGIN

J. Mienert, F.J. Hollender and N. Kenyon

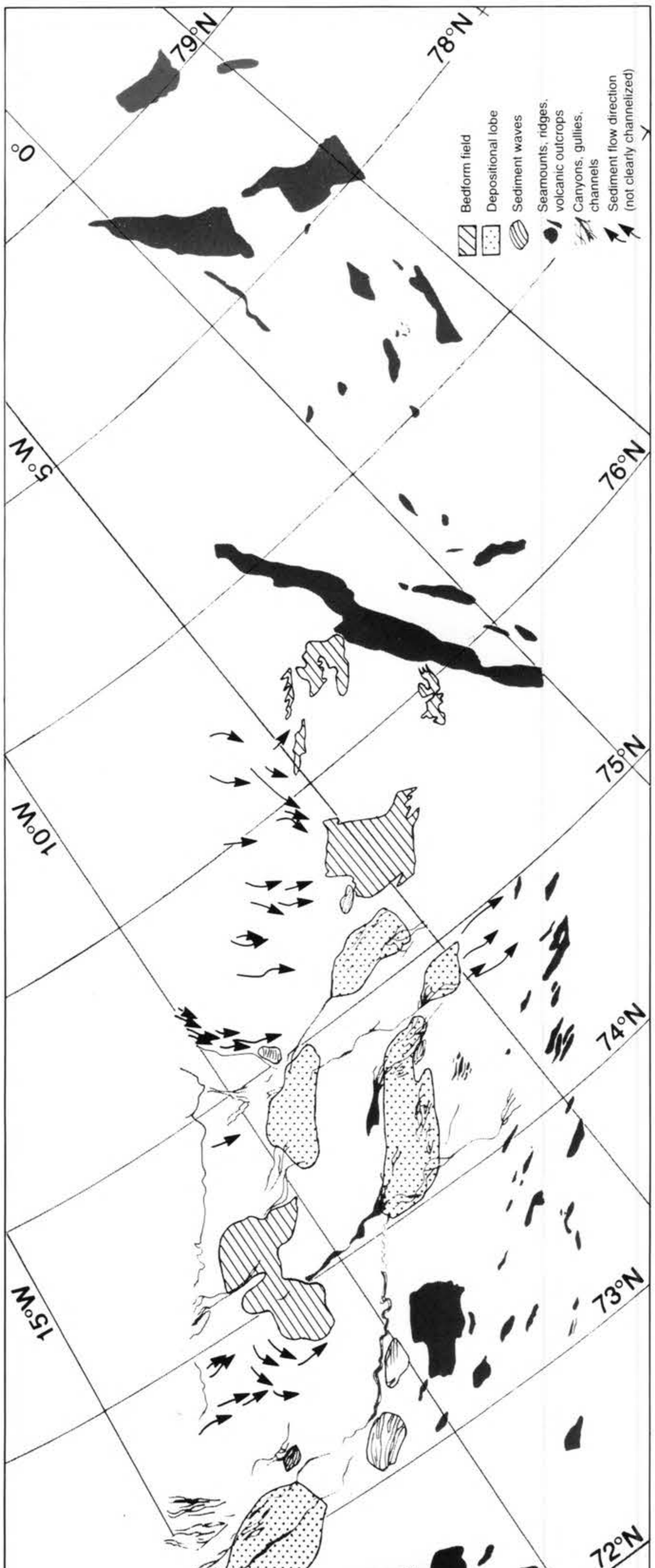

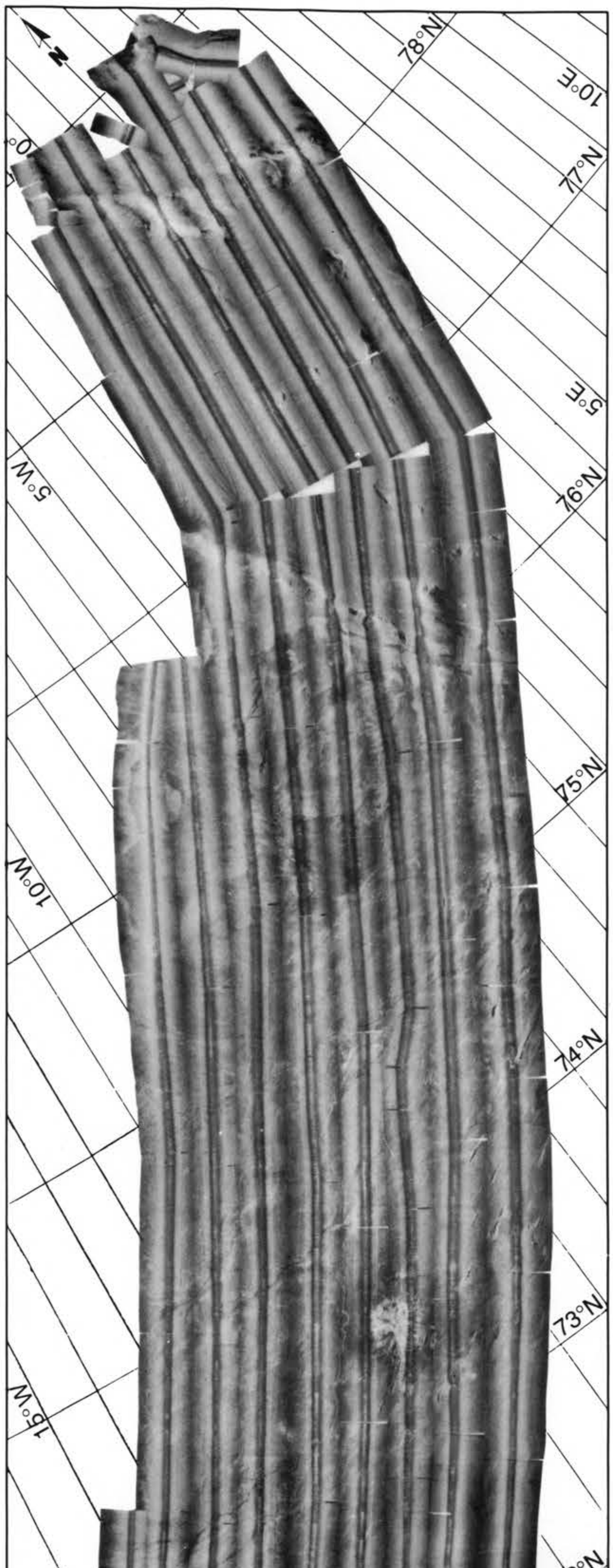

SCALE 1: 3 000 000

0 50 100 km

IV. SEISMIC PROFILING AND STRATIGRAPHY

PLATES 72–75

LATE CENOZOIC SEISMIC STRATIGRAPHY AND CHARACTER OF THE SVALBARD-BARENTS SEA MARGIN

ANDERS SOLHEIM AND ESPEN S. ANDERSEN

Seismic Data

A number of seismic investigations have been carried out on the Svalbard - Barents Sea margin since 1970 by several different institutions. They include both multichannel (MCS) and single channel (SCS) acquisition. Data presented in Plates 72-75 are from the Norwegian Petroleum Directorate (NPD), the Universities of Bergen and Tromsø in Norway, the Norwegian Polar Institute (NPI), and the Bundesanstalt für Geowissenschaften und Rohstoffe (BGR) in Germany (Hinz & Schlüter 1978; Schlüter & Hinz 1978; Sundvor et al. 1978, 1982a, b; Eiken & Austegard 1987; Solheim et al. 1991). An overview of all seismic surveys carried out on the Svalbard margin is presented by Eiken (1994).

Due to many years of hydrocarbon exploration, the Barents Sea margin is relatively well mapped with commercial multichannel seismic data. Both the coverage and the quality are more variable adjacent to Svalbard, and particularly on the western Spitsbergen continental shelf and upper slope. Most of the data are from conventional surveys using small airgun arrays as sources with 6 seconds recording time and 12-24 fold coverage. In 1987, the Norwegian Polar Institute and the University of Bergen jointly carried out a multi-channel survey using a commercial vessel with a 240 channel streamer and airgun arrays up to 7000 cu. inches. Two types of data were acquired: the University of Bergen ran a deep, low resolution survey, using maximum source volume and 15 seconds recording time, while NPI carried out a high resolution survey using a 2000 cu. inch array with 60-fold coverage. In a recent publication, Eiken (1994) presents a comprehensive description of the seismic character from transects of the western and northern Svalbard margins.

The most detailed high resolution data set from the western Svalbard Margin was acquired by NPI in 1990 using single-channel recording and a small array of two 40 cu. inch sleeve guns as a source (Solheim et al. 1991) (Plates 74 & 75). Later, in 1994, the Norwegian Polar Institute carried out a similar survey on the northern margin of Svalbard and the Barents Sea, using a 4 x 40 cubic inch sleeve gun source (Solheim, unpublished). On the Barents Sea margin, the University of Tromsø carried out single channel sparker investigations of the Bear Island Fan for several years. Results from these investigations are presented by Laberg & Vorren 1995 (Plate 76).

Depositional and Glacial Evolution of the Margin

Pre Weichselian

The evolution of the Svalbard-Barents Sea margin as a passive sheared margin is closely connected to the gradual opening of the Norwegian-Greenland Sea, which commenced around the Paleocene-Eocene transition, at ca. 57 Ma, and propagated northwards along the Barents Sea and Svalbard area from early Eocene to early Oligocene (Talwani & Eldholm 1977; Myhre et al. 1982; Reksnes & Vågenes 1985; Eldholm et al. 1987; Crane et al. 1991). Since the Oligocene, oceanic crust has evolved along the entire Svalbard-Barents Sea Margin, with subsequent subsidence and deposition of a thick Cenozoic sediment wedge, with the Barents Sea continental shelf and Svalbard as source areas for the sediments. Recent studies of sediments sampled from commercial wells located in the southwestern Barents Sea indicate that a major part of the sediment wedge is of glacial origin

(Eidvin & Riis 1989; Eidvin et al. 1993). This implies an extensive glacial erosion over the Barents Sea. The main problem, however, when discussing the late Cenozoic evolution along the margin, is the scarcity of chronostratigraphic data. Based on results from the Ocean Drilling Program (ODP) Leg 104 sites on the Vøring Plateau, off northern Norway (Eldholm, Thiede et al. 1989), the initial stage of glaciation occurred at 5.5 Ma, followed by an intensification at 2.57 Ma. Between 1.2 and 0.8 Ma, the glacial-interglacial changes turned into a 100 ky cyclicity and the amplitudes became higher, i.e. the interglacials were warmer and the glacials more severe, creating ice sheets that probably also covered the large continental shelf areas (Jansen & Sjøholm 1991). The sedimentary section at the Deep Sea Drilling Project (DSDP) Site 344, on the eastern flank of the Knipovich Ridge, SW of Svalbard, terminates at a basaltic intrusion K/Ar dated to 3 Ma (Talwani, Udintsev et al. 1976). All the sediments above this show a glacimarine character and therefore indicate that glaciers reached sea level in the mid Pliocene in this region. From the Barents Sea, seismic stratigraphic interpretations indicate that total glaciation occurred on the shelf at least five times (Solheim & Kristoffersen 1984; Vorren et al. 1988). Seismic data from the western Svalbard margin also indicate repeated glacial advances to the shelf edge (Andersen et al. 1994).

Seismic sequences have now been correlated along the entire western Svalbard and Barents Sea margins, a distance of nearly 1,000 km (Fiedler 1992; Hjelstuen 1993; Andersen et al. 1994; Faleide et al., in press). The majority of the data used are conventional multi-channel seismic records, and the correlation is mainly focused on the part of the section which is interpreted to be of glacial origin. Seven regional reflectors, R7-R1, have been identified, of which the most important are shown in plates 72 through 75. R7 is interpreted to represent onset of continental shelf glaciation in the northern areas, and corresponds to the lowermost regional unconformity, U2, defined by Schlüter & Hinz (1978) off the Svalbard Margin. In the northern region, along the Storfjorden Fan and the Svalbard Margin, the sequence bounded by R7 and R6 has a chaotic seismic character (Plate 72, Lines BGR 31-74 and BEL-1, and Plate 73, Lines BGR 23-74 and SVA 2-87) interpreted to result from mass wasting processes. A likely explanation for this is increased deposition on the upper slope and outer shelf when glaciers reached the shelf break already in the early stages of glaciation in this region. Further south, at the Bear Island Fan, large scale mass wasting appears to commence later, at reflector R5 time (Plate 73, Line NPD 7300-75), and can be identified as large scale structures through the sedimentary section up to R2.

R5 forms an important boundary off Svalbard, where it marks the onset of frequent slumping activity on the continental slope, and hence an important change in the depositional environment. To the north of the fan, the seismic sequences form a condensed, well stratified section, whereas the fan proper shows a large increase in the thickness of individual sequences and a major change in their internal seismic character. Typically, the internal reflectors are discontinuous and often define lense shaped bodies. The individual bodies are 10-30 m thick, 2-3 km wide and 10-20 km long. They are interpreted to represent individual slumping events and result from rapid deposition through ice streams directly on the outer shelf and upper slope (Andersen et al. 1994).

No channels are identified on the Isfjorden Fan, an observation which is confirmed by SeaMARC II side-looking sonar data (Crane et al. 1995, Plates 8-63). Although the southern boundary of the fan is less well defined than the northern boundary, the sequences gradually thin to form another condensed section before they thicken again in the next fan southwards, the Bellsund Fan.

The "Upper Regional Unconformity" (URU), identified in the western Barents Sea continental shelf (Solheim & Kristoffersen 1984), corresponds to progressively younger slope reflectors to the south. Off Svalbard, URU corresponds to R5, while it corresponds to R3 and R1 in the areas of the Storfjorden and Bear Island Fans, respectively. One implication of this is that the northern parts of the Barents Sea and Svalbard platform have experienced a greater glacial erosion than the southern parts. This implication is supported by recent calculations of sediment yield from various parts of the Barents Sea and Svalbard (Hjelstuen 1993; Elverhøi et al. 1995).

With the few drill holes in the region, the age constraints for the seismic stratigraphy are sparse. The chronology is based on: a) general plate tectonic evolution and the age of magnetic anomalies in oceanic crust (Talwani & Eldholm 1977; Reksnes & Vågnes 1985; Fiedler 1992), b) DSDP Site 344 (Talwani, Udintsev et al. 1976), c) deep, commercial wells on the southwestern Barents Sea shelf (Eidvin et al. 1993), and d) shallow wells in the outer parts of the Bear Island Trough (Sættem et al. 1992).

Reflector R7 is tied seismically to the base of the glacial sediments in the wells on the Senja Ridge. The age of the boundary in the wells is estimated to be 2.6 Ma, based on biostratigraphy, Sr-isotopes, and correlation with ODP Leg 104 results. In the seaward direction, R7 terminates against oceanic crust of no older than Pliocene age, based on magnetic sea floor anomalies (Fiedler 1992). Furthermore, a seismic tie from the southern Svalbard margin to Site 344 on the flank of the Knipovich Ridge, places the base of the drilled sedimentary section, which has an age of around 3 Ma, within the seismic sequence between R7 and R6, i.e. in the lowermost glacial sequence. Recent K-Ar dates of volcanogenic clasts immediately below the fan sequences in a shallow drillhole on the shelf southwest of Bear Island (Mørk & Duncan 1993; Sættem et al. 1994), however, indicate an age of 2.3 Ma for R7.

Of the other regional reflectors, only R1 can be tied directly to well information. In a shallow well in the Bear Island Trough, the sediments above URU, which in this area is correlated to R1, are interpreted from amino acid analyses to be younger than 440 ka (Sættem et al. 1992). Between R7 and R1, only assumptions based on general knowledge about the paleoclimatic history can be made about the age relationships. The erosion marked by R5 in the Storfjorden area and the change in depositional style on the Svalbard margin at the same time, may be related to the change in the style of the climatic fluctuations at 1.2-0.8 Ma (Jansen & Sjøholm 1991).

Based on the above chronological constraints and seismic correlations, the following glacial history can be suggested:

* Glaciation in the marine shelf areas commenced sometime between 5.2 Ma and 2.3 Ma. Existence of alpine glaciers prior to this is not excluded.
* Glacial influence on the margin sedimentation started earlier adjacent to Svalbard than further south. The main glacial depocenter in an early phase was the Storfjorden Fan.
* A general intensification of the glaciations took place at about R5 time. This led to erosion in the Storfjordrenna area, and a major change in depositional style off western Svalbard.
* The Upper Regional Unconformity (URU), as presently defined on the shelf, developed through repeated glaciations throughout the Middle/Late Pleistocene, with a deeper erosion in the north than in the south.

Weichselian and Post-glacial History

There are strong indications for extensive glaciations of Svalbard and the Barents Sea area during the Early and Middle Weichselian. In western Svalbard, Early, Middle and Late Weichselian tills are found in coastal sections (Mangerud & Svendsen 1992). These also seem to correlate with periods of high glacial input to the deep sea sediments of the Greenland Sea (Hebbeln 1992), and an extension beyond the coast is likely. In the Barents Sea, till and glacial marine sediments older than the Late Weichselian are found in a local sediment accumulation northeast of Bjørnøya (Elverhøi et al. 1992).

Svalbard and the Barents Sea were covered by a marine based ice sheet during the Late Weichselian. Maximum extent of the ice sheet occurred around 18-20 ka. Although the relation between the Svalbard and Barents Sea Ice Sheets during the Late Weich-

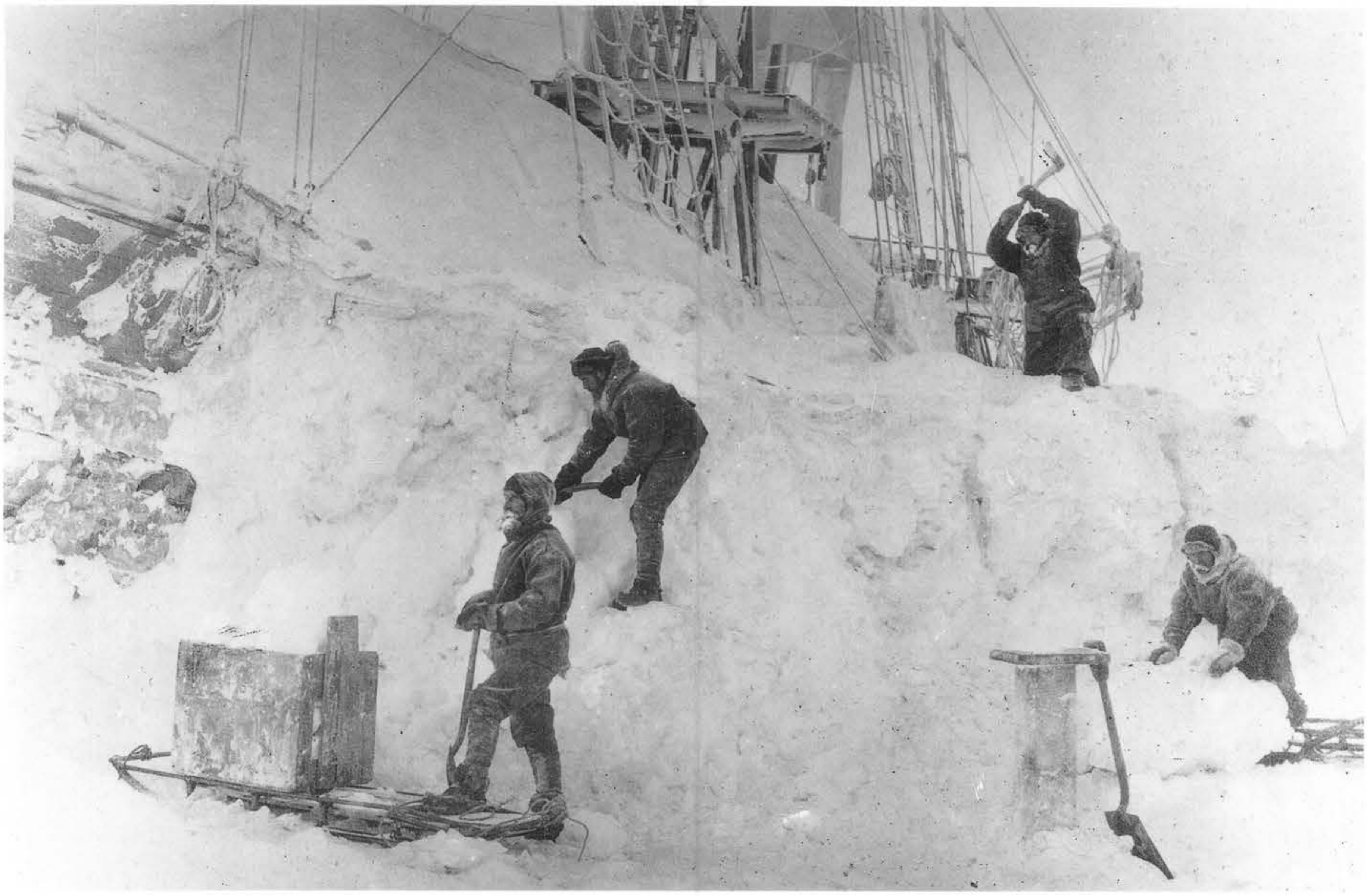

selian seems established, the glacial extent on the west coast of Svalbard has been widely debated. New sedimentological data, combined with radiometric dates, however, show that the continental shelf was covered by grounded ice outside both the two fjords, Isfjorden and Kongsfjorden, and that rapid deglaciation of these areas took place shortly after 15 ka. Present knowledge about the growth and decay of the Late Weichselian Barents Sea ice sheet seems to indicate that it was decoupled from the Fennoscandian Ice Sheet at an early stage of deglaciation (Elverhøi et al. 1994).

Indications both in the continental shelf areas and from the deep sea, point towards rapid, stepwise deglaciation of the entire marine based Barents Sea ice sheet, as well as of the marine based parts of the ice centered over Svalbard (Jones & Keigwin 1988; Solheim et al. 1990). An initial and major event in this deglaciation took place between 15 ka and 14 ka, and by 10 ka, the entire Barents Sea was deglaciated, and the glaciers on Svalbard were approximately at their present locations (Svendsen et al. 1992). The rapid deglaciation occurred through massive calving as a result of destabilization caused by the eustatic sea level rise. Large amounts of IRD were transported and deposited in the Norwegian-Greenland Sea.

Sediments

In the continental shelf areas, the general upper sediment succession consists of overconsolidated Late Weichselian till, covered by an ice proximal glacial marine sediment of up to 2 m thickness, deposited at high rates during ice recession, and Holocene muds with a generally low content of IRD (Elverhøi & Solheim 1983; Svendsen et al. 1992). The lithologies in cores from the continental slope and the deep sea are typical for glacial marine, hemipelagic sedimentation also found further south along the Norwegian continental margin, and include structureless, laminated, layered and bioturbated mud. In addition, the sediments also include silty and sandy turbidites, mostly of pre Late Weichselian age. Further south in the Norwegian Sea, foraminifer- and nanno oozes, with carbonate contents up to 60% occur relatively frequently, reflecting interglacial periods with high surface water productivity (Henrich et al. 1989). In general, carbonate rich deposits become less frequent northwards and towards the continental margins, where the dilution effect caused by terrigeneous input increases. This is seen towards both the Svalbard - Barents Sea margin and the Greenland margin, respectively (Baumann et al. 1993; Hebbeln & Berner 1993).

Holocene sedimentation is generally low, as most of the sediments transported to the marine environment is deposited in fjords and other near coastal areas (Pfirman & Solheim 1989; Elverhøi et al., 1994). Holocene linear sedimentation rates from Isfjorden, western Svalbard, vary between 15 cm/ky and 75 cm/ky, while the average rate in the Barents Sea is 2-7 cm/ky (Elverhøi & Solheim 1983; Elverhøi 1984; Elverhøi et al. 1989). Deep sea linear sedimentation rates from the Norwegian-Greenland Sea also generally fall in the range of 2-6 cm/ky, averaged over the last 100-300 ky, i.e. intervals usually reachable by conventional piston coring devices (Thiede at al. 1986; Henrich et al. 1989).

The lithology and physical properties of the Svalbard margin sediments are exemplified by cores NP90-12 and NP90-39, recovered from the continental slope and rise west of Svalbard, respectively (Figures 4 and 5). The lithology varies between finely laminated and massive muds, all associated with coarse grained IRD. They are normally consolidated, as seen from both the undrained shear strengths and the water content, although the slope core (NP90-12) has a hiatus spanning most of the Holocene. This core is taken immediately north of the Isfjorden Fan proper, and is therefore not affected by the frequent, small scale mass wasting processes associated with the fan (Plate 73). Cores recovered from the fan generally show a higher content of coarse grained material, which gives the sediment a lower water content and higher bulk density. Sediments on the Bear Island Fan, further south on the Barents Sea margin, are affected by debris flow processes on a slope of lower gradient than off Svalbard. The sediments, however, are similar in character to those on the Svalbard margin (Laberg & Vorren 1995, Plate 76).

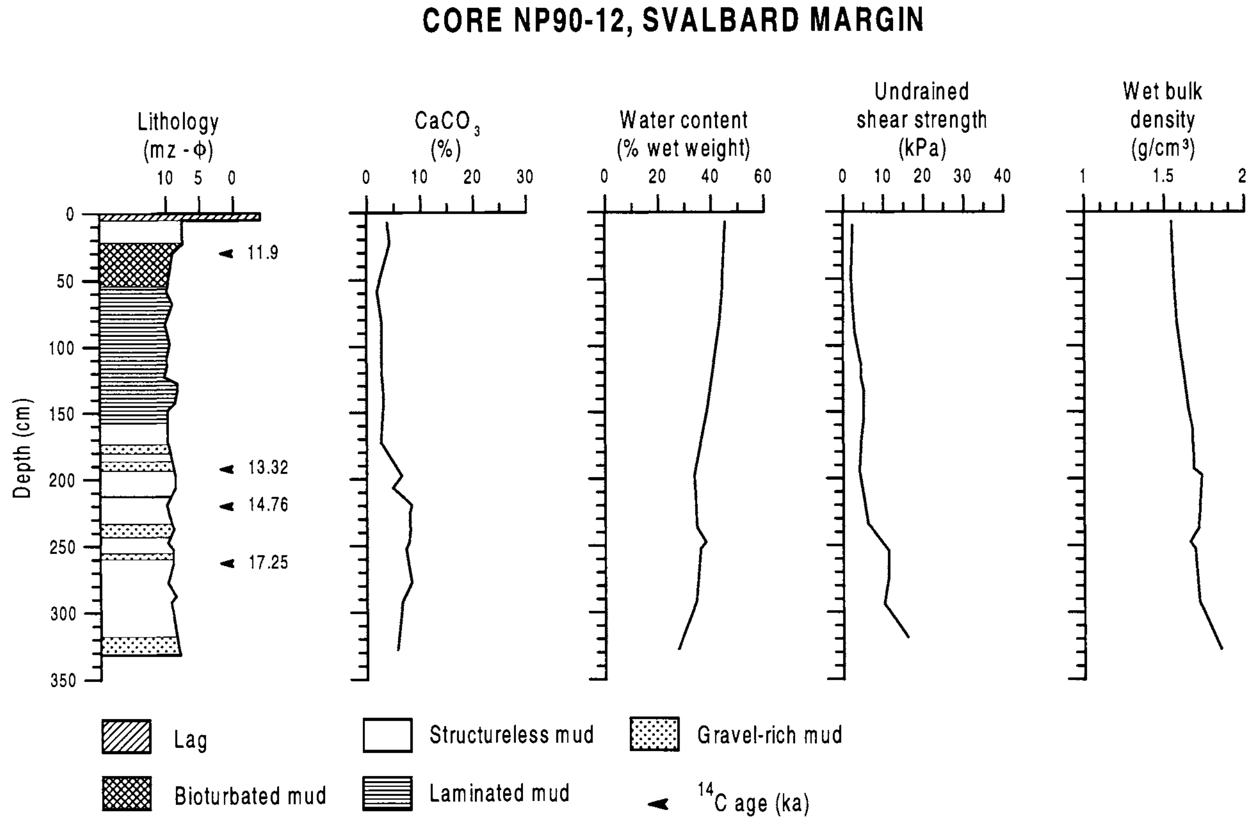

Figure 4. Lithology and Physical Properties of the Svalbard Margin Sediments: Core NP90-12, revovered at 630 m waterdepth. See Plate 7 for location.

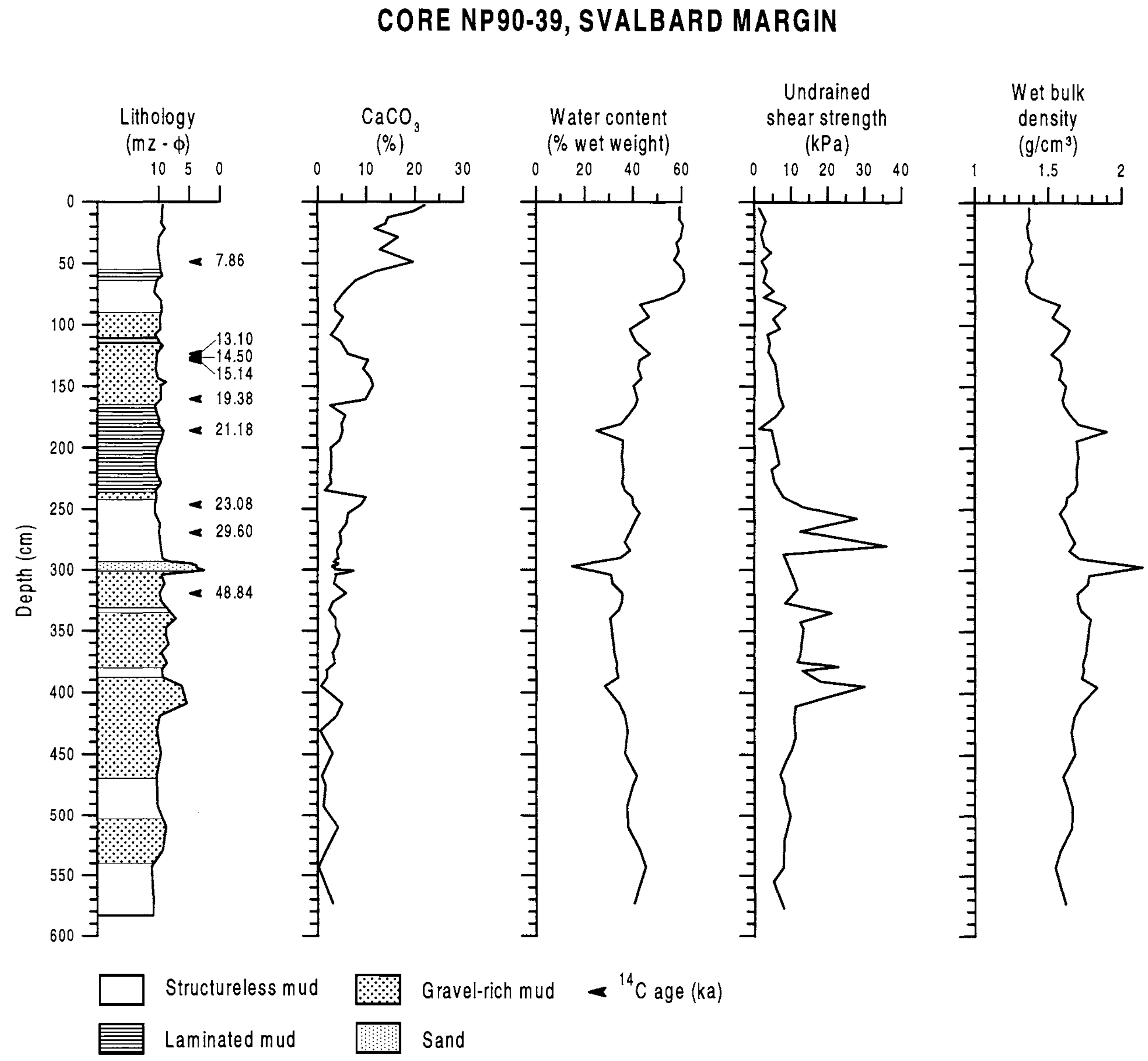

Figure 5. Lithology and Physical Properties of the Svalbard Margin Sediments: Core NP90-39, recovered at 2120 m waterdepth. See Plate 7 for location.

PLATE 72

MULTICHANNEL SEISMIC LINES FROM THE SVALBARD MARGIN

A. Solheim, O. Eiken and K. Hinz

LINE BGR 31 - 74

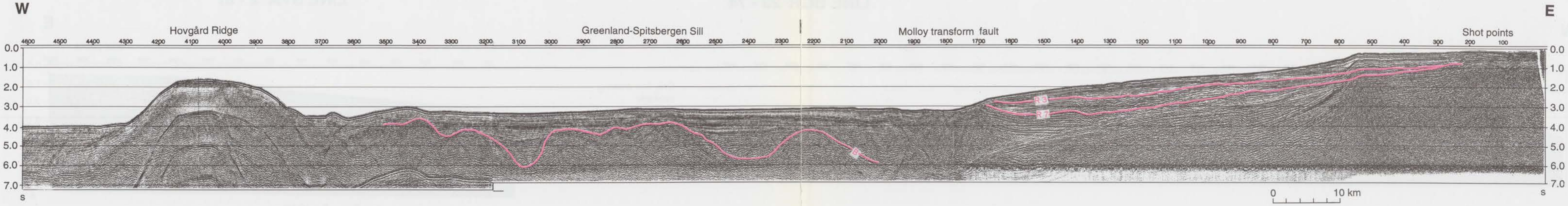

LINE BEL - 1

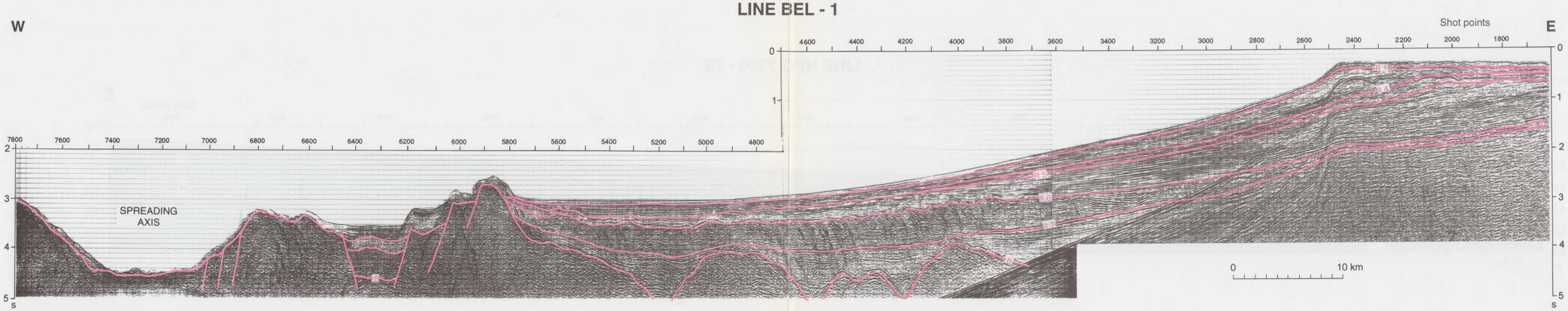

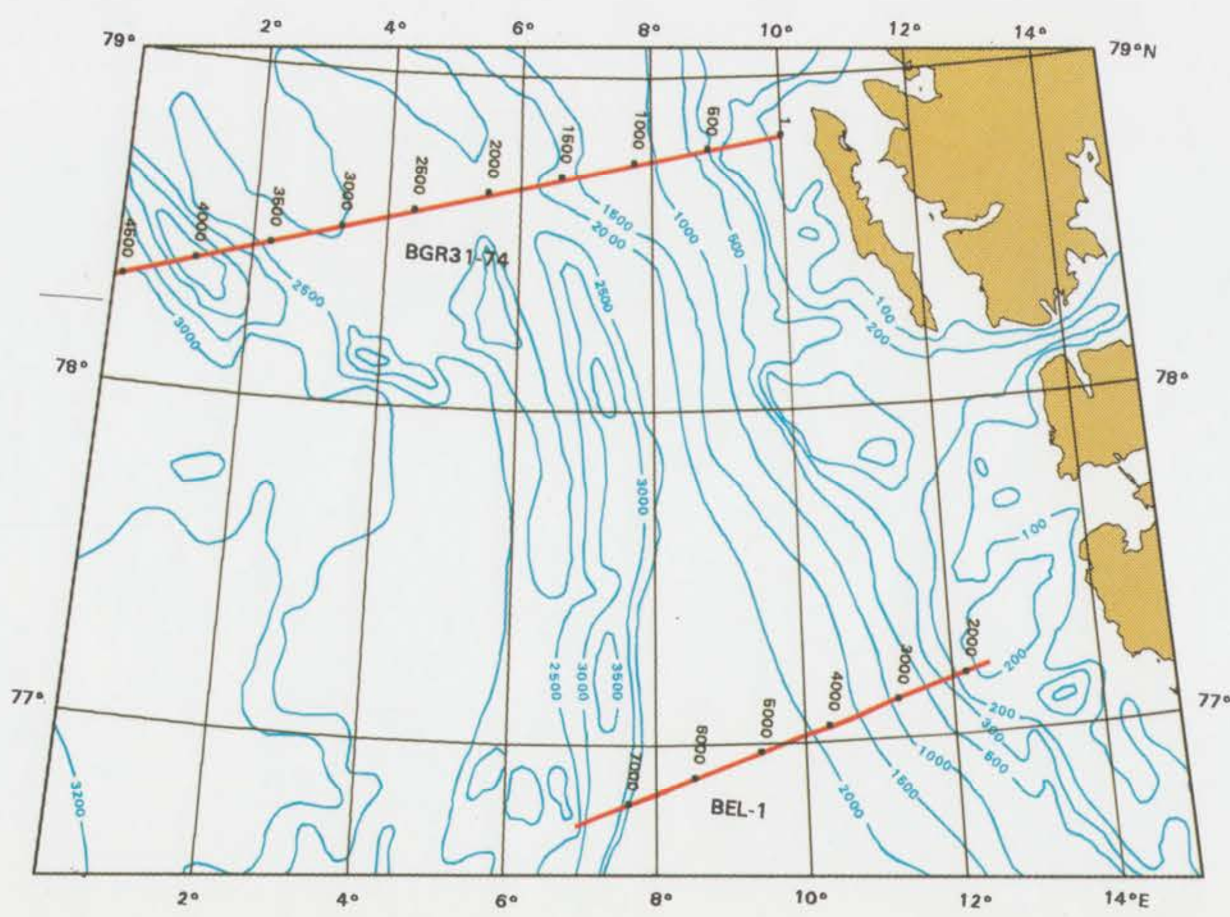

LEGEND

R 1 - R 7 — Seismic Sequence Boundaries

B — Basement

PLATE 73

MULTICHANNEL SEISMIC LINES FROM THE BARENTS SEA MARGIN

A. Solheim, O. Eiken, K. Hinz, Norwegian Petroleum Directorate and Conoco Norway Inc.

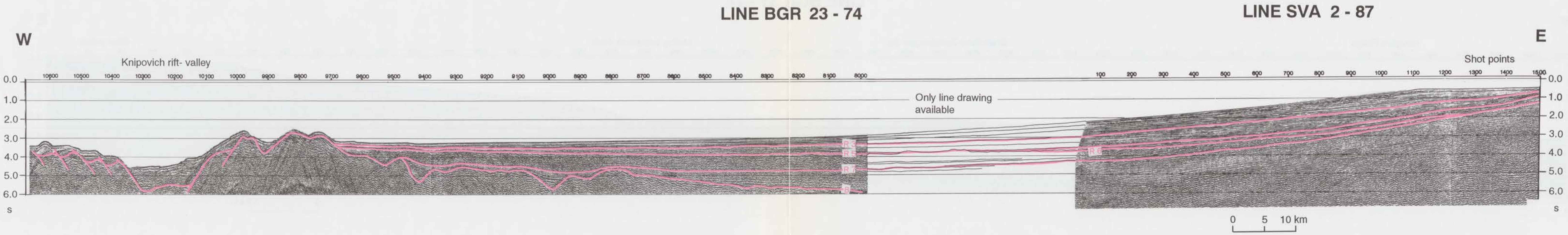

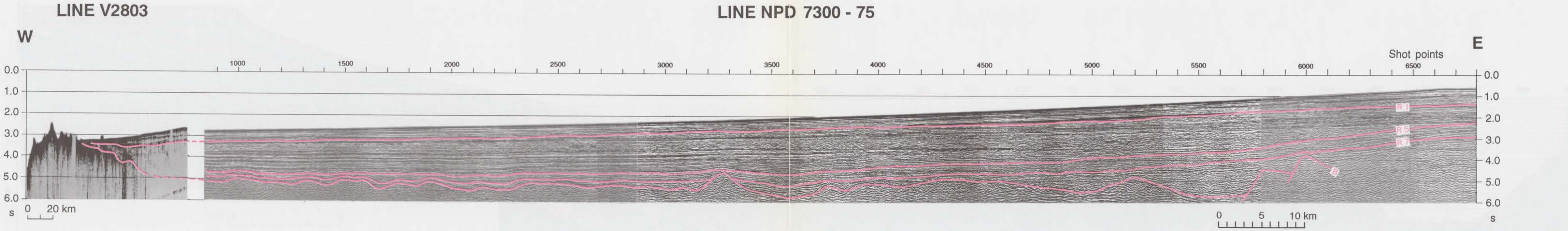

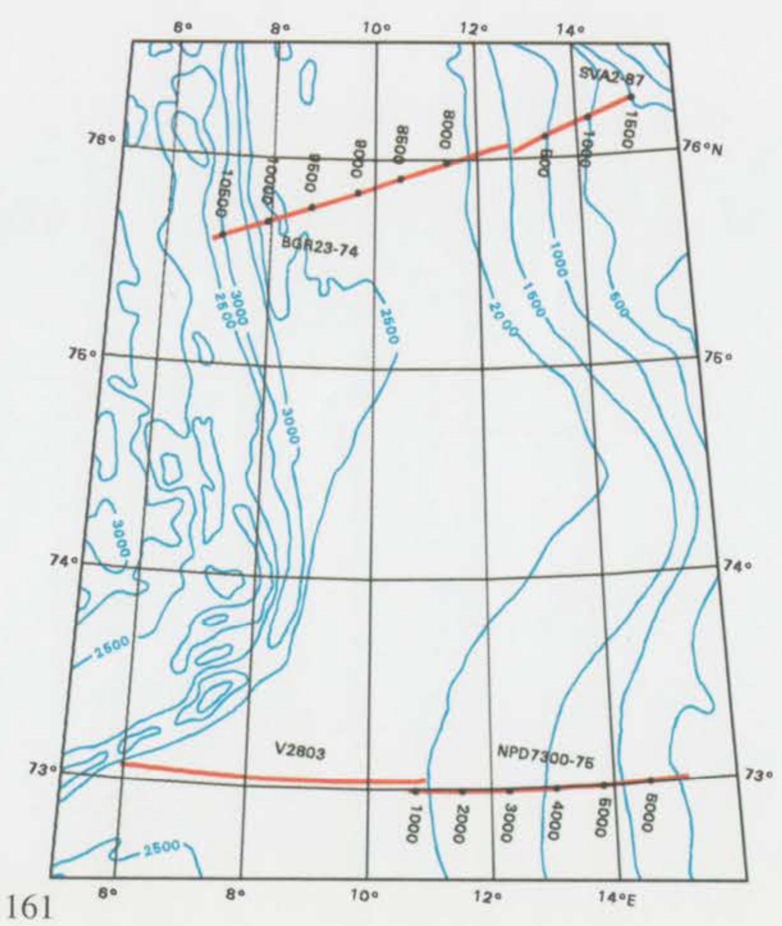

LEGEND

R 1 - R 7 Seismic Sequence Boundaries

B Basement

PLATE 74

SINGLE CHANNEL SEISMIC LINES FROM THE SVALBARD MARGIN; THE CONTINENTAL SLOPE

A. Solheim

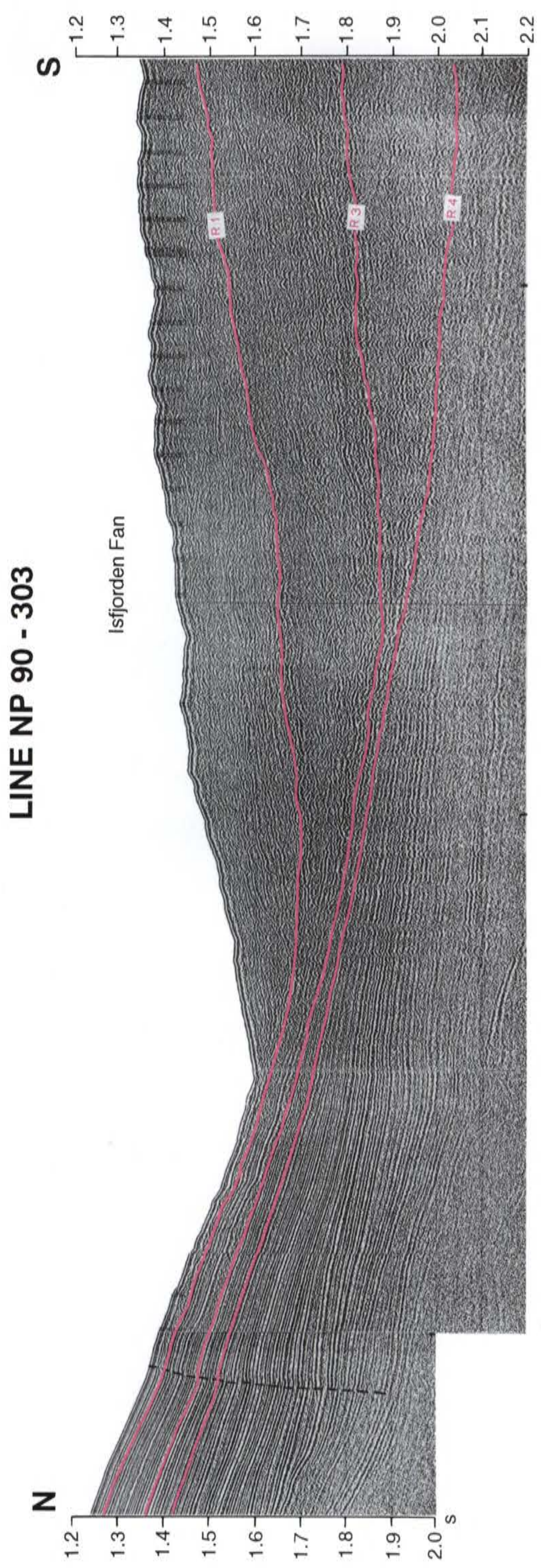

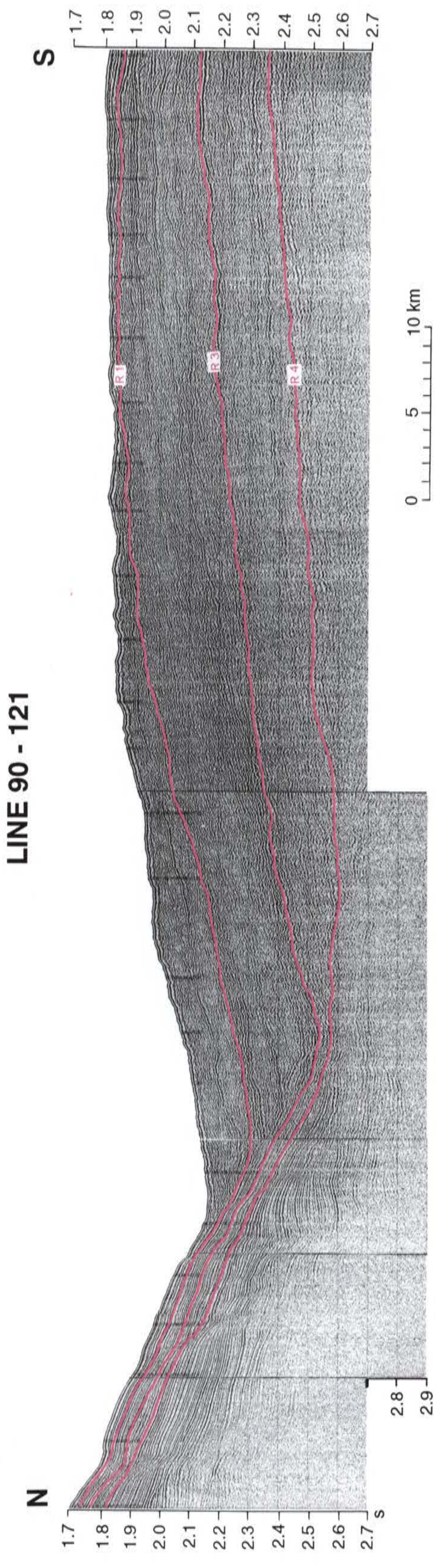

LEGEND

R1 —— Seismic Sequence Boundaries

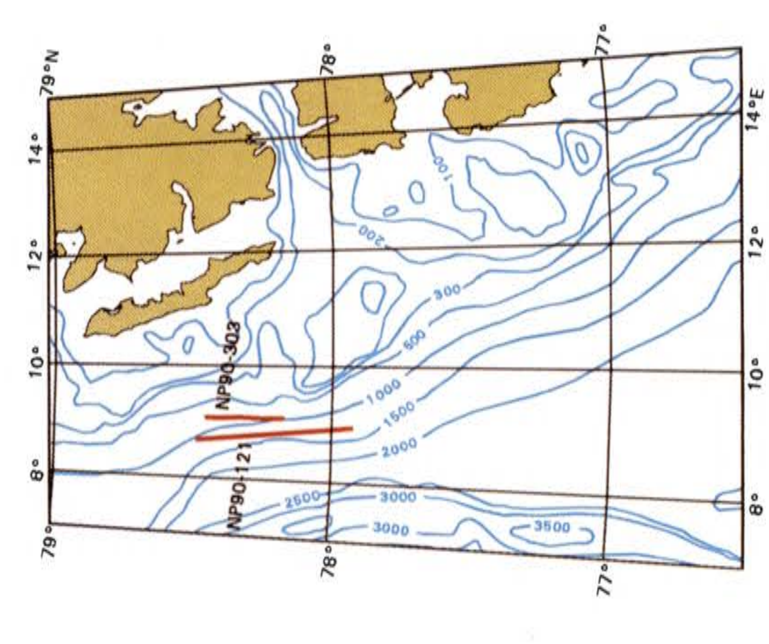

PLATE 75

SINGLE CHANNEL SEISMIC LINES FROM THE SVALBARD MARGIN; THE CONTINENTAL SHELF AND RISE

A. Solheim

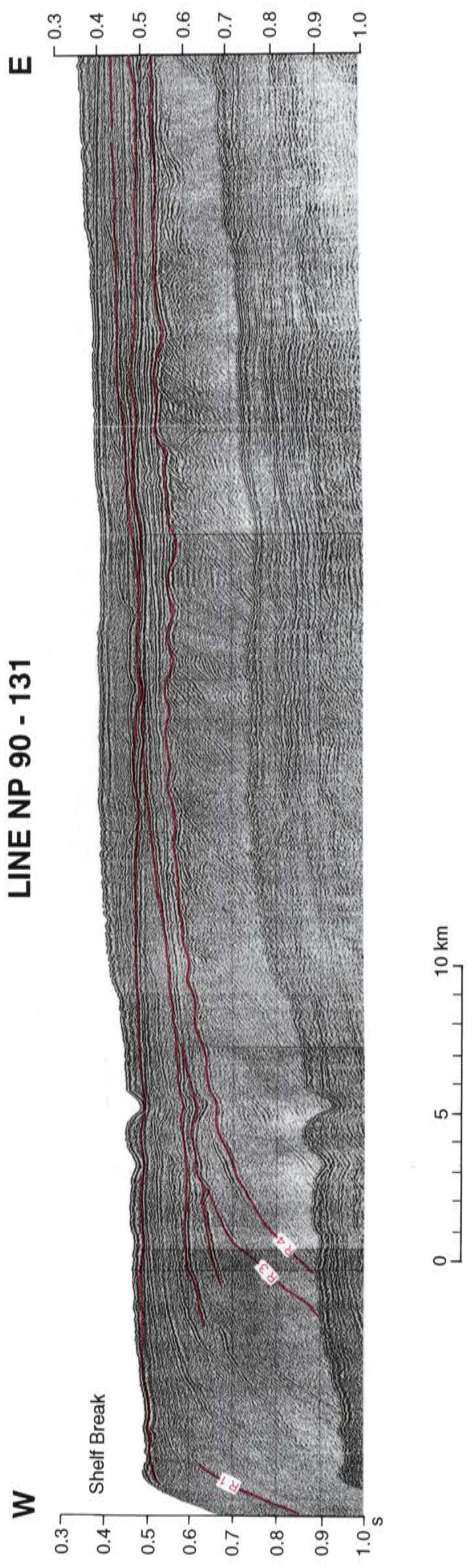

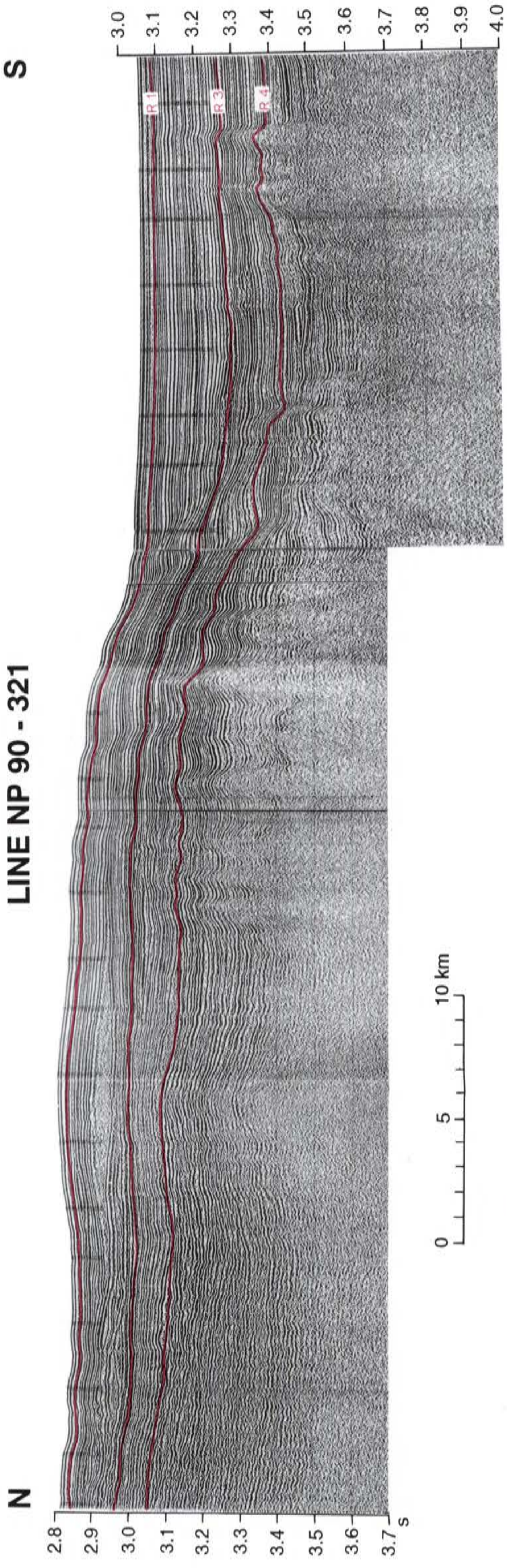

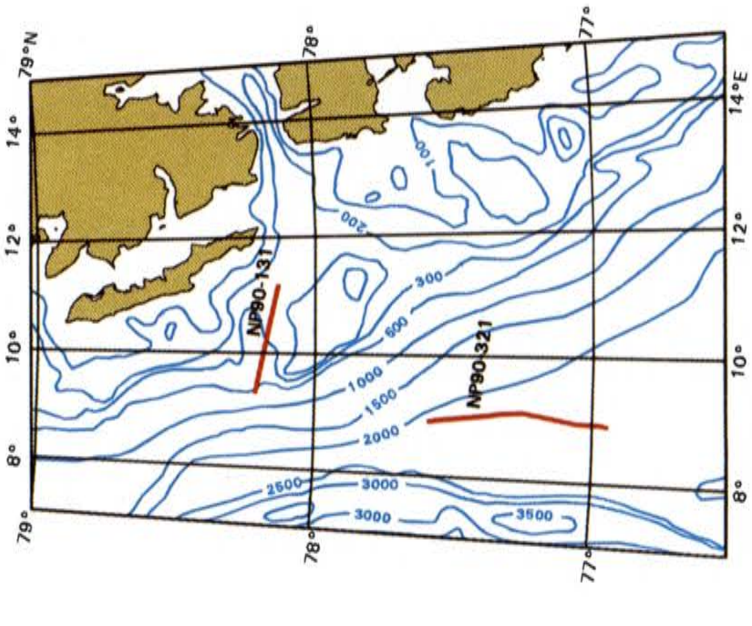

LEGEND

R 1 — Seismic Sequence Boundaries

PLATE 76

HIGH RESOLUTION SEISMIC AND STRATIGRAPHIC DATA FROM THE BEAR ISLAND FAN

JAN SVERRE LABERG AND TORE O. VORREN

Introduction

The large submarine Bear Island Fan dominates the western Barents Sea continental margin. The fan extends from the shelf break downslope to water depths greater than 3,200 m in the Lofoten Basin and covers an area of about 280,000 km^2. During most of the Cenozoic, the fan has acted as an important depocenter, reflecting the evolution of the Norwegian-Greenland and Barents Seas (Spencer et al. 1984; Myhre & Eldholm 1988; Vorren et al. 1991; Vogt et al. 1993). Compilations of data collected during the last decade suggest that the Barents Sea Ice Sheet probably reached the shelf break more than five times during late Cenozoic (Solheim & Kristoffersen 1984; Vorren et al. 1988, 1989; Sættem et al. 1992). Thus, much of the sediment in the upper layers of the Bear Island Fan are probably of a glacigenic origin.

Seismic Stratigraphy

Using high resolution seismic data and gravity cores (Plate 76b,e) (Vorren et al. 1989, 1990), Laberg & Vorren (1993) presented their interpretations of the Late Pleistocene succession on the Bear Island Fan. These data overlap much of the SeaMARC II coverage of the continental slope and rise in this region (Vogt et al. 1993; Vogt et al. 1994 a,b,c).

The Shelf Break

Most profiles crossing the shelf break reveal sedimentary layer transitions that are sigmoidal, oblique and complex. Normally, this implies a history of alternating aggradation and depositional bypass within a high-energy depositional regime (Mitchum et al. 1977). As the upper shelf units contain glacial diamictons and moraine ridges close to the shelf break (Vorren et al. 1989), the truncation "depositional bypass" is interpreted to be due to glacial erosion (Vorren et al. 1990) .

The Slope

On the southern flank of the Bear Island Fan, a large slide has been identified (Plate 76b) which extends over 400 km leaving a slide scar up to 400 m deep. Based on a conservative estimate, about 1,100 km^3 of sediment was removed. Laberg & Vorren (1993) infer an age younger than 330 Ka for the slide by making a tentative correlation with the stratigraphy outside the slide-affected area and with new dating results from the outer Barents Sea continental shelf (Sættem et al. 1992)

North of the large slide scar, the Late Pleistocene part of the Bear Island Fan has been divided into eight (informal) seismic units, unit I (oldest) to unit VIII (Laberg & Vorren 1993). On the upper fan, which extends from the shelf break to about 1,500 m water depth, all the identified units are dominated by a chaotic seismic facies (Plate 76c). Downslope, the seismic pattern within most of the units changes into a mounded geometry. The mounds are about 20 - 50 m thick and form lensoid bodies oriented with their longest axis downslope. Their width varies between about 2 km and 20 km and each lens has a transparent internal seismic facies. Younger lensoid bodies are deposited in bathymetric lows between older ones (Plate 76d) and they can be followed over 100 km downslope, as also seen in SeaMARC II records (Vogt et al. 1991a, b, 1993, 1994b).

The youngest mound shaped deposits within unit VIII have been studied in more detail. Based on: 1) their external shape, characterized by abrupt termination laterally and downslope, 2) the transparent acoustic character within each mound, 3) their sedimentological characteristics, and 4) similarities with previously described deposits from other areas (e.g. Aksu & Hiscott 1992) it is concluded that the mound-shaped deposits are large submarine debris flow deposits. Most of the Late Pleistocene succession on the Bear Island Fan is probably dominated by large debris flow deposits. On the upper fan, the chaotic seismic facies is most likely caused by small scale sliding as is indicated in the SeaMARC II data from the fan (Vogt et al. 1991a, b, 1994b).

Sediments and Stratigraphy

A gravity core at a water depth of 1,317 m (Plate 76a, e), which most likely has penetrated the upper part of a debris flow (unit 1, Plate 76e), sampled a massive diamicton with a transitional upper boundary (Kvilhaug 1990). The grain-size distribution shows a very poorly sorted sediment with a relatively low water content (about 20 %) and an undrained shear strength of about 10-14 kPa. A relatively homogeneous, poorly sorted sediment showing many similarities with glacigenic diamictons found on glaciated shelves often characterize submarine debris flows (Anderson et al. 1979). The stratigraphy above unit 1 includes a gravely pelite (unit 2) characterized by a water content of about 22 % and a shear strength of about 10 % (Kvilhaug 1990). Unit 2 is interpreted to be a glacimarine sediment. Unit 3 is probably a slurry flow deposit according to the terminology of Gravenor et al. (1984) and units 4 and 5 are infered to be different parts of a turbidite. Unit 6 which is a glacimarine pelite carrying dropstones has a water content of between 37% and 41% and an undrained shear strength of 3.5 kPa. Unit 7 is Holocene sediment comprised of clay and silt. Thus, most of the sediments in this core were deposited as gravity flows during the Late Weichselian followed by hemipelagic glacimarine and open marine deposition (Kvilhaug 1990).

Conclusions

1. By analysing high resolution seismic sparker data, eight Late Pleistocene seismic units have been identified north of the large slide scar on the Bear Island Fan. The seismic units are dominated by debris flows up to 50 m thick, 20 km wide and over 100 km long.

2. The debris flows are most likely derived from glacigenic deposits. The sediments of the debris flows consist of diamicton with a relatively low water content (about 20 %) and an undrained shear strength of about 10-14 kPa.

3. The spatial and temporal distribution of the seismostratigraphic units indicate that the Late Pleistocene succession on the Bear Island Fan is dominated by the release of glacigenic sediments on the upper fan during glacial maxima.

Acknowledgements

The authors wish to thank H. Falkseth, F. Strand, J. P. Holm and Gunvor Granaas for drafting and photographic work.

PLATE 76

HIGH RESOLUTION SEISMIC AND STRATIGRAPHIC DATA FROM THE BEAR ISLAND FAN

J.S. Laberg and T. O. Vorren

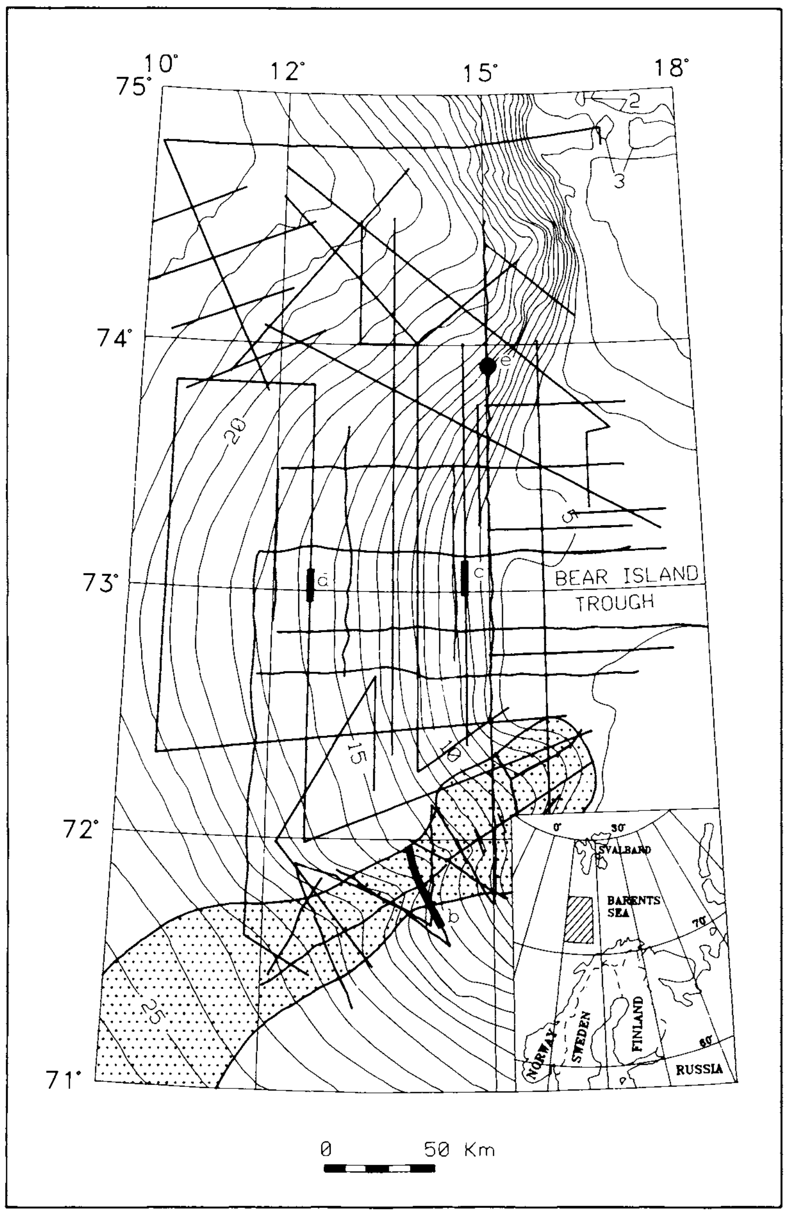

a. Location and bathymetry of the study area. Contour interval is 100 m. Heavy lines indicate the seismic data base and the hatching represents the area affected by mass wasting. Locations of seismic examples (Plate 76 **b-d**) are given. Gravity core location (Plate 76 **e**) is shown by filled circle.

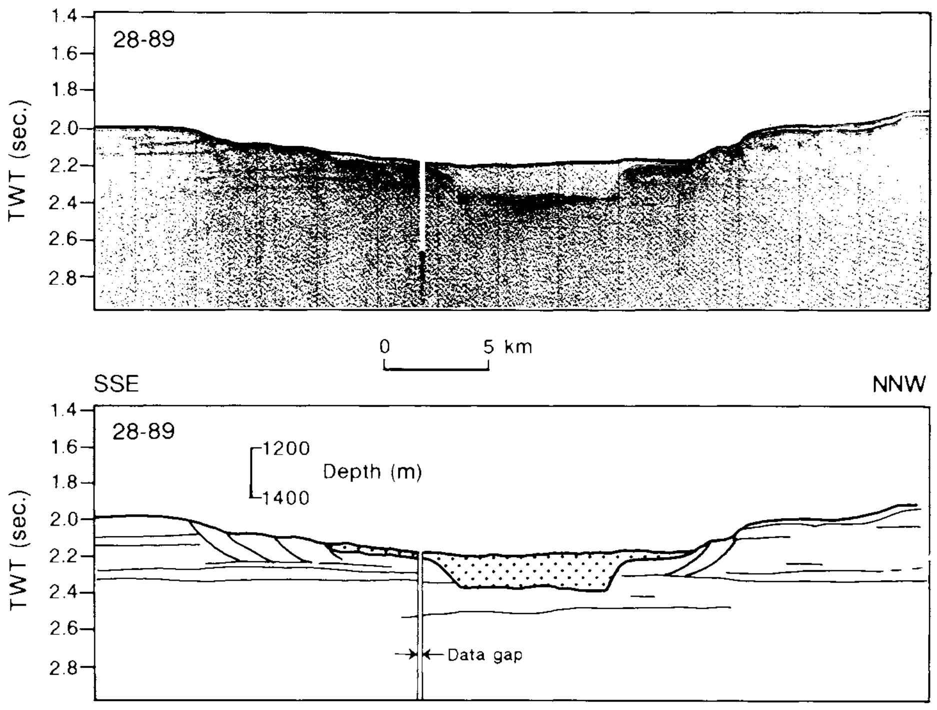

b. Sparker profile across the slide scar at about 2.0 s (TWT) depth showing sediment infill (dotted area) enclosed by a zone of several tilted blocks separated by listric faults. See Plate 76 **a** for location. From Laberg & Vorren (1993).

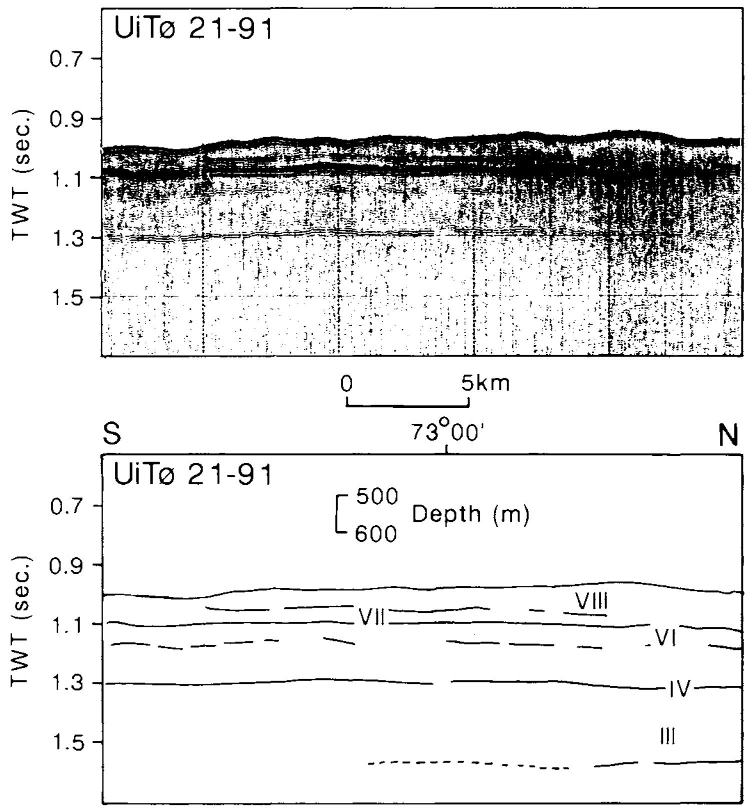

c. Part of sparker profile UiTø 21–91 from the upper part of the fan. Note the chaotic internal seismic facies and uneven unit boundaries, indicative of small scale sliding, See Plate 76 **a** for location.

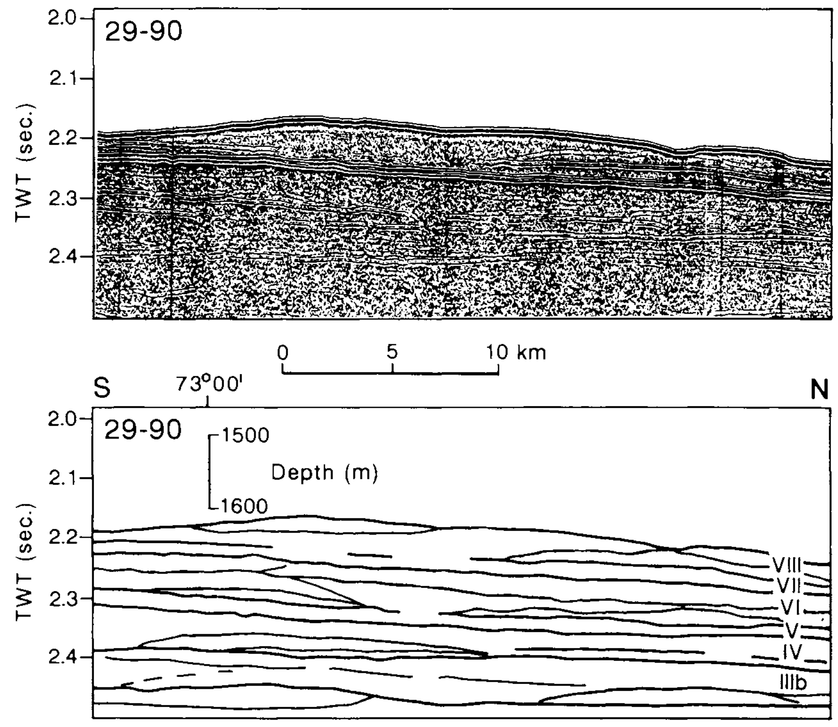

d. Part of sparker profile UiTø 29–90 from the middle part of the fan. At this part, the internal seismic facies is dominated by a mounded geometry, which most likely represents large debris flow deposits. See Plate 76 **a** for location.

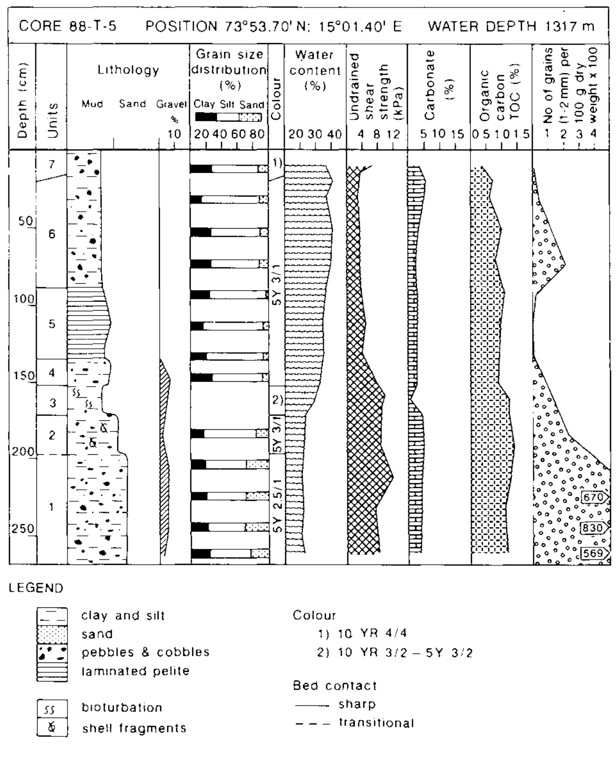

e. Stratigraphy and lithology of core 88–T–5 from the Bear Island Fan (73°57.70'N, 15°01.40'E, depth 1317 m). The stratigraphy includes a debris flow deposit (unit 1), a glacimarine unit (unit 2), a "slurry flow" (unit 3), different parts of a turbidite (units 4 and 5), a glacimarine unit (unit 6) and Holocene hemipelagic unit on top (unit 7) (from Kvilhaug 1990). See Plate 76 **a** for location.

REFERENCES

Aksu, A.E. & Hiscott, R.N. 1992: Shingled Quaternary debris flow lenses on the north-east Newfoundland Slope. *Sedimentology 39*, 193-206.

Alekshin, S.V. & Verba, M.L. 1979: Dinamika tektonicheskih processov i razlomy Yuzhno-Barentsevskoi vpadini kovoi otmeli i okeana. Sbornik nauchnykh trudov (Tectonics of the Arctic. *Fractures of the Continental Shoal and of the Ocean.).* Collection of Scientific Papers) *NIIGA, Leningrad*, 18-26. (in Russian).

Alfred Wegener Institut für Polar and Marine Research (AWI) and Geologisch-Paläontologisches Institut, Kiel, (GIK) 1989: Bathymetrie und geodäsie. In Gersonde, R. (ed.): Die Expedition Arktis III mit FS "Polarstern" 1985. *Ber. Polarforsch. 28*, 82-85.

Andersen, E.S., Solheim, A. & Elverhøi, A. 1994: Development of a glaciated Arctic continental margin: Exemplified by the western margin of Svalbard. *Int. Conference on Arctic Margins, Anchorage 1992, Proceedings,* 155-160.

Anderson, J.B., Kurtz, D.D. & Weaver, F.M. 1979: Sedimentation on the Antarctic Continental slope. *Society of Economic Paleontologists and Mineralogists Special Publication 27*, 265-283.

Austegard, A. & Sundvor, E. 1991: The Svalbard continental margin: Crustal structure from deep seismic profiles and gravity. *Institute of Solid Earth Physics, University of Bergen, Norway, Seismo-Series no.53.*

Baturin, D.G. 1987: Evolution of the northern Barents Sea in the area of junction with the Eurasian Ocean Basin. *Oceanology 27*, 308-312 (AGU transl., 1988).

Baturin, D.G. 1988: Stroyeniye i evolyutsiya kontinental'noy okrainy Yevraziyskogo bassenyna mezhdu arkhipelagani Shpitsbergena i Zemlya Frantsa-Iosifa (Continental Margin of the Eurasian Basin Between Spitsbergen Archipelago and Franz Josef Land: Structure and Evolution). *Doklady Akad. Nauk SSSR 289,* 419-423 (in Russian).

Baturin, D.G. & Yunov, A. Yu. 1987: Evolutsiya Barentsevomorskogo shelfa v svyazi s geologicheskim razvitiem Arkticheskogo regiona (Evolution of the Barents Sea shelf and its connection with the geological development of the Arctic region). Paleogeografiya i paleo kologiya Barentseva i Belogo Moreii v Letberti ii period Izd. *Kolsk Spiliala AN CCCP, r. Anatit* (in Russian).

Baturin, D.G. & Nechkhaev 1989: Glubinnoe Stroeniye Shpitsbergen-skogo Kraevogo Plato Severo-Vostochnoe Chasti Grenlandskogo Morya (Deep Structure of the Spitsbergen Marginal Plateau in the Northeastern Greenland Sea). *Doklady Akademi Nauk SSSR 306*, 925-930 (in Russian).

Baturin, D.G. & Yunov, A. Yu. 1989: Sedimentatsionniya tsiklochnost yuzhno-Karskoiye Sinekliz' po seismicheskim dann'm (Sedimentational cycles in the southern Kara Sea from seismic data). *Problemi' Neftegazonosnosti Mirovogo Okeana,* 197-205. (in Russian).

Baumann, K.-H., Lackschewitz, K.S., Erlenkeuser, H., Henrich, R. & Jünger, B. 1993: Late Quaternary calcium carbonate sedimentation and terrigeneous input along the east Greenland continental margin. *Marine Geology 114*, 13-36.

Beal, M.A. 1969: *Bathymetry and Structure of the Arctic Ocean.* Unpublished PhD thesis, Oregon State Univ., 204 pp.

Birkenmajer, K. 1981: The geology of Svalbard, the western part of the Barents Sea and the continental margin of Scandinavia. Pp. 265-330 in Nairn et al. (eds.): *The ocean basins and margins 5, The Arctic Ocean.* Plenum, New York.

Boyd, L.A. 1935: The fjord region of east Greenland. *American Geographic Society Special Publication 18.* 361 pp.

Boyd, L.A. 1948: The coast of northeast Greenland. *American Geographic Society Special Publication 30.* 339 pp.

Breivik, A.J. 1991: *Årsaker til tyngdeanomaliene på Barentshavsmarginen.* Unpublished Cand.scient. thesis, Univ. of Oslo.

Briseid, E. & Mascle, J. 1975: Structure de la marge continentale norvégienne au debouche de la mer de Barentz. *Marine Geophysical Researches 2*, 231-241.

Buchardt, B. 1981: Tertiary deposits of the Norwegian-Greenland Sea region (Svalbard northeast and east Greenland, Iceland, The Faeroe Islands and the Norwegian-Greenland Sea) and their correlation of northwest Europe. In Kerr, J.W. & Fergusson, A.J.(eds.): *Geology of the North Atlantic Borderlands, Can. Soc. Petrol. Geol. Mem. 7*, 585-610.

Bugge, T., Rise, L. & Rokoengen, K. 1987: *Dybdekart over Midtnorsk Kontinentalsokkel, Målestokk:1:1,000,000.* Institutt for Kontinentalsokkelundersøkelser og Petroleumsteknologi A/S, Trondheim. (in Norwegian).

Chan, W.W. & Mitchell, B.J. 1985: Intraplate earthquakes in northern Svalbard. In Husebye et al. (eds.): Geophysics of the Polar Regions. *Tectonophysics 114 (1-3)*,181-191.

Charov, G.S. & Krasil'shchikov, A.A. 1981: Sostav i nekotorye zakonomernosti raspredeleniya donnogo kamennogo materiala v Barentsevom more po profilyu poluostrov Rybachiy-Zemlya Frantsa-Iosifa (Composition and Some Regularities of Distribution of Bottom Rock Material in the Barents Sea along the profile Rybachiy Fisherman's Peninsula-Franz Josef Land). Pp 33-40 in Litologiya i paleogeografiya Barentseva i Karskogo morey. Sbornik nauchnych trudov *(Lithology and Paleogeography of the Barents and Kara Seas).* Collection of Scientific Papers). *NIIGA, Leningrad.*

Cherkis, N.Z., Max, M.D. & Midthassel, A. 1989: Mass wasting features north of Spitsbergen. *EOS, Trans. Amer. Geophys. Un. 70.* 1348 pp..

Cherkis, N.Z. & Max, M.D. 1991: Bathymetry and geological disposition, tectonics and Pre-Mesozoic terranes in the Barents and Kara Seas continental platform. *EOS, Trans. Amer. Geophys. Un. 72*, Spring Mtg. Prog. 103 pp.

Cherkis, N.Z., Fleming, H.S., Max, M.D., Vogt, P.R., Czarnecki, M.F., Kristoffersen, Y., Midthassel, A. & Rokoengen, K. 1991a: Bathymetry of the Barents and Kara Seas. *Geological Society of America Map and Chart Series, MCH047.*

Cherkis, N., Steinmetz, S. & Theiner, J. 1991b: Bathymetrie-Hydrosweep. Pp. 19-24 in Thiede, J. & Hempel, G. (eds.): The Expedition Arktis-VII/1 of RV "Polarstern" in 1990. *Ber. Polarforsch. 80.*

Cherkis, N.Z. & Max, M.D. 1992: Bathymetry and geological terranes in the Norwegian, Greenland and Barents Seas. In Vorren, T.O., Bergsager, E., Dahl-Stamnes, O.A., Johansen, B., Lie, E. & Lund, T.B. (eds.): *Arctic Geology and Petroleum Potential, Proc. Norw. Petrol. Soc. Conf., 15-17 August 1990.* Elsevier Sci. Publ. Amsterdam.

Cherkis, N.Z., Max, M.D., Midthassel, A., Crane, K., Sundvor, E. & Vogt, P.R. 1992: Deep ice scour and mass-wasting features on the Northern Svalbard insular shelf and slope. *Abs. Int. Conf. on Arctic Margins, Anchorage, AK, Sept 1992.* 10 pp.

Cherkis, N., Steinmetz, S., Schreiber, R., Thiede, J., & Theiner, J. 1994: Verestis Seamount: An enigma in the Greenland Basin. *Marine Geophysical Researches* 16 (4), 287-302.

Crane, K., Eldholm, O., Myhre, A.M. & Sundvor, E. 1982: Thermal implications for the evolution of the Spitsbergen Transform Fault. *Tectonophysics 89,* 1-32.

Crane, K., Sundvor, E., Foucher, J.P., Hobart, M., Myhre, A.M. & LeDouaran, S. 1988: Thermal evolution of the western Svalbard margin, *Marine Geophysical Researches 9*, 165-194.

Crane, K., Sundvor, E., Buck, R. & Martinez, F. 1991: Rifting in the northern Norwegian-Greenland Sea: Thermal tests of asymmetric spreading. *Jour. Geophys. Res. 96, B9,* 14520-14550.

Crane, K., Vogt, P.R. & Sundvor, E. 1992: Arctic Ocean: Basin plate tectonics and sedimentology. Pp. 22-30 in: McGraw - Hill Yearbook of Science and Technology, McGraw-Hill Inc.

Crane, K., Vogt, P. R., Sundvor, E., Shor, A. & Reed, T. 1995: SeaMARC II investigations of the northern Norwegian-Greenland Sea. Pp. 32-34 n Crane, K. & Solheim, A. (Eds.): Seafloor Atlas of the Northern Norwegian-Greenland Sea. *Norsk Polarinstitutt Medd. 137* (this volume).

Damuth, J.E. 1978: Echo character of the Norwegian-Greenland Sea: Relationship to Quaternary sedimentation. *Marine Geology 28*, 1-36.

Dekko, T. & Rokoengen, K. 1980: Submerged beaches off Troms, North Norway. Continental Shelf Institute, *IKU Publication No. 101.* 34 pp.

Dibner, V.D., Basov, V.A., Gerke, A.A., Solov'yeva, M.F., Sisopatrova, G.P. & Shul'gina, N.I. 1970: The age of the Pre-Quaternary deposits on the bottom of the Barents Sea. *Oceanology 10,* 520-529 (AGU translation).

Doss, H., Crane, K., Vogt, P. & Sundvor, E. 1991: Evolution of the western Svalbard margin: results from analysis of Sea-MARC II data: Part II, Tectonics, AGU-MSA, 1991 Spring meeting , *EOS Trans., Amer. Geophys. Un.72(17). p.* 274.

Döscher, T. & Schöne, T. 1992: Bathymetric survey with Hydrosweep. Pp. 44-48 in Fütterer, D. K. (ed.): Arctic 91: The Expedition ARK-VIII/3 of RV Polarstern in 1991. *Ber. Polarforsch. 107*, 44-48.

Eggvin, J. 1963: *Bathymetric chart of the Norwegian Sea and adjacent areas.* Fiskeridir. Havforsk. Inst., Bergen.

Eidvin, T. & Riis, F. 1989: Nye dateringer av de tre vestligste borehullene i Barentshavet. Resultater og konsekvenser for den Tertiære hevingen. *Norw. Petrol. Dir. Contrib. 27,* 44pp.

Eidvin, T., Jansen, E. & Riis, F. 1993: Chronology of Tertiary fan deposits off western Barents Sea: Implications for the uplift and erosion history of the Barents shelf. *Marine Geology 112,* 109-131.

Eiken, O. 1994: Seismic Atlas of Western Svalbard. *Norsk Polarinstituttt Meddelelser 130.* 73pp.

Eiken, O. & Austegard, A. 1987: The Tertiary orogenic belt of West-Spitsbergen: Seismic expressions of the offshore sedimentary basins. *Norsk Geologisk Tidsskrift 67*, 383-394.

Eldholm, O. & Ewing, J. 1971: Marine geophysical survey in the southwestern Barents Sea. *Journal of Geophys. Res. 83*, 3832-3841.

Eldholm, O. & Windisch, C. 1974: Sediment distribution in the Norwegian-Greenland Sea. *Geol. Soc. Am. Bull. 85*, 1661-1676.

Eldholm, O. & Myhre, A.M. 1977: Hovgaard Fracture Zone. *Norsk Polarinstitutt Årbok 1976*, 195-208.

Eldholm, O., Sundvor, E., Myhre, A.M. & Faleide, J.I. 1984: Cenozoic evolution of the continental margin off Norway and western Svalbard. Pp. 3-18 in Spencer, A.M. (ed.): *Petroleum Geology of the North European Margin.* Graham and Trotman, London.

Eldholm, O., Faleide, J.I. & Myhre, A.M. 1987: Continent-ocean transition at the western Barents Sea/Svalbard continental margin. *Geology 15,* 1118 - 1122.

Eldholm, O., Thiede, J., Taylor, E. et al. 1989: *Proceedings of the Ocean Drilling Program, Scientific Results, Vol. 104: College Station, TX: Ocean Drilling Program,* 1141pp.

Eldholm, O., Karasik, A.M. & Reksnes.P.A. 1990: In: Grantz, A., Johnson, G.L & Sweeney, J. (eds.): *The Arctic Ocean region vol. L.* The geology of North America, Boulder, (Geol. Soc. AM.) The North American Plate Boundary. DNAG Synthesis Volume, Geology of the Arctic Ocean Regions, Chapter 12.

Elverhøi, A., 1984: Glacigenic and associated marine sediments in the Weddel Sea, fjords of Spitsbergen and the Barents Sea. A review. *Marine Geology 57*, 52-88.

Elverhøi, A. & Solheim, A. 1983: The Barents Sea ice sheet – a sedimentological discussion. *Polar Research 1*, 23-42.

Elverhøi, A., Pfirman, S.L., Solheim, A. & Larssen, B.B. 1989: Glaciomarine sedimentation and processes in high Arctic epicontinental seas, exemplified by the northern Barents Sea. *Marine Geol. 85*, 225-250.

Elverhøi, A., Solheim A., Nyland Berg, M. & Russwurm, L. 1992: Last interglacial-glacial cycle western Barents Sea. *LUNDQUA Report 35,* 17-24.

Elverhøi, A., Fjeldskaar, W., Solheim, A., Nyland Berg, M. & Russwurm, L. 1994: The Barents Sea ice sheet – A model of its growth and decay during the last ice maximum. *Quaternary Science Reviews, 12,* 863-873.

Elverhøi, A., Svendsen, J.I., Solheim, A., Andersen, E.S., Milliman, J.D., Mangerud, J.. & Hooke, R.LeB. 1995: Late Quaternary sediment yield from the high Arctic Svalbard area, *Journal of Geology 103,* 1-17.

Emery, K.O. 1974: Pagoda structure in some marine sediments. Pp. 309-317 in Kaplan, I.R. (ed.): *Gases in Marine Sediments.* Plenum Press, New York.

Faleide, J.I. & Gudlaugsson, S.T. 1981: *Geology of the western Barents Sea – A regional study based on marine geophysical data.* Unpublished Cand. real. thesis, Univ. of Oslo, 160 pp.

Faleide, J.I., Gudlaugsson S.T. & Jacquart, G. 1984a: Evolution of the western Barents Sea. *Marine and Petroleum Geol. 1*, 123-150.

Faleide, J.I., Gudlaugsson, S.T., Johansen, B., Myhre, A.M. & Eldholm, O. 1984b: Free-air gravity maps of the Greenland Sea and the Barents Sea. *Norsk Polarinstitutt Skrifter 180*, 63-67.

Faleide, J.I., Gudlaugsson, S.T., Eldholm, O., Myhre, A.M. & Jackson, H.R. 1991: Deep seismic transects across the sheared western Barents Sea – Svalbard continental margin. *Tectonophysics 189,* 73-89.

Faleide, J.I., Solheim, A., Fiedler, A., Hjelstuen, B.O., Andersen, E.S. & Vanneste, K. in press: Late Cenozoic evolution of the western Barents Sea - Svalbard continental margin. *Global and Planetary Change.*

Feden, R.H., Vogt, P.R. & Fleming, H.S. 1979: Magnetic and bathymetric evidence for the "Yermak" hot spot northwest of Svalbard in the Arctic Basin. *Earth and Planetary Science Letters 44,* 18-38.

Fiedler, A. 1992: Kenozoisk sedimentasjon i Lofotenbassenget langs vestlige Barentshavmarginen. *Unpublished Cand. Scient. Thesis. Univ. of Oslo* 113pp.

Gammelsrød, T. & Rudels, B. 1983: Hydrographic and current measurements in the Fram Strait, August 1981. *Polar Research 1,* 115-126.

Gayer, R.A., Gee, D.G., Harland, W.B., Miller, J.A., Spall, H.R., Wallis, R.H. & Winsnes, T.S. 1966: Radiometric age determinations on the rocks from Spitsbergen. *Norsk Polarinstitutt Skrifter 137,* 39 pp.

Gramberg, I. C. (ed.) 1988: Barentsevskaya Shel'fovaya Pleta (The Barents Shelf Plate); Ministerstvo Geologii SSSR, "SEVMORGEOLOGIYA", Vsesoyouz Nauch. Issled. Institut Gelogii Mineral'n'kh Resursoc Mirovogo okeana. *"VNIIokeangeologiya" Trudy T. 196,* Nedra, Leningrad, 263 pp.

Grantz, A., Johnson, G.L. & Sweeney, J.F. (editors) 1990: The Geology of North America; The Arctic Ocean Region. *Decade of North American Geology, Geological Society of America,* Boulder, Colorado. 644 pp.

Gravenor, C.P., von Bruun, V. & Dreimanis, A. 1984: Nature and classification of waterlain glacigenic sediments, exemplified by Pleistocene, late Paleozoic and late Precambrium deposits. *Earth Science Review* 20, 105-166.

Grønlie, G. & Talwani, M. 1979: Bathymetry of the Norwegian-Greenland Sea. *VEMA Research Series IV,* Lamont-Doherty Geological Observatory, Palisades, N.Y.

Gudlaugsson, S.T., Faleide, J.I., Fanavoll, S. & Johansen, B. 1987: Deep seismic reflection profiles across the western Barents Sea. *Geophys. J. R. Astr. Soc. 89,* 273-278.

Guterch, A., Pajchel, J., Perchuc, E., Kowalski, J., Duda, S., Komber, J., Bojdys, G. & Sellevoll, M.A. 1978: Seismic reconnaissance measurements on the crustal structure in the Spitsbergen region. *Univ. Bergen Seism. Obs. Rpt.,* 61pp.

Hagevang, T. 1978: *En Maringeofysisk Undersøkelse av Kontinentalmarginen utenfor Helgeland.* Unpublished. Cand. real thesis, Univ. Oslo. 151pp. (in Norwegian).

Hebbeln, D. 1992: Weichselian glacial history of the Svalbard area: correlating the marine and terrestrial records. *Boreas 21,* 295-304.

Hebbeln, D. & Berner, H. 1993: Surface sediment distribution in the Fram Strait. *Deep-Sea Research* 40, 1731-1745.

Heezen, B.C. & Ewing, M. 1961: The Mid-Oceanic Ridge and its extension through the Arctic Basin. Pp. 622-642 in Raasch, G.O. (ed.): *Geology of the Arctic 1. Proceedings of the First International Symposium on Arctic Geology.* University of Toronto Press, Toronto, Ontario.

Heezen, B.C. & Tharp, M. 1975: Bathymetry of the Arctic Region. In Pinther, M. (Chief Cartographer): *Map of the Arctic Region,* American Geographical Society, New York, N.Y.

Heidland, K. 1989: Bathymetrie und geodäsie. In Gersonde, R. (ed.): Die Expedition Arktis III mit FS Polarstern 1985. *Ber. Polarforsch. 28,* 50-53. .

Helland-Hansen, B. & Nansen, F. 1909: The Norwegian Sea. Its physical oceanography based upon the Norwegian researches 1900-1904. *Rpt. on Norw. Fishery and Mar. Invest. II, No. 2,* Det Mallingske Bogtrykkeri, Kristiana, 99 pp.

Hempel, P., Schreiber, R., Johnson, L. & Thiede, J. 1991: The Vesterisbanken Seamount (Greenland Basin), patterns of morphology and sediment distribution. *Marine Geology 96,* 175-185.

Henrich, R., Kassens, H., Vogelsang, E. & Thiede, J. 1989: Sedimentary facies of glacial – interglacial cycles in the Norwegian – Greenland Sea during the last 350 ka. *Marine Geology 86,* 283-319.

Herman, Y. (ed.) 1974: *Marine Geology and Oceanography of the Arctic Seas.* Springer-Verlag, New York, 397.

Hinz, K. & Schlüter, H.U. 1978: The geological structure of the western Barents Sea. *Marine Geology 26,* 199-230.

Hjelle, A. & Lauritzen, Ø. 1982: Geological Map of Svalbard, 1:500.000, Sheet 3G, (Spitsbergen northern part). *Norsk Polarinstitutt Skrifter 154C,* 15 pp, 1 map.

Hjelstuen, B.O. 1993: Sein-Kenozoisk utvikling av Storfjordvifta, basert på reprosesserte multikanals data. *Unpubl. Cand. Scient. Thesis, Univ. of Oslo, 111pp.*

Holtedahl, O. 1940: The submarine relief off the Norwegian coast, with bathymetric maps in seven sheets of the Norwegian coastal waters and adjoining seas. *Vid.-Akad. Special Publication,* Oslo, 1-43.

Holtedahl, O. & Holtedahl, H. 1961: On marginal channels and the problem of their origin. *Bulletin of the Geological Institute of the University of Upsala 49,* 183-187.

Houtz, R. & Windisch, C.C. 1977: Barents Sea continental margin sonobuoy data. *Geol. Soc. Amer. Bull. 88,* 1030-1036.

Hurdle, B.G. (ed.) 1986: *The Nordic Seas.* Springer-Verlag, Berlin, 777 pp.

IGH Institut für Geophysik, Universität Hamburg 1984: SeaBeam, 3.5-kHz-Lot, CTD-Multisonde. In Augstein, E., Hempel, G., Schwarz, J., Thiede, J. & Weigel, W. (eds.): Die Expedition Arktis II des FS "Polarstern" 1984. *Ber. Polarforsch. 20,* 123-124.

Jackson, H.R., Johnson, G.L., Sundvor, E. & Myhre, A.M. 1984: The Yermak Plateau: Formed at a triple junction. *Journal of Geophys. Res. 89 (B5),* 3223-3232.

Jackson, H.R., Faleide, J.I. & Eldholm, O. 1990: Crustal structure of the sheared southwestern Barents Sea continental margin. *Marine Geology 93,* 119-146.

Jansen, E. & Sjøholm, J. 1991: Reconstruction of glaciation over the past 6 Myr from ice-borne deposits in the Norwegian Sea. *Nature 349,* 600-603.

Johnson, G.L. & Eckhoff, O.B. 1966: Bathymetry of the north Greenland Sea. *Deep Sea Res.13,* 1161-1173.

Johnson, G.L. & Heezen. B.C. 1967: Morphology and evolution of the Norwegian-Greenland Sea. *Deep Sea Res. 14,* 755 - 771.

Johnson, G.L., Monahan, D., Grønlie, G. & Sobczak, L. 1979: Bathymetric Chart of the Arctic, *GEBCO sheet 5.17.* Canadian Hydrographic Service, Ottawa, Ontario, Canada.

Jones, G.A. & Keigwin, L.D. 1988: Evidence from Fram Strait (78°N) for early deglaciation. *Nature 336,* 56-59.

Kellogg, H.E. 1975: Tertiary stratigraphy and tectonism in Svalbard and continental drift. *Am. Assn. Petrol. Geol. Bull. 35,* 1505-1522.

Kitterød, N.O. 1986: *Hastighetsvariasjoner med dypet, tolkningsprosedyrer for ESP og sonarbøyedata.* Unpublished Cand. scient. thesis, Univ. of Oslo, 193 pp.

Klenova, M.V. 1960: Geology of the Barents Sea. *Akad. Sci. USSR, Moscow.* (US NavoOceano Transl. 130 by M. Slessers).

Kovacs, L.C. & Vogt, P.R. 1982: Depth-to-magnetic source analysis of the Arctic Ocean region. *Tectonophysics* 89, 255-294.

Kristoffersen, Y., Sand, M., Beskow, B. & Ohta, Y. 1989: Western Barents Sea: Bathymetry. *Norsk Polarinstitutt Skrifter 179E.*

Kvilhaug, T. 1990: *Sedimentologiske undersøkelser på kjerneprøver fra øvre del av kontinentalskråningen utenfor Bjørnøyrenna.* Unpublished Cand. scient. thesis, Univ. Tromsø, 180 pp.

Laberg, J.S. & Vorren, T.O. 1993: A Late

Pleistocene submarine slide on the Bear Island Trough Mouth Fan. *Geo-Marine Letters, 13,* 227-234

Laberg, J.S. & Vorren T. O. 1995: High resolution seismic and stratigraphic data from the Bear Island Fan. Page 165 in Crane, K. & Solheim, A. (Eds.): Seafloor Atlas of the Northern Norwegian-Greenland Sea. *Norsk Polarinstitutt Medd. 137* (this volume).

Lachenbruch, A.H. & Marshall, B.V. 1968: Heat flow and water temperature fluctuations in the Denmark Strait. *Journal of Geophys. Res. 73,* 5829-5842.

Laktionov, A.F. 1959: Bottom topography of the Greenland Sea in the region of Nansen's Sill. *Priroda 10,* 95-97 (DRB-Canada translation T333 R by E.R. Hope, Nov. 19959).

Langseth, M.G. & Zielinski, G.W. 1974: Marine heat flow measurements in the Norwegian-Greenland Sea and in the vicinity of Iceland. Pp. 277-295 in *Geodynamics of Iceland and the North Atlantic.* D. Reidel Publ., Dordrecht, Holland.

Lauritzen, Ø. & Ohta, Y. 1984: Geological Map of Svalbard, 1:500,000, Sheet 4G (Nordaustlandet). *Norsk Polarinstitutt Skrifter 154D.* 14 pp, 1 map.

Litvin, V.M. 1965: Origin of the bottom configuration of the Norwegian Sea. *Oceanology 5,* 90-96.

Lowell, J.D. 1972: Spitsbergen Tertiary orogenic belt and the Spitsbergen Fracture Zone. *Geol. Soc. Am.. Bull. 83,* 3091-3102.

Lubimova, E.A., Alexandrov, A.L. & Duchdov, A.D. 1973: Methods of study of the heat flow through the bottom of the ocean. Moscow, *Nauka,* 179 pp

Løvø, V., Elverhøi, A., Antonsen, P., Solheim, A., Butenko, G., Gregersen, O. & Liestøl, O. 1990: Submarine permafrost and gas hydrates in the northern Barents Sea. *Norsk Polarinstitutt Rapport No. 56.* 171 pp.

Malod, J. & Mascle, J. 1975: Structures géologiques de la marge continentale à l'ouest du Spitsberg. *Marine Geophys. Res. 2,* 215-229.

Mangerud, J. & Svendsen, J.I. 1992: The last interglacial-glacial period on Spitsbergen, Svalbard. *Quaternary Science Reviews 11,* 633-664.

Matishov, G.G. 1975: *Batimetricheckaya Karta Barentseva Morya* (Bathymetric Chart of the Barents Sea). Polyariye Nauchno-issledovatel'skiye i Proektniye Institut Morskogo R'Bnogo Chozyaiestva I Okeanografii Im. N.M. Knipovitch (Polar Research Institute and N.M. Knipovitch Institute of Fisheries Management and Oceanography), Murmansk.

Matishov, G.G. 1979: Geomorphological signs of the action of the Scandinavian, Novaya Zemlya, and Spitsbergen ice sheets on the floor of the Barents Sea. *Oceanology 20,* 440-447 (AGU translation).

Matishov, G.G. 1986a: Bottom geomorphology in marine ecosystems. In Nefedova, N.F. (ed.): Zhizn I Usloviya yeye Sushestvovaniya v Bentali Barentseva Morya (Life and Conditions for its Existence on the Bottom of the Barents Sea I-III).

Matishov, G.G. 1986b: Marginal glacial formations of the ocean floor. *Oceanology 26,* 730-735 (AGU Transl., 1987).

Matishov, G.G. 1987: Mirovoye okean i oledeneniye zemlya (World Oceans and Frozen Lands). *Izdatelstvo* M'sla~, Moscow, 272 (in Russian).

Matishov, G.G., Pavlova, L.G., Tarasov, G.A. & Alekseyev, V.V. 1984:. The complex paleo-oceanological expedition to the Barents Sea and the Norway-Greenland Basin. *Oceanology 24,* 148-149 (AGU transl., 1985).

Medvedev, V.S.& Pavlidis, Yu. A. 1984: New lithological and lithodynamical studies in the Barents Sea shelf (Leg 8 of the R/V Professor Shtokman). *Oceanology 24,* 144-147 (AGU transl., 1985).

Meyer, O., Voppel, D., Fleischer, U., Closs, H. & Gerke, K. 1972: Results of bathymetric, magnetic and gravimetric measurements between Iceland and 70°N. *Deutsches Hydrographisches Inst. Zeits. 25 (5),* 193-201.

Mienert, J., Kenyon, N. H., Thiede, J. & Hollender, F.J. 1993: Polar continental margins. Studies off east Greenland. *EOS Trans. Amer. Geophys. Un.* 74 (20) pp. 225, 234, 236.

Mienert, J., Hollender, F.-J. & Kenyon, N. 1995: Gloria Survey of the East Greenland Margin 70°N to 80 °N. Page 150 in Crane, K. & Solheim, A. (Eds.): Seafloor Atlas of the Northern Norwegian-Greenland Sea. *Norsk Polarinstitutt Medd. 137* (this volume)

Mitchum, R.M., Vail, P.R. & Sangree, J.B. 1977: Stratigraphic interpretation of seismic reflection patterns in depositional sequences. *American Association of Petroleum Geologists Memoir 26,* 117-134.

Myhre, A.M. & Eldholm, O. 1981: Sedimentary and crustal velocities in the Norwegian-Greenland Sea. *Jour. Geophys. Res. 86,* 5012-5022.

Myhre, A.M., Eldholm, O. & Sundvor, E. 1982: The margin between the Senja and Spitsbergen Fracture Zones: implications from plate tectonics. *Tectonophysics 89,* 1-32.

Myhre, A.M., & Eldholm, O. 1988: The western Svalbard margin (74 - 80N). *Marine and Petroleum Geology 5,* 134-156.

Mørk, M.B.E. & Duncan, R.A. 1993: Late Pliocene basaltic volcanism on the Western Barents Shelf margin: implications from petrology and 40Ar - 39Ar dating of vulcaniclastic debris from a shallow drill core. *Norsk Geologisk Tidsskrift 73,* 209-225.

Nansen, F. 1904: The bathymetrical features of the north polar seas with a discussion of continental shelves and previous oscillations of shoreline. Norwegian Polar Expedition, 1893-1896. *Science Research 4,* 232.

Neprochnov, Yu.P., Gol'mshtok, A.Ya. & Yel'nikov, I.N. 1984: Geophysical investigations of the subsurface structure of the bottom of the Barents Sea (4th, 6th and 8th Cruises of the R/V Professor Shtokman) *Oceanology 24,* 141-143 (AGU translation, 1985).

Niederjasper, F. & Focke 1989: Bathymetric surveys. In J.Krause, G., Meincke, J. & Thiede, J. (eds.): Scientific Cruise Reports of Arctic Expeditions ARK IV/1, 2 & 3. *Ber. Polarfosch. 56,* 43-46.

Norges Sjøkartverk 1988: *Den norske los. Arctic Pilot, Sailing Directions-Svalbard-Jan Mayen. 7,* 1st ed. 419 pp., Stavanger.

Nunns, A.G. 1980: *Marine geophysical investigations in the Norwegian-Greenland Sea between the latitudes of 62°N and 74°N.* Ph.D. thesis, Univ. of Durham, U.K.

Nunns, A.G. 1982: The structure and evolution of the Jan Mayen Ridge and surrounding areas. *Memoir 34, American Association of Petroleum Geologists,* 193-208. Tulsa.

ODP Leg 151 Shipboard Scientific Party 1994: Exploring Arctic History Through Scientific Drilling , *EOS 75 No. 25, P. 281, 285-286.*

Ohta, Y. 1982: Morpho-tectonic studies around Svalbard and the northernmost Atlantic. In Embry, A.F. & Balkwill, H.R. (eds.): Arctic Geology and Geophysics. *Can. Soc. Petrol. Geol. Mem. 8,* 415-429.

Okay, N., Crane, K., Vogt, P. & Sundvor, E. 1991: Diffuse rifting and associated volcanism on the Yermak Plateau in the Arctic Ocean. SeaMARC II results; Part IV. *Trans. Amer. Geophys. Un.72* (17), 274 pp.

Okay , N. & Crane, K. 1993: Thermal evolution of the Yermak Plateau. *Marine Geophysical Researches. 15,* 243-263.

Okay, N. 1994, *The Evolution of Volcanic Passive Margins in the Norwegian-Greenland Sea*, Unpublished PhD Thesis, City University of New York

Ostenso, N.A. 1968: Geophysical studies in the Greenland Sea. *Geological Society of America Bulletin 79*, 107-132.

Perry, R.K. 1986: Bathymetry, Ch. 9. Pp. 212-234 in Hurdle, B.G.(ed.): *The Nordic Seas.* Springer-Verlag, New York.

Perry, R.K., Fleming, H.S., Cherkis, N.Z., Feden, R.H. & Vogt, P.R. 1980: Bathymetry of the Norwegian, Greenland and Western Barents Seas. *Geological Society of America. Map and Chart Series, MC 21.*

Perry, R.K., Fleming, H.S., Weber, J.R., Kristoffersen, Y., Hall, J.K., Grantz, A., Johnson, G.L., Cherkis, N.Z. & Larsen, B. 1986: Bathymetry of the Arctic Ocean. *Geological Society of America. Map and Chart Series. MC 56.*

Pfirman, S.L. 1987: Sediment distribution of the Greenland Sea and the Fram Strait. *Polar Research 5 n.s.*, 319-320.

Pfirman, S.L. & Solheim, A. 1989: Subglacial meltwater discharge in the open-marine tidewater glacier environment: Observations from Nordaustlandet, Svalbard archipelago. *Marine Geology 86*, 265-282.

Phillips, J.D., Feden, R., Fleming, H.S. & Tapscott, C. 1982: *Aeromagnetic studies of the Greenland/Norwegian Sea and Arctic Ocean.* Unpublished. Naval Research Laboratory, Washington, D.C.

Ratcliffe, A.E. 1960: The thermal conductivities of ocean sediments. *Jour. Geophys. Res. 65*, 1535-15541.

Reed, T. B., Tucholke, B., Macdonald, K.C., Crane, K., Vogt, P. & Sempere, J.C. 1992: Interactive visualization of 3D-plus data sets: Simulated flights along the Mid-Atlantic Ridge, the East Pacific Rise and the Knipovich Ridge, AGU Montreal. *EOS April 7*, 1992, 46.

Reksnes, P.A. & Vågenes, E. 1985: Evolution of the Greenland Sea and Eurasia Basin. *Unpubl. Cand. Scient. Thesis, Univ. of Oslo,* 136pp.

Renard, V. & Malod, J. 1974: Structure of the Barents Sea from seismic refraction. *Earth and Planetary Science Letters 24,* 33-47.

Renard, V., Avedik, F., Geli, L., Le Comte, I., Le Formal, J.P. & Nercessian, A. 1989: Characteristics of oceanic crust formation of a part of the Mohn's Ridge near 72°N in the Norwegian-Greenland Sea. Part 1: Morphological study and underway geophysics. Abstract. *Terra Cognita 1*, 207.

Rice, A.H.N., Gayer, R.A., Robinson, D. & Bevins, R.E. 1989: Strike-slip restoration of the Barents Sea Caledonides terrane, Finnmark, north Norway. *Tectonics 8*, 247-264.

Riis, F., Vollset, J. & Sand, M. 1986: Tectonic development of the western margins of the Barents Sea and adjacent areas. Pp. 661-676 in Halbouty, M.T. (ed.): Future Petroleum Provinces of the World. *Amer. Assn. Petrol. Geol. Mem. 40.*

Rønnevik, H.C. 1981: Geology of the Barents Sea. Pp. 395-406 in Illing, L.V. & Hobson (eds.): *Petroleum Geology of the Continental Shelf of Northwest Europe.* Inst. of Petrol., London.

Rønnevik, H.C. & Motland, K. 1979: Geology of the Barents Sea. *Norw. Petrol. Soc., NSS/15*, 34 pp.

Rønnevik, H.C., Beskow, B. & Jacobsen, H.P. 1982a: Structural and stratigraphic evolution of the Barents Sea. Pp. 431-440 in Embry, A.F. and Balkwill, H.R. (eds.): Arctic Geology and Geophysics. *Can. Soc. Petrol. Geol. Mem. 8.*

Rønnevik, H.C., Beskow, B. & Jacobsen, H.P. 1982b: Structural and stratigraphic evolution of the Barents Sea. *ONS-82, Norw. Petrol. Soc.* 29 pp.

Rønnevik, H.C., Beskow, B. & Jacobsen, H.P. 1984: Structural and stratigraphic evolution of the Barents Sea. *Norw. Petrol. Soc., Geol. Mem. 8*, 431-440.

Rønnevik, H.C. & Jacobsen, H.P. 1984: Structural highs and basins in the western Barents Sea. Pp. 19-32 in Spencer, A.M. (ed.): *Petroleum Geology of the North European Margin.* Graham and Trotman, London.

Savostin, L.A. & Karasik, A.M. 1981: Recent plate tectonics of the Arctic Basin and of northeastern Asia. *Tectonophysics 74*, 111-145.

Schlüter, H.U. & Hinz. K. 1978: The continental margin of west Spitsbergen. *Polarforschung 48*, 151-169.

Solheim, A. & Kristoffersen, Y. 1984: The Physical Environment, Western Barents Sea, 1:1,500,000: Sheet B, Sediments Above the Upper Regional Unconformity: Thickness, Seismic Stratigraphy and Outline of the Glacial History. *Norsk Polarinstitutt Skrifter 179B*. 26 pp., 1 map.

Solheim, A., Russwurm, L., Elverhøi, A. & Nyland Berg, M. 1990: Glacial geomorphic features: direct evidence for grounded ice in the northern Barents Sea and implications for the pattern of deglaciation and late glacial sedimentation. *Geological Society of London, Special Publication. 53,* 253-268.

Solheim, A., Elverhøi, A., Sletten Andersen, E. & Jahre, H. 1991: Marine geological-geophysical cruise on the western Svalbard margin 1990. Cruise report. *Norsk Polarinstitutt Rapportserie 69,* 96pp.

Solheim, A. & Elverhøi, A. 1993: Gas-related sea floor craters in the Barents Sea. *Geo-Marine Letters, 13,* 235-243.

Somers, M. L., Carson, R. A., Revie, J. H., Edge, R. H., Barrow, B. J. & Andrews A. G. 1978: GLORIA I – An improved long range side scan sonar. *Oceanology International, Proceedings. Offshore Instrumentation and Communications 16-24,* Institute of Electrical Engineers. New York.

Sommerhoff, G. 1973: Formenschatz und morphologische Gliederung des Südostogrönländischen Schelfgebietes und Kontinental-abhanges: "Meteor". *Forsch. eregibn.-Reihe C.* 15, 1-54.

Sorokin, A.L. 1987: The geomorphology of the Barents Shelf off the Kola Peninsula. *Polar Geography and Geology 11*, 117-126.

Spencer, A.M., Home, P.C. & Berglund, L.T. 1984: Tertiary structural development of the western Barents Shelf: Troms to Svalbard. Pp.199-209 in Spencer, A.M. et al. (eds.): *Petroleum Geology of the North European Margin.* Graham and Trotman.

Sundvor, E. 1986: Heat flow measurements on the Barents Sea/Svalbard margin. *Univ. Bergen, Seismol. Observ. Int. rep.*, 8 pp.

Sundvor, E. & Eldholm, O. 1976: Marine geophysical survey of the continental margin from Bear Island to Hornsund, Spitsbergen. *Univ. Bergen Seism. Obs. Ser. Rpt. 3.* 28 pp.

Sundvor, E. & Eldholm, O. 1979: The western and northern margin off Svalbard. *Tectonophys. 59*, 239-250.

Sundvor, E., Eldholm, O., Haugland, K., Sellevoll, M. & Bruland, L. 1975: Seismic measurements on the Norwegian continental margin. *Univ. Bergen Seism. Obs. Rpt. 2,* 30 pp.

Sundvor, E., Eldholm, O., Gidskehaug, A. & Myhre, A.M. 1977: Marine geophysical survey on the western and northern continental margin of Svalbard. *Univ. Bergen Seism. Obs. Rpt. 4*, 35 pp.

Sundvor, E., Gidskehaug, A., Myhre, A.M. & Eldholm. E. 1978: Marine geophysical survey on the northern Svalbard margin. *Univ. Bergen Seism. Obs. Sci. Rpt. 5,* 46 pp.

Sundvor, E., Myhre, A.M. & Eldholm, O. 1979: The Svalbard continental margin. *Norwegian Sea Symposium (Norw. Petrol. Soc.) NSS/6,* 1-25.

Sundvor, E., Johnson, G.L. & Myhre, A.M. 1982a: Some aspects of morphology and structure of the Yermak Plateau, NW of Spitsbergen. *Univ. Bergen Seism. Obs. Sci. Rpt. 8*, 24 pp.

Sundvor, E., Myhre, A.M., Austegard, A., Haugland, K., Eldholm, O. & Gidskehaug, A. 1982b: Marine geophysical survey on the Yermak Plateau. *Univ. Bergen Seism. Obs. Sci. Rpt. 7*, 29 pp.

Sundvor, E. & Torp, J.E. 1987: Measurements of heat flow and thermal conductivity in the Nansen Basin, Arctic Ocean. *Univ. Bergen. Seismol. Observ. Cruise rep.*, 17 pp.

Sundvor, E., Crane, K.,Vogt, P., Jones, C., deMoustier, C., Doss, H., Okay, N., Shor, A., Rognstad, M., Dang, S., Johnson, D.K & Bergersen, D. 1991: SeaMARC II and associated geophysical investigation of the Knipovich Ridge, Molloy Ridge/ Fracture Zone and Barents/Spitsbergen continental margin. Part I, overview of two year program completed. *EOS Trans. Amer. Geophys.Un. 72, (20)*, 232.

Svendsen, J.I., Mangerud, J., Elverhøi, A., Solheim, A. & Schüttenhelm, R.T.E. 1992: The late Weichselian glacial maximum on western Spitsbergen inferred from offshore sediment cores. *Marine Geology 104*, 1-17.

Sverdrup, H.U. 1933: *The Norwegian North Polar Expedition with the "MAUD", 1a, 1918-1925.* Geofysisk Institutt, Bergen.

Sættem, J., Poole, D.A.R., Ellingsen, K.L. & Sejrup, H.P. 1992: Glacial geology of outer Bjørnøyrenna, southwestern Barents Sea. *Marine Geology 103*, 15-51.

Sættem, J., Bugge, T., Fanavoll, S., Goll, R.M., Mørk, M.B.E., Smelror, M. & Verdeniüs, J.G. 1994: Cenozoic margin development and erosion of the Barents Sea: Core evidence from southwest of Bjørnøya, *Marine Geology 118*, 257-281.

Talwani, M. & Grønlie, G. 1976: Free-air gravity field of the Norwegian-Greenland Seas. *Geol. Soc. Am. Map and Chart Series, MC-15.*

Talwani, M., Udintsev, G. et al. 1976: *Initial Reports of the Deep Sea Drilling Project, Vol. 28,* Washington (U.S. Government Printing Office), 389-449.

Talwani, M. & Eldholm, O. 1977: Evolution of the Norwegian-Greenland Sea. *Geol. Soc. America Bull. 88*, 969-999.

Thiede, J., Diesen, G.W., Knudsen, B.-E. & Snåre, T. 1986: Patterns of Cenozoic sedimentation in the Norwegian - Greenland Sea. *Marine Geology 69*, 323-352.

Thiede, J., Pfirman, S., Schenke, H.W. & Reil, W. 1990: Bathymetry of Molloy Deep: Fram Strait between Svalbard and Greenland. *Marine Geophys. Res. 12*, 197-214.

Vogt, P.R. 1968: *A Reconnaissance Geophysical Survey of the North, Norwegian, Greenland, Kara and Barents Seas and the Arctic Ocean.* Unpublished PhD Thesis,. Univ. Wisconsin, 133 pp., 36 fig., 18 charts.

Vogt, P.R. 1986: Geophysical and geochemical signatures and plate tectonics. Pp. 413 - 664 in Hurdle, B.G. (ed): *The Nordic Seas.* Springer-Verlag.

Vogt, P.R. & Avery, O.E. 1974: Tectonic history of the Arctic Basins: partial solutions and unsolved mysteries. Pp. 83-117 in Herman, Y. (ed.): *Marine Geology and oceanography of the Arctic Seas.* Springer Verlag, New York.

Vogt, P.R., Feden, R.H., Eldholm, O. & Sundvor, E. 1978: The ocean crust west and north of the Svalbard Archipelago. Synthesis and review of new results. *Polarforshung 48*, 1-19.

Vogt, P.R., Taylor, P.T., Kovacs, L.C. & Johnson, G.L. 1979: Detailed aeromagnetic investigation of the Arctic Basin. *Jour. Geophys. Res. 84*, 1071-1089.

Vogt, P.R., Perry. R.K., Feden, R.H., Fleming, H.S. & Cherkis, N.Z. 1981: The Greenland-Norwegian Sea and Iceland environment: Geology and geophysics. Pp. 493 - 598 in Nairn, A.E.M., Churkin, M. jr. & Stehli, F.G. (eds.): *The Ocean Basins and Margins 5.* Plenum Publ. Corp., New York.

Vogt, P.R., Kovacs, L.C., Bernero, L.C. & Srivastava, S.P. 1982: Asymmetric geophysical signatures in the Greenland-Norwegian and southern Labrador Seas and the Eurasia Basin. In Johnson, G.L. & Sweeney, J.F. (eds): Structure of the Arctic. *Tectonophysics 89 (1-3)*, 95-160.

Vogt, P.R., Crane, K., Pfirman, S., Sundvor, E., Chayes, D., Cherkis, N.Z., Fleming, H. & Nishimura, C. 1991a: SeaMARC II sidescan sonar imagery and swath bathymetry in the Nordic Basin: Sedimentary processes elucidated by correlation with 3.5 kHz and other data: *EOS, Trans. Amer. Geophys. Un.72 (44), p.* 486 .

Vogt, P.R., Fleming, H., Sundvor, E., Crane, K., Pfirman, S. & Shor, A. 1991b: SeaMARC II and associated geophysical investigation of the Knipovich Molloy Ridge fracture zone, Spitsbergen/Barents/Norwegian continental margin and extinct Aegir Ridge (Norway Basin). Part III, synthesis of sedimentary processes. *EOS Trans., Amer. Geophys. Un.72 (20),* p. 232 .

Vogt, P.R., Crane. K. & Sundvor, E. 1993: Glacigenic mudflows on the Bear Island submarine fan. *EOS, Trans. Amer. Geophys. Un. 74* (40).

Vogt, P.R., Crane, K. & Sundvor, E. 1994a: Deep Pleistocene iceberg plowmarks on the Yermak Plateau: Side scan and 3.5 kHz evidence for thick calving ice fronts and a possible marine ice sheet in the Arctic Ocean. *Geology 22*, 403-406.

Vogt, P.R., Crane, K. & Sundvor, E. 1994b: Glaciagenic mudflows on the Bear Island submarine fan. *EOS Trans. Amer. Geophys. Un.74,40,* 449-453.

Vogt, P.R., Crane, K., Sundvor, E., Max M., & Pfirman, S. L. 1994c: Methane-generated (?) Pockmarks on young thickly sedimented oceanic crust in the Arctic: Vestnesa Ridge, Fram Strait. *Geology 22*, 255-258.

Volkov, P. 1961: New explorations of the bottom topography in the Greenland Sea. *Morskoi Flot 3*, 35-37. Translated by E.R. Hope, DRB Canada, T356R.

Von Herzen, R.P. & Maxwell, A.E. 1959: The measurements of thermal conductivity of deep-sea sediments by a needle probe method. *Jour. Geophys. Res.* 64, 1557-1563.

Vorren, T.O., Hald, M. & Lebesbye, E. 1988: Late Cenozoic environment in the Barents Sea. *Paleoceanography 3*, 601-612.

Vorren, T. O., Lebesbye, E., Andreassen, K. & Larsen, K.B. 1989: Glacigenic sediments on a passive continental margin as exemplified by the Barents Sea. *Mar. Geol. 85*, 251-272.

Vorren, T.O., Lebesbye, E. & Larsen, K.B. 1990: Geometry and genesis of the glacigenic sediments in the southern Barents Sea. Pp. 309-328 in Dowdeswell, J.A. & Scourse, J.D. (eds.): Glacimarine environments, processes and sediments. *Geological Society of London Special Publication 53*, 309-328.

Vorren, T.O., Richardsen, G., Knutsen, S.M. & Henriksen, E. 1991: Cenozoic erosion and sedimentation in the western Barents Sea. *Marine and Petroleum Geology 8*, 317-340.

Winsnes, T.S. & Worsley, D. 1981: Geological Map of Svalbard, 1:500,000, Sheet 2G (Edgeøya). *Norsk Polarinstitutt Skrifter 154B*, one map.

Åm, K. 1975: Magnetic profiling over Svalbard and surrounding shelf areas. *Norsk Polarinstitutt Årbok 1973*, 87-100.

REGIONES
SVB POLO ARCTICO.
Auctore Guilielmo Blaeu
FRIGVS iners illic habitant, Pallorque
Et jejuna FAMES.
Amplissimo Spectatissimo
Prudentiss.mo Viro
GVILIELMO BACKER
DE CORNELIIS.
Reip. Amstelodamensis Consuli et Se-
natori, nec non in Consessu Societa-
tis Indicæ Orientalis Aßessori Tabu-
lam hanc D.D.
Joh. Blaeu.
New South
Wales.
Buttons Bay
New North
Wales
James his Bay
NOVA
BRITANNIA.
Fretum
Hudson
Baffins Bay.
FRETUM DAVIS.
GROENLANDIA.
Terra de
Cortereealis.
TERRA NOVA
YSLANDIA.
OCE
SE
TRION
Linea sub C
Port Nelson
New Severne
Briggs his Bay
Hope check
C. Philips
Hope advanced
Ne Vltra
C. Henriette Maria
Charlton Ile
Danby Ile
Caryes Ile
Ille Hibernavit Hudson
The great Bay of Gods deliverance
C. Southampton
Carye Swans nest
C. Pembrock
C. Comfort
Mansfield Iland
Digges Iland
Salisberis Iland
C. Worsnam
C. Charles
Cumberlants Iles
C. Elisabeth
Salvage I.
Mount Raleg
C. Walsingam
Hornsound
Westmanna eyar
Vogel Scharen
Skalholt
Hekla mons
Grimsey
Langenes
Papey
Bus
Grand Bay
Belisle
C. de Grato
C. Bonavista
Trinite Bay
Conception Bay
C. Farewel
Herwolds ness
50
60
70
80
260
250
240
230
340
350
360
10

Circulus sub Circulo Arctico.
Tenduc
Cambalu
CATHAIA.
A: TARTA: SIÆ
RIÆ
PARS
C. Tabin
MARE TARTARICUM.
Tazata Insula
NOVA ZEMLA
NIAREN MORE
Molgomzaia.
Obi reca
Obdora.
SAMOIEDA.
Staten eylant
Nova Hollandia
Petzora
MOVRMANSKOY MORE.
Fretum Nassovicum
I. Colgoyen
C. Candenos
Spitsberge
Vogelhoeck
Wardhuys
Noordkyn
Finmarchia
Kola
LAPPONIA.
Mare Album
S. Michael Archangel
EVROPÆ
SVECIÆ PARS
NORVEGIÆ PARS
RVSSIÆ PARS
Sinus Bothnicus
Milliaria Germanica communia
pro 60 latit. gradu
pro 70 latit. gradu
pro 80 lat. gradu

VOYAGES TO THE NORWEGIAN-GREENLAND SEA: A SHORT HISTORY

SUSAN BARR

Around the Middle Ages, when speculations about the area north of Norway and Iceland began to evolve beyond the myths of sea dragons and Nordic gods and goddesses, cartographers believed that a continuous land mass stretched from Bjarmeland (the Kola Peninsula) to Greenland. Undoubtedly this idea evolved from various sightings of the impenetrable Arctic ice pack interpreted to be land. The icelandic annals of 1194 indicated that Norwegian and Icelandic ship traffic across the Norwegian and Greenland Seas was primarily aimed at seal and walrus hunting along the edge of the Arctic ice pack. However, coinciding with the arrival of Christianity by the end of the Middle Ages, such voyages northwards were no longer carried out and knowledge of the area was gradually lost.

A renewed interest in the Arctic arose at the end of the 16th century when English and Dutch companies sent ships northwards to find a new trade route to India. Willem Barents discovered and named the archipelago of Spitsbergen (Svalbard) after encountering the ice edge in the northern Norwegian-Greenland Sea. In 1607, Henry Hudson sailed along Greenland's east coast to 81°N, across to Svalbard and back to England, supposedly via the island of Jan Mayen. Hudson observed large numbers of whales in Svalbard's fjords which quickly led to an intensive period of whaling around Svalbard and Jan Mayen in the 17th century, and near the ice edge of the entire Norwegian-Greenland Sea during the 18th and 19th centuries. Together with whaling and also sealing, came scientific expansion. Friderich Martens from Germany (1675), Cornelius G. Zorgdrager from Holland (1720), and William Scoresby Sr. and Jr. from England (1803-22) are four individuals whose scientific observations and publications contributed to the early knowledge of the Norwegian-Greenland Sea.

Many of the scientific expeditions in the 19th century were primarily concerned with mapping the Arctic islands and coastlines. A chart from 1865 by A. Petermann, shows that only the north-eastern coast of Greenland and the western side of the Fram Strait were still unmapped (although controversy about the correct Greenland coastline still puzzles Arctic cartographers to this day). However, British, French, German and Scandinavian expeditions in the 19th century also conducted valuable scientific research at sea. For example Prince Bonaparte's expedition in «La Reine Hortense» and «Le cocyte» in the Norwegian-Greenland Sea in 1856, Karl Koldewey's expeditions in «Germania» and «Hansa» in the Norwegian-Greenland Sea in 1868 and 1869-70, the Norwegian «Voringen» expeditions in 1877 and 1878, A. E. Nordenskiöld's expedition in «Sofia» in 1883, C. F. Wandel's «Ingolf» expedition in 1895 and 1896, and A. G. Nathorst's 1899 expedition in the «Antarctic».

After a several hundred year hiatus, Norway's presence in the Norwegian-Greenland Sea revived in the beginning of the 19th century with major fishing and sealing efforts between the island of Jan Mayen and Greenland. Norwegian scientific investigations naturally followed the sealing and fishing interests. The first ship specially equipped and run by the Norwegian government for marine research commenced operation in 1900. In addition, French, German and American organizations conducted notable research. Amongst the more important were Johan Hjort's expeditions in 1900 and 1901, Duc Philippe d'Orlean's «Belgica» expedition under Adrian de Gerlache in 1905, Fridtjof Nansen's expedition with «Veslemoy» in 1912, Johan Hjort's «Michael Sars» expedition in 1924, the Danish «Dana» expedition in 1925, J.B. Charcot's expeditions with «Pourquoi Pas?» in the years 1925-31 and 1936, the German «Meteor» expeditions in 1929-35, American, Louise Boyd's «Veslekari» expeditions in 1937 and 1938 and Thor Iversen's fishery and other studies off eastern Greenland in 1932.

A new style of scientific exploration arose with the advent of far-ranging submarines during World War II. However, scientific participation was limited to Hubert Wilkins and H.U. Sverdrup in the «Nautilus» in 1931 and Papanin's ice-drift station from the North Pole down the eastern coast of Greenland in 1937-38. After World War II, scientific expeditions in the Norwegian-Greenland Sea increased rapidly, particularly during the last two decades. In recent years, improved technology, increased basic research interests as well as the need to investigate the Arctic fisheries, oil and gas resources, have allowed the development of many new ice-strengthened research vessels. Many of the results from these latest expeditions are presented in this atlas. Nevertheless, the North Polar region remains one of the least understood regions on Earth.

NORSK POLARINSTITUTT

ISBN 82-7666-089-4